SPATIO-TEMPORAL VARIABILITY OF BIOENERGY FEEDSTOCK BIOMASS YIELD AND QUALITY AT FIELD SCALE IN THE GREAT LAKES REGION USA

By

Sichao Wang

A DISSERTATION

Submitted to
Michigan State University
in partial fulfillment of the requirements
for the degree of

Crop and Soil Sciences – Doctor of Philosophy

2023

ABSTRACT

To understand the temporal and spatial variability of switchgrass (*Panicum virgatum*) and restored prairie biomass yield and quality as a bioenergy feedstock at field-scale, a study was conducted at Marshall Farm (42.44° N, -85.32° W) and Lux Arbor Farm (42.48° N, -85.44° W) in southwest Michigan USA from 2018-2021. Switchgrass annual average biomass yield ranged from 4.3 to 9.1 Mg ha^{-1} over the study period. Restored prairie annual average biomass yield ranged from 2.4 to 4.9 Mg ha^{-1}. Under similar field conditions, the monoculture switchgrass cropping system exhibited more temporal and spatial variability of biomass yield than the polyculture restored prairie. In contrast, the polyculture restored prairie exhibited more spatial variability of glucose and xylose content than monoculture switchgrass under similar field conditions. However, minimal spatial variability of glucose, xylose and lignin content was observed in switchgrass and restored prairie. The ratio of interannual temporal variance to spatial variance for glucose, xylose and lignin content of switchgrass at Marshall Farm was 12.2, 3.2 and 5.5, respectively. The ratio of interannual temporal variance to spatial variance for glucose, xylose and lignin content of switchgrass at Lux Arbor Farm was 52.4, 5.8 and 1.0×10^5, respectively. The ratio of interannual temporal variance to spatial variance for glucose, xylose and lignin content of restored prairie at Marshall Farm was 1.3, 1.7 and 9.1, respectively. The ratio of interannual temporal variance to spatial variance for glucose, xylose and lignin content of restored prairie at Lux Arbor Farm was 6.1, 4.3 and 18.8, respectively. Soil ammonium, magnesium, calcium, and phosphorus concentrations as well as the topographic wetness index were important to explain within-field spatial variability in biomass yield, glucose, xylose and lignin content of switchgrass and restored prairie at Lux Arbor Farm and Marshall Farm. Lastly, we evaluated near-infrared spectroscopy as a quick, non-destructive method for analyzing biomass quality.

Compared to chemical analyses, near-infrared sprectroscopy had negative biases for glucose (switchgrass: -72.5 mg g^{-1}, restored prairie: -78.5 mg g^{-1}) and xylose content (switchgrass: -99.6 mg g^{-1}, restored prairie: -91.4 mg g^{-1}) and positive biases for lignin content (switchgrass: 32.6 mg g^{-1}, restored prairie: 47.8 mg g^{-1}). With bias correction, the agreement between near-infrared spectroscopy and chemical analysis was significantly improved. Near-infrared spectroscopy is therefore a promising rapid analytical tool for glucose, xylose, and lignin content of biomass. With expected increases in precipitation and temperature variability associated with future climate change, spatial and temporal variability in biomass quality will likely be exacerbated. Understanding the sources of this variability will facilitate the development of management practices at the field and biorefinery level to help address the issue. Identifying analytical methods to accurately assess variability in biomass quality will be an important step in this process.

This dissertation is dedicated to my family.

ACKNOWLEDGEMENTS

I would like to acknowledge all the wonderful people I have met at Michigan State University. Firstly, I would like to express my deepest gratitude to my advisor, Dr. Kurt Thelen, with whom this work would not have been possible. I also could not have undertaken this journey without my committee: Dr. Alexandra Kravchenko, Dr. Bruno Basso and Dr. Stephen Hamilton, who generously offered expertise and knowledge.

I would like to thank all the lab members—Pavani Tumbalam, Todd Martin, Chris Robbins, and Dileepa Jayawardena—for help and company in the lab and field. I also would like to thank Dr. Bruno Basso's lab members—Ruben Ulbrich and Richard Price—for help during field season.

Particularly, I would like to thank the Center for Statistical Training and Consulting at MSU (CSTAT), where I have learned more than what I could think of. At CSTAT, I got the greatest support and growth. I deeply appreciate Dr. Steve Pierce's generous mentoring and support. He was always available when I needed help and guidance. Dr. Wenjun Ma always provided me the warmest and thoughtful advice. Dr. Dhruv Sharma's course introduced me to CSTAT and helped me grow into a statistical consultant. I cannot say more thanks to Dr. Marianne Huebner, whose leadership at CSTAT and STATCOM has been inspiring me as a professional female. Her encouragement motivated me to finish this work.

Additionally, thanks also goes to my friends at Michigan State University. They made my graduate student life more colorful.

I am tremendously grateful to my family. My mother, Xiping Yu, has consistently provided me with unwavering support. My husband, Chris Vargas, has been a pillar of love and encouragement for me. My son, Liam Vargas, has been a constant source of cheer and strength, helping me stay motivated and focused.

Last but not the least, I also thank the research funding by the US DOE Great Lakes Bioenergy Research Center (DOE Office of Science, DE-FC02-07ER64494 & DOE Office of Energy Efficiency and Renewable Energy, DE-AC05-76RL01830)

TABLE OF CONTENTS

LIST OF ABBREVIATIONS

IEA International Energy Agency

IPCC Intergovernmental Panel on Climate Change

BECCS bioenergy with carbon capture and storage

GHG Greenhouse Gas

CRP Crop Reservation Program

ICC Intraclass correlation coefficient

NDC Nationally Determined Contribution

P phosphorus

K potassium

Ca calcium

Mg magnesium

NH_4^+ ammonium

DEM digital elevation map

LL15 15 bar lower limit of soil water content

DUL upper limit of soil water content

Ksat saturated hydraulic conductivity of soil

SWCON whole profile drainage rate coefficient

SAT saturated water content

CV Coefficient of Variance

EOF Empirical orthogonal function

CI Confidence Interval

AIC Akaike Information Criterion

[Glc] Glucose content

[Xyl] Xylose content

ABSL Acetyl bromide soluble lignin

NIR near infrared

CHAPTER 1 GENERAL INTRODUCTION

Today's global energy challenges, exacerbated by current global geopolitical conflicts, are reshaping the future of energy sustainability, security and affordability. The detrimental effects of climate change make the ongoing energy crisis even more urgent. To face the pressing energy and climate challenges, developing and deploying renewable energy has become a global effort. Among all types of renewable energy, bioenergy is the largest source of renewable energy globally and contributes 55% of renewable energy supply today (IEA, 2022). Especially for liquid transportation fuel, bioenergy is the only practical renewable energy option in the near future (Skeer et al., 2016; Bergero et al., 2023). Furthermore, bioenergy has been seen as instrumental to realize a net zero carbon emission economy globally (Highina et al., 2014; Jeswani et al., 2020). The current U. S. administration set a goal to achieve net zero carbon emission no later than 2050, which is compatible with IPCC's 1.5 °C increase limit (IPCC, 2022). The first U.S. National Blueprint for Transportation Decarbonization (2023) demonstrated that sustainable advanced biofuel has the potential to fully replace fossil fuel in aviation, maritime and rail transportation (Muratori et al., 2023). In addition to supplying carbon neutral energy, bioenergy with carbon capture and storage (BECCS) as a negative carbon emissions technology has been recognized to be essential to offset greenhouse gas emissions from sectors with known difficulty of mitigating carbon emission completely (Azar et al., 2010; Hanssen et al., 2020; Rosa et al., 2021). Under the net zero carbon by 2050 scenario, the International Energy Agency forecasted that the demand for biofuel will increase by 20% from 2022 to 2027 (IEA, 2022). Moreover, other value-added biochemical products from the emerging bioenergy industry have great potential to replace oil-based chemical products (Torres-Mayanga et al., 2019; Meramo et al., 2022). Thus, bioenergy and biochemical products from biomass-based resources are integral parts of the greener

bioeconomy (Rogers et al., 2017; Scarlat et al., 2015). To meet the projected increasing demand of bioenergy and support the bioeconomy, a steady and sustainable biomass feedstock supply is paramount.

Bioenergy feedstocks are generally classified into three groups: 1st, 2nd and 3rd generation bioenergy feedstocks. The 1st generation bioenergy feedstocks come from edible crops such as corn, sugarcane and soy. With the help of enzymes and microorganisms, biofuel such as ethanol is produced from starch in corn or sugar in sugarcane. Via the transesterification process, biodiesel is produced from oil in soy or fat in animals. To date, the majority of the biofuel in the U.S. is still coming from corn ethanol due to supportive policies such as Renewable Fuel Standard (Taxpayers for Common Sense, 2021). The food- or feed-based 1st generation biofuel feedstocks have been criticized for having a negative impact on food security and biodiversity (Tenenbaum, 2008; Hill, 2022; Tudge et al., 2021). Some studies have reported that 1st generation biofuel such as corn ethanol can increase greenhouse gas (GHG) emissions when compared to fossil fuel (Searchinger et al., 2008; Brandão, 2022; Lark et al., 2022). Lark et al. (2022) summarized that the sources of GHG increases are intensive use of synthetic nitrogen fertilizer and land use change to grow more corn. To address the concerns associated with 1st generation bioenergy feedstocks, lignocellulosic biomass as 2nd generation bioenergy feedstocks have gained more attention. Main sources of 2nd generation bioenergy feedstocks are dedicated energy crops such as switchgrass (*Panicum virgatum*), short rotation woody crops such as poplar, agricultural and forestry residues, etc. A review reported that 2nd generation bioenergy feedstocks generally decrease GHG emissions compared to fossil fuel (Highina et al., 2014). Despite the great GHG emission reduction potential, the major technical challenge of using lignocellulosic biomass is developing efficient and cost-effective pathways to convert relatively recalcitrant biomass materials into fuel

or other value-added co-products (Balan, 2014; Singhvi & Gokhale, 2019). Third generation bioenergy feedstocks include lipid rich algal biomass. At the current status of technology, biofuel derived from 3rd generation bioenergy feedstocks is not feasible for commercialization owing to a large requirement of land and high water footprint (Li-Beisson & Peltier, 2013; Maliha & Abu-Hijleh, 2022).

Low input requirements and the perennial nature of candidate crop species make 2nd generation bioenergy feedstocks such as switchgrass and restored prairie good candidates for growing on marginal lands (Tilman et al., 2006; Mitchell et al., 2008). Marginal lands are defined as lands with low biophysical quality and economic marginality for conventional food crop cultivation (Kang et al., 2013; Csikós & Tóth, 2023). Growing bioenergy feedstocks on marginal lands provides multiple benefits: reduced land use conflicts with food crop cultivation (Qin et al., 2015; Jiang et al., 2021), reduced soil erosion (Lai et al., 2018; Næss et al., 2023), increased soil carbon stocks (Slessarev et al., 2020; Bazrgar et al., 2020), and improved biodiversity (Valcu-Lisman et al., 2016; Von Cossel et al., 2020). Lands enrolled in the Crop Reserve Program (CRP) in the U.S. are characterized as low quality and environmentally vulnerable, thus generally considered as marginal lands. Therefore, the CRP lands offer unique opportunities to study agronomic practices, environmental impacts and economic viability of perennial bioenergy crop cultivation on marginal lands. Abraha et al. (2018) reported that converting CRP grassland to perennial bioenergy crops such as switchgrass can repay the carbon debt incurred upon conversion in 8 years. A life-cycle analysis of perennial bioenergy crops on CRP land in the northeastern U.S. found that high biomass price and high share of land rental payments leads to high cumulative GHG savings (Chen et al., 2021). Hartman et al. (2011) summarized that converting CRP land to a bioenergy cropping system closely resembling its original composition such as mixed grasses

would maintain biodiversity (Hartman et al., 2011).

Site specific management or precision agriculture is the key management approach for modern agriculture to maximize crop yield, optimize resource use and minimize negative environmental impacts by following 5 Rs: right input, right amount, right time, right place and right method (Pierce et al., 1994; Mokariya & Malam, 2020). It allows growers to manage not only within-field variability at finer resolution but also the temporal dynamic of crops (Plant, 2001). Site specific management relies on georeferenced data to understand within-field variability. Historically, grid sampling or point sampling was the main data collection method for site specific management. With the advance of technology, yield monitors, on-the-go sensors and remote sensing have become the data collection powerhouse of precision agriculture. Unlike grain yield monitor technology, yield monitoring systems for perennial biomass feedstock yield are not yet commercially available. Studies have used remote sensing, primarily unmanned aerial vehicles with sensors, to monitor biomass yield (Maesano et al., 2020; Hamada et al., 2021; Impollonia et al., 2022). However, the ground truth field level data for bioenergy feedstocks yield are scarce. Therefore, point sampling on the ground is essential to understand the variability of perennial biomass yield and quality.

Studies have shown high spatial variability of perennial bioenergy crop yield among fields based on plot experiments across a wide geographical range (Fike et al., 2006; Wullschleger et al., 2010; Anderson et al., 2011; Ouattara et al., 2022). However, little information is available for within-field spatial variability of perennial bioenergy crop yield. Understanding temporal and spatial variability of crop yield and the causes of the variability will help growers to implement site-specific management. It is well recognized that annual crop yield is affected by inherent soil variability such as soil fertility, soil topography and soil texture (e.g., Marques Da Silva &

Alexandre, 2005; Juhos et al., 2015; Wang et al., 2022). Jiang and Thelen (2004) reported that corn and soybean yield were affected by slope and very fine sand content. Previous studies found that soil properties and topography largely explained within-field variability of corn and soybean grain yield. Kaspar et al. (2004) demonstrated that soil pH, landscape position, and curvature influenced corn and soybean yield. To the best of our knowledge, only two studies have examined within-field spatial variability of early established switchgrass biomass yield using field data (Di Virgilio et al., 2007; Schmer et al., 2010). Di Virgilio et al. (2007) found soil nitrogen, phosphorus, moisture and pH were correlated with switchgrass biomass yield. Schmer et al. (2010) reported soil topography did not significantly affect switchgrass biomass yield. Knowledge of within-field temporal and spatial variability of biomass feedstock yield is critical for bioenergy feedstock supply chain modeling and planning (Kazemzadeh & Hu, 2013; O'Neill et al., 2022). Success of the bioenergy industry not only depends on a sustainable supply of feedstocks but also on the quality of the feedstocks. The inherent heterogeneity of biomass feedstocks poses unique challenges to biorefineries because it influences conversion efficiency and cost (Kenney et al., 2013; Castillo-Villar et al., 2017). Generally, biomass quality includes physical characteristics and chemical composition. Cell wall chemical composition of lignocellulosic biomass feedstock is critical for selecting appropriate conversion pathways and improving conversion efficiency (Li et al., 2016). The major components of cell walls include cellulose, hemicellulose and lignin. High cellulose, high hemicellulose and low lignin are desired for biochemical conversion of lignocellulosic biomass into liquid fuel via enzyme hydrolysis. Although lignin is less desired for biochemical conversion pathways due to its recalcitrance, it is a promising material for value-added chemical production (Weng et al., 2021; Zhou et al., 2022). Previous studies reported that variation in biomass cell wall composition was most likely caused by precipitation and

temperature patterns (Emerson et al., 2014; Crivellaro et al., 2022). Harvesting time and nitrogen fertilization were found to affect switchgrass quality as a biofuel feedstock. Schmer et al. (2012) demonstrated cell wall composition of switchgrass had higher field to field variability than within-field variability. Research on within-field temporal and spatial variability of lignocellulosic biomass cell wall composition and the causes of the variability is still lacking. A full understanding of within-field temporal and spatial of lignocellulosic biomass cell wall composition is critical for developing meaningful biomass quality specifications for various conversion pathways.

The importance of understanding variability in cell wall composition of biomass feedstock underlies the need for rapid, low-cost analytical instrumentation and methods to accurately assess the variability. Traditional chemical analysis of cell wall composition is time-consuming, labor intensive and high cost. Near-infrared spectroscopy coupled with chemometrics as a non-destructive and high-throughput method have shown promising results in analyzing plant cell wall composition (Li et al., 2015; Ai et al., 2022). Increasing portability of near-infrared spectrometers makes it attractive as a biomass quality monitoring and control tool from biomass harvest and storage to conversion at the biorefinery (Zhu et al., 2022). However, near-infrared spectroscopy relies on primary chemical analysis for calibration and validation. More information is still needed regarding its performance and measurement bias.

Crop growth and yield are climate dependent. Ray et al. (2014) reported that one third of the global crop yield variability can be explained by climate. Studies have highlighted the impacts and risks of climate variability and change on crop production globally (Gornall et al., 2010, Wing et al., 2021, Hasegawa et al., 2022). With expected increases in precipitation and temperature variability associated with future climate change, spatial and temporal variability in

biomass yield and quality will likely be exacerbated. Understanding the causes of this variability will facilitate the development of management practices at the field and biorefinery level to help address the issue.

The main aim of this dissertation is to better understand the temporal and spatial variability of the quantity and quality of switchgrass and restored prairie as bioenergy feedstocks at field scale. To do this, this dissertation is organized into three main research chapters, bookended by an introductory chapter at the beginning and a general conclusion chapter at the end. The second chapter focuses on understanding biomass yield variability of switchgrass and restored prairie with two objectives: (1) investigate the temporal and spatial variability of switchgrass and restored prairie biomass yield at field scale; and, (2) examine the effect of soil fertility features and topographical characteristics on switchgrass and restored biomass yield at field scale. The third chapter focuses on understanding the variability of glucose, xylose and lignin content of switchgrass and restored prairie at field scale with two objectives: 1) investigate the temporal and spatial variability of switchgrass and restored prairie biomass quality components at field scale; and, 2) examine the effects of soil fertility features and topographical characteristics on glucose, xylose and lignin content of switchgrass and restored prairie at field scale. In chapter four, the possibility of using near-infrared spectroscopy technique as a low-cost, rapid analytical tool for biomass compositional determination is examined.

REFERENCES

Abraha, M., Gelfand, I., Hamilton, S. K., Chen, J., & Robertson, G. P. (2019). Carbon debt of field-scale conservation reserve program grasslands converted to annual and perennial bioenergy crops. Environmental Research Letters, 14(2). https://doi.org/10.1088/1748-9326/aafc10

Ai, N., Jiang, Y., Omar, S., Wang, J., Xia, L., & Ren, J. (2022). Rapid Measurement of Cellulose, Hemicellulose, and Lignin Content in Sargassum horneri by Near-Infrared Spectroscopy and Characteristic Variables Selection Methods. Molecules, 27(335). https://doi.org/https:// doi.org/10.3390/molecules27020335

Anderson, E., Arundale, R., Maughan, M., Oladeinde, A., Wycislo, A., & Voigt, T. (2011). Growth and agronomy of Miscanthus × giganteus for biomass production. Biofuels, 2(2), 167–183. https://doi.org/10.4155/bfs.10.80

Anderson, E. K., Parrish, A. S., Voigt, T. B., Owens, V. N., Hong, C. H., & Lee, D. K. (2013). Nitrogen fertility and harvest management of switchgrass for sustainable bioenergy feedstock production in Illinois. Industrial Crops and Products, 48(2013), 19–27. https://doi.org/10.1016/j.indcrop.2013.03.029

Azar, C., Lindgren, K., Obersteiner, M., Riahi, K., van Vuuren, D. P., den Elzen, K. M. G. J., Möllersten, K., & Larson, E. D. (2010). The feasibility of low CO2 concentration targets and the role of bio-energy with carbon capture and storage (BECCS). Climatic Change, 100(1), 195–202. https://doi.org/10.1007/s10584-010-9832-7

Balan, V. (2014). Current Challenges in Commercially Producing Biofuels from Lignocellulosic Biomass. ISRN Biotechnology, 2014(i), 1–31. https://doi.org/10.1155/2014/463074

Bazrgar, A. B., Ng, A., Coleman, B., Ashiq, M. W., Gordon, A., & Thevathasan, N. (2020). Long-term monitoring of soil carbon sequestration in woody and herbaceous bioenergy crop production systems onmarginal lands in southern Ontario, Canada. Sustainability (Switzerland), 12(9), 1–16. https://doi.org/10.3390/su12093901

Bergero, C., Gosnell, G., Gielen, D., Kang, S., Bazilian, M., & Davis, S. J. (2023). Pathways to net-zero emissions from aviation. Nature Communications, January. https://doi.org/10.1038/s41893-022-01046-9

Brandão, M. (2022). Indirect Effects Negate Global Climate Change Mitigation Potential of Substituting Gasoline With Corn Ethanol as a Transportation Fuel in the USA. Frontiers in Climate, 4(March), 1–9. https://doi.org/10.3389/fclim.2022.814052

Castillo-Villar, K. K., Eksioglu, S., & Taherkhorsandi, M. (2017). Integrating biomass quality variability in stochastic supply chain modeling and optimization for large-scale biofuel production. Journal of Cleaner Production, 149, 904–918. https://doi.org/10.1016/j.jclepro.2017.02.123

Chen, L., Blanc-Betes, E., Hudiburg, T. W., Hellerstein, D., Wallander, S., Delucia, E. H., &

Khanna, M. (2021). Assessing the Returns to Land and Greenhouse Gas Savings from Producing Energy Crops on Conservation Reserve Program Land. Environmental Science and Technology, 55(2), 1301–1309. https://doi.org/10.1021/acs.est.0c06133

Crivellaro, A., Piermattei, A., Dolezal, J., Dupree, P., & Büntgen, U. (2022). Biogeographic implication of temperature-induced plant cell wall lignification. Communications Biology, 5(1), 1–10. https://doi.org/10.1038/s42003-022-03732-y

Csikós, N., & Tóth, G. (2023). Concepts of agricultural marginal lands and their utilisation: A review. Agricultural Systems, 204(June 2022). https://doi.org/10.1016/j.agsy.2022.103560

Di Virgilio, N., Monti, A., & Venturi, G. (2007). Spatial variability of switchgrass (Panicum virgatum L.) yield as related to soil parameters in a small field. Field Crops Research, 101(2), 232–239. https://doi.org/10.1016/j.fcr.2006.11.009

Emerson, R., Hoover, A., Ray, A., Lacey, J., Cortez, M., Payne, C., Karlen, D., Birrell, S., Laird, D., Kallenbach, R., Egenolf, J., Sousek, M., & Voigt, T. (2014). Drought effects on composition and yield for corn stover, mixed grasses, and Miscanthus as bioenergy feedstocks. Biofuels, 5(3), 275–291. https://doi.org/10.1080/17597269.2014.913904

Fike, J. H., Parrish, D. J., Wolf, D. D., Balasko, J. A., Green, J. T., Rasnake, M., & Reynolds, J. H. (2006). Long-term yield potential of switchgrass-for-biofuel systems. Biomass and Bioenergy, 30(3), 198–206. https://doi.org/10.1016/j.biombioe.2005.10.006

Gornall, J., Betts, R., Burke, E., Clark, R., Camp, J., Willett, K., & Wiltshire, A. (2010). Implications of climate change for agricultural productivity in the early twenty-first century. Philosophical Transactions of the Royal Society B: Biological Sciences, 365(1554), 2973–2989. https://doi.org/10.1098/rstb.2010.0158

Hamada, Y., Zumpf, C. R., Cacho, J. F., Lee, D., Lin, C. H., Boe, A., Heaton, E., Mitchell, R., & Negri, M. C. (2021). Remote sensing-based estimation of advanced perennial grass biomass yields for bioenergy. Land, 10(11). https://doi.org/10.3390/land10111221

Hanssen, S. V., Daioglou, V., Steinmann, Z. J. N., Doelman, J. C., Van Vuuren, D. P., & Huijbregts, M. A. J. (2020). The climate change mitigation potential of bioenergy with carbon capture and storage. Nature Climate Change, 10(11), 1023–1029. https://doi.org/10.1038/s41558-020-0885-y

Hartman, J. C., Nippert, J. B., Orozco, R. A., & Springer, C. J. (2011). Potential ecological impacts of switchgrass (Panicum virgatum L.) biofuel cultivation in the Central Great Plains, USA. Biomass and Bioenergy, 35(8), 3415–3421. https://doi.org/10.1016/j.biombioe.2011.04.055

Hasegawa, T., Wakatsuki, H., Ju, H., Vyas, S., Nelson, G. C., Farrell, A., Deryng, D., Meza, F., & Makowski, D. (2022). A global dataset for the projected impacts of climate change on four major crops. Scientific Data, 9(1), 1–11. https://doi.org/10.1038/s41597-022-01150-7

Highina, B. K., Bugaje, I. M., State, B., Umar, B., & State, B. (2014). A review on second generation biofuel: a comparison of its carbon footprints. European Journal of Engineering and Technology, 2(2), 117–125.

Hill, J. (2022). The sobering truth about corn ethanol. Proceedings of the National Academy of Sciences of the United States of America, 119(11), 9–10. https://doi.org/10.1073/pnas.2200997119

IEA (2022), Bioenergy, IEA, Paris https://www.iea.org/reports/bioenergy, License: CC BY 4.0

Impollonia, G., Croci, M., Ferrarini, A., Brook, J., Martani, E., Blandinières, H., Marcone, A., Awty-Carroll, D., Ashman, C., Kam, J., Kiesel, A., Trindade, L. M., Boschetti, M., Clifton-Brown, J., & Amaducci, S. (2022). UAV Remote Sensing for High-Throughput Phenotyping and for Yield Prediction of Miscanthus by Machine Learning Techniques. Remote Sensing, 14(12). https://doi.org/10.3390/rs14122927

IPCC. (2022). Food, Fibre and Other Ecosystem Products. In IPCC Sixth Assessment Report. https://doi.org/10.1017/9781009325844.007.714

Jeswani, H. K., Chilvers, A., & Azapagic, A. (2020). Environmental sustainability of biofuels: A review: Environmental sustainability of biofuels. Proceedings of the Royal Society A: Mathematical, Physical and Engineering Sciences, 476(2243). https://doi.org/10.1098/rspa.2020.0351

Jiang, C., Guan, K., Khanna, M., Chen, L., & Peng, J. (2021). Assessing Marginal Land Availability Based on Land Use Change Information in the Contiguous United States. Environmental Science and Technology, 55(15), 10794–10804. https://doi.org/10.1021/acs.est.1c02236

Jiang, P., & Thelen, K. D. (2004). SITE-SPECIFIC ANALYSIS Effect of Soil and Topographic Properties on Crop Yield in a North-Central Corn – Soybean Cropping System. 252–258.

Juhos, K., Szabo, S., & Ladanyi, M. (2015). Influence of soil properties on crop yield: A multivariate statistical approach. International Agrophysics, 29(4), 433–440. https://doi.org/10.1515/intag-2015-0049

Kang, S., Post, W. M., Nichols, J. A., Wang, D., West, T. O., Bandaru, V., & Izaurralde, R. C. (2013). Marginal Lands: Concept, Assessment and Management. Journal of Agricultural Science, 5(5), 129–139. https://doi.org/10.5539/jas.v5n5p129

Kaspar, T. C., Pulido, D. J., Fenton, T. E., Colvin, T. S., Karlen, D. L., Jaynes, D. B., & Meek, D. W. (2004). Relationship of corn and soybean yield to soil and terrain properties. Agronomy Journal, 96(3), 700–709. https://doi.org/10.2134/agronj2004.0700

Kazemzadeh, N., & Hu, G. (2013). Optimization models for biorefinery supply chain network design under uncertainty. Journal of Renewable and Sustainable Energy, 5(5). https://doi.org/10.1063/1.4822255

Kenney, K. L., Smith, W. A., Gresham, G. L., & Westover, T. L. (2013). Understanding biomass feedstock variability. Biofuels, 4(1), 111–127. https://doi.org/10.4155/bfs.12.83

Kravchenko, A. N., & Bullock, D. G. (2000). Correlation of corn and soybean grain yield with topography and soil properties. Agronomy Journal, 92(1), 75–83. https://doi.org/10.2134/agronj2000.92175x

Lai, L., Kumar, S., Osborne, S., & Owens, V. N. (2018). Switchgrass impact on selected soil parameters, including soil organic carbon, within six years of establishment. Catena, 163(March 2017), 288–296. https://doi.org/10.1016/j.catena.2017.12.030

Lark, T. J., Hendricks, N. P., Smith, A., Pates, N., Spawn-Lee, S. A., Bougie, M., Booth, E. G., Kucharik, C. J., & Gibbs, H. K. (2022). Environmental outcomes of the US Renewable Fuel Standard. Proceedings of the National Academy of Sciences of the United States of America, 119(9). https://doi.org/10.1073/pnas.2101084119

Li-Beisson, Y., & Peltier, G. (2013). Third-generation biofuels: Current and future research on microalgal lipid biotechnology. OCL - Oilseeds and Fats, Crops and Lipids, 20(6). https://doi.org/10.1051/ocl/2013031

Li, C., Aston, J. E., Lacey, J. A., Thompson, V. S., & Thompson, D. N. (2016). Impact of feedstock quality and variation on biochemical and thermochemical conversion. Renewable and Sustainable Energy Reviews, 65(August 2011), 525–536. https://doi.org/10.1016/j.rser.2016.06.063

Li, X., Sun, C., Zhou, B., & He, Y. (2015). Determination of Hemicellulose , Cellulose and Lignin in Moso Bamboo by Near Infrared Spectroscopy. Nature Publishing Group, October, 1–11. https://doi.org/10.1038/srep17210

Maesano, M., Khoury, S., Nakhle, F., Firrincieli, A., Gay, A., Tauro, F., & Harfouche, A. (2020). UAV-based LiDAR for high-throughput determination of plant height and above-ground biomass of the bioenergy grass arundo donax. Remote Sensing, 12(20), 1–20. https://doi.org/10.3390/rs12203464

Maliha, A., & Abu-Hijleh, B. (2022). A review on the current status and post-pandemic prospects of third-generation biofuels. In Energy Systems (Issue 0123456789). Springer Berlin Heidelberg. https://doi.org/10.1007/s12667-022-00514-7

Marques Da Silva, J. R., & Alexandre, C. (2005). Spatial variability of irrigated corn yield in relation to field topography and soil chemical characteristics. Precision Agriculture, 6(5), 453–466. https://doi.org/10.1007/s11119-005-3679-3

Meramo, S., Fantke, P., & Sukumara, S. (2022). Advances and opportunities in integrating economic and environmental performance of renewable products. Biotechnology for Biofuels and Bioproducts, 15(1), 1–18. https://doi.org/10.1186/s13068-022-02239-2

Mitchell, R., Vogel, K. P., & Sarath, G. (2008). Managing and enhancing switchgrass as a bioenergy feedstock. Biofuels, Bioproducts and Biorefining, 2, 530–539.

https://doi.org/10.1002/bbb.106

Mokariya, L. K., & Malam, K. (2020). Precision Agriculture -A New Smart Way of Farming. Agriculture and Environtment, 1(2), 87–92.

Muratori, M., Kunz, T., Hula, A., & Freedberg, M. (2023). U.S. National Blueprint for Transportation Decarbonization: A Joint Strategy to Transform Transportation. https://rosap.ntl.bts.gov/view/dot/66718

Næss, J. S., Hu, X., Gvein, M. H., Iordan, C. M., Cavalett, O., Dorber, M., Giroux, B., & Cherubini, F. (2023). Climate change mitigation potentials of biofuels produced from perennial crops and natural regrowth on abandoned and degraded cropland in Nordic countries. Journal of Environmental Management, 325(October 2022). https://doi.org/10.1016/j.jenvman.2022.116474

O'Neill, E. G., Martinez-Feria, R. A., Basso, B., & Maravelias, C. T. (2022). Integrated spatially explicit landscape and cellulosic biofuel supply chain optimization under biomass yield uncertainty. Computers and Chemical Engineering, 160, 107724. https://doi.org/10.1016/j.compchemeng.2022.107724

Ouattara, M. S., Laurent, A., Berthou, M., Borujerdi, E., Butier, A., Malvoisin, P., Romelot, D., & Loyce, C. (2022). Identifying Factors Explaining Yield Variability of Miscanthus x giganteus and Miscanthus sinensis Across Contrasting Environments: Use of an Agronomic Diagnosis Approach. Bioenergy Research, 15(2), 672–685. https://doi.org/10.1007/s12155-021-10332-x

Pierce, F. J., Robert, P. C., & Mangold, G. (1994). Site Specific Management: The Pros, the Cons, and the Realities. Proceedings of the 1994 Integrated Crop Management Conference. https://doi.org/10.31274/icm-180809-454

Plant, R. E. (2001). Site-specific management: The application of information technology to crop production. Computers and Electronics in Agriculture, 30(1–3), 9–29. https://doi.org/10.1016/S0168-1699(00)00152-6

Qin, Z., Zhuang, Q., & Cai, X. (2015). Bioenergy crop productivity and potential climate change mitigation from marginal lands in the United States: An ecosystem modeling perspective. GCB Bioenergy, 7(6), 1211–1221. https://doi.org/10.1111/gcbb.12212

Ray, D. K., Gerber, J. S., Macdonald, G. K., & West, P. C. (2015). Climate variation explains a third of global crop yield variability. Nature Communications, 6, 1–9. https://doi.org/10.1038/ncomms6989

Rogers, J. N., Stokes, B., Dunn, J., Cai, H., Wu, M., Haq, Z., & Baumes, H. (2017). An assessment of the potential products and economic and environmental impacts resulting from a billion ton bioeconomy. Biofuels, Bioproducts and Biorefining, 11(1), 110–128. https://doi.org/10.1002/bbb.1728

Rosa, L., Sanchez, D. L., & Mazzotti, M. (2021). Assessment of carbon dioxide removal

potential: Via BECCS in a carbon-neutral Europe. Energy and Environmental Science, 14(5), 3086–3097. https://doi.org/10.1039/d1ee00642h

Scarlat, N., Dallemand, J. F., Monforti-Ferrario, F., & Nita, V. (2015). The role of biomass and bioenergy in a future bioeconomy: Policies and facts. Environmental Development, 15(2015), 3–34. https://doi.org/10.1016/j.envdev.2015.03.006

Schmer, M. R., Mitchell, R. B., Vogel, K. P., Schacht, W. H., & Marx, D. B. (2010). Spatial and temporal effects on switchgrass stands and yield in the Great Plains. Bioenergy Research, 3(2), 159–171. https://doi.org/10.1007/s12155-009-9045-y

Schmer, M. R., & Vogel, K. P. (2012). DigitalCommons @ University of Nebraska - Lincoln Temporal and Spatial Variation in Switchgrass Biomass Composition and Theoretical Ethanol Yield.

Searchinger, T., Heimlich, R., Houghton, R. A., Dong, F., Elobeid, A., Fabiosa, J., Tokgoz, S., Hayes, D., & Yu, T. (2008). Emissions from Land-Use Change. 423(February), 1238–1240.

SENSE, T. F. C. (2021). Understanding U.S. Corn Ethanol and Other Corn-Based Biofuels Subsidies (Issue May). https://www.taxpayer.net/energy-natural-resources/understanding-u-s-corn-ethanol-and-other-corn-based-biofuels-subsidies/

Singhvi, M. S., & Gokhale, D. V. (2019). Lignocellulosic biomass: Hurdles and challenges in its valorization. Applied Microbiology and Biotechnology, 103(23–24), 9305–9320. https://doi.org/10.1007/s00253-019-10212-7

Skeer, J., Boshell, F., & Ayuso, M. (2016). Technology Innovation Outlook for Advanced Liquid Biofuels in Transport. ACS Energy Letters, 1(4), 724–725. https://doi.org/10.1021/acsenergylett.6b00290

Slessarev, E. W., Nuccio, E. E., McFarlane, K. J., Ramon, C. E., Saha, M., Firestone, M. K., & Pett-Ridge, J. (2020). Quantifying the effects of switchgrass (Panicum virgatum) on deep organic C stocks using natural abundance 14C in three marginal soils. GCB Bioenergy, 12(10), 834–847. https://doi.org/10.1111/gcbb.12729

Tenenbaum DJ. Food vs. fuel: diversion of crops could cause more hunger. Environ Health Perspect. 2008 Jun;116(6):A254-7. doi: 10.1289/ehp.116-a254. PMID: 18560500; PMCID: PMC2430252.

Tilman, D., Hill, J., & Lehman, C. (2006). Carbon-negative biofuels from low-input high-diversity grassland biomass. Science, 314(5805), 1598–1600. https://doi.org/10.1126/science.1133306

Torres-Mayanga, P. C., Lachos-Perez, D., Mudhoo, A., Kumar, S., Brown, A. B., Tyufekchiev, M., Dragone, G., Mussatto, S. I., Rostagno, M. A., Timko, M., & Forster-Carneiro, T. (2019). Production of biofuel precursors and value-added chemicals from hydrolysates resulting from hydrothermal processing of biomass: A review. Biomass and Bioenergy,

130(September), 105397. https://doi.org/10.1016/j.biombioe.2019.105397

Tudge, S. J., Purvis, A., & De Palma, A. (2021). The impacts of biofuel crops on local biodiversity: a global synthesis. Biodiversity and Conservation, 30(11), 2863–2883. https://doi.org/10.1007/s10531-021-02232-5

Valcu-Lisman, A. M., Kling, C. L., & Gassman, P. W. (2016). The optimality of using marginal land for bioenergy crops: Tradeoffs between food, fuel, and environmental services. Agricultural and Resource Economics Review, 45(2), 217–245. https://doi.org/10.1017/age.2016.20

Von Cossel, M., Winkler, B., Mangold, A., Lask, J., Wagner, M., Lewandowski, I., Elbersen, B., van Eupen, M., Mantel, S., & Kiesel, A. (2020). Bridging the Gap between Biofuels and Biodiversity through Monetizing Environmental Services of Miscanthus Cultivation. Earth's Future, 8(10). https://doi.org/10.1029/2020EF001478

Wang, L., He, Z., Zhao, W., Wang, C., & Ma, D. (2022). Fine Soil Texture Is Conducive to Crop Productivity and Nitrogen Retention in Irrigated Cropland in a Desert-Oasis Ecotone, Northwest China. Agronomy, 12(7). https://doi.org/10.3390/agronomy12071509

Weng, C., Peng, X., & Han, Y. (2021). Depolymerization and conversion of lignin to value-added bioproducts by microbial and enzymatic catalysis. Biotechnology for Biofuels, 14(1), 1–22. https://doi.org/10.1186/s13068-021-01934-w

Wing, I. S., De Cian, E., & Mistry, M. N. (2021). Global vulnerability of crop yields to climate change. Journal of Environmental Economics and Management, 109(March), 102462. https://doi.org/10.1016/j.jeem.2021.102462

Wullschleger, S. D., Davis, E. B., Borsuk, M. E., Gunderson, C. A., & Lynd, L. R. (2010). Biomass production in switchgrass across the United States: Database description and determinants of yield. Agronomy Journal, 102(4), 1158–1168. https://doi.org/10.2134/agronj2010.0087

Zhou, N., Thilakarathna, W. P. D. W., He, Q. S., & Rupasinghe, H. P. V. (2022). A Review: Depolymerization of Lignin to Generate High-Value Bio-Products: Opportunities, Challenges, and Prospects. Frontiers in Energy Research, 9(January), 1–18. https://doi.org/10.3389/fenrg.2021.758744

Zhu, C., Fu, X., Zhang, J., Qin, K., & Wu, C. (2022). Review of portable near infrared spectrometers: Current status and new techniques. Journal of Near Infrared Spectroscopy, 30(2), 51–66. https://doi.org/10.1177/09670335211030617

CHAPTER 2 SPATIO-TEMPORAL VARIABILITY OF SWITCHGRASS AND RESTORED PRAIRIE BIOMASS YIELD IN THE GREAT LAKES REGION USA

Abstract

To date, little research has been done on the spatio-temporal variability of switchgrass (*Panicum virgatum*) and restored prairie biomass yield at the within-field scale. Spatio-temporal variability of biomass yield for mature switchgrass and restored prairie fields were examined at Marshall Farm (42.44° N, -85.32° W) and Lux Arbor Farm (42.48° N, -85.44° W) in southwest Michigan USA from 2018-2021. Average biomass yield for switchgrass at Marshall Farm ranged from a low of 5.9 Mg ha^{-1} in 2020 to a high of 9.1 Mg ha^{-1} in 2021. Biomass yield for switchgrass at Lux Arbor Farm ranged from 4.3 Mg ha^{-1} in 2019 to 5.8 Mg ha^{-1} in 2020. Biomass yield for restored prairie at Marshall Farm ranged from a low of 2.4 Mg ha^{-1} in 2020 to a high of 3.7 Mg ha^{-1} in 2021. Biomass yield for restored prairie at Lux Arbor Farm ranged from 3.0 Mg ha^{-1} in 2021 to 4.9 Mg ha^{-1} in 2020. Under similar field conditions, biomass yield of switchgrass had higher within-field spatial variability than restored prairie. Temporal variability for biomass yield of switchgrass with higher average interannual correlation (Intraclass correlation coefficient (ICC): 0.63) at Lux Arbor was lower than switchgrass at Marshall Farm (ICC: 0.06). Similarly, temporal variability for biomass yield of restored prairie with higher average interannual correlation (ICC: 0.48) at Lux Arbor was lower than restored prairie at Marshall (ICC: 0.17). Soil ammonium was positively correlated with biomass yield of switchgrass at Lux Arbor Farm and Marshall Farm. Profile curvature had a positive effect on biomass yield of switchgrass at Lux Arbor Farm. In contrast, profile curvature had negative effect on biomass yield of switchgrass at Marshall Farm. Soil calcium and relative elevation played a critical role to explain within-field spatial variability in biomass yield of restored prairie at Lux Arbor Farm and

Marshall Farm.

Introduction

In the foreseeable future, biofuel as one form of renewable energy will be an integral part of a greener future with its inherent ability to mitigate carbon emissions. IPCC states that by the end of the century, atmospheric CO_2 concentrations need to be brought down to the preindustrial era levels in order to maintain temperature increase within 1.5 or 2 °C (IPCC, 2022). By rejoining the Paris agreement in 2021, the United States of America set its nationally determined contribution (NDC) of greenhouse gas emissions to 50-52% below 2005 levels in 2030 (United Nations Climate Change, 2021). One study argued that greenhouse gas (GHG) emissions increase the carbon debt of bioenergy cropping systems up to 50% when switching from corn to switchgrass (Searchinger et al., 2008). However, perennial cropping systems like switchgrass and restored prairie have a shorter carbon debt repayment period than annual cropping systems such as corn (Abraha et al., 2019). Furthermore, Fargione et al. (2008) estimated that perennial cropping systems on degraded agricultural land either have no or little carbon debt due to land use change. Converting to perennial cropping system with no-till management brought down the C debt to zero or even negative (Ruan & Robertson, 2020). In addition, Hussain et al. (2019) reported on the potential of established perennial bioenergy cropping systems to ameliorate nitrogen pollution from the agricultural landscape. Adkins et al. (2019) found that choosing a cultivar based on phenological features and associated microbial community could further increase the potential of C sequestration in switchgrass.

Perennial crops coupled with sustainable management practices will help to realize the goal of mitigating atmospheric CO_2 from the agricultural sector. Due to low fertilizer input requirements, perennial grasses for biomass production have great potential to be grown on

marginal lands, which are not ideal for food production. Doing so fundamentally removes the food vs. fuel concern associated with first generation bioenergy feedstocks. A review demonstrates that growing perennial bioenergy crops on marginal lands offers a wealth of benefits, such as soil erosion control, soil carbon sequestration, increased biodiversity and improved water quality (Jacot et al., 2021). A recent study estimated that there are potentially 2230 million hectares of marginal lands available for switchgrass production globally, and among that total, the USA accounts for 297.5 million hectares (Fan et al., 2020).

Often the assumption of having a readily available, reliable supply of biomass feedstock for biofuel purposes is made by researchers and the general public, but this assumption should not be naively made without validation. In agreement, a US government report stated that a reliable supply of biomass feedstock is critical for the success of a biofuel economy and in realizing the economy of scale necessary to maintain low fuel prices (U.S. Department of Agriculture, 2021). Previous studies suggested within-field variability in yields of perennial bioenergy crops like switchgrass (Di Virgilio et al., 2007, Schmer et al., 2010). One unanswered question is identifying the dominant contributors to spatial and temporal variability of perennial bioenergy feedstock yield. To be able to effectively use agronomic inputs and increase average biomass yield, it is imperative to understand the spatial and temporal variation of the specific growing environment. Once dominant causes of variability are determined, field management plans can be tailored to address the identified causes of variability.

The objectives of this study are to 1) Investigate the temporal and spatial variability of switchgrass (*Panicum virgatum*), restored prairie biomass yield at field scale; and 2) Study the effect of soil fertility characteristics and soil topographical features on the temporal and spatial variability of switchgrass and restored prairie biomass yield. The knowledge gained from this

study will facilitate agronomic management planning for perennial bioenergy cropping systems to help ensure a reliable future bioenergy feedstock supply.

Materials and methods

Experimental Site Description

Field-scale experiments were conducted at Marshall Farm (42.44° N, -85.32° W) and Lux Arbor Farm (42.48° N, -85.44° W) from 2018 to 2021 (Figure A2.1 and A2.2), which are part of the Great Lakes Bioenergy Research Center experimental infrastructure located at Michigan State University's W.K. Kellogg Biological Station (KBS) in southwest Michigan. Soils in southwest Michigan are developed on glacial till and outwash from the last retreat of the Wisconsin glaciation (circa 12,500 years BP). Most soils are sandy loam and silty clay loams of moderate fertility and belong to the Alfisol, Mollisol, Histosol and Entisol soil orders in this area (Crum & Collins, 1995). All the fields at Marshall were enrolled in the USDA CRP program in 1987, with smooth brome grass (*Bromus inermis*) planted in the fields. Annual crops had been planted in these fields for decades prior to CRP program enrollment. Prior to conversion, all the fields at Lux Arbor had been cultivated with a tilled corn-soybean rotation since 1987. In early May 2009, fields at Marshall and Lux Arbor were planted with glyphosate resistant soybean as a breakout crop for one growing season and then converted to switchgrass and restored prairie fields.

Restored prairie (5 grass and 14 forb species, see details in Table A2.1) and switchgrass (cultivar Cave-in-rock) were planted following the soybean breakout crop at both farms, which created a total of 4 fields varying in size from 11-14 ha. Switchgrass was planted at a seeding rate of 11.2 kg ha^{-1} with oats (*Avena sativa*) as nurse crop in 2010. Restored prairie was planted at a bulk seeding rate of 7.8 kg ha^{-1} with oats as nurse crop in 2010.

Switchgrass was fertilized with 28-0-0 liquid urea-ammonium nitrate at the rate of 56 kg ha^{-1} nitrogen every spring beginning in 2011. Based on low soil test levels, potash at rate of 140 kg ha^{-1} was applied to restored prairie at Lux Arbor in 2009. No other phosphorus or potassium applications were made to switchgrass or restored prairie fields.

In each field, 30 georeferenced points were randomly selected. In late May 2018 and late May 2020, soil samples were collected at 0-25 cm depth ‘sat all georeferenced points and sent to MSU soil lab for measurements of pH, phosphorus (P: mg kg^{-1}), potassium (K: mg kg^{-1}), calcium (Ca: mg kg^{-1}), magnesium (Mg: mg kg^{-1}), ammonium (NH_4^+: mg kg^{-1}), and total soil carbon (C: wt%) and organic matter (wt%) content, which collectively indicate soil fertility characteristics. Soil fertility characteristics were assumed unchanged from 2018 to 2019 and 2020 to 2021. Elevation at a resolution of 5 meters was collected by Lidar at all fields in 2008, which were used to generate digital elevation maps (DEMs) for each field. Slope, aspect, plane curvature, profile curvature, and Topographical Wetness Index (TWI) were obtained and used as soil topographical features in R Statistical Programming Language (R Core Team, 2022) with the raster (Hijmans, R.J., 2021), rgdal (Bivand, R., et al., 2021), maptools (Bivand, R. & Lewin-Koh, N., 2021) and dynatopmodel packages (Metcalfe, P., et al., 2018). Soil sand, and clay content were obtained from either deep core (0-50 cm) samples analysis in 2009 or USDA Web Soil Survey for all georeferenced sampling points (Web Soil Survey, 2022). The 15 bar lower limit of soil water content (LL15), drained upper limit of soil water content (DUL), saturated hydraulic conductivity of soil (Ksat), whole profile drainage rate coefficient (SWCON), and saturated water content (SAT) were calculated from soil sand content, clay content and total carbon content (Saxton & Rawls, 2006). Details on biomass samples and soil samples parameters are located in Figure A2.3. Descriptive statistics for soil fertility characteristics and topographical

features are located in Table A2.4 to A2.7. In late fall of 2018-2021, switchgrass and restored prairie biomass samples were cut at ground level at 30 fixed georeferenced points by using 1×1 m^2 quadrat and clipper at both farms after the first killing frost. In 2019, 2020 and 2021 harvesting seasons, switchgrass and restored prairie samples were also collected at an additional distinct 12 georeferenced points at both farms giving a total of 42 sampling points per field. All biomass samples were dried at 65 °C to a constant weight and biomass yield was expressed on a dry weight basis.

Statistical Analysis

All statistical analyses were done in the R statistical computational environment (R Core Team, 2022) with packages sf (Pebesma, 2018), sp (Pebesma et al., 2005), gstat (Pebesma, 2004), automap (Hiemstra et al., 2008), ape (Paradis & Schliep, 2019), lme4 (Bates et al., 2015), DHARMa (Hartig, 2021), and spaMM (Rousset & Ferdy, 2014). All figures were made in R statistical computational environment with package ggplot2 (Wickham, 2016). Empirical semi-variograms were fitted to the data and interpolations were made for switchgrass and restored prairie at both farms separately for the years 2018-2021 to visually examine the biomass yield variability. Null linear mixed model with intercept for sampling station as random effect were fitted to four-year biomass yield data. Then, intra-class correlations were obtained for the null models to determine interannual variability of biomass yield. Two-level residuals for sampling stations were extracted to study field spatial variability of biomass yield. From 2-level residuals, Moran's I values (Moran, 1950) were calculated for each cropping system at both Lux Arbor and Marshall. Linear mixed models with farm, crop, and year coupled with their two- and three-way interactions were fitted to obtain the estimated means of biomass yield. The linear mixed model was explicitly incorporated with Matern spatial covariance. In order to control family-wise error

(α=0.05), only predetermined comparisons were conducted when three-way interaction was significant. The comparisons were biomass yield between crops within the same location and year (N=8), biomass yield between locations within the same crop and year (N=24) and biomass yield between years within the same locations and crops (N=8). Empirical orthogonal functions (EOFs) as a dimension reduction technique were used to reveal spatial and temporal patterns for switchgrass and restored prairie biomass yield at both Marshall and Lux Arbor with centered values. Spatially centered values were used to decompose the dataset into corresponding spatial EOFs and paired time series of expansion coefficients (ECs), which together revealed the spatial variability patterns. In addition, temporally centered values were similarly used to reveal corresponding temporal EOFs and paired time series of expansion coefficients (ECs), which together revealed the temporal variability pattern. Ordinary kriging with Matern covariance structure was used to generate interpolated spatial and temporal EOF maps.

Moran's I value formula:

$$I = \frac{N}{W} \frac{\sum_{i=1}^{N} \sum_{j=1}^{N} (x_i - \bar{x})(x_j - \bar{x})}{\sum_{i=1}^{N} (x_i - \bar{x})^2}$$

where N is the number of the sampling points; W is the sum of weights; w_{ij} is weight from a distance decay function; x_i is the residuals; $\bar{x}$ is the mean of the residuals.

Spatially centered values:

$$Y_{spatial\ (s,\ t)} = y_{(s,\ t)} - \bar{y}_{(t)},$$

Where $y_{(s,\ t)}$ is the observed value at location s and in year t. $\bar{y}_{(t)}$ is the mean of observed value over sampling points within farm.

Temporally centered values:

$$Y_{temporal\ (s,\ t)} = y_{(s,\ t)} - \bar{y}_{(s)}$$

Where $y_{(s,\ t)}$ is the observed value at location s and in year t. $\bar{y}_{(s)}$ is the mean of observed value

over years for each sampling point.

A spatio-temporal Gaussian process unconditional model was fitted to examine spatial and temporal variability of switchgrass and restored prairies separately at both farms. In addition, a spatio-temporal Gaussian process model with selected variables in the final model was fitted to investigate the change of spatial variability of switchgrass and restored prairie separately at both farms.

The spatio-temporal Gaussian Process model took the form below:

$y_{(s,\,t)} = Y_{(s,t)} + \epsilon_{(s,\,t)}$

Where $Y_{(s,\,t)}$ is mean process part and $\epsilon_{(s,\,t)}$ is noise or error process part. Index s indicates location with x, y coordinates; t indicates discrete time point.

The error part $\epsilon_{(s,\,t)}$ is assumed to have identical independent and distributed normal distribution with 0 mean and variance σ^2. The mean process part $Y_{(s,\,t)}$ is consist of a systematic part and error part $\eta_{(s,\,t)}$. Error part $\eta_{(s,\,t)}$ in mean process is assumed to have 0 mean and variance-covariance term, which takes account of spatial and temporal dependency. Matern spatial correlation was used to model the spatial dependency. Stationarity was also assumed from examining the trends along longitude and latitude for dry biomass yield. Since the temporal resolution was one measurement per year and only 4 years of data were available, within-field spatial variability is assumed static over the study period. Temporal variability was examined by including year as random intercept for each crop at both farms. Therefore, independence of random variations due to year and Matern spatial covariance was assumed.

Multi-model inference with backward selection was adopted to study the possible associative effects of soil fertility characteristics, soil topographical features and seasonal precipitation on switchgrass and restored prairie biomass yield over the study period (2018-2021). Since variable

selection techniques often suffer from model instability, checking model stability is recommended is an integral part of model fitting (Burnham & Anderson, 2004, Symonds & Moussalli, 2011). To this end, a bootstrapping resampling (replication: 1000) technique was used to examine stability of the final model chosen by lowest AIC. Variables with at least 70% inclusion probability were considered to be the constantly selected variables. Soil P, K, Ca, Mg, NH_4^+, pH, and total carbon (C: wt%) were included in the models as soil fertility characteristics. Elevation, slope, aspect, plane curvature, profile curvature, TWI, LL15, DUL, Ksat, SAT, sand, and clay as soil topographical features were included in the models. Cumulative precipitation (mm) from April to May as early growing season precipitation (early), June to July as middle growing season precipitation (middle), and August to September as late growing season precipitation (late) were included in the models. All of soil features and growing season precipitation were standardized by abstracting means and dividing by standard deviations before model fitting.

Results

Air Temperature and Precipitation

As shown in Table 2.1, 30-year monthly average maximum air temperatures in the area range from 0.7 °C in January to 29.7 °C in July. Thirty-year monthly average minimum air temperature values range from -7.6 °C in January to 16.1 °C in July. Climatological data (2018-2021) at the MSU Kellogg Weather Station represents monthly temperature and monthly cumulative precipitation at Marshall. Growing seasons 2019 and 2020 both had higher monthly average maximum air temperature and higher monthly average minimum air temperature in July than the 30-year monthly averages. Thirty-year monthly average total precipitation ranges from 63.8 mm in March to 106.4 mm in May. Compared to 30-year monthly average cumulative precipitation,

the 2018 growing season was the driest among the four growing seasons under study. In comparison with growing season 2019, growing season 2020 had relatively lower cumulative precipitation earlier in the season from April to July and relatively higher total precipitation later in the season from August to September. The 2021 growing season had substantial lower cumulative precipitation earlier in the season from April to May and significantly higher later in the season from June to September compared to other growing seasons and the 30 year average (Figure A2.4).

Figure 2.1 shows that both maximum and minimum air temperature had a general trend of gradual increase from April until July and August during the four growing seasons under study. Precipitation during the study period mainly clustered in two time periods, May to July and September to October, respectively. The 2018 growing season had relatively lower precipitation than the 2019 and 2020 growing seasons (April to September). The 2021 growing season had the highest precipitation from June to September over the four study years.

At Lux Arbor, early growing season cumulative precipitation (April and May) and late growing season cumulative precipitation (August and September) were generally lower in 2021 than 2018 to 2020, respectively (Table 2.2). The years 2018 and 2020 had similar cumulative precipitation over the growing season (April to September)

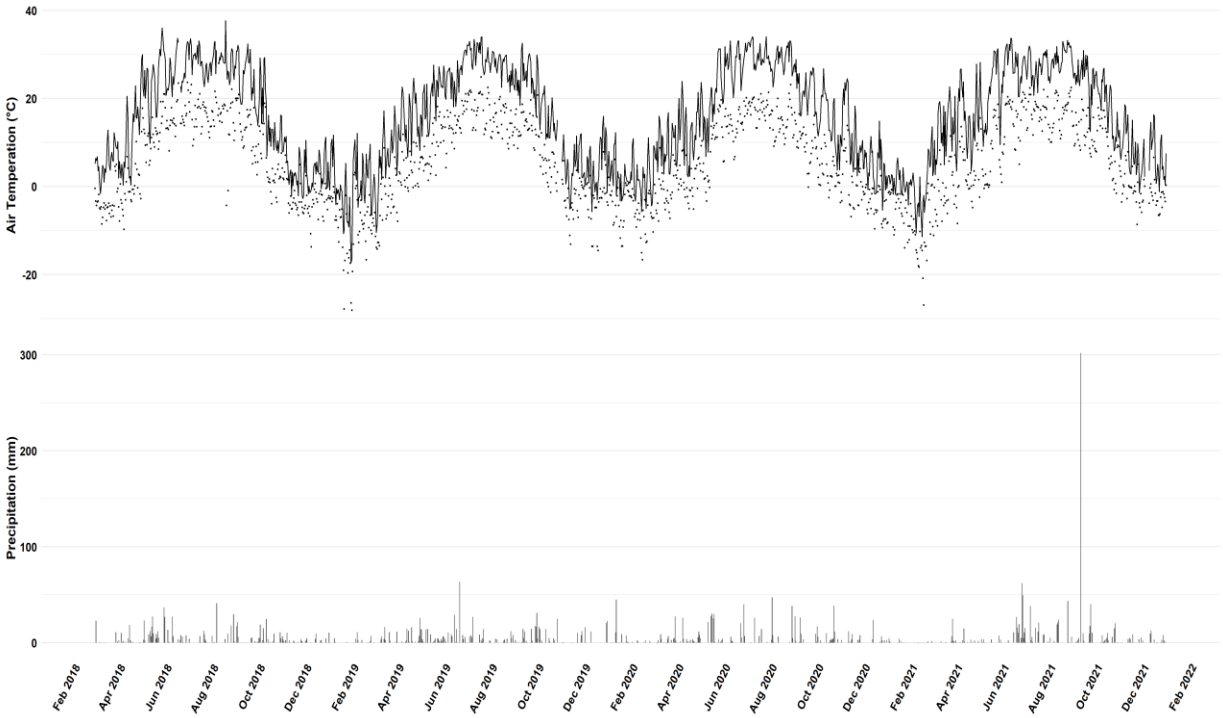

Figure 2.1. Daily air temperature (°C) and precipitation (mm) at Michigan State University's Kellogg Weather Station (42.41°N, -85.37°W). Vertical bars represent precipitation. Dots represent minimum air temperature and continuous lines represent maximum air temperature. Data were obtained from Michigan State University Enviro-weather Automated Weather Station Network. Available online: https://mawn.geo.msu.edu/station.asp?id=kbs [1/19/2023].

Table 2.1. Monthly climatological data for 2018-2021 growing seasons at Michigan State University Kellogg Weather Station (42.41° N, -85.37°W) and 30-year average at Battle Creek Weather Station (42.37°N, -85.26°W).

Month	3	4[a]	5[a]	6[b]	7[b]	8[c]	9[c]	10	11	12	1	2
	2018-2019[d]											
Tmax[1]	5.9	10.1	24.6	26.1	28.4	28.5	24.5	15.1	3.8	3.3	-1.9	1.8
Tmin[1]	-3.6	-0.8	12.5	15.6	16.4	15.4	13.0	5.3	-1.8	-3.5	-10.1	-7.4
PRCP[1]	36.3	44.4	208.3	77.7	37.6	111.3	58.2	103.1	39.6	32.2	16.8	30.2
	2019-2020[d]											
Tmax	5.9	15.0	20.3	25.2	30.1	27.2	24.8	16.4	4.8	4.8	2.5	1.4
Tmin	-4.2	3.5	9.0	14.4	18.3	14.5	14.0	5.8	-2.7	-3.3	-3.9	-6.7
PRCP	58.7	86.4	110.0	157.0	80.5	44.2	119.4	91.2	32.0	71.4	76.2	10.2
	2020-2021[d]											
Tmax	8.9	12.4	19.6	28.0	30.1	28.8	22.2	14.6	12.2	4.1	1.1	-0.7
Tmin	-1.0	1.6	8.9	14.1	17.7	14.8	10.1	3.2	1.6	-3.7	-5.4	-11.3
PRCP	70.1	73.1	152.4	82.5	48.8	109.2	80.5	107.7	42.4	42.4	13.2	5.3
	2021-2022[d]											
Tmax	12.3	15.4	21.1	28.1	27.1	29.3	24.7	18.1	7.9	6.6	-2.0	1.0
Tmin	-0.9	3.2	7.3	15.8	17.0	16.9	12.2	9.5	-0.1	-2.0	-11.5	-8.8
PRCP	40.1	28.2	21.6	233.4	114.1	121.7	400.2	74.7	31.5	42.7	2.5	46.5
	30 Year Average[e]											
Tmax	9.3	16.4	22.7	27.8	29.7	28.1	24.5	17.8	9.8	2.7	0.7	2.7
Tmin	-2.4	3.2	9.0	14.2	16.1	15.5	11.2	5.8	0.7	-5.1	-7.6	-7.0
PRCP	63.8	91.7	106.4	104.2	103.1	105.9	92.4	89.1	79.0	62.2	62.6	47.9

1. Abbreviation: Tmax: Max Air Temperature (°C), Tmin: Minimum Air Temperature (°C) and PRCP: Total Precipitation (mm).

a. April and May are defined as early growing season.

b. June and July are defined as middle growing season.

c. August and September are defined as late growing season.

d. 2018-2021 climatological data were obtained from Michigan State University Enviro-weather Automated Weather Station Network.
Available online: https://mawn.geo.msu.edu/station.asp?id=kbs [4/27/2022]

e. 30-year average climatological data were obtained from National Centers for Environmental Information (Station ID: USC00200552) at National Oceanic and Atmospheric Administration (NOAA).
Available online: https://www.ncdc.noaa.gov/cdo-web/datatools [1/19/2023].

Table 2.2. Monthly precipitation for 2018-2021 growing seasons at Lux Arbor Marginal Land Experiment Weather Station (42.48°N, -85.45°W).

Month	3	4[a]	5[a]	6[b]	7[b]	8[c]	9[c]	10	11	12	1	2
						2018-2019[d]						
PRCP[1]	43.4	64.3	199.4	112.5	46.7	101.9	130.8	98.3	52.6	53.8	24.1	80.0
						2019-2020[d]						
PRCP	61.0	133.9	140.7	178.8	52.6	61.2	127.5	136.9	43.9	81.8	96.8	26.2
						2020-2021[d]						
PRCP	77.2	79.0	152.9	88.4	78.0	139.2	93.2	99.6	45.2	60.7	25.7	8.6
						2021-2022[d]						
PRCP	39.9	31.5	27.4	199.1	64.5	87.1	74.2	132.6	44.7	60.2	2.5	60.2

1. Abbreviation: PRCP: Total Precipitation (mm).
a. April and May are defined as early growing season.
b. June and July are defined as middle growing season.
c. August and September are defined as late growing season.
d. 2018-2022 climatological data were obtained from Great Lake Bioenergy Research Center online database: https://data.sustainability.glbrc.org/datatables/507 [1/19/2023].

Descriptive statistics

Both switchgrass and restored prairie show within-field spatial variability of dry biomass yield over the study period (2018-2021) with a relatively higher coefficient of variation (CV: 0.40 to 0.49, 0.39 to 0.51 for switchgrass and restored prairie respectively) at Lux Arbor and relatively low CV (0.24 to 0.39 and 0.27 to 0.47 for switchgrass and restored prairie respectively) at Marshall (Table 2.3). In 2020, switchgrass (mean 5.9 Mg ha^{-1}; standard deviation (SD): 2.0 Mg ha^{-1}) and restored prairie (2.4 ± 1.1 Mg ha^{-1}) recorded the lowest biomass yield at Marshall over the study period (Table 2.3). Conversely, Lux Arbor recorded its highest biomass yield (switchgrass: 5.8 ± 2.6 Mg ha^{-1}; restored prairie: 4.9 ± 1.9 Mg ha^{-1}) over the study period (2018-2021) in 2020. Switchgrass dry biomass yields were higher at Marshall than Lux Arbor across all four years. However, restored prairie dry biomass yields were lower at Marshall than Lux Arbor from 2018 to 2020. In the relatively high precipitation year of 2021, restored prairie yield was higher at Marshall than Lux Arbor. This implies differences in the underlying mechanisms driving switchgrass and restored prairie biomass yields.

Table 2.3. Descriptive statistics of dry biomass yield (Mg ha^{-1}) for switchgrass and restored prairie during the study period (2018-2021) at Marshall Farm and Lux Arbor Farm.

Dry Biomass Yield (Mg ha^{-1})							
		Marshall			Lux Arbor		
Crop	Year	Mean	SD[1]	CV[1]	Mean	SD[1]	CV[1]
Switchgrass	2018	6.1	2.3	0.39	4.8	1.9	0.40
	2019	6.1	1.5	0.24	4.3	2.1	0.49
	2020	5.9	2.0	0.34	5.8	2.6	0.44
	2021	9.1	2.7	0.29	4.8	2.1	0.44
	Average	6.9	2.5	0.37	4.9	2.3	0.46
Restored prairie	2018	3.5	0.9	0.27	4.2	2.0	0.47
	2019	3.7	1.4	0.38	3.8	1.6	0.41
	2020	2.4	1.1	0.47	4.9	1.9	0.39
	2021	3.7	1.4	0.39	3.0	1.5	0.51
	yearly	3.3	1.4	0.41	3.9	1.9	0.47

1. Abbreviation: SD: standard deviation, CV: coefficient of variance.

As shown in Table 2.4, neither switchgrass nor restored prairie at Lux Arbor showed statistically significant spatial autocorrelation based on Moran's I values. Switchgrass showed statistically significant spatial autocorrelation in 2020 and 2021 at Marshall. Restored prairie showed statistically significant autocorrelation in 2018 and 2020 at Marshall.

Further examination of spatial autocorrelation by empirical variograms (Figures A2.5, A2.7, A2.9 and A2.11 in appendix) corroborate the Moran's I value results. Best fitted empirical variograms show that only switchgrass and restored prairie at Marshall had relatively high pill: nugget ratios, indicating spatial dependency. In addition, most of the predicted maps (Figures A2.6, A2.8, A2.10 and A2.12 in appendix) from ordinary kriging show a lack of spatial dependency. The directional variograms (Figures A2.13 to A2.16 in appendix) show that spatial autocorrelations were similar at different directions, which confirmed the stationarity of the spatial autocorrelations.

Table 2.4. Moran's I values of observed dry biomass yield (Mg ha^{-1}) for switchgrass and restored prairie fields at Marshall Farm and Lux Arbor Farm during the study period (2018-2021).

		Marshall			
Crop	Year	Observed Value	Expected Value	Standard Deviation	P-value
Switchgrass	2018	-0.031	-0.035	0.026	0.892
	2019	-0.025	-0.024	0.022	0.989
	2020	0.041	-0.024	0.022	**0.003**[a]
	2021	0.072	-0.024	0.023	**<0.001**
Restored prairie	2018	0.065	-0.035	0.028	**<0.001**
	2019	-0.045	-0.024	0.023	0.364
	2020	0.098	-0.024	0.023	**<0.001**
	2021	0.018	-0.024	0.023	0.063
		Lux Arbor			
		Observed Value	Expected Value	Standard Deviation	P-value
Switchgrass	2018	-0.028	-0.035	0.028	0.819
	2019	-0.048	-0.024	0.022	0.287
	2020	-0.039	-0.024	0.022	0.494
	2021	-0.028	-0.024	0.022	0.879
Restored prairie	2018	-0.006	-0.035	0.031	0.363
	2019	-0.052	-0.024	0.024	0.250
	2020	-0.040	-0.024	0.023	0.513
	2021	-0.050	-0.024	0.023	0.273

a. *p*-value < 0.05 is in bold.

According to the observed biomass yield (Figure 2.3), switchgrass at Marshall in 2020 and 2021 presented an obvious cluster of relatively high biomass yield at the southeastern corner and relatively low yield at the northwestern corner. As shown in Figures 2.2 and 2.3, restored prairie had relatively stable biomass yield at both Marshall and Lux Arbor over the study period (2018-2021).

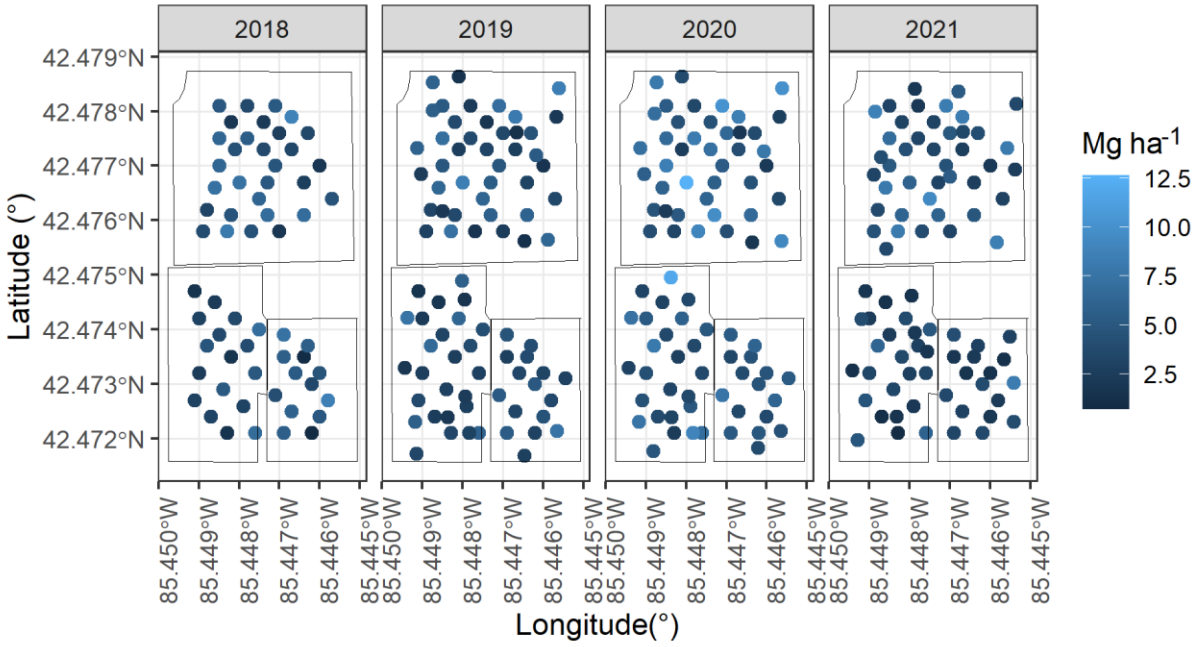

Figure 2.2. Dry biomass yield (Mg ha^{-1}) for switchgrass (upper panel) and restored prairie (lower panel) at sampling points during the study period (2018-2021) at Lux Arbor Farm.

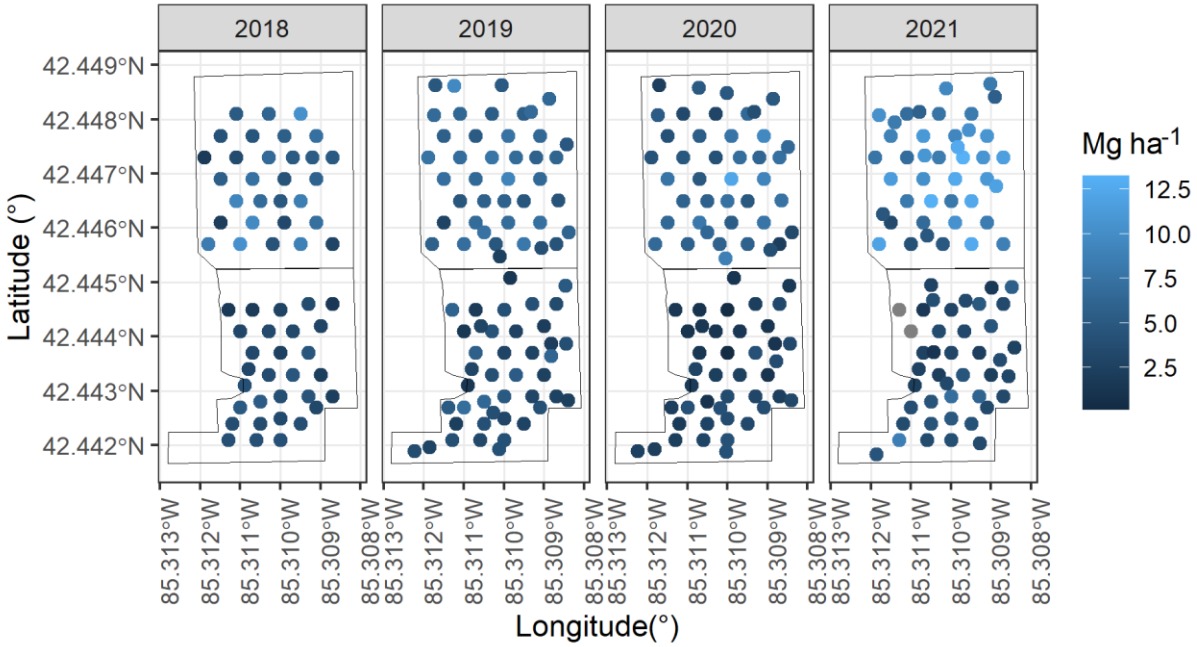

Figure 2.3. Dry biomass yield (Mg ha^{-1}) for switchgrass (upper panel) and restored prairie (lower panel) at sampling points during the study period (2018-2021) at Marshall Farm.

Temporal Variability of Dry Biomass Yield

Via examination of intraclass correlation (ICC) for null models for switchgrass and restored prairie at Marshall and Lux Arbor, prominently higher intraclass correlations existed for switchgrass and restored prairie at Lux Arbor compared to switchgrass and restored prairie respectively at Marshall (Table 2.5). Higher ICC reflects lower annually temporal variability (Liljequist, D., et al. 2019). Temporal variability of environmental conditions during the study period such as precipitation did not significantly lead to temporal yield variability of switchgrass and restored prairie biomass yield at Lux Arbor. Lower temporal variability at Lux Arbor could be caused by persistent nutrient limitation. Since this study is limited to four growing seasons, more growing seasons are needed to confirm the observed lower temporal variability of dry biomass yield for switchgrass and restored prairie at Lux Arbor.

Table 2.5. Intraclass correlation (ICC) of dry biomass yield from null models for switchgrass and restored prairie at Marshal Farm and Lux Arbor Farm.

Croping System	Marshall	Lux Abor
switchgrass	0.06	0.63
restored prairie	0.17	0.48

Within-field Spatial Autocorrelation of Dry Biomass Yield

Spatial correlation of residuals from null models of switchgrass and restored prairie at Marshall and Lux Arbor provides a methodology to evaluate spatial autocorrelation. As shown in Table 2.6, after stripping off the temporal component, only restored prairie at Marshall presented statistically significant spatial autocorrelation (p-value: 0.016), which implies that potential underlying spatially correlated factors drive the spatially correlated dry biomass yield of restored prairie at Marshall.

Table 2.6. Moran's I test statistics of level-2 residuals of dry biomass yield from null models for switchgrass and restored prairie at Marshall Farm and Lux Arbor Farm.

	Marshall		Lux Arbor	
	Switchgrass	Restored prairie	Switchgrass	Restored prairie
Observed Moran I value	0.013	0.064	0.029	0.004
Expected Moran I value	-0.017	-0.017	-0.018	-0.018
Standard Deviation	0.035	0.034	0.030	0.027
P-value	0.406	0.016	0.125	0.429

Linear mixed model with spatial covariance structure

The three-way interaction between location, crop and year had a statistically significant effect (p=0.02) on biomass yield. As shown in Figure 2.4, restored prairie biomass yield was significantly lower than switchgrass at Marshall over the study period (2018-2021). Restored prairie biomass yield was only significantly lower than switchgrass in 2021 at Lux Arbor. Switchgrass biomass yield was significantly higher at Marshall than Lux Arbor in 2019 and 2021 respectively. At Marshall, switchgrass biomass yield in 2021 (9.1 Mg ha^{-1}; 95% Confidence Interval (95% CI): 8.4 to 9.7 Mg ha^{-1}) was significantly higher than in 2018 (5.9 Mg ha^{-1}; 95% CI: 5.1 to 6.6 Mg ha^{-1}), 2019 (6.1 Mg ha^{-1}; 95% CI: 5.4 to 6.7 Mg ha^{-1}) and 2020 (5.9 Mg ha^{-1}; 95% CI: 5.3 to 6.6 Mg ha^{-1}). Restored prairie biomass yield at Marshall was significantly higher in 2021 (3.7 Mg ha^{-1}; 95% CI: 2.8 to 4.5 Mg ha^{-1}) than in 2020 (2.3 Mg ha^{-1}; 95% CI: 1.5 to 3.2 Mg ha^{-1}). At Lux Arbor, switchgrass biomass yield in 2020 (5.9 Mg ha^{-1}; 95% CI: 5.2 to 6.5 Mg ha^{-1}) was significantly higher than 2019 (4.4 Mg ha^{-1}; 95% CI: 3.7 to 5.1 Mg ha^{-1}). There was no significant difference of restored prairie biomass yield at Lux Arbor over the study period (2018-2021). The numerical ranking of restored prairie biomass yield at Lux Arbor was 2020 (4.9 Mg ha^{-1}; 95% CI: 4.3 to 5.4 Mg ha^{-1}) > 2018 (4.3 Mg ha^{-1}; 95% CI: 3.6 to 4.9 Mg ha^{-1}) > 2019 (3.8 Mg ha^{-1}; 95% CI: 3.3 to 4.4 Mg ha^{-1}) > 2021 (3.1 Mg ha^{-1}; 95% CI: 2.6 to 3.7 Mg ha^{-1}).

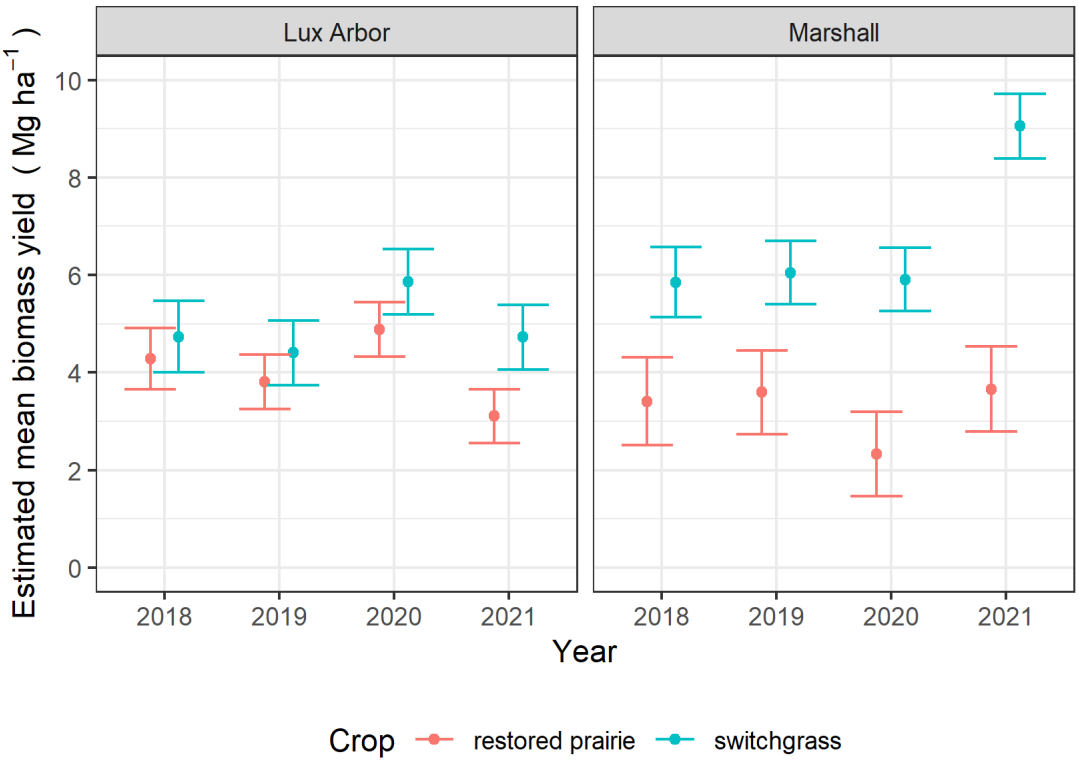

Figure 2.4. Estimated mean biomass yield (Mg ha^{-1}) of switchgrass and restored prairie at Lux Arbor Farm and Marshall Farm from linear mixed models with spatial covariance structure. Dots present estimated mean biomass yield. Vertical bars represent 95% confidence intervals of estimated mean biomass yield.

Empirical orthogonal functions (EOFs)

The first two spatial EOFs accounted for most of the variation of dry biomass yield for switchgrass and restored prairie at both farms (Table 2.7). The first spatial EOF explained 63.2% and 49.4% of variation in switchgrass and restored prairie biomass yield, respectively, at Lux Arbor. The first temporal EOFs explained 45.1% and 45.4% of variation in switchgrass and restored prairies biomass yield, respectively, at Marshall. Because the spatial EOFs depict the normalized contribution to within-field spatial variability, a 0 value of spatial EOF indicates no departure from annual mean biomass yield within the field. Figures A2.17 and A2.19 show that both switchgrass and restored prairie presented within-field spatial variability of biomass yield at both farms. There are isolated pockets of high and low biomass yield in both switchgrass and restored prairie at Lux Arbor, which indicate higher within-field spatial variability of biomass yield at Lux Arbor (Figure A2.17 in appendix). The expansion efficient (EC) values, which represent the amplitude of EOF in each year, had highest values for both switchgrass and restored prairie at Lux Arbor in 2020. Figure A2.19 shows that switchgrass biomass yield was relatively high in the central area of the Marshall and relatively low at the edge of the field. Conversely, restored prairie exhibited more positive departure from the annual mean biomass yield at the southern side than northern side of the field at Marshall. Both switchgrass and restored prairie had highest EC values in 2021. On a practical basis, this implies that EOF analysis could be used to target customized management to address field areas varying substantially in yield potential.

The first two temporal EOFs accounted for most of the variation of dry biomass yield for switchgrass and restored prairie at both farms (Table 2.8). The first temporal EOFs explained 61.4% and 55.4% of variation in switchgrass and restored prairie, respectively, at Lux Arbor.

The first temporal EOFs explained 73.7% and 56.4% of variation in switchgrass and restored prairie, respectively, at Marshall. Because the temporal EOFs depict the normalized contribution to interannual regionalized variability, a 0 value of EOFs indicates no departure from average biomass yield over years. Switchgrass at Lux Arbor showed a latitudinal trend of interannual variability (Figure A2.18 in appendix). From the south to north side of the switchgrass at Lux Arbor, year to year biomass variation gradually increased. The only interannual restored prairie biomass yield variability observed at Lux Arbor occurred at the north end of the field (Figure A2.18 in appendix). In Figure A2.20, switchgrass at Marshall shows more interannual regionalized variability in the center of the field. Similarly, the contribution of the first temporal EOFs to temporal variation showed that restored prairie did not exhibit apparent spatial structure of interannual variability at Marshall (Figure A2.20 in appendix). The restored prairie exhibited biomass yield resilience to annual changes of field environmental conditions.

Table 2.7. Spatial empirical orthogonal functions (EOFs) explained variance of dry biomass yield for switchgrass and restored prairie at Marshall Farm and Lux Arbor Farm over the study period (2018-2021).

		Swithcgrass		Restored prairie	
		Proportion of Variance	Cumulative Proportion	Proportion of Variance	Cumulative Proportion
Mashall	EOF1	0.451	0.451	0.454	0.454
	EOF2	0.244	0.695	0.272	0.726
	EOF3	0.200	0.894	0.198	0.923
	EOF4	0.105	1	0.077	1
Lux Arbor	EOF1	0.632	0.632	0.494	0.494
	EOF2	0.219	0.852	0.209	0.703
	EOF3	0.096	0.947	0.172	0.875
	EOF4	0.053	1	0.125	1

Table 2.8. Temporal empirical orthogonal functions (EOFs) explained variance of dry biomass yield for switchgrass and restored prairie at Marshall Farm and Lux Arbor Farm over the study period (2018-2021).

		Switchgrass		Restored prairie	
		Proportion of Variance	Cumulative Proportion	Proportion of Variance	Cumulative Proportion
Marshall	EOF1	0.737	0.737	0.564	0.564
	EOF2	0.163	0.9	0.314	0.878
	EOF3	0.1	1	0.1223	1
Lux Arbor	EOF1	0.614	0.614	0.554	0.554
	EOF2	0.258	0.872	0.278	0.832
	EOF3	0.128	1	0.168	1

Gaussian process unconditional models

Based on empirical semivariograms and Moran's I values, different spatial dependencies were observed for switchgrass and restored prairie at Marshall and Lux Arbor. Therefore, models were fitted separately by cropping systems and farms. As shown in Table 2.9, spatial correlations, represented by the decay parameter (ρ =0.006) from Matern spatial correlation, confirmed that only restored prairie at Marshall had relatively high spatial dependency. Both switchgrass and restored prairie at Lux Arbor had relatively low spatial dependency (ρ =0.296 and 0.253). Spatial correlations reduce rapidly and reach 0 approximately at a distance of 60 meters for switchgrass and restored praire at Lux Arbor (Figure A2.21 in appendix). Spatial correlation reduced to 0 around 100 meters for switchgrass at Marshall. Spatial correlations did not reach 0 within the maximum sampling distance for restored prairie at Marshall. Except for switchgrass at Marshall, switchgrass and restored prairie showed similar interannual variability (variance: 0.302 to 0.399). Spatial variability (variance: 3.561 and 1.896 for switchgrass and restored prairie) accounted for a substantial amount of total biomass yield variability at Lux Arbor, respectively. Within the same farm, switchgrass showed more spatial variability than restored prairie.

Table 2.9. Gaussian process model results of unconditional models for dry biomass yield (Mg ha^{-1}) of switchgrass and restored prairie at Marshall Farm and Lux Arbor Farm.

		Spatial Correlation		Random Part (Variance)		
Location	Crop	ν^1	ρ^2	Year	spatial	residual
Marshall	Switchgrass[3]	16.67	0.185	1.784	0.967	3.644
	Restored prairies	0.20	0.006	0.313	0.334	1.148
Lux Arbor	Switchgrass	16.67	0.296	0.302	3.561	1.559
	Restored prairies	16.67	0.253	0.399	1.896	1.469

1. ν: smoothness parameter.
2. ρ: decay parameter.

Multimodel inference for variable selection

Figure 2.5 shows that soil fertility characteristics Mg, K, NH_4^+, pH as well as soil topographic features profile curvature and TWI were selected based on Akaike information criterion (AIC) and included over 70% among 1000 bootstrap resampling models for switchgrass dry biomass yield at Lux Arbor. Soil topographical features TWI and profile curvature were main drivers for switchgrass biomass yield at Lux Arbor. The estimated coefficient of TWI was consistently estimated positive (1.30 Mg ha^{-1}/SD; 95% Bootstrap CI: 0.66 to 2.02 Mg ha^{-1}/SD). According to Pearson's second moment correlation, TWI was positively correlated with switchgrass biomass yield at Lux Arbor over the study period (2018: R = 0.47; 2019: 0.57; 2020:0.49; 2021: 0.70). Even though profile curvature has an estimated coefficient of 3.03 Mg ha^{-1}/SD, the 95% bootstrap CI lower bound rested on 0. Potassium and pH had a moderate positive estimated coefficient of 0.50 Mg ha^{-1}/SD (95% Bootstrap CI: 0 to 1.05 Mg ha^{-1}/SD) and 0.55 Mg ha^{-1}/SD (95% Bootstrap CI: 0 to 0.98 Mg ha^{-1}/SD), respectively. Magnesium was found to be negatively associated with switchgrass biomass yield (EM: -1.12 Mg ha^{-1}/SD; 95% Bootstrap CI: -1.89 to 0 Mg ha^{-1}/SD). Ammonium with 0.713 inclusion probability showed a positive estimated coefficient of 0.41 Mg ha^{-1}/SD (95% Bootstrap CI: 0 to 0.97 Mg ha^{-1}/SD). Late growing season precipitation had 0.957 inclusion probability, which was higher than early season precipitation and middle season precipitation, respectively. Late growing season precipitation had a positive

estimated coefficient of 5.13 Mg ha^{-1}/SD (95% Bootstrap CI: 0 to 10.66 Mg ha^{-1}/SD). In contrast, early growing season precipitation had a negative estimated coefficient of -0.61 Mg ha^{-1}/SD (95% Bootstrap CI: -1.37 to 0 Mg ha^{-1} / SD). Details on model results are located in Table 2.8 in the appendix.

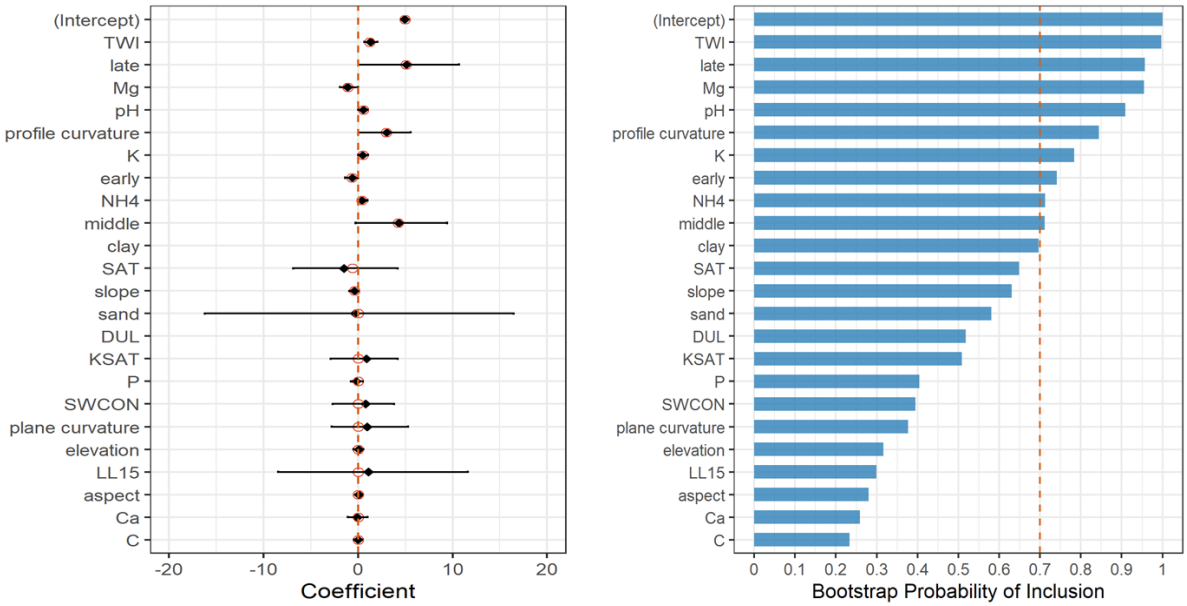

Figure 2.5. Model results from 1000 bootstrap resampling for switchgrass biomass yield (Mg ha^{-1}) at Lux Arbor Farm. Left panel: estimated coefficients: black diamond is the estimation from full model. Black horizontal is 95% bootstrap confidence interval, open red circle is bootstrap median. Coefficient is not included when standard error is greater than 10. Right panel: bootstrap probability of inclusion. Red dashed vertical bar indicates probability of 0.7.

In Figure 2.6, soil fertility characteristics Mg, Ca, P as well as soil topographic features aspect, Ksat, DUL, elevation, sand content and SAT were selected based on AIC and included over 70% among 1000 bootstrap resampling models for restored prairie dry biomass yield at Lux Arbor. Similar to switchgrass at Lux Arbor, Mg was negatively associated with restored prairie yield at Lux Arbor (-1.87 Mg ha^{-1}/SD; 95% Bootstrap CI: -2.81 to -0.70 Mg ha^{-1}/SD). The relation of yield to aspect was estimated reliably with a positive estimated coefficient of 0.61 Mg ha^{-1}/SD (95% Bootstrap CI: 0.25 to 0.89 Mg ha^{-1}/SD). Elevation showed a negative relation of -0.52 Mg

ha^{-1}/SD (95% Bootstrap CI: -1.16 to 0 Mg ha^{-1}/SD). The positive relations of yield with Ca and P were 1.11 (95% Bootstrap CI: 0 to 2.04 Mg ha^{-1}/SD) and 0.37 Mg ha^{-1}/SD (95% Bootstrap CI: 0 to 0.82 Mg ha^{-1}/SD), respectively. The relations of yield with Ksat, DUL and sand had substantial standard errors, therefore cannot be reliably estimated from this study. Late growing season cumulative precipitation (August to September) was the only precipitation parameter selected over 70% of the time among the 1000 bootstrap resampling models. The positive estimated coefficient of late growing season cumulative precipitation (August to September) was 2.70 Mg ha^{-1}/SD (95% Bootstrap CI: 0 to 7.25 Mg ha^{-1}/SD). Details on model results are located in Table 2.9 in the appendix.

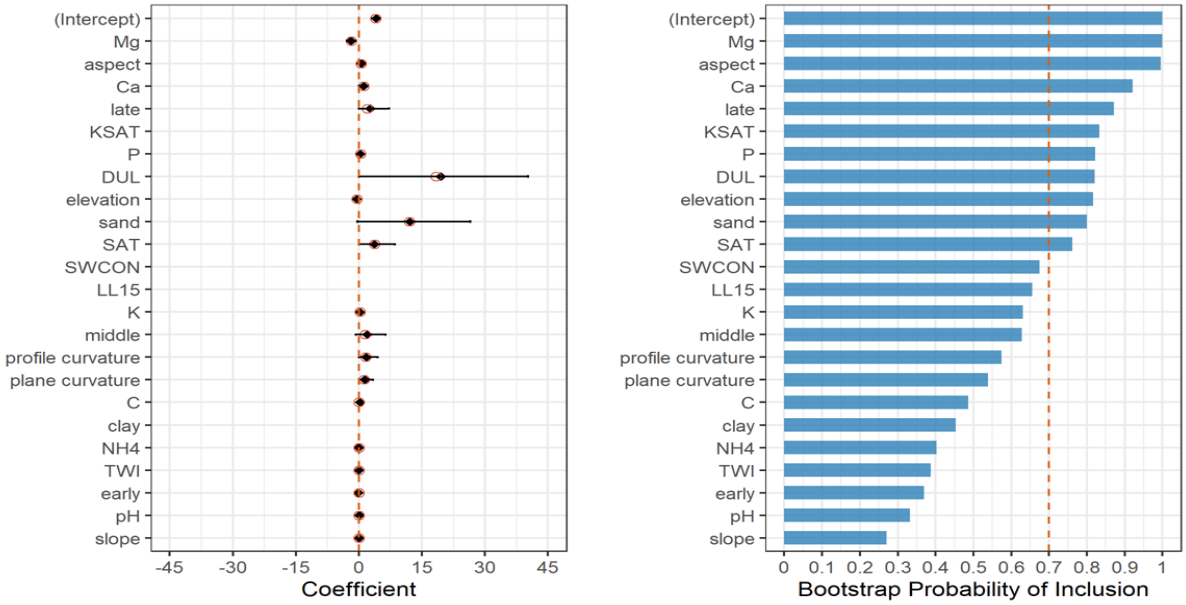

Figure 2.6. Model results from 1000 bootstrap resampling for restored prairie biomass yield (Mg ha^{-1}) at Lux Arbor Farm. Left panel: estimated coefficients: black diamond is estimation from full model. Black horizontal is 95% bootstrap confidence interval, open red circle is bootstrap median. Coefficient is not included when standard error is greater than 10. Right panel: bootstrap probability of inclusion. Red dash vertical bar indicates probability of 0.7.

At Marshall only total C as soil fertility and profile curvature as topographical characteristics met the 70% inclusion criteria for switchgrass biomass yield (Figure 2.7). Profile curvature with 0.709 inclusion probability had a negative estimated coefficient of -2.61 Mg ha^{-1}/SD (95%

Bootstrap CI: -6.60 to 0 Mg ha^{-1}/SD). Total C with 0.701 inclusion probability had a negative effect of -0.44 Mg ha^{-1}/SD (95% Bootstrap CI: -1.04 to 0 Mg ha^{-1}/SD). Late growing season cumulative precipitation (August to September) had 0.816 inclusion probability and had a positive effect of 2.30 Mg ha^{-1}/SD (95% Bootstrap CI: 0 to 5.54 Mg ha^{-1}/SD). Details on model results are located in Table 2.10 in the appendix.

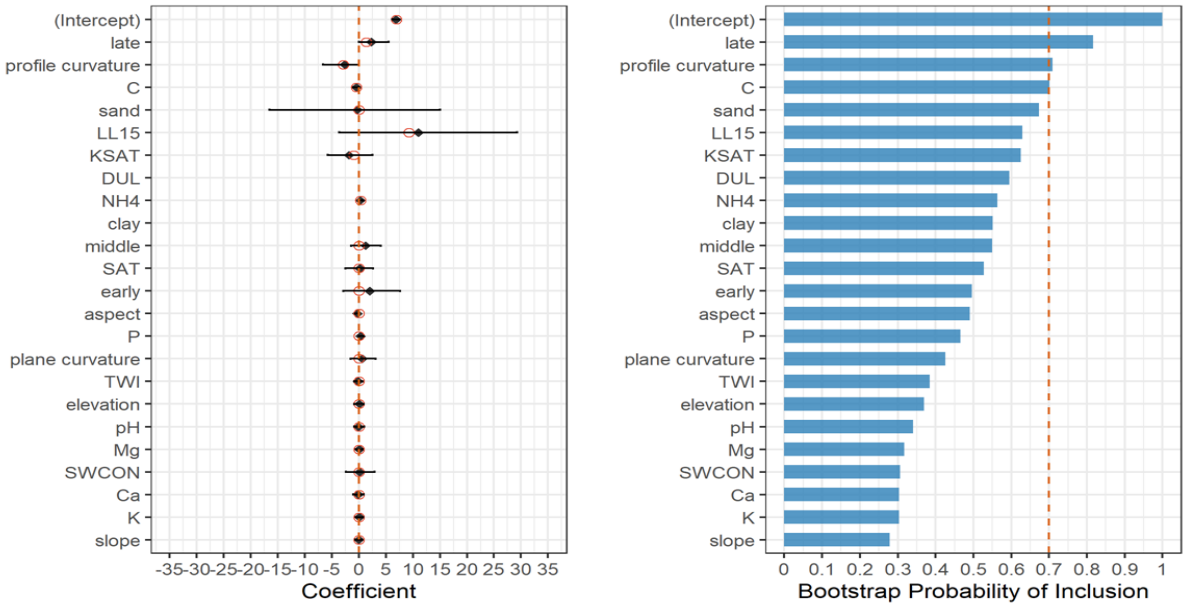

Figure 2.7. Model results from 1000 bootstrap resampling for switchgrass biomass yield (Mg ha^{-1}) at Marshall Farm. Left panel: estimated coefficients: black diamond is estimation from full model. Black horizontal is 95% bootstrap confidence interval, open red circle is bootstrap median. Coefficient is not included when standard error is greater than 10. Right panel: bootstrap probability of inclusion. Red dash vertical bar indicates probability of 0.7.

Figure 2.8 shows that total C, Ca, NH_4^+, pH as soil fertility characteristics and slope, elevation as soil topographic features were selected based on AIC and included over 70% among 1000 bootstrap resampling models for restored prairies dry biomass yield at Marshall. Calcium showed a positive effect of 0.42 Mg ha^{-1}/SD (95% Bootstrap CI: 0 to 0.91 Mg ha^{-1}/SD). Total C (-0.82 Mg ha^{-1}/SD, 95% Bootstrap CI: -1.21 to -0.41 Mg ha^{-1}/SD) and NH_4^+ (-0.25 Mg ha^{-1}/SD, 95% Bootstrap CI: -0.51 to 0 Mg ha^{-1}/SD) were negatively associated with restored prairie yield at Marshall. Slope, elevation and pH had a negative estimated coefficient on restored prairie

yield. Early growing season cumulative precipitation (April and May), middle growing season cumulative precipitation (June and July) and late growing season cumulative precipitation (August and September) were all selected in over 70% of the 1000 bootstrap resampling models and had positive relationships with restored prairie yield. Details on model results are located in Table 2.11 in the appendix.

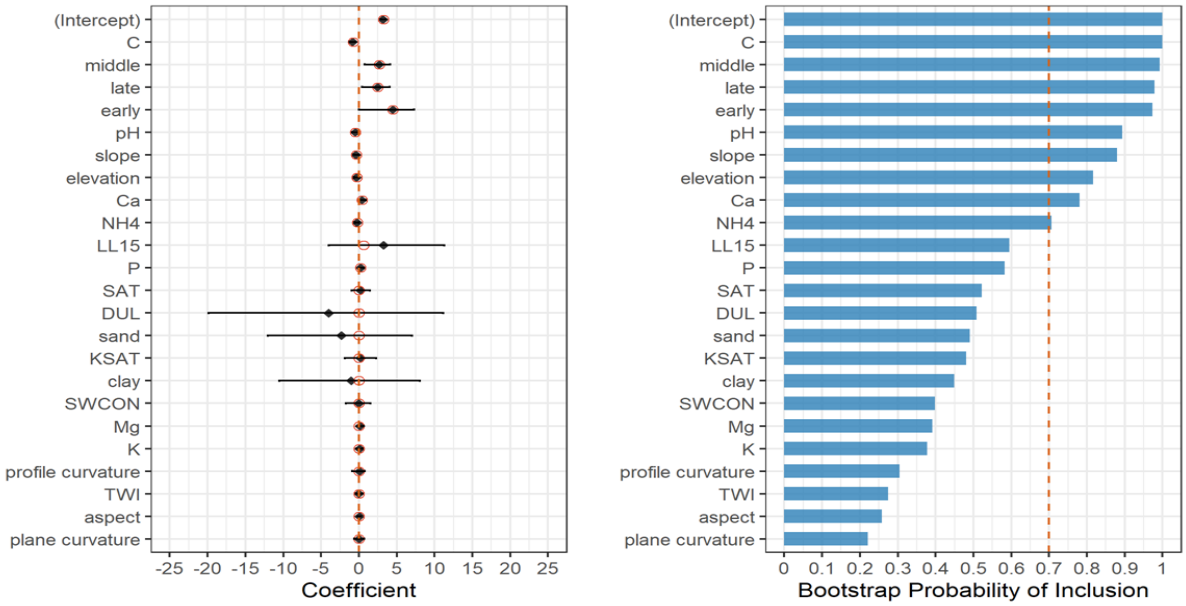

Figure 2.8. Model results from 1000 bootstrap resampling for restored prairie biomass yield (Mg ha^{-1}) at Marshall Farm. Left panel: estimated coefficients: black diamond is estimation from full model. Black horizontal is 95% bootstrap confidence interval, open red circle is bootstrap median. Right panel: bootstrap probability of inclusion. Red dash vertical bar indicates probability of 0.7.

For switchgrass, NH_4^+ had a positive estimated coefficient of 0.29 Mg ha^{-1}/SD (95% Bootstrap CI: 0 to 0.79 Mg ha^{-1}/SD) and 0.41 Mg ha^{-1}/SD (95% Bootstrap CI: 0 to 0.97 Mg ha^{-1}/SD) Mg ha^{-1} at Marshall and Lux Arbor, respectively. Profile curvature had positive estimated coefficient (3.03 Mg ha^{-1}/SD, 95% Bootstrap CI: 0 to 5.58 Mg ha^{-1}/SD) on switchgrass yield at Lux Arbor. On the other hand, profile curvature had negative estimated coefficient (-2.61 Mg ha^{-1}/SD, 95% Bootstrap CI: -6.60 to 0 Mg ha^{-1}/SD) on switchgrass yield at Marshall.

For restored prairie biomass, Ca had positive relationships with yield at Marshall and Lux Arbor.

The magnitude of the relationship with Ca was higher at Lux Arbor (1.11 Mg ha^{-1}/SD; 95% Bootstrap CI: 0 to 1.98 Mg ha^{-1}/SD) than Marshall (0.42 Mg ha^{-1}/SD; 95% Bootstrap CI: 0 to 0.91 Mg ha^{-1}/SD). Elevation was negatively associated with restored prairie biomass yield at both farms.

Gaussian process models with selected variables and Gaussian process full models

Only variables selected by backward step selection and over 70% inclusion according to bootstrapping were included in the final models for biomass yield of switchgrass and restored prairie at both Lux Arbor and Marshall. In comparison of unconditional models, Table 2.10 shows that spatial variability decreased for switchgrass and restored prairie at both farms after including selected variables. Matern's spatial correlation plot with model estimated parameters shows that switchgrass and restored prairie grown at Marshall had a spatial dependency of biomass yield (Figure A2.22 in the appendix).

Table 2.10. Gaussian process model results for models with selected variables for biomass yield (Mg ha^{-1}) of switchgrass and restored prairie at Marshall Farm and Lux Arbor Farm.

		Spatial Correlation		Random Part (Variance)		
Location	Crop	ν^1	ρ^2	Year	spatial	residual
Marshall	Switchgrass	0.252	0.009	1.946	0.899	3.527
	Restored prairies	16.667	0.025	0.334	0.149	1.112
Lux Arbor	Switchgrass	16.667	0.471	0.320	0.988	1.554
	Restored prairies	9.622	1.621	0.347	0.182	1.327

1. ν: smoothness parameter.
2. ρ: decay parameter

Models including all soil fertility characteristics and topographical features are referred to as full models. The spatial variability from full models for switchgrass and restored prairie at both farms decreased to a negligible amount (Table 2.11). The spatial variability of switchgrass and restored prairie at Marshall reduced to 0.00003 (SD: 0.005) and 0.00001(SD: 0.003), respectively. The spatial variability of switchgrass and restored prairie at Lux Arbor reduced to 0.624 (SD: 0.790) and 0.092 (SD: 0.303), respectively. According to Matern's spatial correlation

plot with model estimated parameters, switchgrass at Marshall and restored prairie at Lux Arbor show substantial spatial dependency from full model estimation (Figure A2.23 in appendix).

Table 2.11. Gaussian process model results of full models for dry biomass yield (Mg ha^{-1}) of switchgrass and restored prairie at Marshall and Lux Arbor Farms.

		Spatial Correlation		Random Part (Variance)		
Location	Crop	ν[1]	ρ[2]	Year	spatial	residual
Marshall	Switchgrass[3]	13.149	0.001	1.792	0.00003	3.169
	Restored prairie	0.005	0.117	0.278	0.00001	0.984
Lux Arbor	Switchgrass	16.667	0.751	0.206	0.624	1.492
	Restored prairie	16.667	0.036	0.367	0.092	1.236

1. ν: smoothness parameter.
2. ρ: decay paramter

Discussion

This study provides important evidence of within-field spatial and interannual temporal variability of switchgrass and restored prairie biomass yields at the field scale. The four-year mean annual biomass yields of switchgrass and restored prairie at Marshall were 6.9 Mg ha^{-1} (SD: 2.5 Mg ha^{-1}) and 3.3 Mg ha^{-1} (SD: 1.4 Mg ha^{-1}), respectively. The four-year mean annual biomass yield of switchgrass and restored prairie at Lux Arbor were 4.9 Mg ha^{-1} (SD: 2.3 Mg ha^{-1}) and 3.9 Mg ha^{-1} (SD: 1.9 Mg ha^{-1}), respectively. Switchgrass grown in monocultures near the study site as well as at a site in central Wisconsin (USA) yielded as high as 10.9 Mg ha^{-1} (Wang et al., 2010). A 30- year simulation study concluded that switchgrass rgown across the U.S. had an average annual yield of 6.2 Mg ha^{-1} and maximum annual yield of 15.5 Mg ha^{-1} (Thomson et al., 2009). Kordbacheh et al. (2019) reported that prairie in low fertility land produced 4.79 to 15.5 Mg ha^{-1} in Iowa, USA. Biomass yield in this study falls into the ranges previously reported but may not have reached its maximum potential, especially for switchgrass. Bransby and Huang (2014) investigated switchgrass biomass yield over a 20 years study period and found that switchgrass increased yield in the first 12 years and slowly declined thereafter. The experiment in this study started in 2009. Therefore, the relatively low biomass yield from this study could

have been influenced by the advancing stand age.

Concordantly, a three-way interaction of crop, location and year for biomass yield was observed in this study (p=0.02). Switchgrass (5.9 Mg ha^{-1}; 95% CI: 5.3 to 6.5 Mg ha^{-1}) and restored prairie (4.9 Mg ha^{-1}; 95% CI: 4.3 to 5.4 Mg ha^{-1}) produced the highest biomass yield in 2020, at Lux Arbor. At Marshall, switchgrass (9.1 Mg ha^{-1}; 95% CI: 8.4 to 9.7 Mg ha^{-1}) and restored prairie (3.7 Mg ha^{-1}; 95% CI: 2.8 to 4.5 Mg ha^{-1}) yielded highest in 2021. The highest yield of switchgrass and restored prairie in 2021 at Marshall was likely attributable to higher precipitation during June to September in 2021. The higher yield of switchgrass and restored prairie in 2020 at Lux Arbor could be attributed to higher precipitation during the later months (July to September) of the growing season as well. Several studies reported precipitation to be a yield limiting factor for switchgrass (Hui et al., 2018, Wullschleger et al., 2010, Berdahl et al., 2005, Sanderson et al., 1999, Lee & Boe, 2005, Muir et al., 2001). Evidence shows that precipitation from April to September is critical to biomass yield (Berdahl et al., 2005, Sanderson et al., 1999). Interestingly, this study shows that cumulative late season (August and September) precipitation was the best predictor for switchgrass and restored prairie biomass yield.

In this study, switchgrass (temporal variance: 1.784; SD: 1.336 Mg ha^{-1}) showed more interannual temporal variability of biomass yield than restored prairie (temporal variance: 0.313; SD: 0.559 Mg ha^{-1}) at Marshall. At Lux Arbor, interannual temporal variability of biomass yield was similar between switchgrass (temporal variance: 0.302; SD: 0.549 Mg ha^{-1}) and restored prairie (temporal variance: 0.399; SD: 0.632 Mg ha^{-1}). Considerable year-to year-temporal variability of biomass yield has been reported in most experiments intended to test switchgrass yield potential as bioenergy feedstocks (Lasorella et al., 2011, Tulbure et al., 2012, Alexopoulou

et al., 2015, Sanford et al., 2016, Reichmann et al., 2018). Conversely, biomass yield of restored prairie has shown resilience to unfavorable weather conditions such as drought (Bajgain et al., 2020). One theory on prairie resilience to unfavorable conditions is based on compensation theory. According to this theory, the multiple species associated with prairie grants the ability of compensating poor performance of some species by good performance of others (Pfisterer & Schmid, 2002). This suggests future research to investigate relationships between species composition and interannual variability of prairie biomass yield. Given future weather predictions for higher variability and uncertainty (Lopez-Cantu et al., 2020, Dollan et al., 2022), lower interannual variability of restored prairie makes it attractive as a bioenergy feedstock, especially when considering additional co-benefits such as increased biodiversity.

Within-field biomass variability reported in this study is consistent with other studies (Di Virgilio et al., 2007, Schmer et al., 2010). Our reported CV of switchgrass ranged from 0.24 to 0.39 at Marshall and 0.44 to 0.49 at Lux Arbor over the study period (2018-2021); and the CV of restored prairie ranged from 0.27 to 0.47 at Marshall and 0.39 to 0.51 at Lux Arbor over the study period (2018-2021). The slightly greater CV range we report for Lux Arbor relative to Marshall implies that microenvironments associated with specific areas influence within-field variability. This might be due to the generally more consistently fertile soil at Marshall resulting in more stable biomass yield, thereby reducing within-field variability. More fertile soil in Marshall can be attributable to a long history of livestock pasturing and 22 years as CRP grassland at Marshall. In this study, switchgrass showed higher within-field biomass variability than restored prairie at both locations. The estimated spatial variance representing within-field biomass variability for switchgrass was 0.967 (SD: 0.983 Mg ha^{-1}) and 3.561 (SD: 1.887 Mg ha^{-1}) at Marshall and Lux Arbor, respectively. The estimated spatial variance representing within-

field biomass variability for restored prairie was 0.334 (SD: 0.578 Mg ha^{-1}) and 1.896 (SD: 1.377 Mg ha^{-1}) at Marshall and Lux Arbor, respectively. Under similar soil conditions, restored prairie presented less within-field spatial variability than switchgrass. Previous studies showed that switchgrass had a wider range of biomass yield than restored prairie under the same weather and soil conditions (Sanford et al. 2016, Wang et al., 2020).

There were sizable residual variance components that remained unexplained for switchgrass and restored prairie after accounting for interannual temporal and within-field spatial variability. Switchgrass biomass yield at Marshall had unexplained residual variance of 3.644, which was higher than both the interannual temporal and within-field spatial variability. It is well established that plant traits such as yield are a function of environment, agronomic management and genetics**.** Studies have shown that the inherent genetic variation of switchgrass leads to biomass yield variability (Nayak et al., 2020). Future research on switchgrass varietal differences in biomass yield are warranted. There is a plethora of evidence showing that species richness, evenness and floristic quality influence grass productivity (Henschell et al., 2015, Boeck et al., 2008). The unexplained biomass variability we observed in restored prairie fields may possibly be due to variability of prairie species composition. In this study, there was no consistently reliable spatial dependency found for switchgrass (range: < 60 m) and restored prairie (range: <100 m). Similarly, Di Virgilio et al. (2007) demonstrated switchgrass biomass yield presented weak spatial dependency in a 2-year study. On other hand, failure to observe a reliable spatial dependency could be caused by insufficient sampling within the field. This makes it difficult to extrapolate spatial covariance out of the range of sampling distances.

A recent study utilizing a global grassland dataset demonstrated relationships of soil physiochemical qualities such as CEC, soil organic matter, and soil nutrients including N, P,

Zn, and Fe with biomass yield (Radujković et al., 2021). Avohou et al. (2009) showed that topographical features like slope, aspect and curvature do not significantly influence biomass yield in grasslands. In this study, we observed soil Ca had a positive relationship with biomass yield of restored prairie at both farms. Soil Mg had a negative relationship with switchgrass and restored prairie at Lux Arbor. Schmer et al. (2012) found that switchgrass responsivity to soil Ca supplementation depended on cultivar. Another study reported that prairie strips adjacent to row crops increased soil Ca content (Dutter, 2022). The positive soil Ca effect on prairie biomass yield could be due to a reverse causal relationship since the experiment started in 2009. We observed soil NH_4^+ had a positive relationship with switchgrass biomass yield at Marshall and Lux Arbor. This agrees with other studies claiming N and P are the most limiting nutrients for switchgrass and grasslands (Craine & Jackson, 2010, Fay, 2015, Edwards & Venterink, 2016, Niu et al., 2018). Previous studies showed that the leading drivers of switchgrass biomass yield are nitrogen fertilization and then climate (Heaton et al., 2004; Wang et al., 2010).

Soil topographical characteristics related to soil moisture availability such as elevation and slope had a negative relationship with TWI had a positive relationship with biomass yield. TWI represents soil water accumulation tendency has been used as a proxy for soil moisture availability (Beaudette & Geen, 2013, Radu et al., 2018, Winzeler et al., 2022). Virgilio et al. (2007) reported a negative effect of slope on switchgrass biomass yield. Previous studies demonstrated that the relationship of topographical features such as TWI with biomass yield of major grain crops varied year to year due to different precipitation patterns (Kravchenko & Bullock, 2000, Jiang & Thelen, 2004, Huang et al., 2008). Jager et al. (2010) reported a positive relationship of TWI with yield on upland ecotype switchgrass based on an analysis of published switchgrass field trial data across a wide geographical region. Madugundu et al. (2022)

demonstrated a positive relationship between Topographical Wetness Index (TWI) and forage crop yield. Studies on annual crops have shown that elevation was negatively correlated with annual crop yield (Bronson et al., 2002, Iqbal et al., 2005). In contrast, Schmer et al. (2012) found no relationship between slope and switchgrass biomass yield, and reasoned it was due to the established root system of switchgrass in the study.

Switchgrass and restored prairie as bioenergy feedstocks are unlikely to receive intensive management like high levels of fertilization or irrigation. Nevertheless, this study contributes to the identification of potential soil factors affecting crop biomass yield. In practical terms, a grower's understanding of spatial and temporal variability plays a critical role in making management decisions for maximizing biomass crop yield. Similarly, at the biorefinery level, a better understanding of regional spatial and temporal variability is critical in developing strategic plans for bioenergy feedstocks logistics.

Conclusion

The restored prairie polyculture cropping system exhibited a different spatial variation pattern in biomass yield relative to the monoculture cropping system of switchgrass under similar soil conditions, with the switchgrass cropping system showing greater spatial variability than the restored prairie cropping system. In addition, biomass yield of the switchgrass cropping system appeared to be driven more by environmental factors at the more fertile Marshall, which may explain its greater interannual variability than the restored prairie cropping system. Polycultures of restored prairie had relatively low temporal variability in biomass yield. This was likely due in part to the multi-species buffering capacity afforded by a mix of grass and forb species having a wider range of environmental adaptability relative to a monoculture system. Both switchgrass and restored prairie biomass yields were likely limited by multiple factors. Switchgrass biomass

yield was positively related to soil NH_4^+, but negatively related to soil Mg. Profile curvature had a significant influence on switchgrass biomass yield, but with uncertainty of the direction. In the restored prairie, biomass yield was positively influenced by soil Ca and negatively influenced by elevation. This study had typical scope limitations of sample size, therefore an uncertainty of effect of soil characteristics on biomass yield is unavoidable. Future studies should consider increasing spatial resolution to reveal finer spatial patterns for biomass yield of switchgrass and restored prairie.

REFERENCES

Abraha, M., Gelfand, I., Hamilton, S. K., Chen, J., & Robertson, G. P. (2019). Carbon debt of field-scale conservation reserve program grasslands converted to annual and perennial bioenergy crops. Environmental Research Letters, 14(2). https://doi.org/10.1088/1748-9326/aafc10

Adkins, J, Jastrow, J.D., Morris, G.P., Six, J. (2016). Effects of switchgrass cultivars and intraspecific differences in root structure on soil carbon inputs and accumulation. Geoderma, 262. https://doi.org/10.1016/j.geoderma.2015.08.019

Alexopoulou, E., Zanetti, F., Scordia, D., Zegada-Lizarazu, W., Christou, M., Testa, G., Cosentino, S. L., & Monti, A. (2015). Long-Term Yields of Switchgrass, Giant Reed, and Miscanthus in the Mediterranean Basin. Bioenergy Research, 8(4), 1492–1499. https://doi.org/10.1007/s12155-015-9687-x

Avohou, He, T., Sinsin, B. (2009). The Effects of Topographic Factors on Aboveground Biomass Production of Grasslands in the Atacora Mountains in Northwestern Benin.Mountain. Research and Development, 29(3), 250-254

Bajgain, R., Xiao, X., Basara, J., Doughty, R., Wu, X., Wagle, P., Zhou, Y., Gowda, P., & Steiner, J. (2020). Differential responses of native and managed prairie pastures to environmental variability and management practices. Agricultural and Forest Meteorology, 294(August). https://doi.org/10.1016/j.agrformet.2020.108137

Bates, D., Maechler, M., Bolker, B., Walker, S., 2015. Fitting Linear Mixed-Effects Models Using lme4. Journal of Statistical Software, 67(1), 1-48. doi:10.18637/jss.v067.i01.

Beaudette, D. E., & Geen, A. T. O. (2013). Terrain-Shape Indices for Modeling Soil Moisture Dynamics. https://doi.org/10.2136/sssaj2013.02.0048

Berdahl, J. D., Frank, A. B., Krupinsky, J. M., Carr, P. M., Hanson, J. D., & Johnson, H. A. (2005). Biomass yield, phenology, and survival of diverse switchgrass cultivars and experimental strains in western North Dakota. Agronomy Journal, 97(2), 549–555. https://doi.org/10.2134/agronj2005.0549

Bivand, R., Keitt, T. and Rowlingson, B., 2021. rgdal: Bindings for the 'Geospatial' Data Abstraction Library. R package version 1.5-23. https://CRAN.R-project.org/package=rgdal

Bivand, R. and Lewin-Koh, N., 2021. maptools: Tools for Handling Spatial Objects. R package version 1.1-1. https://CRAN.R-project.org/package=maptools

Boeck, H. J. De, Lemmens, C. M. H. M., Zavalloni, C., Gielen, B., Malchair, S., Carnol, M., & Merckx, R. (2008). Biomass production in experimental grasslands of different species richness during three years of climate warming. 585–594.

Bransby, D., & Huang, P. (2014). Twenty-Year Biomass Yields of Eight Switchgrass Cultivars

in Alabama. Bioenergy Research, 7(4), 1186–1190. https://doi.org/10.1007/s12155-014-9448-2

Bronson, K., Nesmith, D. M., & Xu, W. (2002). Spatial and Temporal Variability of Corn Growth and Grain Yield : Implications for Site-Specific Farming. 1576(June 2001), 1564–1576.

Burnham, K. P., & Anderson, D. R. (2004). Multimodel inference: Understanding AIC and BIC in model selection. Sociological Methods and Research, 33(2), 261–304. https://doi.org/10.1177/0049124104268644

Craine, J. M., & Jackson, R. D. (2010). Plant nitrogen and phosphorus limitation in 98 North American grassland soils Plant nitrogen and phosphorus limitation in 98 North American grassland soils. August 2015. https://doi.org/10.1007/s11104-009-0237-1

Crum, J. R., & Collins, H. P. (1995). KBS Soils. Kellogg Biological Station Long-term Ecological Research Special Publication. Zenodo, http://doi.org/10.5281/zenodo.2581504.

Di Virgilio, N., Monti, A., & Venturi, G. (2007). Spatial variability of switchgrass (Panicum virgatum L.) yield as related to soil parameters in a small field. Field Crops Research, 101(2), 232–239. https://doi.org/10.1016/j.fcr.2006.11.009

Dollan, I. J., Maggioni, V., Johnston, J., Coelho, G. de A., & Kinter, J. L. (2022). Seasonal variability of future extreme precipitation and associated trends across the Contiguous U.S. Frontiers in Climate, 4. https://doi.org/10.3389/fclim.2022.954892

Dutter, C. R. (2022). The spatial and temporal effects of prairie strip restoration on soil health (Order No. 29320966). Available from ProQuest Dissertations & Theses Global. (2725294458).

Edwards, P. J., & Venterink, H. O. (2016). Native and alien herbaceous plants in the Brazilian Cerrado are co-limited by different nutrients. 231–243. https://doi.org/10.1007/s11104-015-2725-9

Fan, P., Hao, M., Ding, F., Jiang, D., & Dong, D. (2020). Quantifying global potential marginal land resources for switchgrass. Energies, 13(23), 1–13. https://doi.org/10.3390/en13236197

Fargione, J., Hill, J., Tilman, D., Polasky, S., & Hawthorne, P. (2008). Land clearing and the biofuel carbon debt. Science, 319(5867), 1235–1238. https://doi.org/10.1126/science.1152747

Fay, P. A. (2015). Grassland productivity limited by multiple nutrients. July, 1–5. https://doi.org/10.1038/nplants.2015.80

Hartig, F., 2021. DHARMa: Residual Diagnostics for Hierarchical (Multi-Level / Mixed) Regression Models. R package version 0.4.3. https://CRAN.R-

project.org/package=DHARMa

Henschell, M. A., Webster, C. R., Flaspohler, D. J., & Fortin, C. R. (2015). Influence of Plant Community Composition on Biomass Production in Planted Grasslands. 1–14. https://doi.org/10.1371/journal.pone.0125758

Hiemstra, P.H., Pebesma, E.J., Twenhofel, C.J.W. and G.B.M. Heuvelink, 2008. Real-time automatic interpolation of ambient gamma dose rates from the Dutch Radioactivity Monitoring Network. Computers & Geosciences, accepted for publication.

Hijmans, R.J., 2021. raster: Geographic Data Analysis and Modeling. R package version 3.4-13. https://CRAN.R-project.org/package=raster

Huang, X., Wang, L., Yang, L., & Kravchenko, A. N. (2008). Management Effects on Relationships of Crop Yields with Topography Represented by Wetness Index and Precipitation. 1463–1471. https://doi.org/10.2134/agronj2007.0325

Hui, D., Yu, C. L., Deng, Q., Kudjo Dzantor, E., Zhou, S., Dennis, S., Sauve, R., Johnson, T. L., Fay, P. A., Shen, W., & Luo, Y. (2018). Effects of precipitation changes on switchgrass photosynthesis, growth, and biomass: A mesocosm experiment. PLoS ONE, 13(2), 1–18. https://doi.org/10.1371/journal.pone.0192555

Hussain, M. Z., Bhardwaj, A. K., Basso, B., Robertson, G. P., & Hamilton, S. K. (2019). Nitrate Leaching from Continuous Corn, Perennial Grasses, and Poplar in the US Midwest. Journal of Environmental Quality, 48(6), 1849–1855. https://doi.org/10.2134/jeq2019.04.0156

IPCC. (2022). Climate Change 2022, Mitigation of Climate Change Summary for Policymakers (SPM). In Cambridge University Press (Issue 1). https://www.ipcc.ch/report/ar6/wg2/

Iqbal, J., Read, J. J., Thomasson, A. J., & Jenkins, J. N. (2005). Relationships between Soil – Landscape and Dryland Cotton Lint Yield. https://doi.org/10.2136/sssaj2004.0178

Jacot, J., Williams, A. S., & Kiniry, J. R. (2021). Biofuel benefit or bummer? A review of North American native perennial grass biofuels' environmental effects, economics, and feasibility compared to annual crops. Agronomy, 11(7). https://doi.org/10.3390/agronomy11071440

Jager, H. I., Baskaran, L. M., Brandt, C. C., Davis, E. B., Gunderson, C. A., & Wullschleger, S. D. (2010). Empirical geographic modeling of switchgrass yields in the United States. GCB Bioenergy, 2(5), 248–257. https://doi.org/10.1111/j.1757-1707.2010.01059.x

Jiang, P., & Thelen, K. D. (2004). Effect of Soil and Topographic Properties on Crop Yield in a North-Central Corn–Soybean Cropping System. Agron. J., 96: 252-258. https://doi.org/10.2134/agronj2004.0252

Kordbacheh, F., Jarchow, M., English, L., & Liebman, M. (2019). Productivity and diversity of annually harvested reconstructed prairie communities. Journal of Applied Ecology, 56(2),

330–342. https://doi.org/10.1111/1365-2664.13267

Kravchenko, A. N., & Bullock, D. G. (2000). Correlation of corn and soybean grain yield with topography and soil properties. In Agronomy Journal (Vol. 92, Issue 1, pp. 75–83). https://doi.org/10.2134/agronj2000.92175x

Lasorella, M. V., Monti, A., Alexopoulou, E., Riche, A., Sharma, N., Cadoux, S., van Diepen, K., Elbersen, B., Atzema, A. J., & Elbersen, H. W. (2011). Yield comparison between switchgrass and miscanthus based on multi-year side by side comparison in Europe. Conference Proceedings of 19th European Biomass Conference and Exhibition, June, 729–733.

Lee, D. K., & Boe, A. (2005). Biomass production of switchgrass in Central South Dakota. Crop Science, 45(6), 2583–2590. https://doi.org/10.2135/cropsci2005.04-0003

Lopez-Cantu, T., Prein, A. F., & Samaras, C. (2020). Uncertainties in Future U.S. Extreme Precipitation from Downscaled Climate Projections. Geophysical Research Letters, 47(9), 1–11. https://doi.org/10.1029/2019GL086797

Liljequist D, Elfving B, Skavberg Roaldsen K (2019) Intraclass correlation – A discussion and demonstration of basic features. PLoS ONE 14(7): e0219854. https://doi.org/10.1371/journal.pone.0219854

Madugundu, R., Al-Gaadi, K. A., Tola, E. K., Zeyada, A. M., Alameen, A. A., Edrris, M. K., Edrees, H. F., & Mahjoop, O. (2022). Impact of Field Topography and Soil Characteristics on the Productivity of Alfalfa and Rhodes Grass: RTK-GPS Survey and GIS Approach. Agronomy, 12(12). https://doi.org/10.3390/agronomy12122918

Metcalfe, P., Beven, K. and Freer, J., 2018. dynatopmodel: Implementation of the Dynamic TOPMODEL Hydrological Model. R package version 1.2.1. https://CRAN.R-project.org/package=dynatopmodel

Muir, J. P., Sanderson, M. A., Ocumpaugh, W. R., Jones, R. M., & Reed, R. L. (2001). Biomass Production of 'Alamo' Switchgrass in Response to Nitrogen, Phosphorus, and Row Spacing. Agron. J., 93: 896-901. https://doi.org/10.2134/agronj2001.934896x

Nayak, S., Bhandari, H., Sams, C., Sykes, V., Hilafu, H., Dalid, C., Senseman, S., & Pantalone, V. (2020). Genetic variation for biomass yield and predicted genetic gain in lowland switchgrass "kanlow." Agronomy, 10(12), 1–18. https://doi.org/10.3390/agronomy10121845

Niu, D., Yuan, X., Cease, A. J., Wen, H., Zhang, C., Fu, H., & Elser, J. J. (2018). Science of the Total Environment The impact of nitrogen enrichment on grassland ecosystem stability depends on nitrogen addition level. 618(768), 1529–1538. https://doi.org/10.1016/j.scitotenv.2017.09.318

Paradis, E. & Schliep, K. 2019. ape 5.0: an environment for modern phylogenetics and evolutionary analyses in R. Bioinformatics 35: 526-528.

Pebesma, E.J., 2004. Multivariable geostatistics in S: the gstat package. Computers & Geosciences, 30: 683-691.

Pebesma, E.J., Bivand, R.S., 2005. Classes and methods for spatial data in R. R News 5 (2), https://cran.r-project.org/doc/Rnews/.

Pebesma, E.J., 2018. Simple Features for R: Standardized Support for Spatial Vector Data. The R Journal 10 (1), 439-446, https://doi.org/10.32614/RJ-2018-009

Pfisterer, A. B., & Schmid, B. (2002). Diversity-dependent production can decrease the stability of ecosystem functioning. Nature, 416(6876), 84–86. https://doi.org/10.1038/416084a

Radu, W., Szymura, T. H., & Szymura, M. (2018). Topographic wetness index explains soil moisture better than bioindication with Ellenberg's indicator values. 85(November 2017), 172–179. https://doi.org/10.1016/j.ecolind.2017.10.011

Radujković, D., Verbruggen, E., Seabloom, E. W., Bahn, M., Biederman, L. A., Borer, E. T., Boughton, E. H., Catford, J. A., Campioli, M., Donohue, I., Ebeling, A., Eskelinen, A., Fay, P. A., Hansart, A., Knops, J. M. H., MacDougall, A. S., Ohlert, T., Olde Venterink, H., Raynaud, X., … Vicca, S. (2021). Soil properties as key predictors of global grassland production: Have we overlooked micronutrients? Ecology Letters, 24(12), 2713–2725. https://doi.org/10.1111/ele.13894

R Core Team (2021). R: A language and environment for statistical computing. R Foundation for Statistical Computing, Vienna, Austria. URL https://www.R-project.org/.

Reichmann, L. G., Collins, H. P., Jin, V. L., Johnson, M. V. V., Kiniry, J. R., Mitchell, R. B., Polley, H. W., & Fay, P. A. (2018). Inter-Annual Precipitation Variability Decreases Switchgrass Productivity from Arid to Mesic Environments. Bioenergy Research, 11(3), 614–622. https://doi.org/10.1007/s12155-018-9922-3

Rousset, F. and Ferdy, J., 2014. Testing environmental and genetic effects in the presence of spatial autocorrelation. Ecography 37(8): 781-790 URL: http://dx.doi.org/10.1111/ecog.00566

Ruan, L., & Robertson, G. P. (2020). No-till establishment improves the climate benefit of bioenergy crops on marginal grasslands. Soil Science Society of America Journal, 84(4), 1280–1295. https://doi.org/10.1002/saj2.20082

Sanderson, M. A., Reed, R. L., Ocumpaugh, W. R., Hussey, M. A., Van Esbroeck, G., Read, J. C., Tischler, C. R., & Hons, P. M. (1999). Switchgrass cultivars and germplasm for biomass feedstock production in Texas. Bioresource Technology, 67(3), 209–219. https://doi.org/10.1016/S0960-8524 (98)00132-1

Sanford, G. R., Oates, L. G., Jasrotia, P., Thelen, K. D., Robertson, G. P., & Jackson, R. D. (2016). Comparative productivity of alternative cellulosic bioenergy cropping systems in the North Central USA. Agriculture, Ecosystems and Environment, 216, 344–355. https://doi.org/10.1016/j.agee.2015.10.018

Saxton, K. E., & Rawls, W. J. (2006). Soil Water Characteristic Estimates by Texture and Organic Matter for Hydrologic Solutions. Soil Science Society of America Journal, 70(5), 1569–1578. https://doi.org/10.2136/sssaj2005.0117

Schmer, M. R., Hanson, J. D., Johnson, H. A., Schmer, M. R., Hanson, J. D., Switchgrass, H. A. J., Schmer, M. R., Hanson, J. D., & Johnson, H. A. (2012). Switchgrass and Intermediate Wheatgrass Aboveground and Belowground Response to Nitrogen and Calcium. 4167(May). https://doi.org/10.1080/01904167.2012.671409

Schmer, M. R., Mitchell, R. B., Vogel, K. P., Schacht, W. H., & Marx, D. B. (2010). Spatial and temporal effects on switchgrass stands and yield in the Great Plains. Bioenergy Research, 3(2), 159–171. https://doi.org/10.1007/s12155-009-9045-y

Searchinger, T., Heimlich, R., Houghton, R. A., Dong, F., Elobeid, A., Fabiosa, J., Tokgoz, S., Hayes, D., Yu, T.H. (2008). Use of U.S. Croplands for Biofuels Increases Greenhouse Gases through Emissions from Land-Use Change. Science. 319. 10.1126/science.1151861.

Symonds, M. R. E., & Moussalli, A. (2011). A brief guide to model selection, multimodel inference and model averaging in behavioural ecology using Akaike's information criterion. Behavioral Ecology and Sociobiology, 65(1), 13–21. https://doi.org/10.1007/s00265-010-1037-6

Soil Survey Staff, Natural Resources Conservation Service, United States Department of Agriculture. Web Soil Survey. Available online at http://websoilsurvey.nrcs.usda.gov/ accessed [05/08/2022]

Thomson, A. M., Izarrualde, R. C., West, T. O., Parrish, D. J., Tyler, D. D., & Williams, J. R. (2009). Simulating potential switchgrass production in the United States. Available at Http://Www.Pnl.Gov/Main/Publications/External/Technical_reports/Pnnl-19072.Pdf, 12, 1–22. papers2://publication/uuid/713A684A-15A4-4BC9-BC34-F57C48723E96

Tulbure, M. G., Wimberly, M. C., Boe, A., & Owens, V. N. (2012). Climatic and genetic controls of yields of switchgrass, a model bioenergy species. Agriculture, Ecosystems and Environment, 146(1), 121–129. https://doi.org/10.1016/j.agee.2011.10.017

U.S. Department of Agriculture. (2021). Increasing Feedstock Production for Biofuels Photos credits for front cover: Top photos. http://www.afdc.energy.gov/pdfs/increasing_feedstock_revised.pdf

United Nations Climate Change. (2021). The United States of America: Nationally Determined Contributions. 1–23. https://www4.unfccc.int/sites/ndcstaging/PublishedDocuments/United States of America First/United States NDC April 21 2021 Final.pdf

Wang, D., Lebauer, D. S., & Dietze, M. C. (2010). A quantitative review comparing the yield of switchgrass in monocultures and mixtures in relation to climate and management factors. GCB Bioenergy, 2(1), 16–25. https://doi.org/10.1111/j.1757-1707.2010.01035.x

Winzeler, H. E., Owens, P. R., Read, Q. D., Libohova, Z., Ashworth, A., & Sauer, T. (2022). Topographic Wetness Index as a Proxy for Soil Moisture in a Hillslope Catena: Flow Algorithms and Map Generalization. Land, 11(11), 2018. MDPI AG. Retrieved from http://dx.doi.org/10.3390/land11112018

Wickham, H. (2016). ggplot2: Elegant Graphics for Data Analysis. Springer-Verlag New York.

Wullschleger, S. D., Davis, E. B., Borsuk, M. E., Gunderson, C. A., & Lynd, L. R. (2010). Biomass production in switchgrass across the United States: Database description and determinants of yield. Agronomy Journal, 102(4), 1158–1168. https://doi.org/10.2134/agronj2010.0087

Wang, S., Sanford, G.R., Robertson, G.P. et al. Perennial Bioenergy Crop Yield and Quality Response to Nitrogen Fertilization. Bioenerg. Res. 13, 157–166 (2020). https://doi.org/10.1007/s12155-019-10072-z

APPENDIX

Table A2.1. Plant species and seeding rate at Marshall Farm and Lux Arbor Farm.

Cropping System	Species		Seeding Rate (kg ha^{-1})
Restored prairie	*Aster azureus*	forb	0.07
	Asclepias tuberosa L.		0.04
	Monarda fistulosa L.		0.07
	Asclepias syriaca L.		0.07
	Penstemon digitalis		0.07
	Coreopsis lanceolata		0.14
	Verbena stricta Vent.		0.14
	Rudbeckia triloba L.		0.18
	Rudbeckia hirta L.		0.21
	Ratibida pinnata (Vent.) Barnh.		0.21
	Eryngium yuccifolium Michx.		0.21
	Cassia fasciculata Michx.		0.28
	Echinacea purpurea (L.) Moench		0.28
	Heliopsis helianthoides (L.) Sweet		0.28
	Panicum virgatum var. Southlow	grass	0.56
	Andropogon gerardii		0.56
	Schizacyrium scoparium (Michx.) Nash		1.12
	Sorghastrum nutans (L.) Nash ex Small		1.12
	Elymus canadensis		2.24
Switchgrass	*Panicum virgatum* var. Cave-in-Rock	grass	11.21

Table A2.2. Land use history at Marshall Farm and Lux Arbor Farm.

Farm	Cropping System	Field Size	Pre-conversion (from 1987)	2009 Conversion Year	2010 First Establishment Year	2011 Second Establishement Year
Marshall	Switchgrass	13 ha	CRP Brome grass	No-till soybean	Restored prairie species and oats as nurse crop	Restored prairie species
	Restored prairie	11 ha			Switchgrass and oats as nurse crop	Switchgrass
Lux Arbor	Switchgrass	14 ha	Tilled corn-soybean rotation	No-till soybean	Restored prairie species and oats as nurse crop	Restored prairie species
	Restored prairie	13 ha			Switchgrass and oats as nurse crop	Switchgrass

Table A2.3. Number and distance range (meter) of sampling points for switchgrass and restored prairie at Marshall Farm and Lux Arbor Farm.

		Marshall			Lux Arbor		
Crop	Year	Minimum	Maximum	Number	Minimum	Maximum	Number
Switchgrass	2018	41.1	331.7	30	33.2	297.7	30
	2019	14.4	408.8	42	22.9	398.0	42
	2020	14.4	408.8	42	22.9	398.0	42
	2021	23.0	400.3	42	22.9	397.7	42
Restored prairie	2018	27.6	350.5	30	23.7	374.5	30
	2019	22.0	458.4	42	19.2	401.2	42
	2020	22.0	458.4	42	19.2	401.2	42
	2021	21.6	441.5	42	16.3	402.0	42

Table A2.4. Descriptive statistics of soil fertility characteristics and topographical features at Lux Arbor Farm in 2018.

	Restored prairie				Switchgrass			
	MIN[1]	MAX[1]	MEAN	SD[1]	MIN	MAX	MEAN	SD
Elevation, m	292.56	298.37	296.64	1.61	285.02	294.71	289.85	2.98
pH	5.7	6.4	6.04	0.19	5.8	6.6	6.22	0.22
Phosphorus, mg kg^{-1}	6	37	17.87	7.84	9	61	23.37	10.49
Soil potassium, mg kg^{-1}	30	135	74.83	28.17	37	125	66.07	22.99
Calcium, mg kg^{-1}	566	1455	975.33	238.58	490	1489	1011.70	261.79
Magnesium, mg kg^{-1}	110	313	185.73	52.20	80	302	178.77	51.60
Total soil carbon(C) , wt%	0.64	1.75	1.09	0.26	0.40	1.51	1.00	0.28
Ammonium (NH_4^+), mg kg^{-1}	1.70	5.15	2.97	0.78	1.30	5.20	2.73	0.85
Sand content, wt%	10.60	73.75	44.54	14.23	16.90	81.25	50.94	18.29
Clay content, wt%	7.50	30.70	20.48	5.99	0.00	38.10	19.00	10.27
Slope, °	0.23	6.03	1.98	1.55	0.38	5.95	2.95	1.41
Aspect,	42.59	359.42	223.55	84.11	9.71	356.04	279.84	90.96
Plane curvature, km^{-1}	-0.30	0.30	0.01	0.13	-0.30	0.41	0.03	0.16
Profile curvature, km^{-1}	-0.57	0.34	0.00	0.18	-0.23	0.38	0.00	0.14
Topographical wetness index	4.67	11.36	7.07	1.67	4.83	13.35	7.33	1.96
15 bar lower limit of soil water content (LL15), v%	4.4	18.5	12.36	3.61	1.0	22.7	11.36	6.22
Drained upper limit of soil water content (DUL), v%	13.70	35.60	24.48	5.27	7.50	37.20	22.17	8.72
Saturated water content (SAT), v%	38.10	44.40	39.67	1.52	38.10	45.70	40.07	2.06
Whole profile drainage rate coefficient (SWCON)	17.0	59.1	26.45	9.08	16.6	90.0	38.03	25.87
Saturated hydraulic conductivity (Ksat), mm h^{-1}	2.00	44.09	11.45	9.08	1.58	113.16	25.89	32.59

1. Abbreviation: MIN: minimum, MAX: maximum, SD: standard deviation.

Table A2.5. Descriptive statistics of soil fertility characteristics and topographical features at Lux Arbor Farm in 2020.

	Restored prairie				Switchgrass			
	MIN[1]	MAX[1]	MEAN	SD[1]	MIN	MAX	MEAN	SD
Elevation, m	292.05	298.37	296.51	1.61	284.11	296.43	289.80	3.32
pH	5.5	6.4	5.82	0.22	5.5	6.6	5.97	0.27
Phosphorus, mg kg^{-1}	10	69	21.69	13.95	11	56	24.63	11.60
Soil potassium, mg kg^{-1}	27	169	76.15	29.20	49	141	76.32	21.67
Calcium, mg kg^{-1}	442	1477	971.46	254.85	552	1589	1036.18	280.54
Magnesium, mg kg^{-1}	75	275	181.26	50.39	86	296	179.53	49.76
Total soil carbon(C) , wt%	0.69	1.81	1.17	0.31	0.58	1.75	0.97	0.31
Ammonium (NH_4^+), mg kg^{-1}	2.26	32.81	5.07	4.99	3.16	10.26	4.96	1.53
Sand content, wt%	10.60	73.75	47.94	14.10	16.90	81.25	54.58	17.44
Clay content, wt%	7.50	30.70	20.58	5.44	0.00	38.10	18.69	8.95
Slope, °	0.14	6.82	2.06	1.81	0.38	6.55	3.15	1.63
Aspect,	29.75	359.42	203.02	88.73	9.71	356.04	271.54	97.10
Plane curvature, km^{-1}	-0.30	0.30	0.02	0.13	-0.30	0.41	0.02	0.14
Profile curvature, km^{-1}	-0.57	0.34	0.00	0.16	-0.23	0.38	-0.01	0.13
Topographical wetness index	4.70	14.64	7.53	2.49	4.67	13.34	7.34	1.96
15 bar lower limit of soil water content (LL15), v%	4.4	18.5	12.27	3.40	1.0	22.7	11.02	5.65
Drained upper limit of soil water content (DUL), v%	13.70	35.60	23.79	5.24	7.50	37.20	21.21	8.17
Saturated water content (SAT), v%	38.10	44.40	39.53	1.37	38.10	45.70	39.78	1.92
Whole profile drainage rate coefficient (SWCON)	17.0	59.1	27.43	9.63	16.6	90.0	38.42	23.35
Saturated hydraulic conductivity (Ksat), mm h^{-1}	2.00	44.09	12.42	9.63	1.58	113.16	25.68	29.20

1. Abbreviation: MIN: minimum, MAX: maximum, SD: standard deviation.

Table A2.6. Descriptive statistics of soil fertility characteristics and topographical features at Marshall Farm in 2018.

	Restored prairie				Switchgrass			
	MIN[1]	MAX[1]	MEAN	SD[1]	MIN	MAX	MEAN	SD
Elevation, m	284.96	294.32	290.40	2.69	289.94	298.48	295.87	2.21
pH	5.40	6.40	6.05	0.25	5.30	5.80	5.60	0.13
Phosphorus, mg kg^{-1}	15	126	54.17	22.51	16	119	61.07	23.11
Soil potassium, mg kg^{-1}	8	363	61.47	65.27	10	333	126.73	66.39
Calcium, mg kg^{-1}	396	1182	671.73	159.01	488	890	715.03	90.05
Magnesium, mg kg^{-1}	44	137	66.33	19.09	77	191	114.10	24.45
Total soil carbon(C) , wt%	0.70	2.05	1.12	0.29	0.94	1.88	1.31	0.22
Ammonium (NH_4^+), mg kg^{-1}	3.02	12.85	5.48	2.11	2.95	18.20	6.56	3.61
Sand content, wt%	20.00	88.30	69.58	16.66	24.60	86.25	57.40	12.98
Clay content, wt%	1.25	20.70	9.47	5.09	1.25	27.40	13.69	7.59
Slope, °	0.65	12.64	4.86	2.97	0.44	7.32	2.41	1.68
Aspect,	18.44	318.08	163.87	94.61	120.29	355.52	208.20	67.28
Plane curvature, km^{-1}	-1.00	0.61	0.07	0.36	-1.54	0.31	-0.03	0.37
Profile curvature, km^{-1}	-0.77	0.75	0.08	0.36	-0.26	0.52	0.05	0.17
Topographical wetness index	4.27	14.38	7.02	2.72	4.96	12.43	7.14	1.99
15 bar lower limit of soil water content (LL15), v%	1.0	12.4	5.43	3.21	1.0	16.6	8.18	4.67
Drained upper limit of soil water content (DUL), v%	4.90	28.20	13.27	5.87	5.80	31.90	18.19	6.45
Saturated water content (SAT), v%	38.10	41.60	39.25	0.99	38.00	42.20	39.05	0.96
Whole profile drainage rate coefficient (SWCON)	20.1	90.0	61.98	23.83	18.1	90.0	45.17	24.31
Saturated hydraulic conductivity (Ksat), mm h^{-1}	5.07	144.82	58.60	41.84	3.11	137.14	35.83	37.64

1. Abbreviation: MIN: minimum, MAX: maximum, SD: standard deviation.

Table A2.7. Descriptive statistics of soil fertility characteristics and topographical features at Marshall Farm in 2020.

	Restored prairie				Switchgrass			
	MIN[1]	MAX[1]	MEAN	SD[1]	MIN	MAX	MEAN	SD
Elevation, m	284.96	294.32	290.34	2.62	289.94	299.01	295.61	2.31
pH	5.70	7.50	6.17	0.38	5.10	7.70	5.59	0.43
Phosphorus, mg kg^{-1}	17	127	50.54	23.75	16	124	58.64	23.87
Soil potassium, mg kg^{-1}	22	245	66.43	48.57	25	266	105.81	49.58
Calcium, mg kg^{-1}	405	2023	818.73	329.05	393	3438	687.94	489.28
Magnesium, mg kg^{-1}	45	126	74.78	22.17	58	177	91.97	25.37
Total soil carbon(C) , wt%	0.64	2.28	1.31	0.37	0.87	2.04	1.33	0.31
Ammonium (NH_4^+), mg kg^{-1}	3.15	14.30	6.10	2.48	3.35	31.40	9.47	6.20
Sand content, wt%	20.00	88.30	72.30	14.80	24.60	86.25	60.31	13.58
Clay content, wt%	1.25	20.70	9.89	4.45	1.25	27.40	14.36	7.06
Slope, °	0.65	12.64	4.71	2.93	0.21	7.32	2.33	1.66
Aspect,	10.16	353.16	164.70	104.53	22.84	355.52	205.70	76.38
Plane curvature, km^{-1}	-1.00	0.61	0.01	0.38	-1.54	0.36	-0.04	0.36
Profile curvature, km^{-1}	-0.83	0.86	0.04	0.42	-0.26	0.52	0.03	0.16
Topographical wetness index	4.27	14.38	7.06	2.66	4.96	12.40	7.54	2.16
15 bar lower limit of soil water content (LL15), v%	1.0	12.5	5.60	2.96	1.0	16.6	8.42	4.47
Drained upper limit of soil water content (DUL), v%	4.90	28.20	13.05	5.35	5.80	31.90	18.09	6.26
Saturated water content (SAT), v%	38.10	41.60	39.21	0.91	38.10	42.20	39.03	0.88
Whole profile drainage rate coefficient (SWCON)	20.1	90.0	62.18	21.91	18.1	90.0	44.74	23.12
Saturated hydraulic conductivity (Ksat), mm h^{-1}	5.07	144.82	56.64	38.10	3.11	137.14	34.46	35.04

1. Abbreviation: MIN: minimum, MAX: maximum, SD: standard deviation.

Table A2.8. Results of full model, backward selection model and bootstrap models with backward selection procedure (1000 replications) for switchgrass biomass yield (Mg ha^{-1}) at Lux Arbor Farm.

	Full Model		Backward Select Model		Bootstrap (1000 replications)			
	Coef[1]	SE[1]	Coef[1]	SE[1]	Inclusion[1]	M[1]	2.5%[1]	97.5%[1]
(Intercept)	4.95	0.19	4.96	0.13	1	4.94	4.59	5.30
Topographical wetness index (TWI)	1.30	0.37	1.04	0.16	0.997	1.24	0.66	2.02
Late growing season precipitation (late), mm	5.13	2.64	5.47	2.44	0.957	5.08	0	10.66
Magnesium (Mg), mg kg^{-1}	-1.12	0.42	-1.08	0.20	0.955	-1.12	-1.89	0
pH	0.55	0.21	0.55	0.17	0.909	0.55	0	0.98
Profile curvature, km^{-1}	3.03	1.43	2.93	1.18	0.844	2.96	0	5.58
Potassium (K), mg kg^{-1}	0.50	0.24	0.47	0.19	0.784	0.50	0	1.05
Early growing season precipitation (early), mm	-0.61	0.34	-0.71	0.29	0.741	-0.63	-1.37	0
Ammonium (NH_4^+), mg kg^{-1}	0.41	0.23	0.29	0.17	0.713	0.41	0	0.97
Middle growing season precipitation (middle), mm	4.32	2.48	4.62	2.30	0.712	4.22	-0.25	9.43
Sand content, wt%	1.00	14.62	0.00	0.00	0.697	0	-32.77	28.34
Saturated water content(SAT), v%	-1.50	2.68	-1.23	0.40	0.649	-0.61	-6.86	4.18
Slope, °	-0.38	0.34	-0.44	0.16	0.631	-0.41	-0.93	0
Sand content, wt%	-0.32	8.39			0.581	0	-16.21	16.44
Drained upper limit of soil water content (DUL), v%	-0.12	16.68			0.518	0	-32.35	32.56
Saturated hydraulic conductivity (Ksat), mm h^{-1}	0.89	1.84			0.509	0	-2.92	4.19
Phosphorus (P), mg kg^{-1}	-0.20	0.26			0.404	0	-0.79	0.50
Whole profile drainage rate coefficient (SWCON)	0.80	1.57	1.25	0.62	0.395	0	-2.69	3.79
Plane curvature, km^{-1}	0.96	2.23			0.377	0	-2.79	5.29
Elevation, m	0.09	0.25			0.316	0	-0.47	0.57
15 bar lower limit of soil water content (LL15), v%	1.08	5.97	1.67	0.79	0.299	0	-8.46	11.64
Aspect	0.07	0.20			0.280	0	-0.29	0.46
Calcium (Ca), mg kg^{-1}	-0.09	0.48			0.259	0	-1.12	0.98
Total soil carbon (C) , wt%	0.01	0.22			0.233	0	-0.44	0.47

1. Abbreviation: Coef: estimation of coefficient, SE: standard error for the estimation of coefficient, Inclusion: inclusion probability, M: median, 2.5%: 2.5 percentile, 97.5%: 97.5 percentile.

Table A2.9. Results of full model, backward selection model and bootstrap models with backward selection procedure (1000 replications) for restored prairie biomass yield (Mg ha^{-1}) at Lux Arbor Farm.

	Full Model		Backward Select Model		Bootstrap (1000 Replications)			
	Coef[1]	SE[1]	Coef[1]	SE[1]	Inclusion[1]	M[1]	2.5%[1]	97.5%[1]
(Intercept)	4.11	0.43	4.07	0.13	1	3.97	3.23	4.95
Magnesium (Mg), mg kg^{-1}	-1.87	0.43	-1.83	0.30	0.999	-1.87	-2.81	-0.70
Aspect	0.61	0.15	0.66	0.14	0.995	0.56	0.25	0.89
Calcium (Ca), mg kg^{-1}	1.11	0.41	1.21	0.31	0.921	1.17	0	2.04
Late growing season precipitation (late), mm	2.70	2.00	0.61	0.11	0.872	2.05	0	7.25
Saturated hydraulic conductivity (Ksat), mm h^{-1}	-83.63	57.04	-2.07	0.98	0.833	-71.31	-206.94	0
Phosphorus (P), mg kg^{-1}	0.37	0.20	0.51	0.14	0.822	0.41	0	0.82
Drained upper limit of soil water content (DUL), v%	19.49	9.55	23.89	8.65	0.821	18.31	0	40.2
Elevation, m	-0.52	0.23	-0.55	0.19	0.816	-0.51	-1.16	0
Sand content, wt%	12.13	6.24	14.97	5.47	0.800	12.00	-0.37	26.52
Saturated water content (SAT), v%	3.67	2.22	4.51	1.70	0.761	3.72	0	8.53
Whole profile drainage rate coefficient (SWCON)	81.85	57.24			0.675	60.76	-3.52	206.11
15 bar lower limit of soil water content (LL15), v%	-18.76	23.81	-17.88	6.34	0.655	-11.50	-66.34	34.36
Potassium (K), mg kg^{-1}	0.27	0.19	0.32	0.14	0.631	0.27	0	0.73
Middle growing season precipitation (middle), mm	2.03	1.87			0.628	1.52	-0.70	6.36
Profile curvature	1.76	1.26	1.70	1.11	0.575	1.63	0	4.49
Plane curvature	1.43	1.06	1.71	0.90	0.538	1.20	0	3.35
Total soil carbon(C) , wt%	0.27	0.26			0.487	0	0	0.83
Clay content, wt%	3.96	22.58			0.454	0	-38.25	48.44
Ammonium (NH_4^+), mg kg^{-1}	-0.03	0.19			0.402	0	-0.43	0.74
Topographical wetness index (TWI)	0.01	0.20			0.388	0	-0.47	0.53
Early growing season precipitation (early), mm	-0.10	0.25			0.369	0	-0.61	0.47
pH	0.09	0.20			0.333	0	-0.34	0.49
Slope, °	0.03	0.22			0.271	0	-0.35	0.48

1. Abbreviation: Coef: estimation of coefficient, SE: standard error for the estimation of coefficient, Inclusion: inclusion probability, M: median, 2.5%: 2.5 percentile, 97.5%: 97.5 percentile.

Table A2.10. Results of full model, backward selection model and bootstrap models with backward selection procedure (1000 replications) for switchgrass biomass yield (Mg ha^{-1}) at Marshall Farm.

	Full Model		Backward Select Model		Bootstrap (1000 Replications)			
	Coef[1]	SE[1]	Coef[1]	SE[1]	Inclusion[1]	M[1]	2.50%[1]	97.50%[1]
(Intercept)	6.86	0.35	7.12	0.17	1	6.93	6.18	7.57
Late growing season precipitation (late), mm	2.30	1.61	1.39	0.18	0.816	1.39	0	5.54
Profile curvature	-2.61	1.72	-3.42	1.17	0.709	-2.90	-6.60	0
Total soil carbon (C), wt%	-0.44	0.28	-0.41	0.17	0.701	-0.46	-1.04	0
Sand content, wt%	-0.29	8.56	0.00	0.00	0.674	0	-16.54	15.07
15 bar lower limit of soil water content (LL15), v%	11.04	8.87	0.00	0.00	0.629	9.25	-3.63	29.30
Saturated hydraulic conductivity (Ksat), mm h^{-1}	-1.81	2.17	-1.87	0.41	0.625	-0.99	-5.80	2.51
Drained upper limit of soil water content (DUL), v%	-3.39	17.49	-1.44	0.40	0.595	0	-36.17	29.19
Ammonium (NH_4^+), mg kg^{-1}	0.29	0.22	0.29	0.18	0.563	0.28	0	0.75
Clay content, wt%	-9.12	13.29			0.551	0	-29.93	18.75
Middle growing season precipitation (middle), mm	1.25	1.50			0.549	0	-1.46	4.07
Saturated water content (SAT), v%	0.19	1.51			0.527	0	-2.51	2.61
Early growing season precipitation (early), mm	2.01	2.95			0.496	0	-2.92	7.66
Aspect	-0.27	0.25			0.491	0	-0.71	0
Phosphorus (P), mg kg^{-1}	0.29	0.31			0.466	0	0	0.84
Plane curvature	0.63	1.12			0.426	0	-1.49	3.13
Topographical wetness index (TWI)	-0.15	0.38			0.385	0	-0.82	0.67
Elevation, m	0.10	0.38			0.369	0	-0.86	0.92
pH	-0.06	0.44			0.34	0	-0.90	0.97
Magnesium (Mg), mg kg^{-1}	0.07	0.32			0.317	0	-0.56	0.69
Whole profile drainage rate coefficient (SWCON)	0.14	1.46			0.306	0	-2.38	2.93
Calcium (Ca), mg kg^{-1}	-0.13	0.43			0.304	0	-1.08	0.88
Potassium (K), mg kg^{-1}	0.09	0.35			0.303	0	-0.52	0.75
Slope, °	0.02	0.33			0.278	0	-0.67	0.57

1. Abbreviation: Coef: estimation of coefficient, SE: standard error for the estimation of coefficient, Inclusion: inclusion probability, M: median, 2.5%: 2.5 percentile, 97.5%: 97.5 percentile.

Table A2.11. Results of full model, backward selection model and bootstrap models with backward selection procedure (1000 replications) for restored prairie biomass yield (Mg ha^{-1}) at Marshall Farm.

	Full Model		Backward Select Model		Bootstrap (1000 Replications)			
	Coef[1]	SE[1]	Coef[1]	SE[1]	Inclusion[1]	M[1]	2.50%[1]	97.50%[1]
(Intercept)	3.20	0.18	3.32	0.09	1	3.25	2.87	3.57
Total soil carbon(C), wt%	-0.82	0.19	-0.71	0.15	1	-0.78	-1.21	-0.41
Middle growing season precipitation (middle), mm	2.68	0.76	2.76	0.72	0.993	2.66	0.74	4.13
Late growing season precipitation (late), mm	2.49	0.84	2.55	0.81	0.979	2.51	0.43	4.06
Early growing season precipitation (early), mm	4.49	1.50	4.62	1.44	0.974	4.47	0	7.28
pH	-0.47	0.19	-0.56	0.14	0.893	-0.48	-0.88	0
Slope, °	-0.39	0.15	-0.37	0.10	0.88	-0.34	-0.70	0
Elevation, m	-0.31	0.16	-0.31	0.10	0.817	-0.29	-0.61	0
Calcium (Ca), mg kg^{-1}	0.42	0.23	0.56	0.17	0.781	0.45	0	0.91
Ammonium (NH_4^+), mg kg^{-1}	-0.25	0.13	-0.27	0.10	0.706	-0.23	-0.51	0
15 bar lower limit of soil water content (LL15), v%	3.25	3.19			0.595	0.61	-3.98	11.31
Phosphorus, mg kg^{-1}	0.23	0.17	0.18	0.11	0.583	0.19	0	0.62
Saturated water content (SAT), v%	0.21	0.57	0.28	0.10	0.522	0	-0.93	1.43
Drained upper limit of soil water content (DUL), v%	-4.01	8.56			0.509	0	-19.84	11.12
Sand content, wt%	-2.30	5.35			0.49	0	-12.06	6.99
Saturated hydraulic conductivity (Ksat), mm h^{-1}	0.22	0.99			0.481	0	-1.86	2.25
Clay content, wt%	-1.02	4.75			0.449	0	-10.50	8.06
Whole profile drainage rate coefficient (SWCON)	-0.02	0.78			0.399	0	-1.73	1.54
Magnesium (Mg), mg kg^{-1}	0.15	0.19			0.392	0	-0.24	0.61
Potassium (K), mg kg^{-1}	0.11	0.18			0.378	0	-0.34	0.49
Profile curvature	0.09	0.38			0.305	0	-0.88	0.78
Topographical wetness index (TWI)	-0.02	0.22			0.274	0	-0.44	0.47
Aspect	0.07	0.13			0.258	0	-0.17	0.31
Plane curvature	0.04	0.38			0.221	0	-0.64	0.67

1. Abbreviation: Coef: estimation of coefficient, SE: standard error for the estimation of coefficient, Inclusion: inclusion probability, M: median, 2.5%: 2.5 percentile, 97.5%: 97.5 percentile

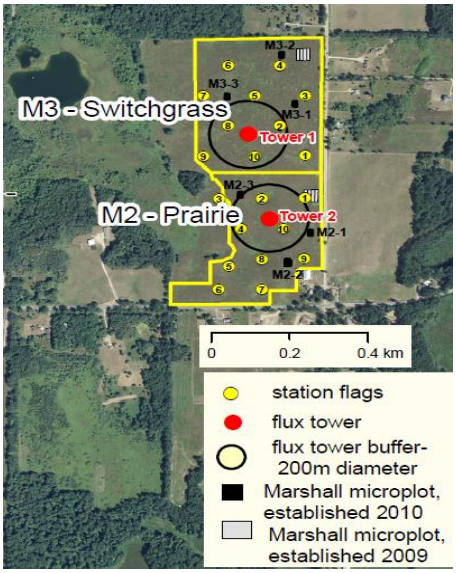

Figure A2.1. Great Lakes Bioenergy Research Center Scale-up Experiment: aerial view of Marshall Farm with field boundaries.

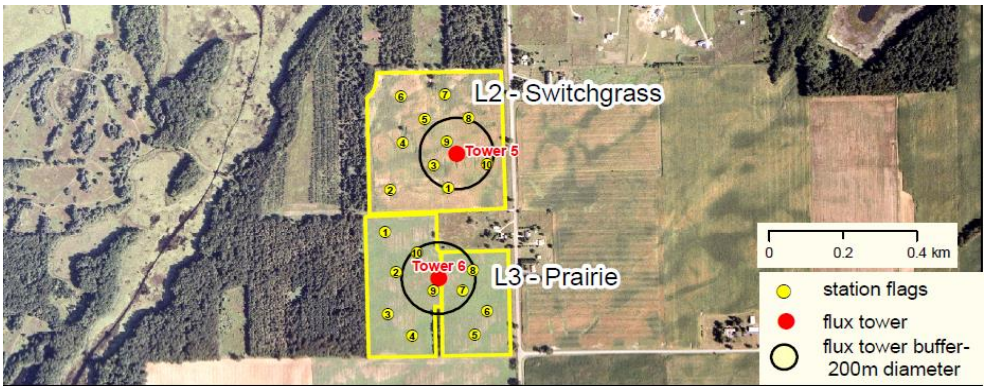

Figure A2.2. Great Lake Bioenergy Research Center Scale-up Fields: aerial view of Lux Arbor Farm with field boundaries.

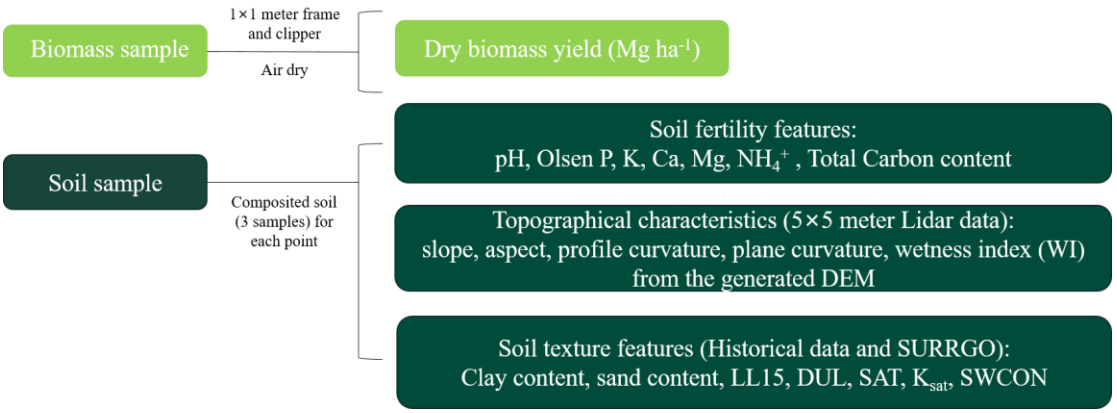

Figure A2.3. Flow chart of biomass samples and soil samples parameters.

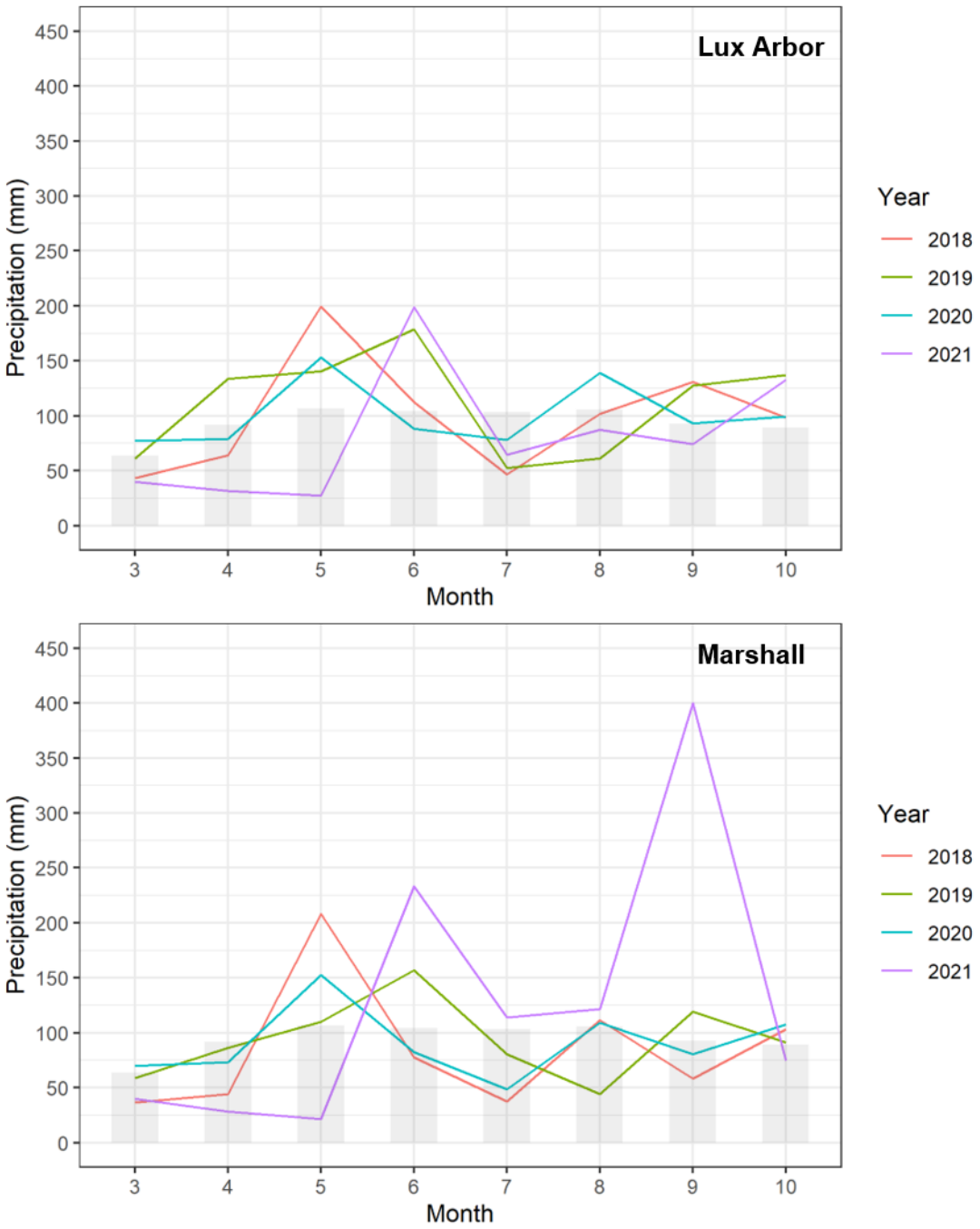

Figure A2.4. Monthly precipitation (mm) during growing season (March-October) at Lux Arbor Farm (upper panel) and Marshall Farm (lower panel) over the study period (2018-2021) and 30 years average.

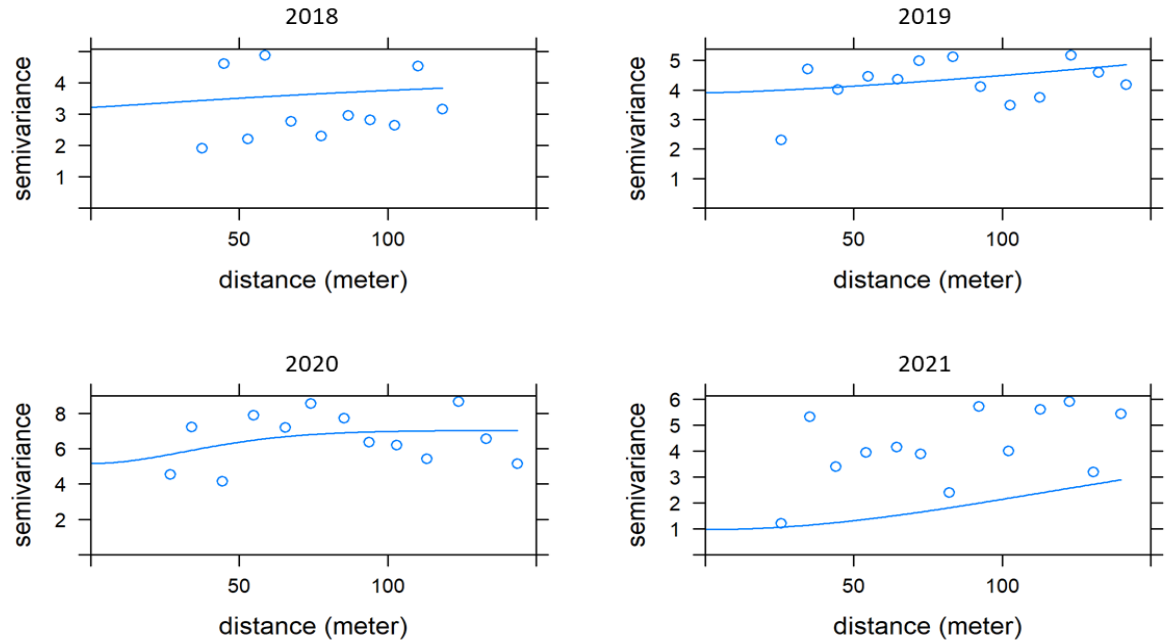

Figure A2.5. Empirical semi-variograms with best fitted Matern correlation models of switchgrass biomass yield (Mg ha^{-1}) at Lux Arbor Farm over the study period (2018-2021).

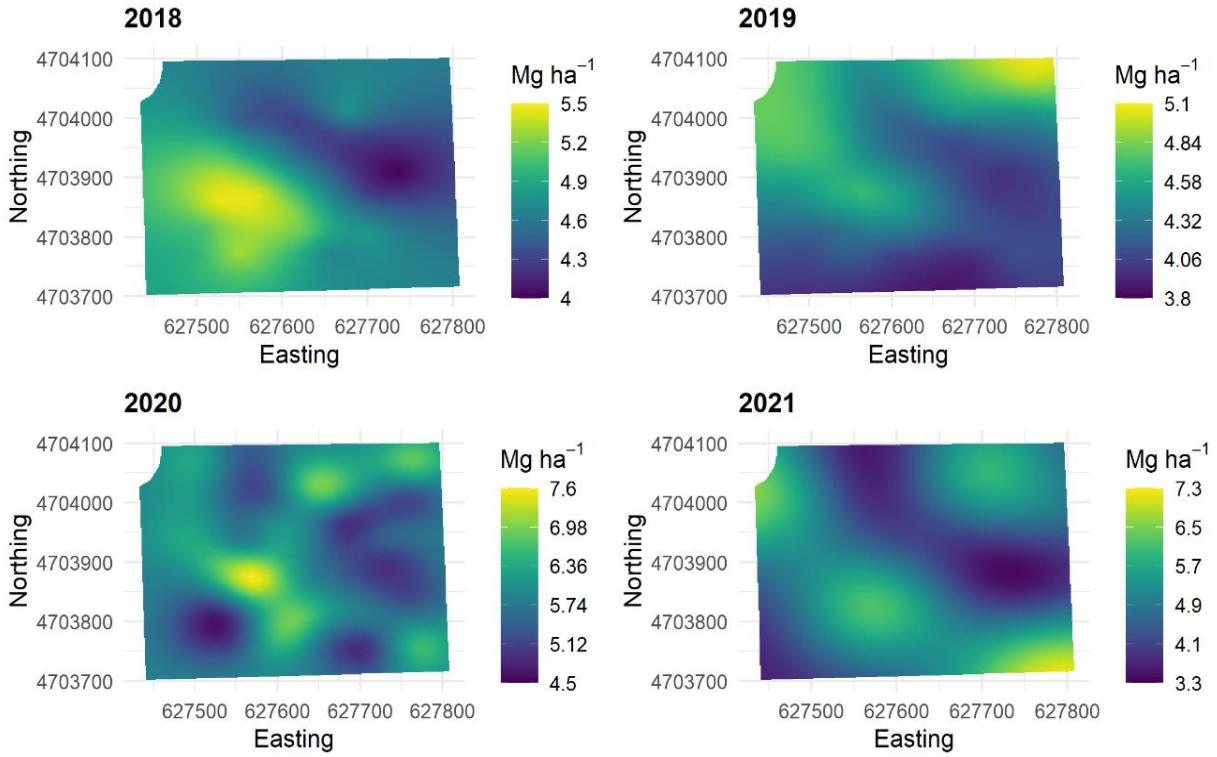

Figure A2.6. Ordinary kriging maps for switchgrass biomass yield (Mg ha^{-1}) at Lux Arbor Farm over the study period (2018-2021).

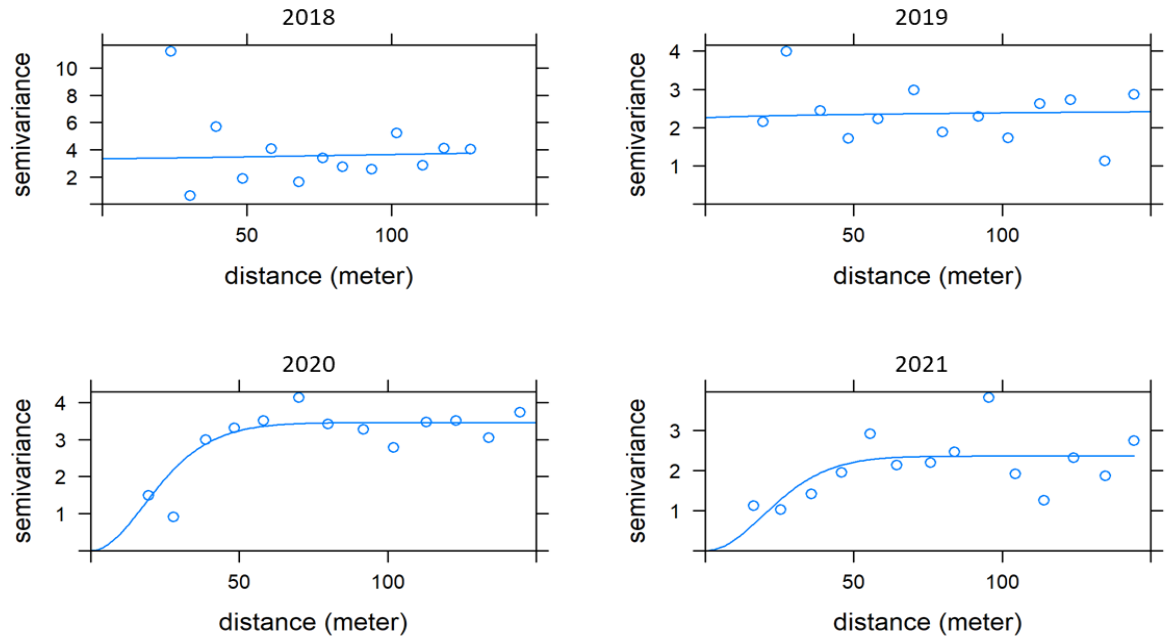

Figure A2.7. Empirical semi-variograms with best fitted Matern correlation models of restored prairie biomass yield (Mg ha^{-1}) at Lux Arbor Farm over the study period (2018-2021).

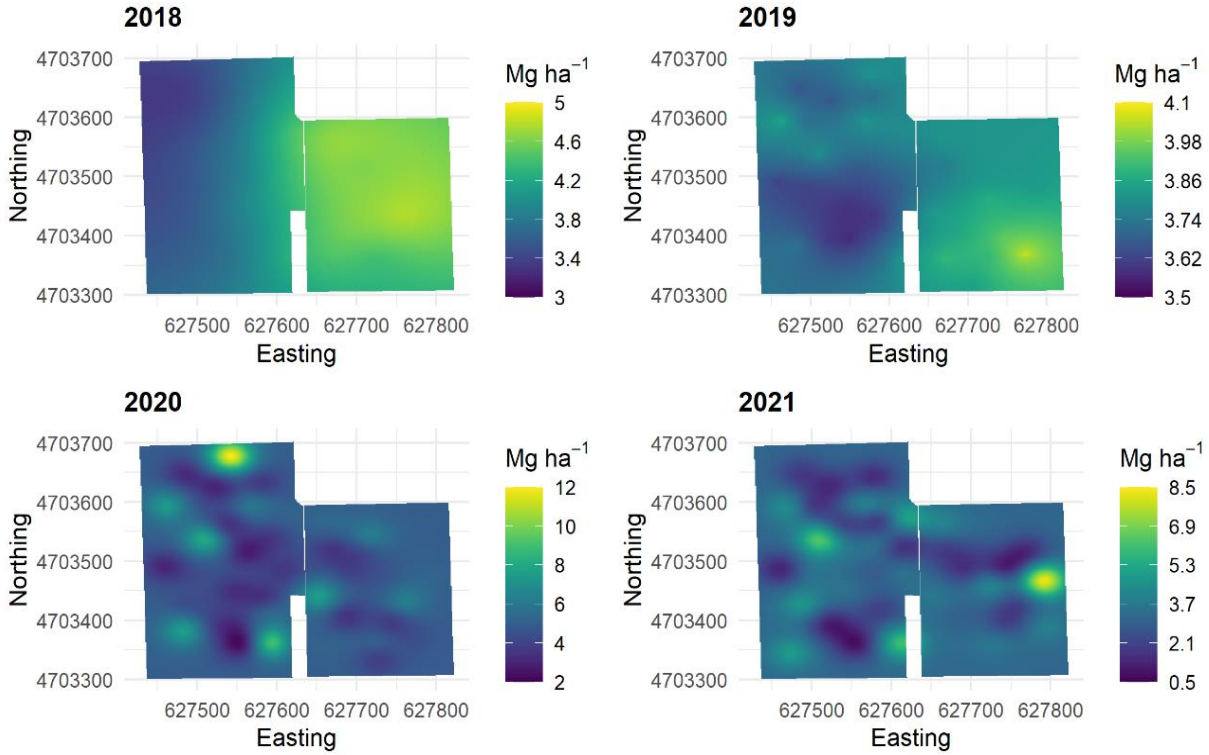

Figure A2.8. Ordinary kriging maps for restored prairie biomass yield (Mg ha^{-1}) at Lux Arbor Farm over the study period (2018-2021).

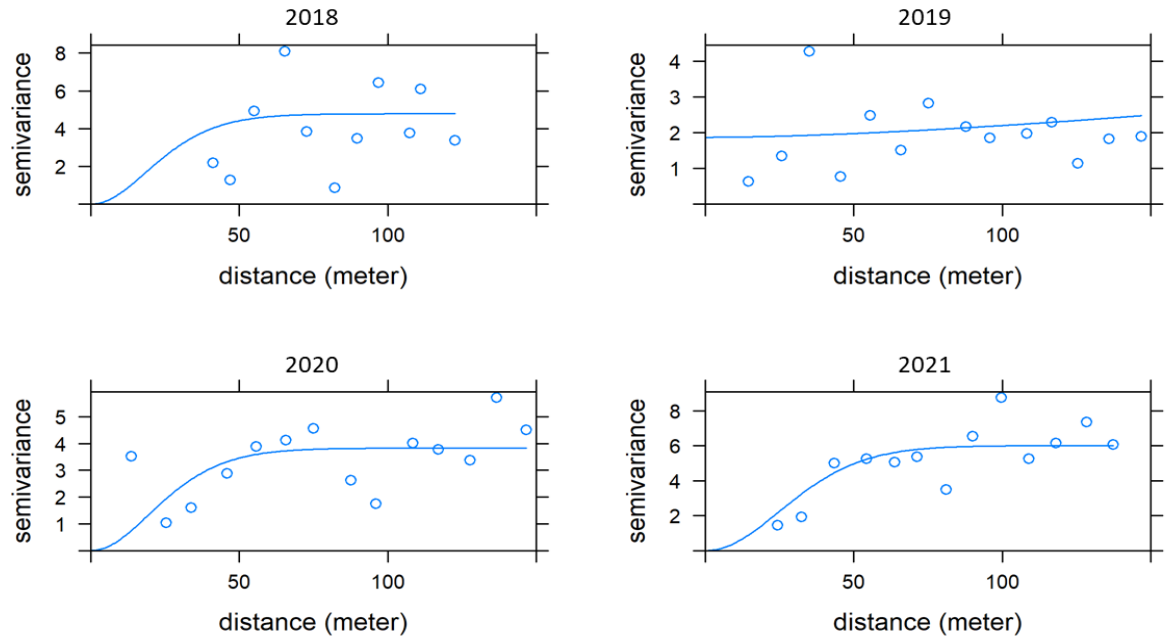

Figure A2.9. Empirical semi-variograms with best fitted Matern correlation models of switchgrass biomass yield (Mg ha^{-1}) at Marshall Farm over the study period (2018-2021).

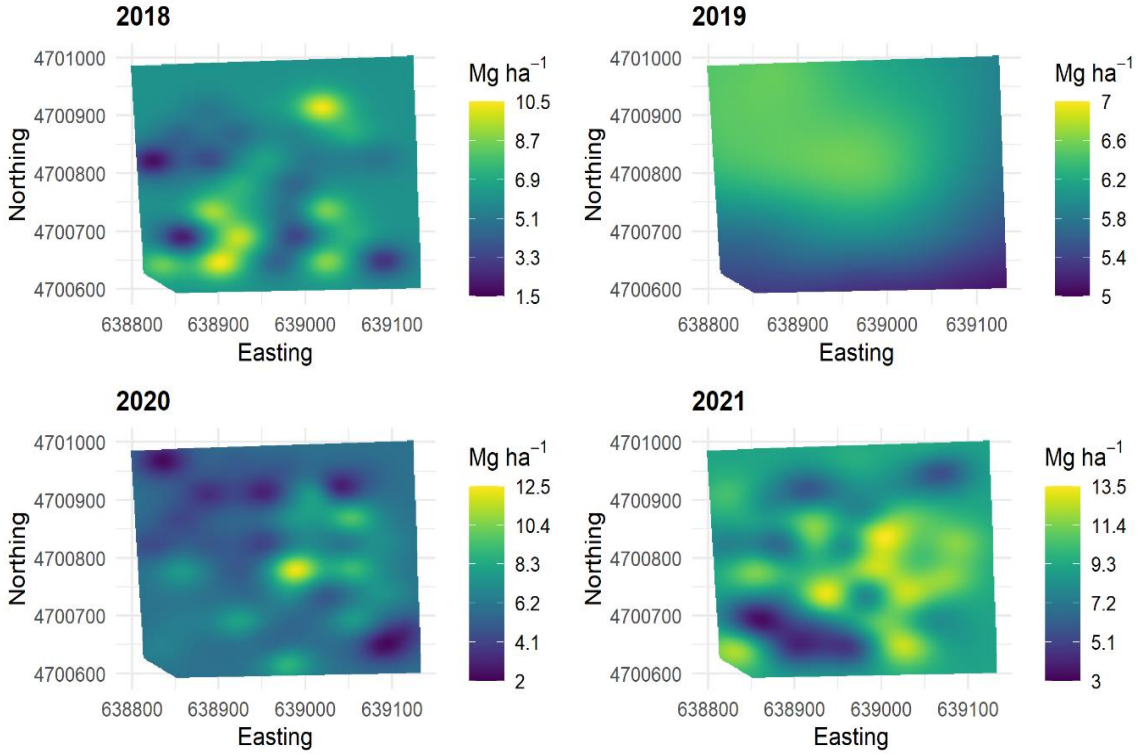

Figure A2.10. Ordinary kriging maps for switchgrass biomass yield (Mg ha^{-1}) at Marshall Farm over the study period (2018-2021).

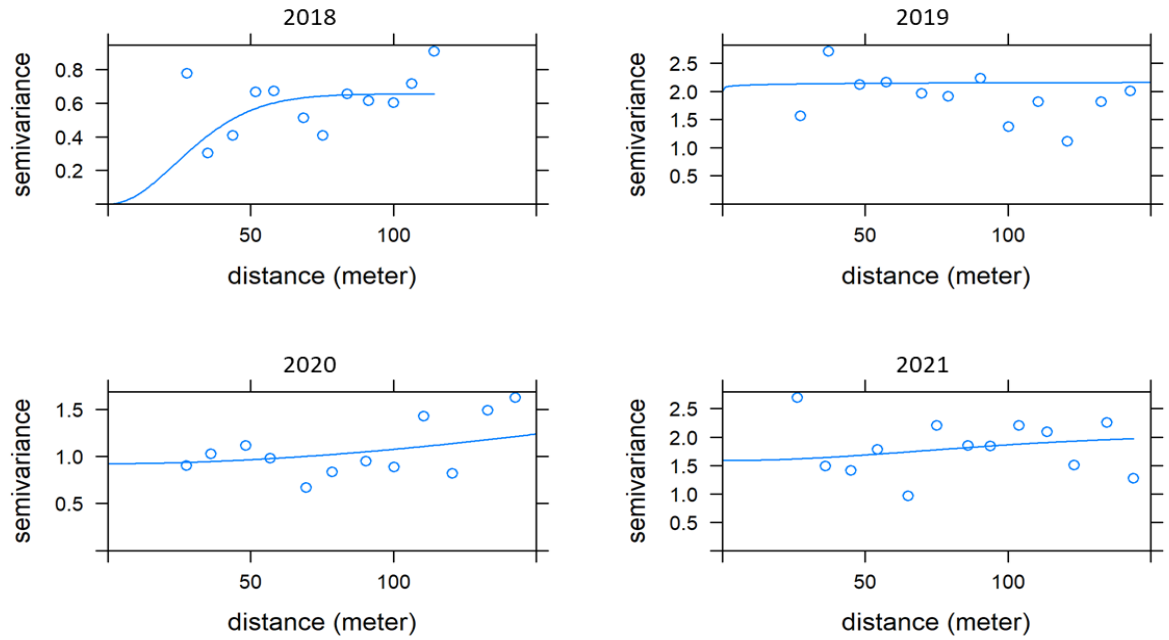

Figure A2.9. Empirical semi-variograms with best fitted Matern correlation models of restored prairie biomass yield (Mg ha^{-1}) at Marshall Farm over the study period (2018-2021).

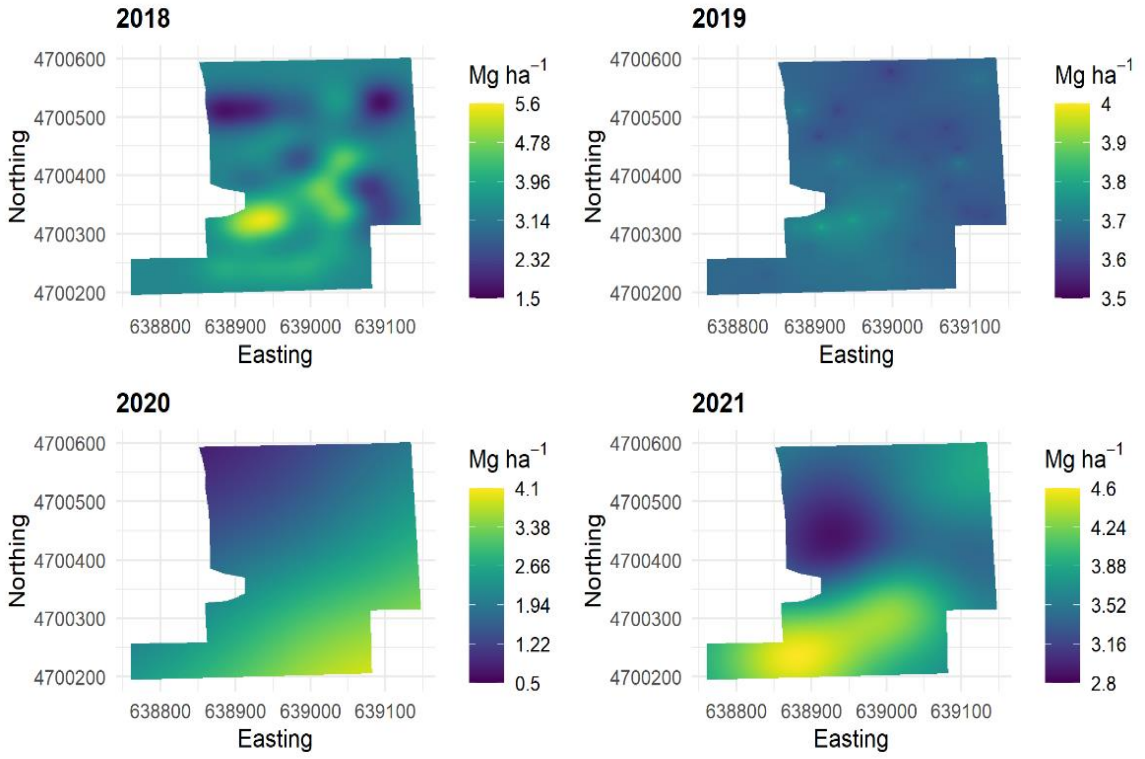

Figure A2.12. Ordinary kriging maps for restored prairie biomass yield (Mg ha^{-1}) at Marshall Farm over the study period (2018-2021).

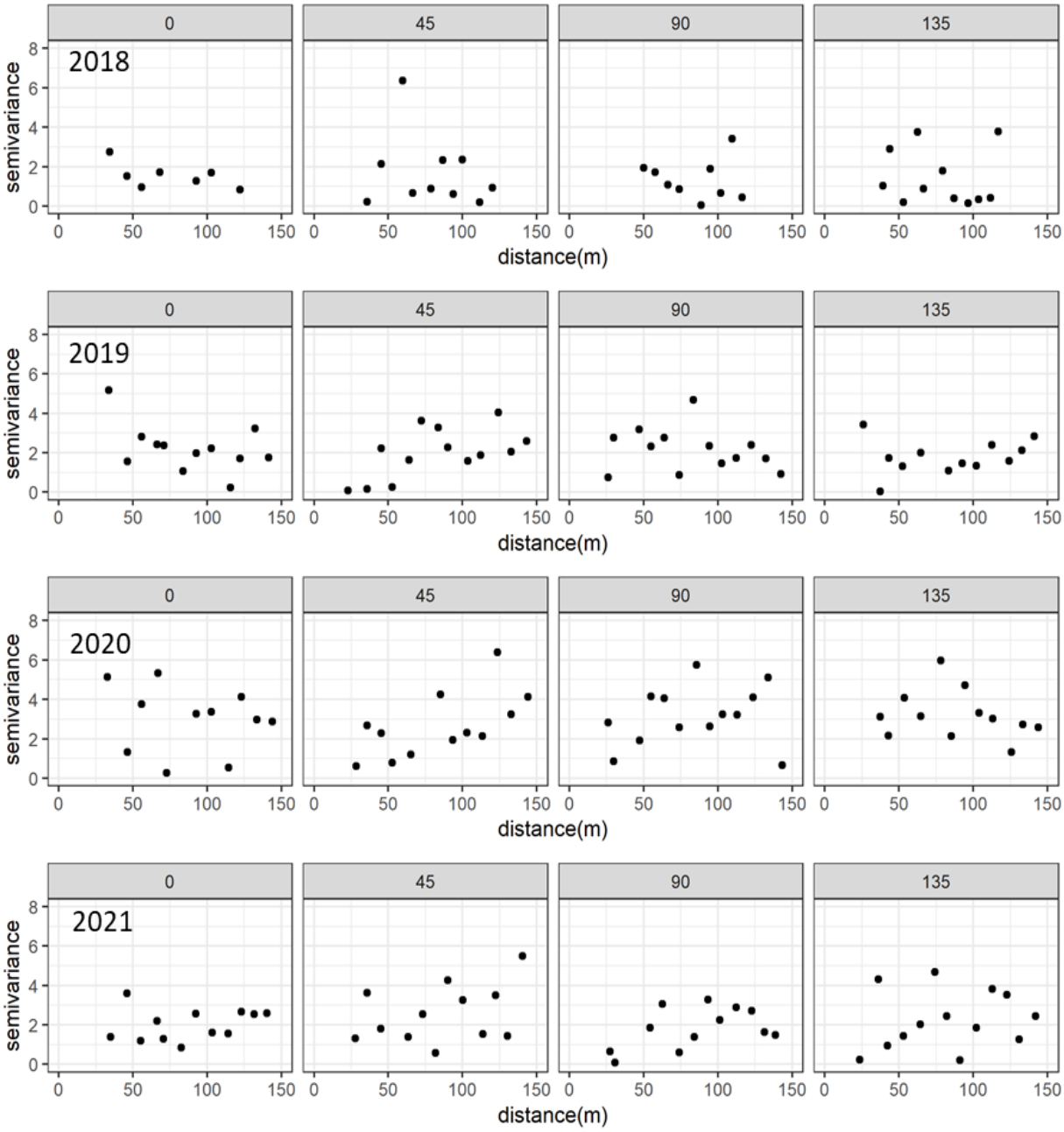

Figure A2.13. Directional semi-variograms for switchgrass biomass yield (Mg ha^{-1}) at Lux Arbor Farm over the study period (2018-2021). Direction at 0, 45, 90 and 135 degrees.

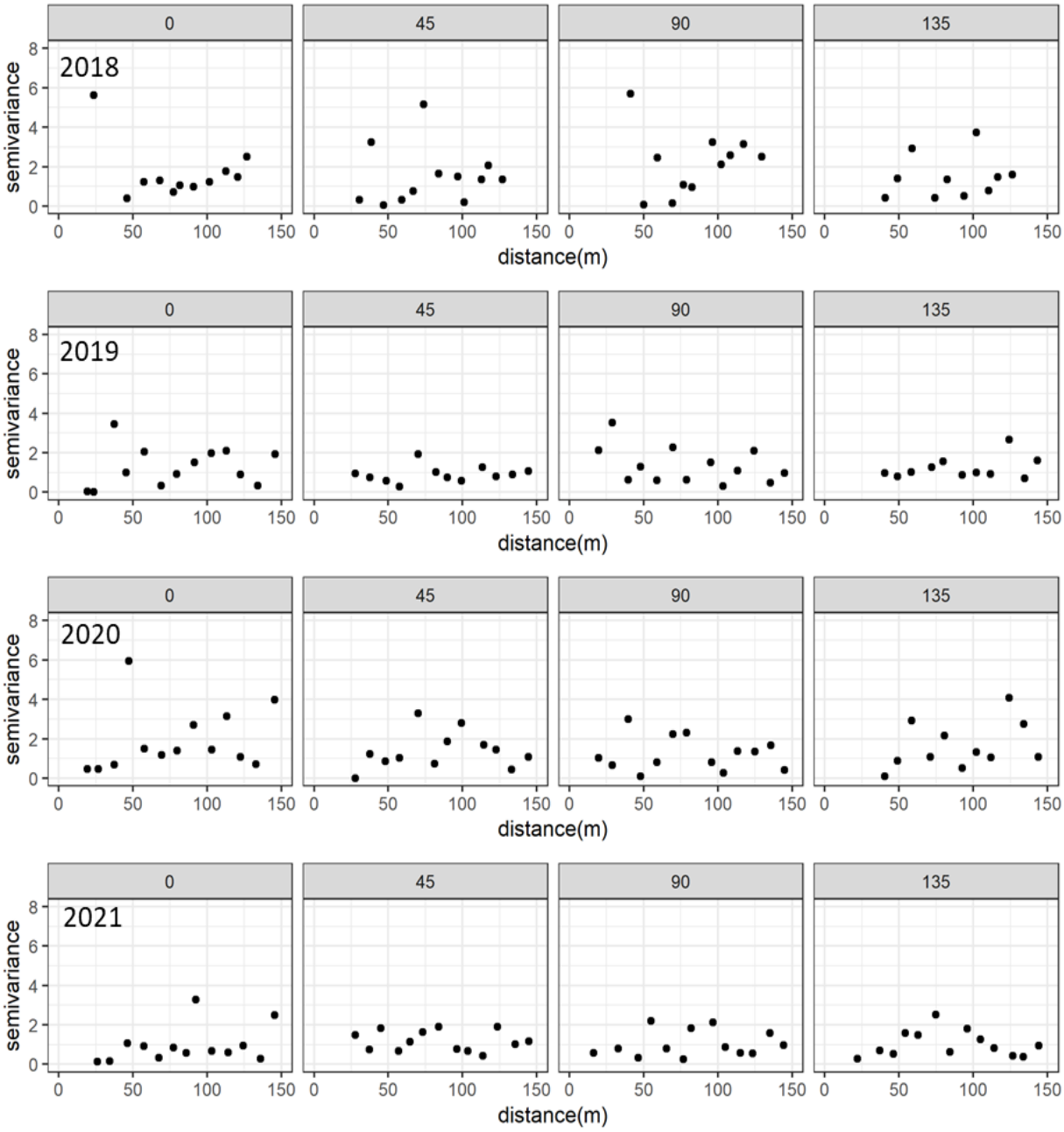

Figure A2.14. Directional semi-variograms of restored prairie biomass yield (Mg ha^{-1}) at Lux Arbor Farm over the study period (2018-2021). Direction at 0, 45, 90 and 135 degrees.

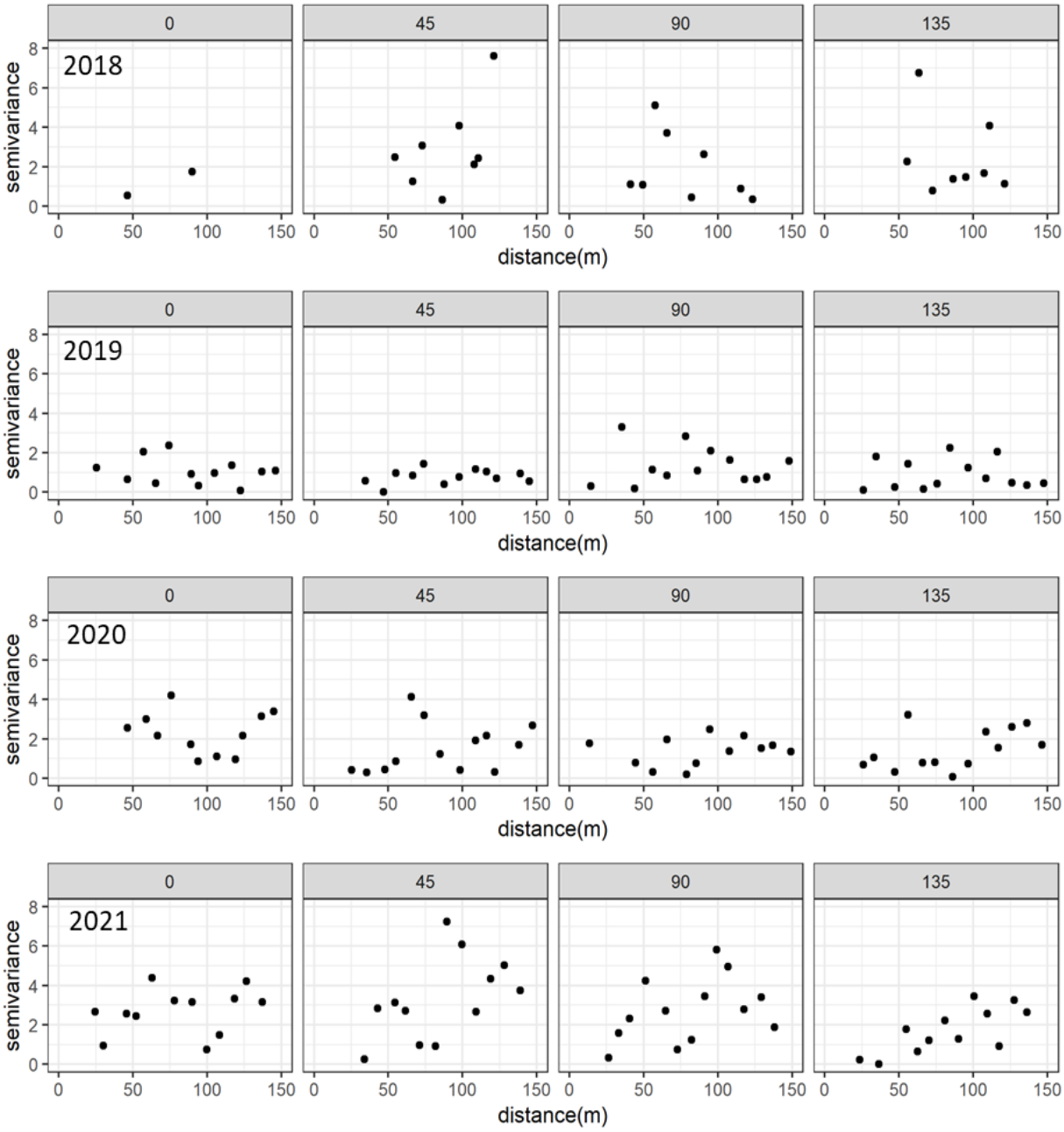

Figure A2.15. Directional semi-variograms for switchgrass biomass yield (Mg ha^{-1}) at Marshall Farm over the study period (2018-2021). Direction at 0, 45, 90 and 135 degrees.

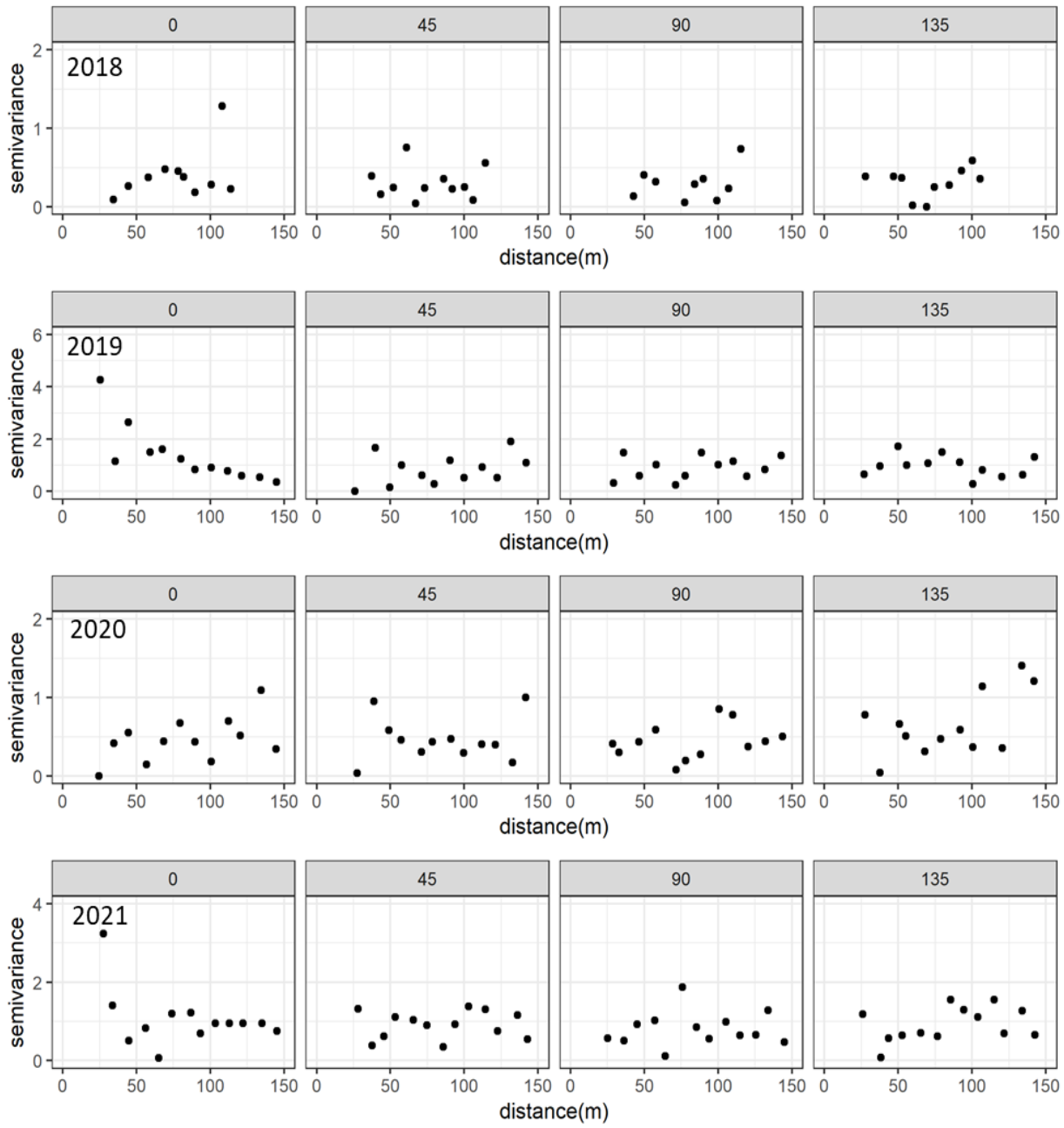

Figure A2.16. Directional semi-variograms of restored prairie biomass yield (Mg ha^{-1}) at Lux Arbor Farm over the study period (2018-2021). Direction at 0, 45, 90 and 135 degrees.

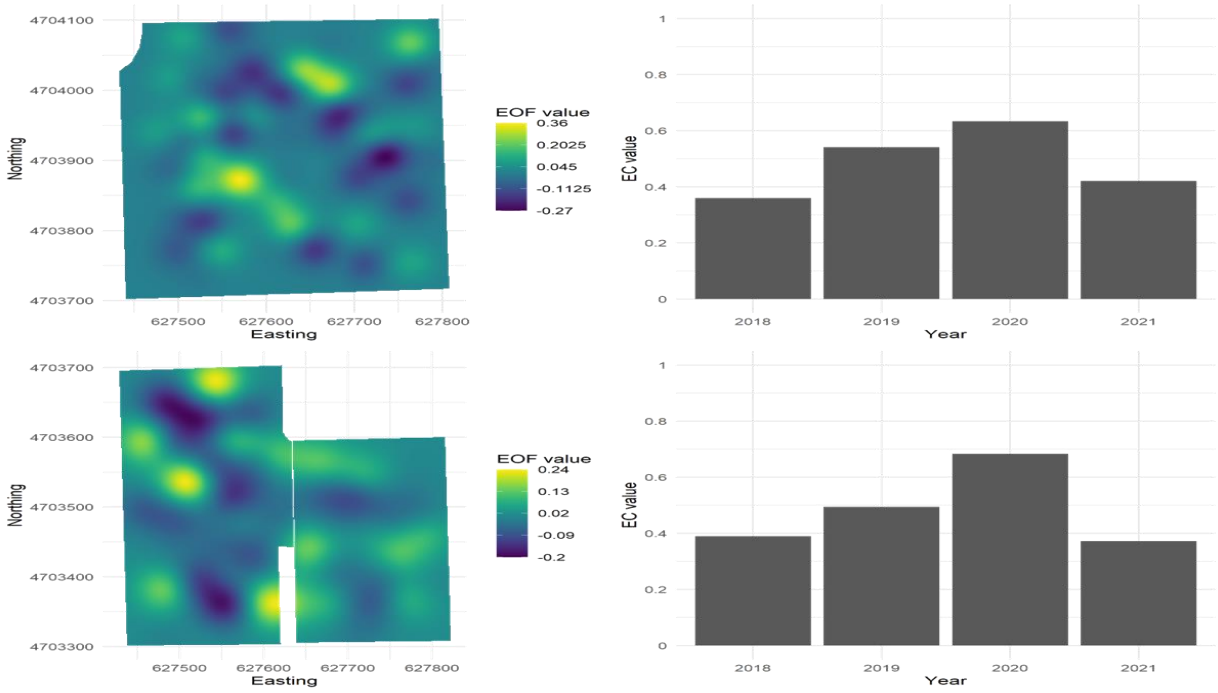

Figure A2.17. The leading spatial empirical orthogonal function (EOF) and time series of expansion efficient (EC) for switchgrass biomass yield (upper panel) and restored prairie biomass yield (lower panel) at Lux Arbor Farm.

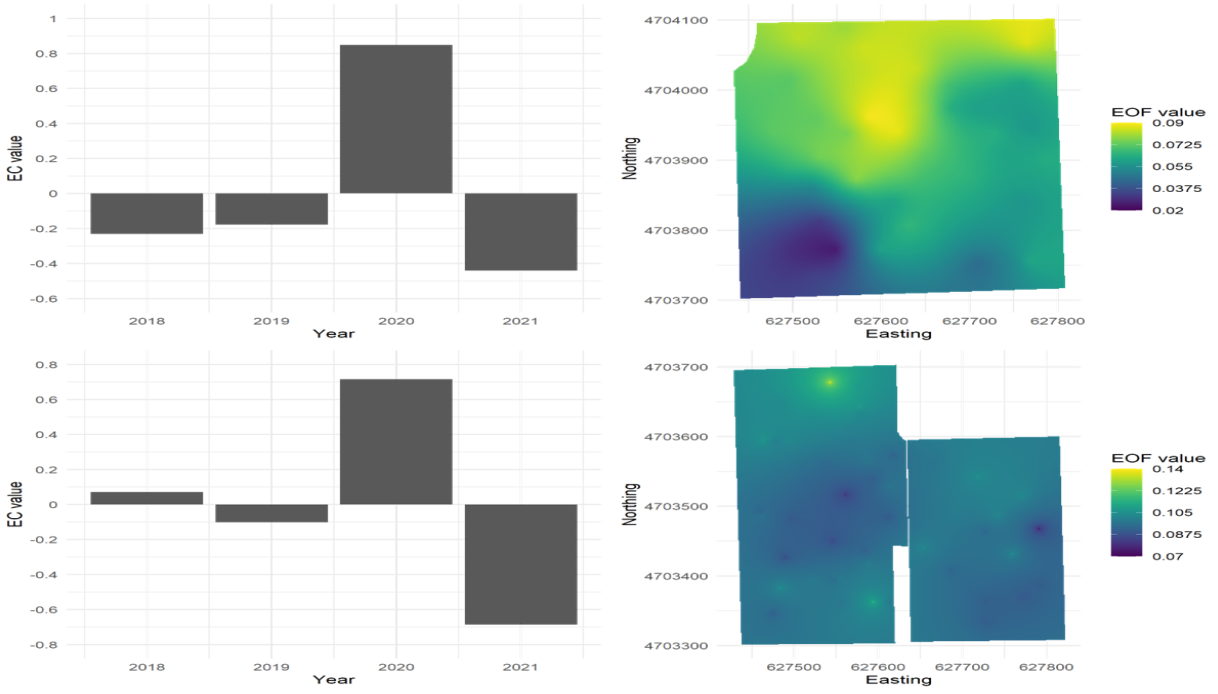

Figure A2.18. The leading temporal empirical orthogonal function (EOF) and time series of expansion efficient (EC) for switchgrass biomass yield (upper panel) and restored prairie biomass yield (lower panel) at Lux Arbor Farm.

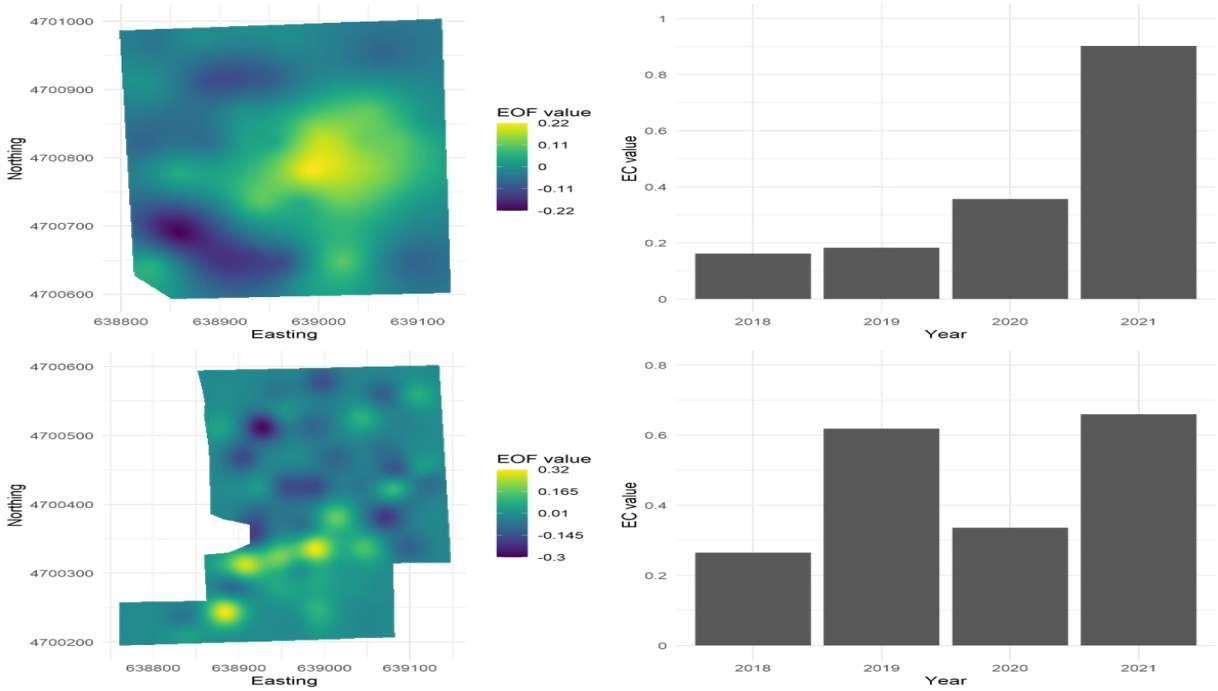

Figure A2.19. The leading spatial empirical orthogonal function (EOF) and time series of expansion efficient (EC) for switchgrass biomass yield (upper panel) and restored prairie biomass yield (lower panel) at Marshall Farm.

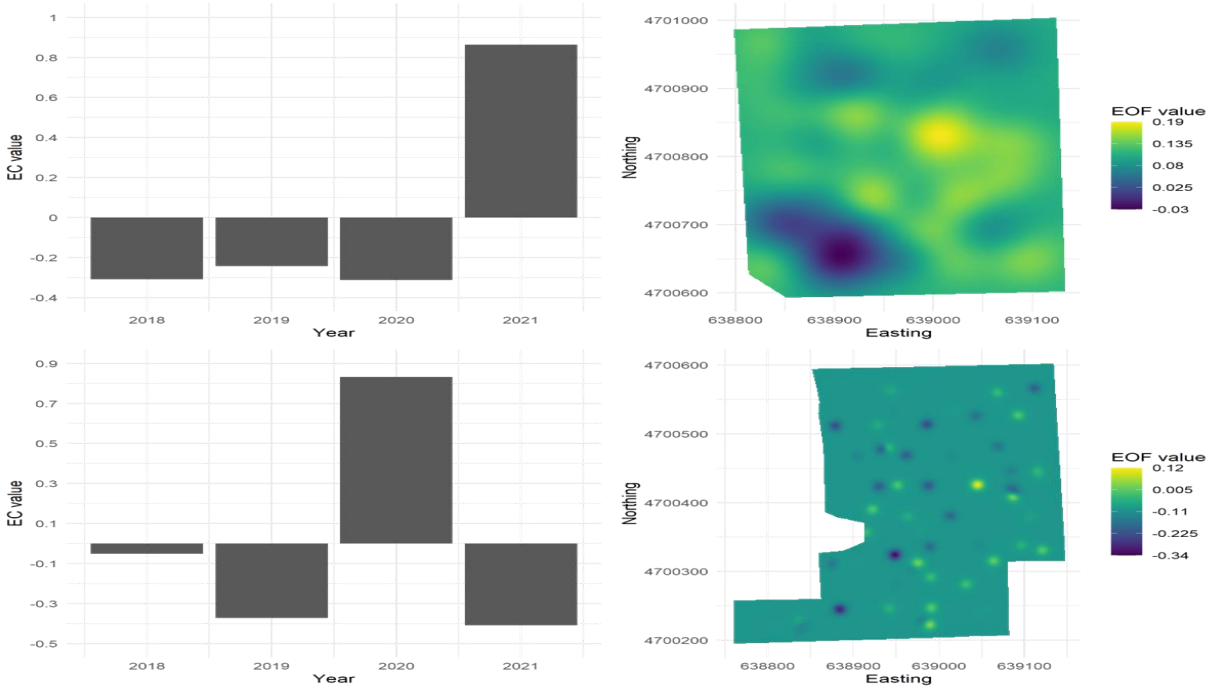

Figure A2.20. The leading temporal empirical orthogonal function (EOF) and time series of expansion efficient (EC) for switchgrass biomass yield (upper panel) and restored prairie biomass yield (lower panel) at Marshall Farm.

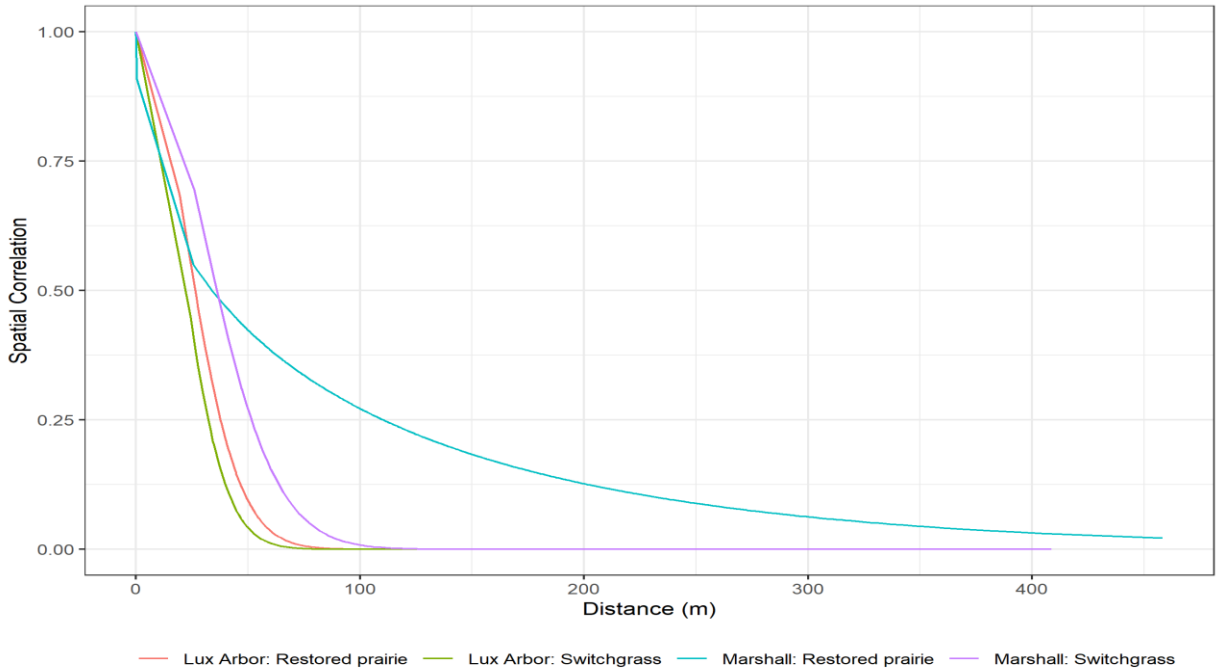

Figure A2.21. Matern spatial correlation from null model for switchgrass biomass yield and restored prairie biomass yield at Marshall Farm and Lux Arbor Farm.

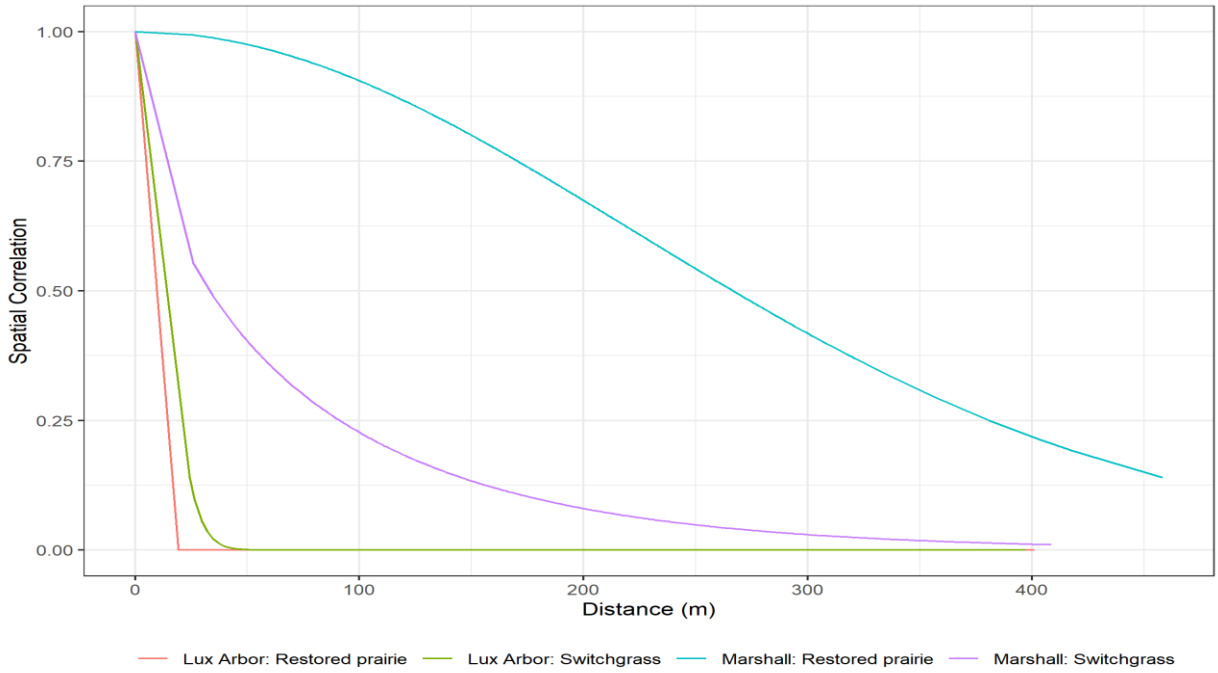

Figure A2.22. Matern spatial correlation from models with selected variables for switchgrass biomass yield and restored prairie biomass yield at Marshall Farm and Lux Arbor Farm.

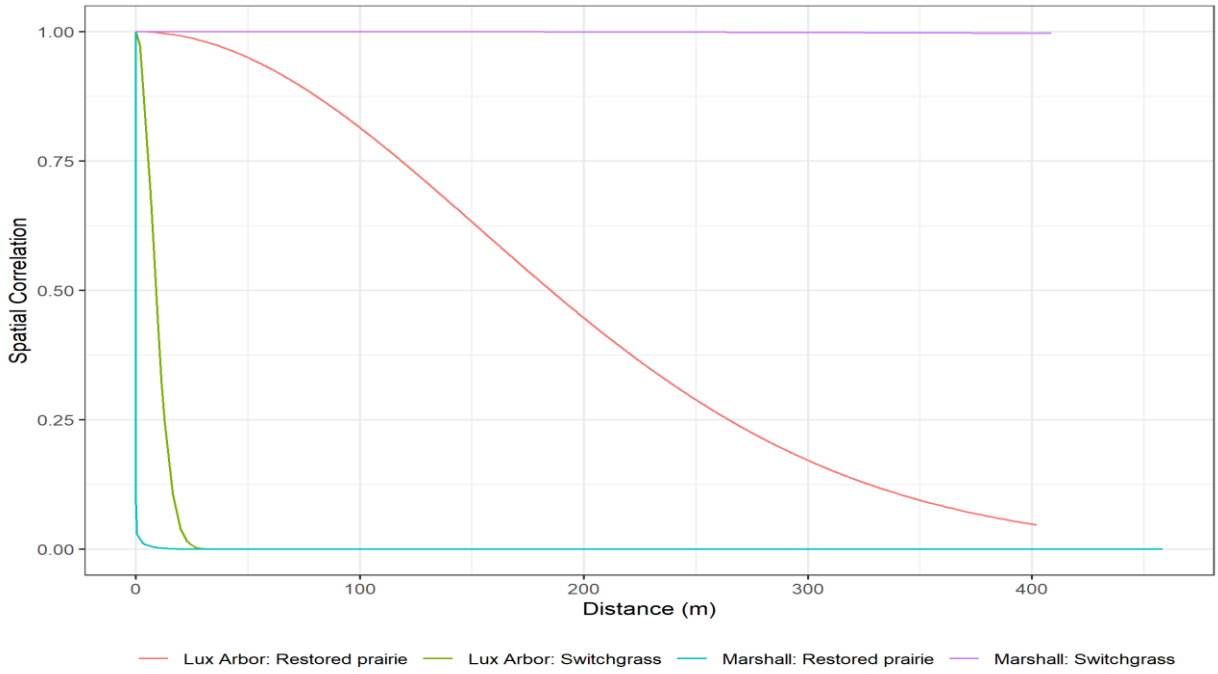

Figure A2.23. Matern spatial correlation plot from full models for switchgrass biomass yield and restored prairies biomass yield at Marshall Farm and Lux Arbor Farm.

CHAPTER 3 SPATIO-TEMPORAL VARIABILITY OF BIOMASS QUALITY COMPONENT LEVELS IN SWITCHGRASS AND RESTORED PRAIRIE IN THE GREAT LAKES REGION USA

Abstract

To help fill the research gap of spatio-temporal variability of biomass feedstock crop quality at field scale, an experiment on switchgrass (*Panicum virgatum*) and restored prairie quality variability was conducted at Marshall Farm (42.44° N, -85.32° W) and Lux Arbor Farm (42.48° N, -85.44° W) in southwest Michigan USA from 2018 to 2020. Randomly located biomass samples were collected during fall before senescence and analyzed for glucose ([Glc]: mg g^{-1}), xylose ([Xyl]: mg g^{-1}) and lignin (mg g^{-1}) content. Interannual temporal variability was higher than within-field spatial variability of [Glc], [Xyl] and lignin content for switchgrass and restored prairie at both farms. The ratio of interannual temporal variance to spatial variance for glucose [Glc] was 12.2 and 52.4 in switchgrass and 1.30 and 6.14 in restored prairie at Marshall Farm and Lux Arbor Farm, respectively. The ratio of interannual temporal variance to spatial variance for [Xyl] was 3.2 and 5.8 in switchgrass and 1.7 and 4.3 in restored prairie at Marshall Farm and Lux Arbor Farm, respectively. The ratio of interannual temporal variance to spatial variance for lignin was 5.5 and 1.0×10^5 in switchgrass and 9.1 and 18.8 in restored prairie at Marshall Farm and Lux Arbor Farm, respectively. Generally, [Glc] and [Xyl] of switchgrass and restored prairie were positively correlated within fields at both farms across the study period (2018-2020). Soil phosphorus and calcium concentrations were negatively related to [Glc] and [Xyl] of restored prairie at Lux Arbor Farm. Elevation, slope and sand content were positively associated with both [Glc] and [Xyl] of switchgrass at Marshall. Topographic wetness index (TWI) was negatively related to [Glc], [Xyl] and lignin content of restored prairie at Marshall Farm.

Introduction

Bioenergy is considered to be one of the most promising alternative energy sources for a greener energy future, especially for providing liquid transportation fuels (Calvin et al., 2021, IEA, 2022). Due to the fuel vs. food debate surrounding first generation biofuel feedstocks (grain-based), research focus has switched to second generation biofuel feedstocks (ligno-cellulosic based) (Valentine et al., 2012, Rai et al., 2022). Per current energy policy such as the Renewable Fuel Standard as authorized by the U.S. Energy Independence and Security Act of 2007, demand for renewable fuel is expected to increase in the future (OECD/FAO, 2021, IEA, 2022). The success of meeting the increasing demand of biofuel relies largely on developing a sustainable biomass feedstock supply (Kline et al., 2007).

Bioenergy feedstock production faces unique challenges, including yield and quality variability (Stoof et al., 2012). Earlier research focused more on feedstock biomass yield, and rarely explored within-field biomass quality variability (Heaton et al., 2004, D. K. Lee et al., 2018, Gill et al., 2022). Sanford et al. (2017) stated that biomass yield is the main driver of final product ethanol yield on a land area basis. Nonetheless, feedstock quality affects the final biofuel product through biomass processing and conversion. Concerns have been raised regarding increased biorefinery production costs due to inconsistency or poor quality of biomass feedstocks (Castillo-Villar et al., 2017). It has been well documented that quality of biomass such as moisture, ash and lignin content impact biofuel production and production costs (Castillo-villar et al., 2016, Metzner et al., 2019, Lan et al., 2020). The tradeoff between achieving high biomass yield per land unit and high quality of biomass has been highlighted by researchers (A. Hoover et al., 2019). Different feedstock quality features are desired for differing conversion routes. Thermochemical conversion processes work best with high caloric content of biomass feedstock

such as high lignin content and low mineral content including nitrogen and sulfur (Tanger et al., 2013). Biochemical conversion routes work best with biomass having more accessible polysaccharides and a lower lignin content (Brethauer & Studer, 2015). Recent research has demonstrated the possibility of blending biomass feedstocks, termed as feedstock formulation, to reduce overall quality variability (Kenney et al., 2013, Allison, 2018). Nevertheless, uniform quality of biomass is crucial for optimizing biofuel production from storage to conversion.

First generation biofuel feedstocks such as corn grain and sugarcane rely on starch and soluble sugar to produce fermentable biofuel. Unlike first generation biofuel feedstocks, the main energy source of the 2nd generation biofuel feedstocks (ligno-cellulosic based) originates from structural biochemicals in the plant cell wall. Plant cell wall material constitutes the largest available photosynthesized carbon reservoir (Carpita et al., 2020). The major components of plant cell walls are cellulose, hemicellulose and the polyphenol lignin. Cellulose is a linear polymer of β-1,4-linked glucose and makes up about 40-50% of plant material (Cosgrove, 2005). Multiple cellulose chains further form cellulose microfibril bundles, which function as the backbone of the cell wall (Maleki et al., 2016). Hemicellulose is assembled as amorphous heterogeneous polymers with β-1, 4-linked xylose as the main component (Scheller & Ulvskov, 2010). Through physico-chemical interaction, hemicellulose crosslinks cellulose microfibrils to form a complex network (Scheller & Ulvskov, 2010). This structural feature reduces the accessibility and digestibility of cellulose. Another major component of ligno-cellulosic biomass cell walls is lignin, a complex phenolic polymer embedded in the network of cellulose and hemicellulose (Liu et al., 2018). It provides plants with rigidity and functions as a defense system to increase plant resistance to lodging, pests, drought and other stresses (Liu et al., 2018). However, the recalcitrance of lignin hinders biofuel production during the conversion stage (Smith et al.,

2016). Recent studies on biomass pretreatment focusing on removing lignin and increasing accessibility of cellulose and hemicellulose for hydrolysis and fermentation have shown substantial increases of biofuel production (Wi et al., 2015, Prasad & Ankit, 2015). In addition to biofuel products, biomass feedstocks can also be used to produce platform chemicals and value-added chemicals such as glycerol, cellulose fiber, resin and bioplastics (Yang et al., 2012, De Bhowmick et al., 2018, Takkellapati et al., 2018, Ma et al., 2021). Recent research has shown that integrating value-added chemical production with biofuel production in a biorefinery is more sustainable and economically feasible than producing biofuel alone (Cheali et al., 2015, Zhang et al., 2020, Sharma et al., 2020).

Differences in biomass quality were not only found between species but also within species of bioenergy cropping systems. Bhandari et al. (2014) showed that the switchgrass upland ecotype yielded 2% higher lignin concentration than lowland ecotypes. Even within a single plant, stems had higher cellulose, hemicellulose and lignin content than leaves (Bergs et al., 2019, Ghasemi et al., 2013). In addition to genetic variability, environmental factors such as temperature and soil moisture content also play a critical role in biomass quality variability. Hoover et al. (2018) have shown that drought leads to high year to year variability of biomass quality. Moreover, research showed that agronomic practices such as harvesting time introduce significant variability of biomass quality (Gorlitsky et al., 2015).

Information regarding within-field variability in biomass feedstock quality at the field scale is lacking in the literature. This study evaluates the quality of bioenergy feedstocks on the field scale to facilitate the determination of crop species and potential agronomic management practices to optimize biomass quality for use as a bioenergy feedstock. Therefore, the objectives of this study are to 1) Examine within-field spatial and temporal variability of switchgrass and

restored prairie [Glc], [Xyl], and lignin content, and 2) Study the relationships between soil fertility characteristics and topographical features with the [Glc], [Xyl], and lignin content of switchgrass and restored prairie on the field scale.

Materials and methods

Experimental Site Description

Field-scale experiments were conducted at Marshall Farm (42.44° N, -85.32° W) and Lux Arbor Farm (42.48° N, -85.44° W) from 2018 to 2020, which are part of the Great Lakes Bioenergy Research Center experimental infrastructure located at Michigan State University's W.K. Kellogg Biological Station (KBS) in southwest Michigan. Soils in southwest Michigan are developed on glacial till and outwash from the last retreat of the Wisconsin glaciation (circa 12,500 years BP). Most soils are sandy loam and silty clay loams of moderate fertility and belong to the Alfisol, Mollisol, Histosol and Entisol soil orders in this area (Crum & Collins, 1995). All the fields at Marshall were enrolled in the USDA CRP program in 1987, with smooth brome grass (*Bromus inermis*) planted in the fields. Annual crops had been planted in these fields for decades prior to CRP program enrollment. Prior to conversion, all the fields at Lux Arbor had been cultivated with a tilled corn-soybean rotation since 1987. In early May 2009, field at Marshall and Lux Arbor were planted with glyphosate resistant soybean as a breakout crop for one growing season and then converted to switchgrass and restored prairie fields.

Restored prairie (5 grass and 14 forb species, see details in Table A3.1) and switchgrass (cultivar Cave-in-rock) were planted following the soybean breakout crop at both farms, which created a total of 4 fields varying in size from 11-14 ha. Switchgrass was planted at a seeding rate of 11.2 kg ha^{-1} with oats (*Avena sativa*) as a nurse crop in 2010. Restored prairie was planted at a bulk seeding rate of 7.8 kg ha^{-1} with oats as a nurse crop in 2010.

Switchgrass was fertilized with 28-0-0 liquid urea-ammonium nitrate at the rate of 56 kg ha^{-1} nitrogen every spring beginning in 2011. Based on low soil test levels, potash at a rate of 140 kg ha^{-1} was applied to restored prairie at Lux Arbor in 2009. No other phosphorus or potassium applications were made to switchgrass or restored prairie fields.

Thirty georeferenced points were randomly selected in each field at both Marshall and Lux Arbor. In late May 2018 and late May 2020, soil samples were collected at 0-25 cm depth at all georeferenced points and sent to the MSU soil lab for measurements of pH, phosphorus (P: mg kg^{-1}), potassium (K: mg kg^{-1}), calcium (Ca: mg kg^{-1}), magnesium (Mg: mg kg^{-1}), ammonium (NH_4^+: mg kg^{-1}), and total carbon (C: wt%) analysis, which collectively indicate soil fertility characteristics. Soil fertility characteristics were assumed unchanged from 2018 to 2019. Elevation at a resolution of 5 meters was collected by Lidar at all fields in 2008, which was used to generate digital elevation maps (DEMs) for each field. Slope, aspect, plane curvature, profile curvature, and Topographical Wetness Index (TWI) were obtained and used as soil topographical features in R Statistical Programming Language (R Core Team, 2022) with the raster (Hijmans, 2021), rgdal (Bivand et al., 2021), maptools (Bivand & Lewin-Koh, 2021) and dynatopmodel packages (Metcalfe et al., 2018). Soil sand, and clay levels were obtained from either deep core (0-50 cm) samples analysis in 2009 or USDA Web Soil Survey for all georeferenced sampling points (Web Soil Survey, 2022). The 15 bar lower limit of soil water content (LL15), drained upper limit of soil water content (DUL), saturated hydraulic conductivity of soil (Ksat), whole profile drainage rate coefficient (SWCON) and saturated water content (SAT) were calculated from soil sand content, clay content and total carbon content (Saxton & Rawls, 2006). Details on biomass samples and soil samples parameters are located in Figure A3.1. Descriptive statistics for soil fertility characteristics and topographical features are located in Table A3.4 to A3.7 in

the appendix. In late fall of 2018-2020, switchgrass and restored prairie biomass samples were cut at ground level at 30 fixed georeferenced points by using 1x1 m^2 quadrat and hand-clipper at both farms after the first killing frost. In 2019 and 2020 harvesting seasons, switchgrass and restored prairie samples were also collected at an additional distinct 12 georeferenced points at both farms giving a total of 42 sampling points per field. All biomass samples were dried at 65 °C to a constant weight and biomass yield was corrected for dry weight.

Chemical compositional analysis (Enzymatic hydrolysis)

All biomass samples were dry ground using a Wiley mill (Thomas Scientific, Swedesboro, NJ) to pass a 5 mm screen. Then subsamples were analyzed to determine [Glc], [Xyl], and lignin concentration. The protocol is summarized as follows: 10 mg dry biomass samples were held in plastic tubes, which were loaded on a robotic arm system to further ball mill with 5.56 mm stainless steel balls (Salem Specialty Ball Co, Canton, CT). After that, a 1.5 mg subsample of each dry biomass sample was pretreated with 750 µL 0.25% (w/v) NaOH (62.5 mM) solution and kept in a water bath set at 90°C for 3 hours. About 7.5 µl of 6N hydrochloric acid was used to neutralize the reaction if necessary. Then, the pretreated subsamples were added to 0.5 µL of Accellerase 1000 (Genencor, Rochester, NY), 33.3 µl of 1 M citrate buffer (pH 4.5) plus 10 µl of 1% w/v sodium azide; 72 nL of C-Tec2 and 8 nL of H-tec2 enzymes and incubated in a rotisserie oven at 50°C for 20 hours. Supernatants after centrifuge were obtained and transferred to 0.8 mL deep-well plates. Finally, enzyme-based assay kits K-GLUC (Megazyme, Ireland) and K-XYLOSE (Megazyme, Ireland) were used for [Glc] concentration and [Xyl] concentration determination, respectively. The analytical extraction methods used for [Glc] and [Xyl] estimation as described above were designed for high throughput analysis providing accurate qualitative differences between samples. However, they represent a conservative approach with

regard to quantitative estimation, and industrial scale lignocellulosic bioethanol conversions will likely be slightly higher. For lignin content determination, 1-1.5 mg subsample of each dry biomass sample was added to 100 µl of freshly made acetyl bromide solution (25% v/v acetyl bromide in glacial acetic acid) and heated in a capped flask at 50°C for 2 hours initially. Then, the samples were heated for an additional hour with vertexing every 15 minutes. After cooling on ice to room temperature, 400 µl of 2 M sodium hydroxide and 70 µl of freshly prepared 0.5 M hydroxylamine hydrochloride were added to the samples in flasks. Then, flasks were filled with glacial acetic acid to the 2.0 ml mark. Absorbance (abs) at 280 nm was read in an ELISA reader from a UV specific 96 well plate containing 200 µl of the solution in each well. Detailed protocols are available in Santoro et al. (2010) and Foster et al. (2010).

Statistical Analysis

All statistical analyses were done in the R statistical computational environment (R Core Team, 2022) with package sf (Pebesma, 2018), sp (Pebesma et al., 2005), gstat (Pebesma, 2004), automap (Hiemstra et al., 2008), ape (Paradis & Schliep, 2019), lme4 (Bates et al., 2015), DHARMa (Hartig, 2021), and spaMM (Rousset & Ferdy, 2014). All figures were made in R statistical computational environment with package ggplot2 (Wickham, 2016). Empirical semi-variograms were fitted to the data and ordinary kriging regression interpolations were made for switchgrass and restored prairie at both farms separately for the years 2018-2020 to visually examine the [Glc], [Xyl] and lignin content variability. Moran's I values (Moran, 1950) were calculated for [Glc], [Xyl] and lignin content of each cropping system at both Lux Arbor and Marshall. A linear mixed model with location, crop, and year coupled with their two-way and three-way interactions was fitted to obtain the estimated means of [Glc], [Xyl] and lignin content. Due to the lack of spatial autocorrelation based on Moran's I values, a linear mixed

model was fitted without spatial covariance structure. When a significant three-way interaction was found, predetermined comparisons with Bonferroni adjusted p-values were conducted between crop within the same location and year (N=6), between location within the same crop and year (N=12), and between year within the same location and crop (N=6).

Moran's I value formula:

$$I = \frac{N}{W} \frac{\sum_{i=1}^{N} \sum_{j=1}^{N} (x_i - \bar{x})(x_j - \bar{x})}{\sum_{i=1}^{N} (x_i - \bar{x})^2},$$

where N is the number of the sampling points; W is the sum of weights; w_{ij} is weight from a distance decay function; x_i is the observed value; $\bar{x}$ is the mean of the observed value.

The spatio-temporal Gaussian process unconditional model was fitted to examine spatial and temporal variability of [Glc], [Xyl] and lignin content of switchgrass and restored prairies separately at both farms.

The spatio-temporal Gaussian Process model takes the form as below:

$$y_{(s,\,t)} = Y_{(s,\,t)} + \epsilon_{(s,\,t)}$$

Where $Y_{(s,\,t)}$ is mean process part and $\epsilon_{(s,\,t)}$ is noise or error process part. Index s indicates location with x, y coordinates; t indicates discrete time point.

The error part $\epsilon_{(s,\,t)}$ is assumed to have identical independent and distributed normal distribution with 0 mean and variance σ^2. The mean process part $Y_{(s,\,t)}$ consists of a systematic part and error part $\eta_{(s,\,t)}$. Error part $\eta_{(s,\,t)}$ in mean process is assumed to have 0 mean and variance-covariance term, which takes account of spatial dependency and temporal dependency. Matern spatial covariance was used to model the spatial dependency. Stationarity was also assumed from examining the trends along longitude and latitude for [Glc], [Xyl] and lignin content. Since the temporal resolution was one measurement per year and only 3 years of data were available, within-field spatial variability is assumed static over the study period. Temporal variability was

examined by including year as the random intercept for each crop at both farms. Therefore, independence of random variations due to year and Matern spatial covariance was assumed.

To understand within-field relationships among biomass yield, [Glc], [Xyl] and lignin contents, Pearson's second moment correlation coefficients were computed for these four measurements of switchgrass and restored prairie at both farms separately from 2018-2020.

Multi-model inference with backward selection was adopted to study the possible associations between soil fertility characteristics and soil topographical features and switchgrass, restored prairie [Glc], [Xyl] and lignin content over the study period (2018-2020). A bootstrapping resampling technique (replication: 1000) was used to examine stability of the final model chosen by lowest AIC. Variables with at least 70% inclusion probability were considered to be the constantly selected variables. Soil P, K, Ca, Mg, NH_4^+, pH, and total carbon were included in the models as soil fertility characteristics. Elevation, slope, aspect, plane curvature, profile curvature, TWI, LL15, DUL, Ksat, SAT, sand, and clay were included in the models as soil topographical features. Cumulative precipitation (mm) from April to June was included as early growing season precipitation (Early), and cumulative precipitation from July to August as late growing season precipitation (Late). All soil features and growing season precipitation amounts were standardized by abstracting means and dividing by standard deviations before model fitting.

Results

Monthly climatological data

Table 3.1 shows Marshall had relatively lower precipitation from April to September in 2018 compared to the 2019, 2020, and the 30 year average. Compared to 2019, the cumulative precipitation from April to June was lower in 2020. Table 3.2 shows that cumulative precipitation from April to June was relatively higher in 2019 than the 2018 and 2020 growing

seasons at Lux Arbor. However, the cumulative precipitation from July to September was relatively lower in 2019.

Table 3.1. Monthly climatological data for 2018-2020 growing seasons at Michigan State University's Kellogg Weather Station (42.41° N, -85.37°W) and 30-year average at the Battle Creek Weather Station (42.37°N, -85.26°W).

Month	3	4[a]	5[a]	6[a]	7[b]	8[b]	9[b]	10	11	12	1	2
	2018-2019[c]											
Tmax[1]	5.9	10.1	24.6	26.1	28.4	28.5	24.5	15.1	3.8	3.3	-1.9	1.8
Tmin[1]	-3.6	-0.8	12.5	15.6	16.4	15.4	13.0	5.3	-1.8	-3.5	-10.1	-7.4
PRCP[1]	36.3	44.4	208.3	77.7	37.6	111.3	58.2	103.1	39.6	32.2	16.8	30.2
	2019-2020[c]											
Tmax	5.9	15.0	20.3	25.2	30.1	27.2	24.8	16.4	4.8	4.8	2.5	1.4
Tmin	-4.2	3.5	9.0	14.4	18.3	14.5	14.0	5.8	-2.7	-3.3	-3.9	-6.7
PRCP	58.7	86.4	110.0	157.0	80.5	44.2	119.4	91.2	32.0	71.4	76.2	10.2
	2020-2021[c]											
Tmax	8.9	12.4	19.6	28.0	30.1	28.8	22.2	14.6	12.2	4.1	1.1	-0.7
Tmin	-1.0	1.6	8.9	14.1	17.7	14.8	10.1	3.2	1.6	-3.7	-5.4	-11.3
PRCP	70.1	73.1	152.4	82.5	48.8	109.2	80.5	107.7	42.4	42.4	13.2	5.3
	30 Year Average[d]											
Tmax	9.3	16.4	22.7	27.8	29.7	28.1	24.5	17.8	9.8	2.7	0.7	2.7
Tmin	-2.4	3.2	9.0	14.2	16.1	15.5	11.2	5.8	0.7	-5.1	-7.6	-7.0
PRCP	63.8	91.7	106.4	104.2	103.1	105.9	92.4	89.1	79.0	62.2	62.6	47.9

1. Abbreviation: Tmax: Max Air Temperature (°C), Tmin: Minimum Air Temperature (°C) and PRCP: Total Precipitation (mm).
a. April, May and June are defined as early growing season.
b. July, August and September are defined as middle growing season.
c. 2018-2020 climatological data were obtained from Michigan State University Enviro-weather Automated Weather Station Network.
Available online: https://mawn.geo.msu.edu/station.asp?id=kbs [10/31/2021]
d. 30-year average climatological data were obtained from National Centers for Environmental Information (Station ID: USC00200552) at National Oceanic and Atmospheric Administration (NOAA).
Available online: https://www.ncdc.noaa.gov/cdo-web/datatools [1/19/2023].

Table 3.2. Monthly precipitation for 2018-2020 growing seasons at Lux Arbor Marginal Land Experiment Weather Station (42.48°N, -85.45°W).

Month	3	4[a]	5[a]	6[b]	7[b]	8[c]	9[c]	10	11	12	1	2
	2018-2019[d]											
PRCP[1]	43.4	64.3	199.4	112.5	46.7	101.9	130.8	98.3	52.6	53.8	24.1	80.0
	2019-2020[d]											
PRCP	61.0	133.9	140.7	178.8	52.6	61.2	127.5	136.9	43.9	81.8	96.8	26.2
	2020-2021[d]											
PRCP	77.2	79.0	152.9	88.4	78.0	139.2	93.2	99.6	45.2	60.7	25.7	8.6

1. Abbreviation: PRCP: Total Precipitation (mm).
a. April and May are defined as early growing season.
b. June and July are defined as middle growing season.
c. August and September are defined as late growing season.
d. 2018-2020 climatological data were obtained from Great Lake Bioenergy Research Center online database: https://data.sustainability.glbrc.org/datatables/507 [1/19/2023].

Descriptive statistics

As shown in Table 3.3, restored prairie had higher [Glc] than switchgrass each year at both farms with a lone exception of 2018 at Lux Arbor. During the study period (2018-2020), both switchgrass (161.1 ± 13.3 mg g^{-1}) and restored prairie (167.3 ± 33 mg g^{-1}) had the highest [Glc] in 2019 at Marshall. The [Glc] of switchgrass increased from the lowest value in 2018 (100 ± 6.9 mg g^{-1}) to the highest value in 2019 (143.3 ± 9.6 mg g^{-1}) at Lux Arbor. Across years, [Glc] of restored prairie continued to increase from 2018 to 2020 at Lux Arbor. At Marshall, restored prairie (SD: 24 to 35.5 mg g^{-1}; CV: 0.2 to 0.27) had a higher SD and CV than switchgrass (SD: 6.3 to 13.3 mg g^{-1}; CV: 0.07 to 0.09). At Lux Arbor, restored prairie (SD: 8.1 to 22.3 mg g^{-1}; CV: 0.09 to 0.13) had a higher SD and CV than switchgrass (SD: 6.9 to 13.2 mg g^{-1}; CV: 0.07 to 0.09). Compared to switchgrass, more within-field variability of [Glc] was observed in the restored prairie in each of the three years.

Table 3.3. Descriptive statistics of glucose content (mg g^{-1}) for switchgrass and restored prairie at Marshall Farm and Lux Arbor Farm during the study period (2018-2020).

Glucose (mg g^{-1})							
		Marshall			Lux Arbor		
Crop	Year	Mean	SD[1]	CV[1]	Mean	SD[1]	CV[1]
Switchgrass	2018	95.7	6.3	0.07	100	6.9	0.07
	2019	161.1	13.3	0.08	143.3	9.6	0.07
	2020	119.7	10.9	0.09	143.1	13.2	0.09
	Average	128.7	28.8	0.22	131.8	21.8	0.17
Restored prairie	2018	98.7	24	0.24	91.3	8.1	0.09
	2019	167.3	33.3	0.2	154.2	16.5	0.11
	2020	133.7	35.5	0.27	165.8	22.3	0.13
	Average	136.9	41.7	0.3	141.9	35.3	0.25

1. Abbreviation: SD: standard deviation, CV: coefficient of variance.

Table 3.4 shows that switchgrass had higher [Xyl] (61.7 to 93.6 mg g^{-1}) than restored prairie (52.8 to 86 mg g^{-1}) at Marshall across the three study years (2018-2020). In contrast, restored prairie had higher [Xyl] than switchgrass at Lux Arbor in 2019 and 2020. The [Xyl] of both cropping systems at both farms increased from 2018-2019 and then decreased in 2020, particularly in the restored prairie. Similar to [Glc], restored prairie had higher CV and SD than switchgrass across the three study years (2018-2020) at both Lux Arbor and Marshall.

Table 3.4. Descriptive statistics of xylose content (mg g^{-1}) for switchgrass, restored prairie at Marshall Farm and Lux Arbor Farm during the study period (2018-2020).

Xylose (mg g^{-1})							
		Marshall			Lux Arbor		
Crop	Year	Mean	SD[1]	CV[1]	Mean	SD[1]	CV[1]
Switchgrass	2018	61.7	3.9	0.06	66.1	2.7	0.04
	2019	93.6	10.7	0.11	88.8	6	0.07
	2020	72.6	8.5	0.12	80.9	6.9	0.09
	Average	77.5	15.6	0.2	79.9	10.6	0.13
Restored prairie	2018	52.8	10.5	0.2	65.7	6.2	0.09
	2019	86	17.3	0.2	89.3	10	0.11
	2020	66.4	17.9	0.27	83.4	10.2	0.12
	Average	70	20.8	0.3	80.9	13.2	0.16

1. Abbreviation: SD: standard deviation, CV: coefficient of variance.

As shown in Table 3.5, switchgrass had consistently higher lignin content than restored prairie within year and farm. At Lux Arbor, the lignin content decreased from 2018 to 2019 then

increased in 2020. Lignin content kept increasing from 2018 to 2020 at Marshall. Over the study period (2018-2020), both switchgrass and restored prairie had low CV values at Marshall and Lux Arbor (2018-2020). A low CV implies that there is lower within-field variability of [Glc], [Xyl] and lignin content for both switchgrass and restored prairie over the study period (2018-2020).

Table 3.5. Descriptive statistics of lignin content (mg g^{-1}) for switchgrass and restored prairie at Marshall Farm and Lux Arbor Farm during the study period (2018-2020).

Lignin (mg g^{-1})							
		Marshall			Lux Arbor		
Crop	Year	Mean	SD[1]	CV[1]	Mean	SD[1]	CV[1]
Switchgrass	2018	199.1	9.7	0.05	197.4	11.6	0.06
	2019	185.3	11.5	0.06	175.1	9.3	0.05
	2020	177.4	10.3	0.06	192.3	6.9	0.04
	Average	186.0	13.6	0.07	187.3	13.2	0.07
Restored prairie	2018	186.7	11.5	0.06	195.9	7.2	0.04
	2019	169.3	11.8	0.07	169.6	8.1	0.05
	2020	159.3	13.0	0.08	185.4	8.8	0.05
	Average	170.2	16.2	0.10	182.4	13.4	0.07

1. Abbreviation: SD: standard deviation, CV: coefficient of variance.

Neither switchgrass nor restored prairie showed statistically significant spatial autocorrelations among [Glc], [Xyl] and lignin content based on Moran's I (Table A3.8- A3.10 in appendix). In addition, empirical semi-variograms (Figures A3.9, A3.11, A3.13, A3.15, A3.17, and A3.19 in appendix) did not show discernable spatial autocorrelations among [Glc], [Xyl] and lignin content of switchgrass and restored prairie at Marshall and Lux Arbor. Higher [Glc] variability was observed across years than the within-field spatial variability for both switchgrass and restored prairie at both farms (Figures A3.3- A3.4 in appendix). For [Xyl] and lignin content, temporal variability was still higher than within-field spatial variability for switchgrass and restored prairie. However, the temporal variability of [Xyl] and lignin content was reduced compared to [Glc] for switchgrass and restored prairie at both farms (Figures A3.3- A3.8 in

appendix). Ordinary kriging maps (Figures A3.10, A3.12, A3.14, A3.16, A3.18 and A3.20 in appendix) after fitting Matern covariance structure to empirical semi-variograms provided more empirical evidence that within-field spatial variability of [Glc], [Xyl] and lignin content for switchgrass and restored prairie at both farms was smaller than the corresponding temporal variability.

Linear mixed model result

As evident from Figure 3.1, the three-way interaction between farm, crop and year was statistically significant (p-value: 0.003) for [Glc]. At Lux Arbor, restored prairie (167.0 mg g^{-1}; 95% CI: 160.4 to 173.5 mg g^{-1}) had a significantly higher [Glc] than switchgrass (143.7 mg g^{-1}; 95% CI: 137.0 to 150.4 mg g^{-1}) in 2020 (Bonferroni adjusted p-value: <0.0001). There was no significant difference of [Glc] between switchgrass and restored prairie at Marshall across the study period (2018-2020). For switchgrass, [Glc] was significantly higher at Marshall than Lux Arbor in 2019. Marshall had significantly lower [Glc] of switchgrass and restored prairie than Lux Arbor in 2020. At Lux Arbor, switchgrass [Glc] in 2018 (100.6 mg g^{-1}; 95% CI: 93.0 to 108.2 mg g^{-1}) was significantly lower than in 2019 (143.9 mg g^{-1}; 95% CI: 137.4 to 150.4 mg g^{-1}) and 2020 (143.7 mg g^{-1}; 95% CI: 137.0 to 150.4 mg g^{-1}) respectively. The ranking of restored prairie [Glc] at Lux Arbor was 2020 (167.0 mg g^{-1}; 95% CI: 160.4 to 173.5 mg g^{-1}) > 2019 (154.9 mg g^{-1}; 95% CI: 148.3 to 161.4 mg g^{-1}) > 2018 (89.5 mg g^{-1}; 95% CI: 81.9 to 97.0 mg g^{-1}). At Marshall, the highest [Glc] was in 2019 for switchgrass (161.8 mg g^{-1}; 95% CI: 155.3 to 168.3 mg g^{-1}) and restored prairie (169.4 mg g^{-1}; 95% CI: 162.9 to 176.0 mg g^{-1}) and lowest in 2018 for switchgrass (96.0 mg g^{-1}; 95% CI: 88.4 to 103.5 mg g^{-1}) and restored prairie (104.0 mg g^{-1}; 95% CI: 96.5 to 111.6 mg g^{-1}).

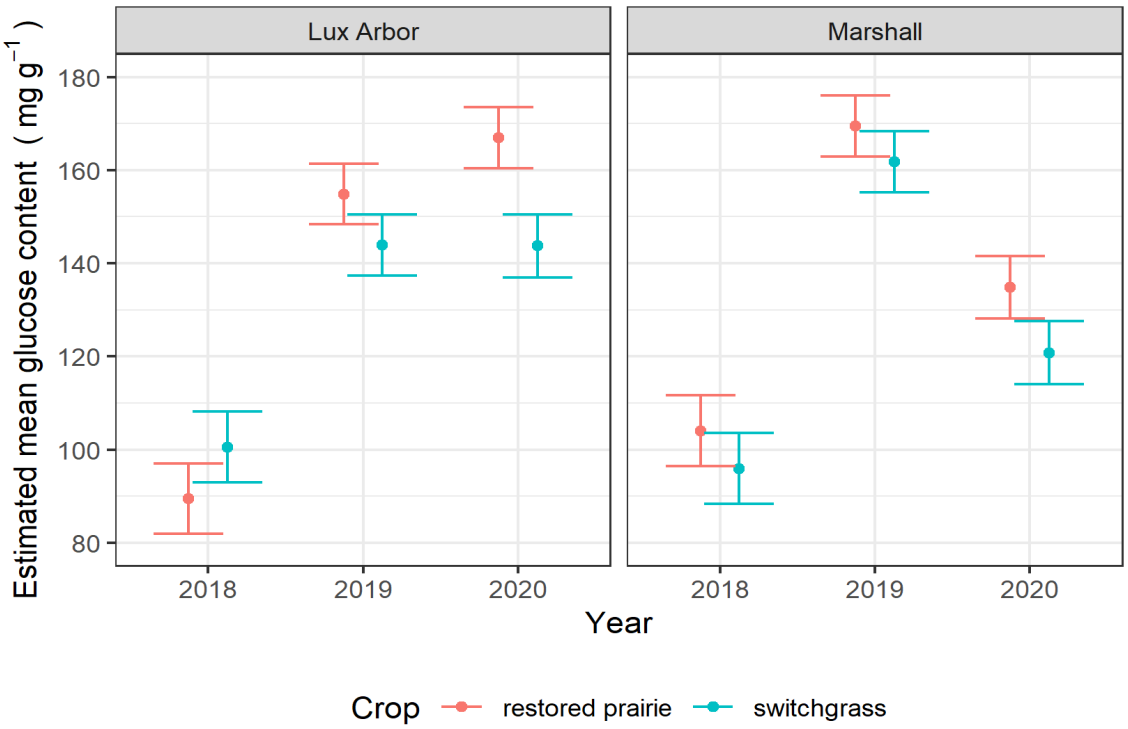

Figure 3.1. Estimated mean glucose content (mg g^{-1}) of switchgrass and restored prairie at Lux Arbor Farm and Marshall Farm during study period (2018-2020). Dots present estimated mean glucose content. Vertical bars represent 95% confidence intervals of estimated mean glucose content.

As evident from Figure 3.2, the two-way interactions between farm and year and farm and crop were statistically significant for [Xyl] (p-value: <0.0001 and 0.0209 respectively). At Lux Arbor, there was no significant difference in [Xyl] between switchgrass (78.5 mg g^{-1}; 95% CI: 75.8 to 81.3 mg g^{-1}) and restored prairie (79.1 mg g^{-1}; 95% CI: 76.3 to 81.8 mg g^{-1}) averaged over the study period (2018-2020). Conversely, switchgrass [Xyl] (76.3 mg g^{-1}; 95% CI: 73.5 to 79.1 mg g^{-1}) was significantly higher than restored prairie [Xyl] (70.3 mg g^{-1}; 95% CI: 67.5 to 73.0 mg g^{-1}) averaged over the study period (2018-2020) at Marshall. At Lux Arbor, the [Xyl] ranking was 89.0 mg g^{-1} (95% CI: 86.5 to 91.5 mg g^{-1}) in 2019 > 82.2 mg g^{-1} (95% CI: 79.6 to 84.7 mg g^{-1}) in 2020 > 65.2 mg g^{-1} (95% CI: 62.3 to 68.1 mg g^{-1}) in 2018. At Marshall, [Xyl] ranking was 90.6 mg g^{-1} (95% CI: 88.1 to 93.1 mg g^{-1}) in 2019 > 70.5 mg g^{-1} (95% CI: 68.0 to 73.1 mg g^{-1}) in 2020 > 58.7 mg g^{-1} (95% CI: 55.8 to 61.6 mg g^{-1}) in 2018.

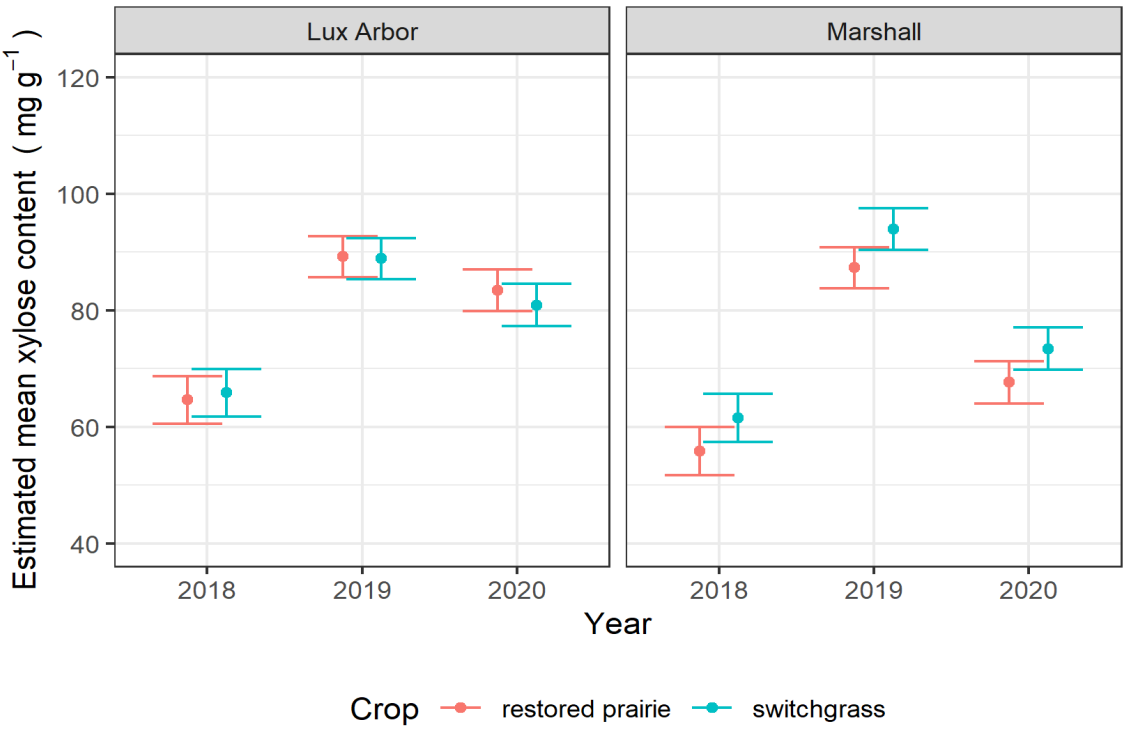

Figure 3.2. Estimated mean xylose content (mg g^{-1}) of switchgrass and restored prairie at Lux Arbor Farm and Marshall Farm during study period (2018-2020). Dots present estimated mean xylose content. Vertical bars represent 95% confidence intervals of estimated mean xylose content.

As evident from Figure 3.3, the two-way interactions between farm and year, farm and crop, crop and year were statistically significant for lignin content (p-value: <0.0001, p< 0.0001 and 0.0162 respectively). At Lux Arbor, there was no significant difference in lignin content between switchgrass (187.5 mg g^{-1}; 95% CI: 185.0 to 190.0 mg g^{-1}) and restored prairie (183.4 mg g^{-1}; 95% CI: 181.0 to 185.9 mg g^{-1}) averaged over the study period (2018-2020). Conversely, switchgrass lignin content (187.3 mg g^{-1}; 95% CI: 184.8 to 189.8 mg g^{-1}) was significantly higher than restored prairie lignin content (172.3 mg g^{-1}; 95% CI: 169.8 to 174.9 mg g^{-1}) averaged over the study period (2018-2020) at Marshall. In 2019, Lux Arbor (172.0 mg g^{-1}; 95% CI: 169.6 to 174.3 mg g^{-1}) had significantly lower lignin content than Marshall (177.5 mg g^{-1};

95% CI: 175.1 to 179.8 mg g^{-1}). In 2020, Lux Arbor (188.6 mg g^{-1}; 95% CI: 186.2 to 190.9 mg g^{-1}) had significantly higher lignin content than Marshall (168.8 mg g^{-1}; 95% CI: 166.4 to 171.2 mg g^{-1}) averaged over crops. The ranking for restored prairie lignin content averaged over farms was: 2018 (191.7 mg g^{-1}; 95% CI: 188.9 to 194.4 mg g^{-1}) > 2020 (172.5 mg g^{-1}; 95% CI: 170.1 to 174.9 mg g^{-1}) > 2019 (169.5 mg g^{-1}; 95% CI: 167.2 to 171.9 mg g^{-1}). The ranking of lignin content in switchgrass averaged over farms was: 2018 (197.4 mg g^{-1}; 95% CI: 194.7 to 200.2 mg g^{-1}) > 2020 (184.9 mg g^{-1}; 95% CI: 182.5 to 187.3 mg g^{-1}) >2019 (179.9 mg g^{-1}; 95% CI: 177.6 to 182.3 mg g^{-1}).

Figure 3.3. Estimated mean lignin content (mg g^{-1}) of switchgrass and restored prairie at Lux Arbor Farm and Marshall Farm during study period (2018-2020). Dots present estimated mean lignin content. Vertical bars represent 95% confidence intervals of estimated mean lignin content.

Gaussian process unconditional model results

Results from unconditional models (Table 3.6) reveal that both switchgrass and restored prairie had significantly lower estimated within-field spatial variance compared to interannual temporal

variance in [Glc], [Xyl] and lignin content. The ratio of interannual temporal variance to spatial variance is 12.2 for [Glc] of switchgrass and 1.3 for restored prairie at Marshall. At Lux Arbor, the ratio of interannual temporal variance to spatial variance of [Glc] is 52.4 for switchgrass and 6.1 for restored prairie. For [Xyl], the ratios of interannual temporal variance to spatial variance are 3.2 and 1.7 for switchgrass and restored prairie at Marshall, respectively. At Lux Arbor, the ratios of interannual temporal variance to spatial variance for [Xyl] are 5.8 and 4.3 for switchgrass and restored prairie, respectively. For lignin content, the ratios of interannual temporal variance to spatial variance are 5.5 and 9.1 for switchgrass and restored prairie at Marshall, respectively. Switchgrass at Lux Arbor had extremely low spatial variance (0.0008) for lignin content. The ratio of interannual temporal variance to spatial variance for restored prairie was 18.8 at Lux Arbor. It is worth noting that the magnitude of spatial variance was similar to residual variance in [Glc], [Xyl] and lignin content for both switchgrass and restored prairie at both farms.

Table 3.6. The Gaussian process model results of unconditional models for glucose content (mg g^{-1}), xylose content (mg g^{-1}) and lignin content (mg g^{-1}) of switchgrass and restored prairies at Marshall Farm and Lux Arbor Farm.

			Spatial correlation		Random part (Variance)		
Variable	Location	Crop	ν^2	ρ^3	Year	spatial	residual
[Glc][1]	Marshall	Switchgrass	16.67	0.48	743	61	69
		Restored prairie	16.67	0.72	705	543	492
	Lux Arbor	Switchgrass	16.67	0.01	419	8	110
		Restored prairie	16.67	0.46	1178	192	131
[Xyl][1]	Marshall	Switchgrass	16.67	0.52	183	58	24
		Restored prairie	0.25	2.51	164	94	167
	Lux Arbor	Switchgrass	16.67	0.48	92	16	20
		Restored prairie	1.91	1.07	107	25	62
Lignin	Marshall	Switchgrass	16.67	0.03	83	15	106
		Restored prairie	16.67	0.40	128	14	106
	Lux Arbor	Switchgrass	5.06	0.0003	82	0.0008	81
		Restored prairie	1.99	1.63	113	6	59

1. Abbreviation: [Glc]: Glucose content, [Xyl]: Xylose content.
2. ν: smoothness parameter.
3. ρ: decay parameter.

Pearson's second moment correlation

Within-field Pearson's second moment product correlations among biomass yield, [Glc], [Xyl] and lignin content for switchgrass and restored prairie by farm and year are shown in Table 3.7. Correlations between [Glc] and [Xyl] were positive for switchgrass and restored prairie at both farms over the study period (2018-2020), ranging from 0.71 to 0.82 for restored prairie at Lux Arbor and from 0.83 to 0.88 at Marshall. For switchgrass, Lux Arbor in 2019 presented the lowest correlation (0.14) between [Glc] and [Xyl] across the three study years. In contrast, switchgrass at Marshall in 2019 presented the highest correlation between [Glc] and [Xyl] across the three study years. [Glc] was negatively associated with biomass yield for switchgrass and restored prairie at both farms across years except in the 2019 switchgrass (0.41) at Marshall. Lignin content had a positive correlation with biomass yield except in the 2018 switchgrass (-0.39), the 2019 restored prairie (-0.02) at Lux Arbor, and the 2020 restored prairie (-0.14) at

Marshall. A positive correlation between [Glc] and lignin content, [Xyl] and lignin content was statistically significant for restored prairie at Marshall across all three years. At Lux Arbor, the correlations between [Glc] and lignin content for restored prairie ranged from -0.01 to 0.37, which were lower than Marshall in the same year. In switchgrass, a negative correlation was observed between [Glc] and lignin content at Lux Arbor across all three years. Conversely, the correlation between [Glc] and lignin content for switchgrass at Marshall was positive in 2019 and 2020. Correlation between [Xyl] and lignin content was positive for switchgrass and restored prairie at both farms in 2019. In 2018, switchgrass and restored prairie had a positive correlation between [Xyl] and lignin content at Marshall. Conversely, switchgrass and restored prairie biomass had a negative correlation between [Xyl] and lignin content at Lux Arbor in 2018.

Table 3.7. Pearson product-moment correlation for biomass yield (Mg ha^{-1}), glucose content (mg g^{-1}), xylose content (mg g^{-1}) and lignin content (mg g^{-1}) for switchgrass and restored prairie at Marshall Farm and Lux Arbor Farm.

			Marshall				Lux Arbor			
			Yield	[Glc][1]	[Xyl][1]	lignin	Yield	[Glc]	[Xyl]	lignin
2018	Switchgrass	Yield	1	-0.03	0.14	0.26	1	-0.13	0.01	-0.39
		[Glc]		1	0.21	-0.31		1	0.30	-0.15
		[Xyl]			1	0.03			1	-0.06
		lignin				1				1
	Restored Prairie	Yield	1	-0.13	0.02	0.16	1	-0.17	-0.18	0.01
		[Glc]		1.00	0.83***	0.56**		1	0.71*	-0.01
		[Xyl]			1.00	0.67***			1	-0.20
		lignin				1.00				1
2019	Switchgrass	Yield	1	0.41*	0.46*	0.21	1	-0.19	0.17	0.26
		[Glc]		1	0.87***	0.25		1	0.14	-0.17
		[Xyl]			1	0.44*			1	0.02
		lignin				1				1
	Restored Prairie	Yield	1	-0.20	0.05	0.12	1	-0.34	-0.15	-0.02
		[Glc]		1	0.84***	0.65***		1	0.79*	0.37
		[Xyl]			1	0.82***			1	0.42*
		lignin				1				1
2020	Switchgrass	Yield	1	-0.05	0.14	0.23	1	-0.31	-0.23	0.31
		[Glc]		1	0.81***	0.53***		1	0.80*	-0.46*
		[Xyl]			1	0.54***			1	-0.12
		lignin				1				1
	Restored Prairie	Yield	1	-0.18	-0.09	-0.14	1	-0.27	0.02	0.37
		[Glc]		1	0.88***	0.75***		1	0.82***	0.14
		[Xyl]			1	0.83***			1	0.29
		lignin				1				1

1. Abbreviation: [Glc]: Glucose content, [Xyl]: Xylose content.

* P-value < 0.05.

** P-value < 0.01.

*** P-value < 0.001.

Multimodel inference for variables selection

In Figure 3.4, only soil K concentration was included over 70% of the time over 1000 bootstrapping models for [Glc] of switchgrass biomass yield at Lux Arbor. As shown in Table A3.11 in the appendix, the estimated coefficient of K on [Glc] of switchgrass at Lux Arbor was -4.19 mg g^{-1}/SD (95% Bootstrap CI: -7.16 to 0 mg g^{-1}/SD). Soil P and Ca as soil fertility properties, and clay, LL15, SAT, and aspect as soil topographical characteristics were included 70% of the time in 1000 bootstrapping models for [Glc] of restored prairie biomass yield at Lux Arbor (Figure 3.5). Soil P and Ca had negative estimated coefficients of -7.86 mg g^{-1}/SD (95% Bootstrap CI: -14.16 to 0 mg g^{-1}/SD) and -7.80 mg g^{-1}/SD (95% Bootstrap CI: -16.08 to 0 mg g^{-1}/SD), respectively. The estimated coefficients of clay and LL15 cannot be reliably estimated due to a significantly high standard error. This could be due to collinearity with other variables in the model. SAT and aspect had positive estimated coefficients of 47.2 mg g^{-1}/SD and 3.71 mg g^{-1}/SD, respectively. Slope, elevation, sand content and K_{sat} were included over 70% of the time in over a 1000 bootstrapping models for [Glc] of switchgrass at Marshall (Figure 3.6). Slope and elevation had a positive estimated coefficients of 3.41 mg g^{-1}/SD (95% Bootstrap CI: 0 to 6.47 mg g^{-1}/SD) and 3.08 mg g^{-1}/SD (95% Bootstrap CI: 0 to 6.77 mg g^{-1}/SD), respectively. Soil sand content had a positive estimated coefficient of 16.63 mg g^{-1}/SD (95% Bootstrap CI: -58.39 to 80.05 mg g^{-1}/SD). Ksat had a negative estimated coefficient of -13.52 mg g^{-1}/SD (95% Bootstrap CI: -29.8 to 0 mg g^{-1}/SD). Topographical wetness index, DUL, sand, SAT and total soil C were included over 70% of the time over 1000 bootstrapping models for [Glc] of restored prairie at Marshall (Figure 3.7). Topographical wetness index and total soil C had negative estimated coefficients of -13.04 mg g^{-1}/SD (95% Bootstrap CI: -25.09 to 0 mg g^{-1}/SD) and -8.02 mg g^{-1}/SD (95% Bootstrap CI: -18.70 to 0 mg g^{-1}/SD), respectively. SAT had a positive estimated

coefficient of 23.02 mg g^{-1}/SD (Bootstrap CI: 0 to 54.80 mg g^{-1}/SD). Details on model results are located in Table A3.11- A3.14 in the appendix.

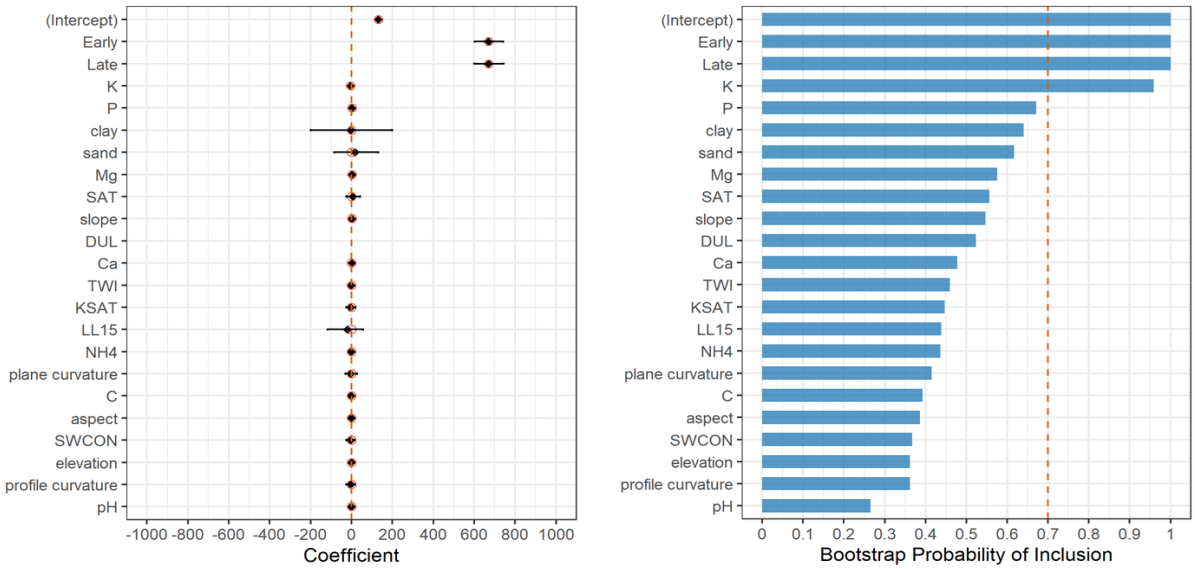

Figure 3.4. Model results from 1000 bootstrap resampling for switchgrass biomass glucose content (mg g^{-1}) at Lux Arbor Farm. Left panel: estimated coefficients: black diamond is estimation from full model. Black horizontal is 95% bootstrap confidence interval, open red circle is bootstrap median. Coefficient is not included when standard error is greater than 100. Right panel: bootstrap probability of inclusion. Red dash vertical bar indicates probability of 0.7.

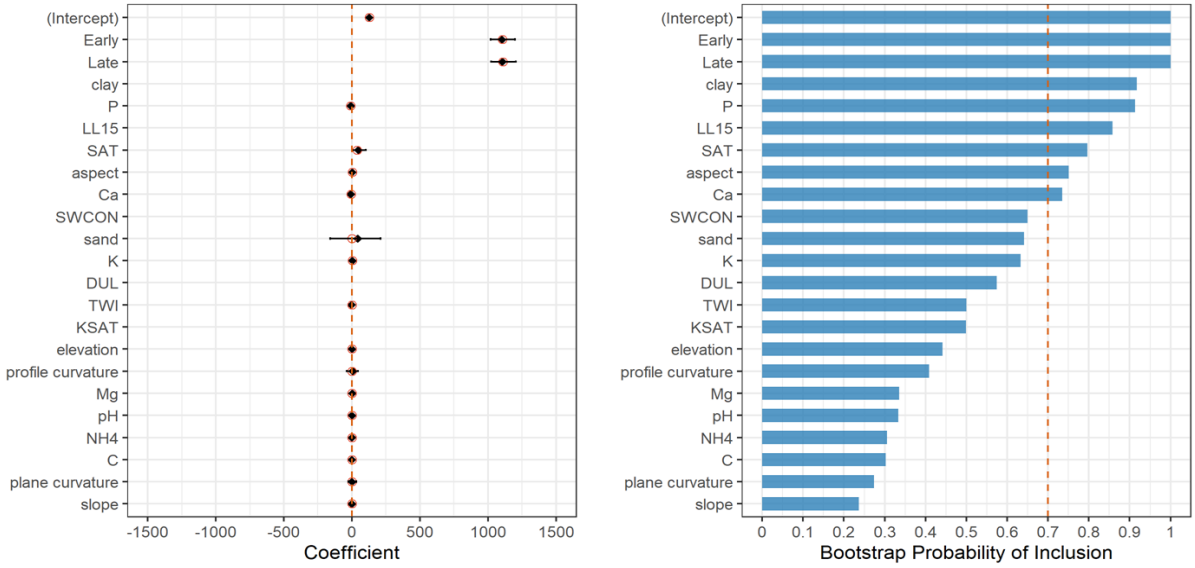

Figure 3.5. Model results from 1000 bootstrap resampling for restored prairie biomass glucose content (mg g^{-1}) at Lux Arbor Farm. Left panel: estimated coefficients: black diamond is estimation from full model. Black horizontal is 95% bootstrap confidence interval, open red circle is bootstrap median. Coefficient is not included when standard error is greater than 100. Right panel: bootstrap probability of inclusion. Red dash vertical bar indicates probability of 0.7.

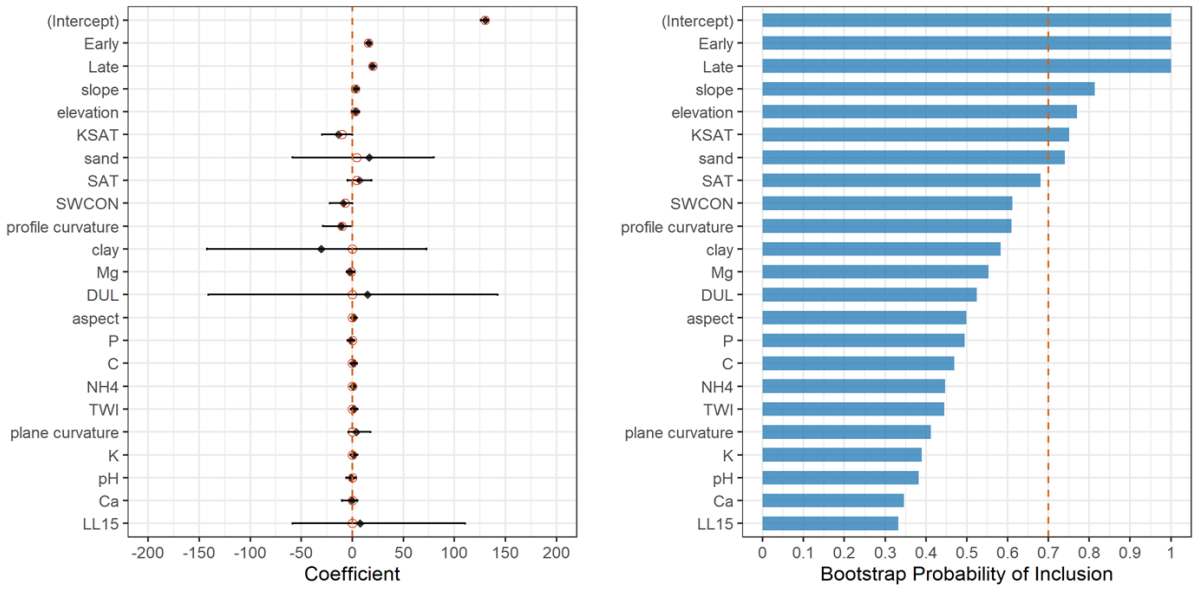

Figure 3.6. Model results from 1000 bootstrap resampling for switchgrass biomass glucose content (mg g^{-1}) at Marshall Farm. Left panel: estimated coefficients: black diamond is estimation from full model. Black horizontal is 95% bootstrap confidence interval, open red circle is bootstrap median. Right panel: bootstrap probability of inclusion. Red dash vertical bar indicates probability of 0.7.

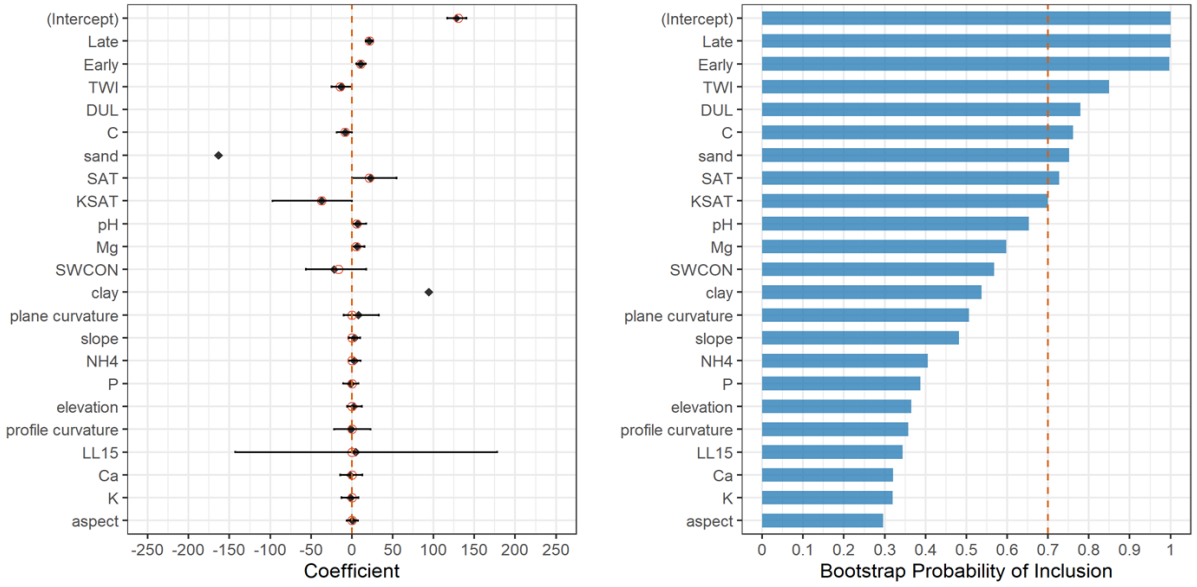

Figure 3.7. Model results from 1000 bootstrap resampling for restored prairie biomass glucose content (mg g^{-1}) at Marshall Farm. Left panel: estimated coefficients: black diamond is estimation from full model. Black horizontal is 95% bootstrap confidence interval, open red circle is bootstrap median. Coefficient is not included when standard error is greater than 100. Right panel: bootstrap probability of inclusion. Red dash vertical bar indicates probability of 0.7.

Topographical wetness index with 0.696 probability of inclusion was negatively associated with [Xyl] of switchgrass at Lux Arbor (EM: -1.75 mg g^{-1}/SD; 95% Bootstrap CI: -3.66 to 0.02 mg g^{-1}/SD). At Lux Arbor, P and Ca as soil fertility characteristics and LL15 and clay content as soil topographical features were included over 70% of the time in over 1000 bootstrapping models for [Xyl] of restored prairie (Figure 3.9). Soil P and Ca had a negative estimated coefficient of -4.26 mg g^{-1}/SD and -5.25 mg g^{-1}/SD, respectively. Sand content, Ksat, SAT, elevation, clay, SWCON, profile curvature, slope and DUL were included over 70% of the time in over 1000 bootstrapping models for [Xyl] of switchgrass at Marshall (Figure 3.10). Among them, sand content had been estimated consistently with a positive estimated coefficient of 64.93 mg g^{-1}/SD (95% Bootstrap CI: 4.54 to 105.33 mg g^{-1}/SD). Elevation, slope, SAT and DUL had positive estimated coefficients on [Xyl] of switchgrass at Marshall. Total soil C, Ksat, Mg, SAT, TWI, sand content, and clay content were included over 70% of the time in over 1000 bootstrapping models for [Xyl] of restored prairie at Marshall (Figure 3.11). Total soil C, Ksat and TWI had a negative estimated coefficient of -7.22 mg g^{-1}/SD, -32.86 mg g^{-1}/SD and -6.29 mg g^{-1} /SD, respectively. Soil Mg had a positive estimated coefficient of 5.43 mg g^{-1}/SD. The standard errors of sand content and clay content were considerably higher. Therefore, the coefficients of sand content and clay content cannot be reliably estimated. Details on model results are located in Tables A3.15-A3.18 in the appendix.

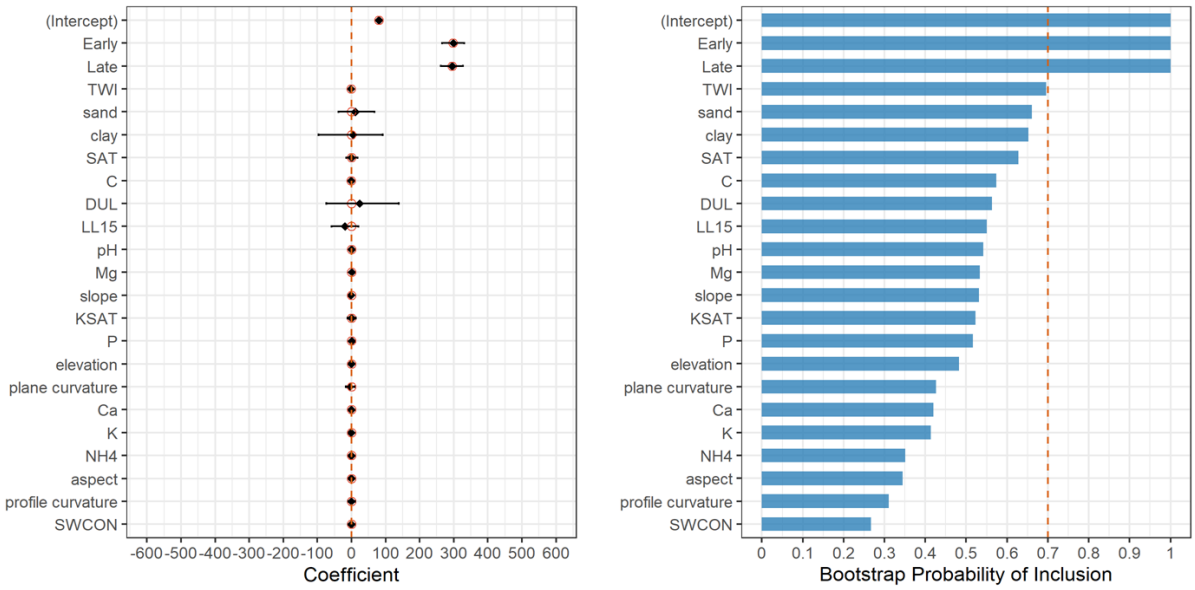

Figure 3.8. Model results from 1000 bootstrap resampling for switchgrass biomass xylose content (mg g^{-1}) at Lux Arbor Farm. Left panel: estimated coefficients: black diamond is estimation from full model. Black horizontal is 95% bootstrap confidence interval, open red circle is bootstrap median. Right panel: bootstrap probability of inclusion. Red dash vertical bar indicates probability of 0.7.

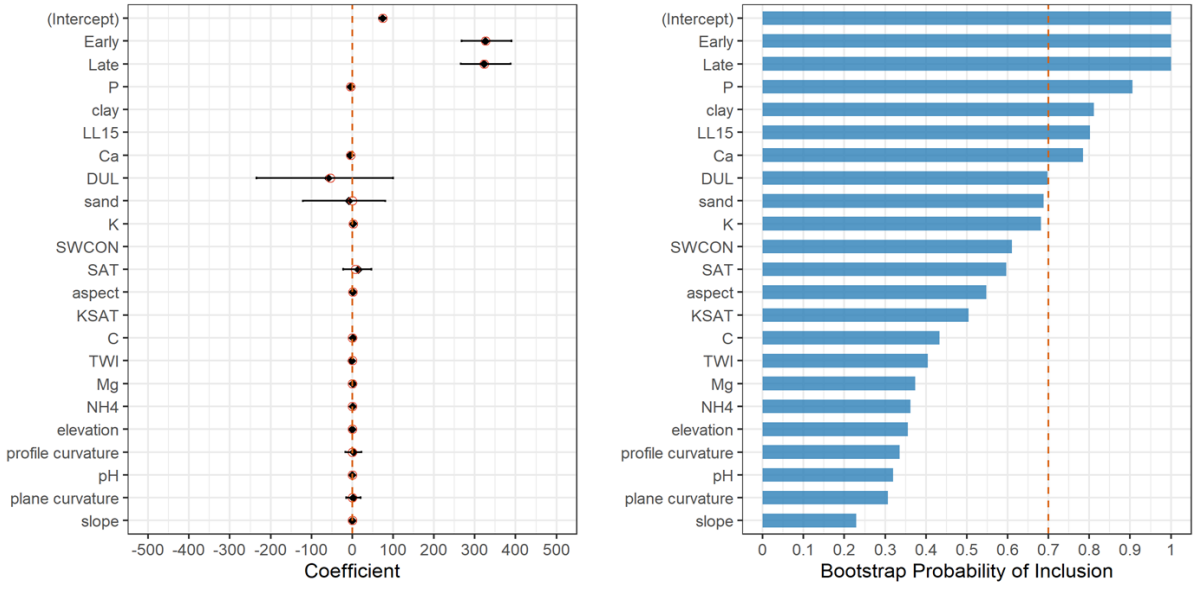

Figure 3.9. Model results from 1000 bootstrap resampling for restored prairie biomass xylose content (mg g^{-1}) at Lux Arbor Farm. Left panel: estimated coefficients: black diamond is estimation from full model. Black horizontal is 95% bootstrap confidence interval, open red circle is bootstrap median. Coefficient is not included when standard error is greater than 100. Right panel: bootstrap probability of inclusion. Red dash vertical bar indicates probability of 0.7.

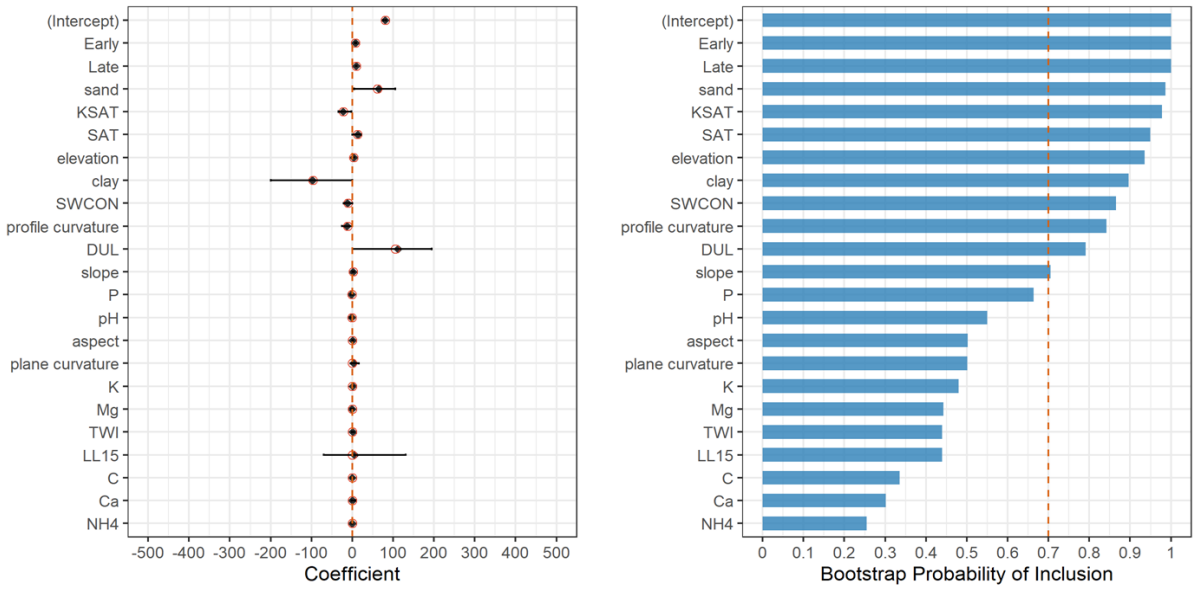

Figure 3.10. Model results from 1000 bootstrap resampling for switchgrass biomass xylose content (mg g^{-1}) at Marshall Farm. Left panel: estimated coefficients: black diamond is estimation from full model. Black horizontal is 95% bootstrap confidence interval, open red circle is bootstrap median. Right panel: bootstrap probability of inclusion. Red dash vertical bar indicates probability of 0.7.

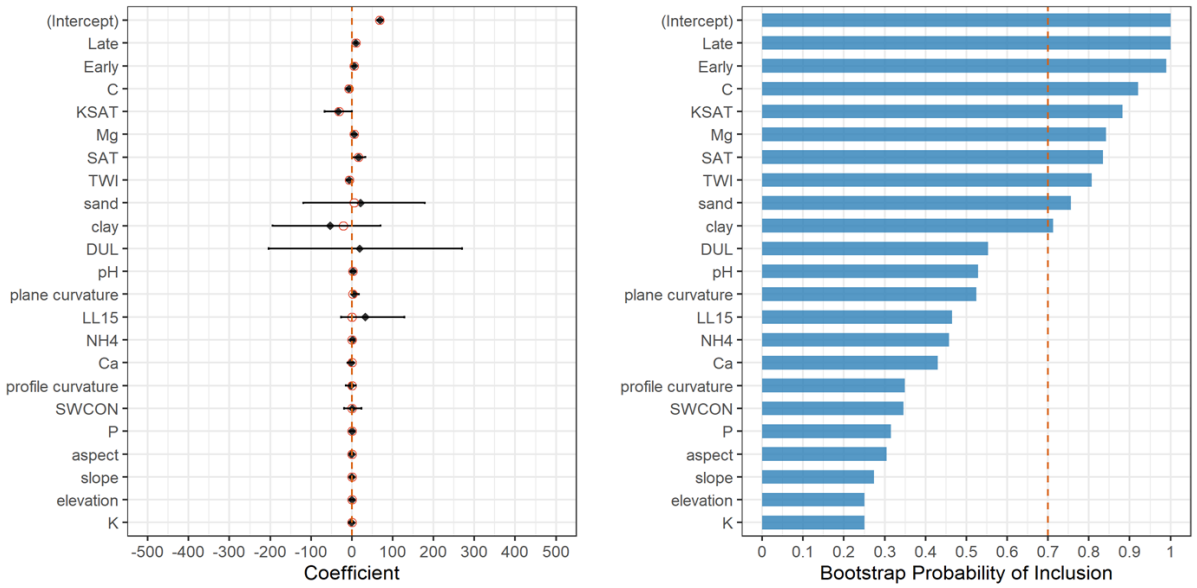

Figure 3.11. Model results from 1000 bootstrap resampling for restored prairie biomass xylose content (mg g^{-1}) at Marshall Farm. Left panel: estimated coefficients: black diamond is estimation from full model. Black horizontal is 95% bootstrap confidence interval, open red circle is bootstrap median. Right panel: bootstrap probability of inclusion. Red dash vertical bar indicates probability of 0.7.

In Figure 3.12, sand content and SWCON were included over 70% of the time in over 1000 bootstrapping models for lignin content of switchgrass biomass at Lux Arbor. A positive estimated coefficient of 25.12 mg g^{-1}/SD (95% Bootstrap CI: 0 to 43 mg g^{-1}/SD) was found for SWCON. Soil K with a 0.699 probability of inclusion had estimated coefficient of 2.42 mg g^{-1}/SD (95% Bootstrap CI: 0 to 4.98 mg g^{-1}/SD) for lignin content of restored prairie at Lux Arbor (Figure 3.13). At Marshall, only clay was included over 70% of the time in over 1000 bootstrapping models for lignin content of switchgrass (Figure 3.14). Clay had a substantial positive estimated coefficient of 114.95 mg g^{-1}/SD (95% Bootstrap CI: 0 to 237 mg g^{-1}/SD). On the opposite, soil Mg, Ca, TWI and DUL were included over 70% of the time in over 1000 bootstrapping models for lignin content of restored prairie biomass at Marshall (Figure 3.15). Soil Mg and Ca had conflicting estimated coefficient s of 5.72 mg g^{-1}/SD (95% Bootstrap CI: 0 to 9.75 mg g^{-1}/SD) and -5 mg g^{-1}/SD (95% Bootstrap CI: -11.52 to 0 mg g^{-1}/SD), respectively. Topographical wetness index (TWI) was negatively associated with lignin content of restored prairie at Marshall (-5.22 mg g^{-1}/SD; 95% Bootstrap CI: -10.26 to 0 mg g^{-1}/SD). Details on model results are located in Tables A3.19-A3.22 in the appendix.

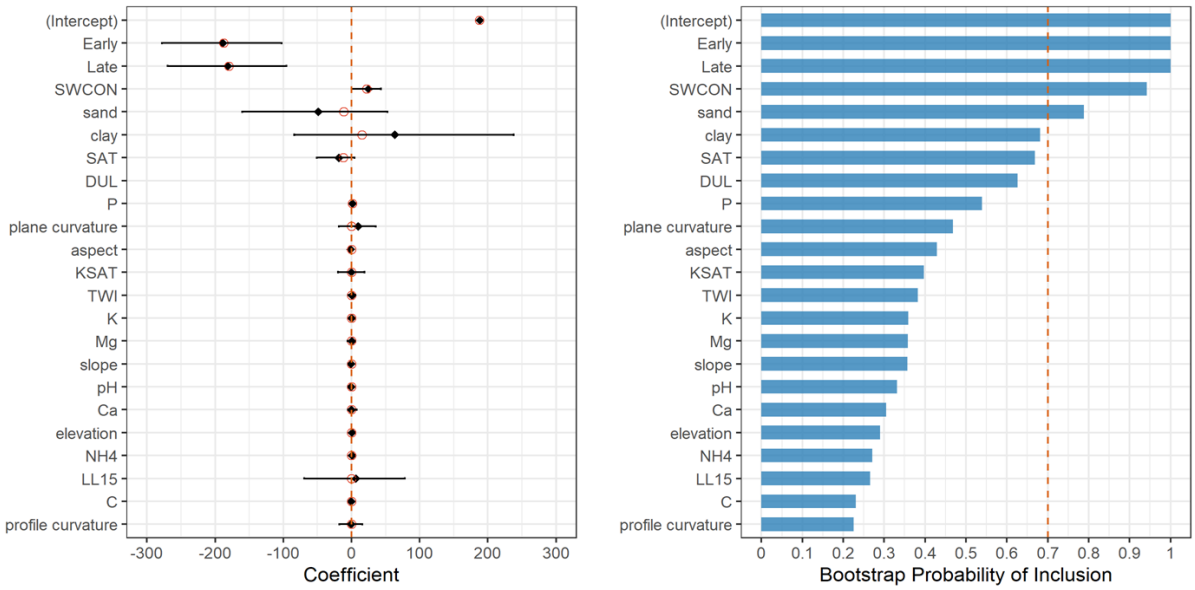

Figure 3.12. Model results from 1000 bootstrap resampling for switchgrass biomass lignin content (mg g^{-1}) at Lux Arbor Farm. Left panel: estimated coefficients: black diamond is estimation from full model. Black horizontal is 95% bootstrap confidence interval, open red circle is bootstrap median. Coefficient is not included when standard error is greater than 100. Right panel: bootstrap probability of inclusion. Red dash vertical bar indicates probability of 0.7.

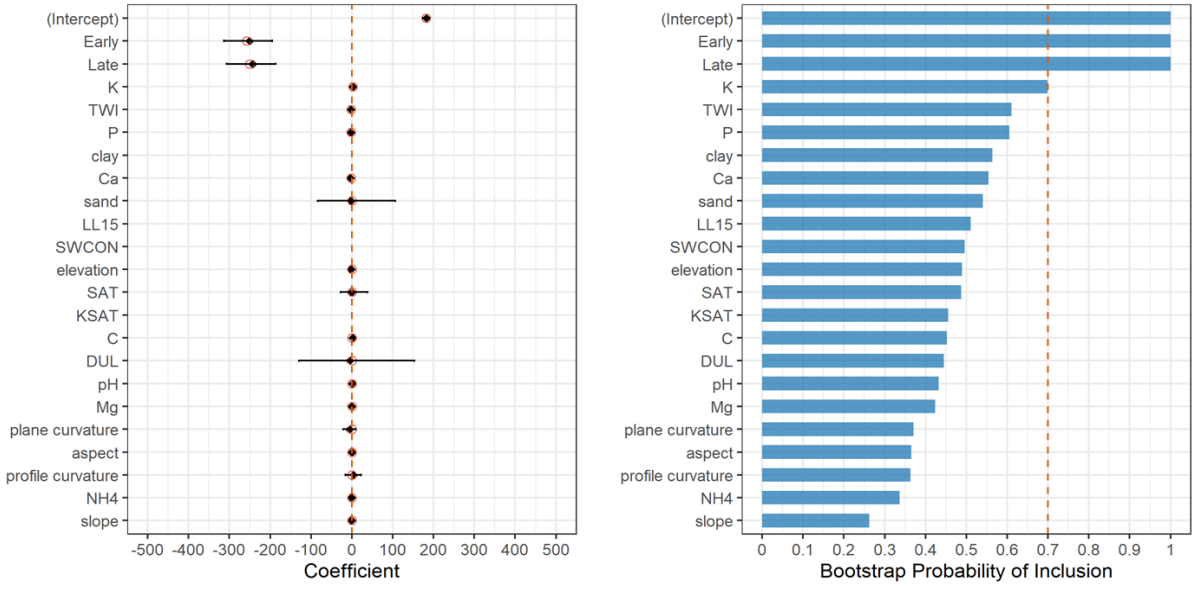

Figure 3.13. Model results from 1000 bootstrap resampling for restored prairie biomass lignin content (mg g^{-1}) at Lux Arbor Farm. Left panel: estimated coefficients: black diamond is estimation from full model. Black horizontal is 95% bootstrap confidence interval, open red circle is bootstrap median. Coefficient is not included when standard error is greater than 100. Right panel: bootstrap probability of inclusion. Red dash vertical bar indicates probability of 0.7.

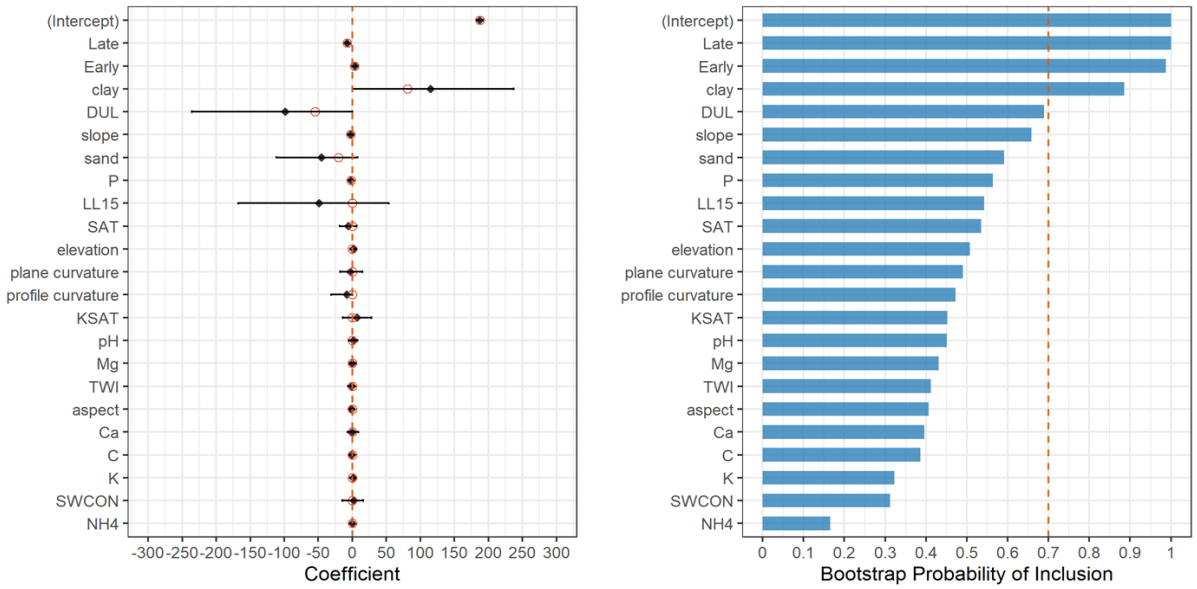

Figure 3.14. Model results from 1000 bootstrap resampling for switchgrass biomass lignin content (mg g^{-1}) at Marshall Farm. Left panel: estimated coefficients: black diamond is estimation from full model. Black horizontal is 95% bootstrap confidence interval, open red circle is bootstrap median. Right panel: bootstrap probability of inclusion. Red dash vertical bar indicates probability of 0.7.

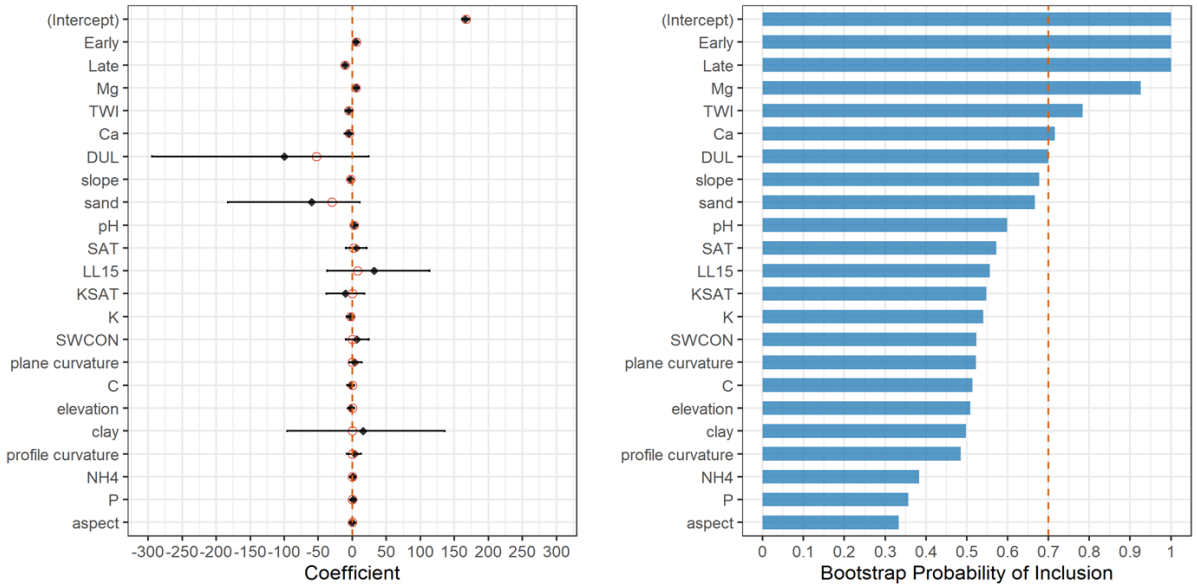

Figure 3.15. Model results from 1000 bootstrap resampling for restored prairie biomass lignin content (mg g^{-1}) at Marshall Farm. Left panel: estimated coefficients: black diamond is estimation from full model. Black horizontal is 95% bootstrap confidence interval, open red circle is bootstrap median. Right panel: bootstrap probability of inclusion. Red dash vertical bar indicates probability of 0.7.

At Lux Arbor, soil P and Ca had negative estimated coefficients on both [Glc] and [Xyl] of restored prairie. At Marshall, sand, elevation and slope were positively associated with both [Glc] and [Xyl] of switchgrass. Topographical wetness index had negative estimated coefficients on [Glc], [Xyl] and lignin content of restored prairie at Marshall.

The early season (April to June) cumulative precipitation and late season (July to September) cumulative precipitation were selected 100% of the time in over 1000 bootstrapping models for the interannual variation in [Glc], [Xyl] and lignin content of switchgrass and restored prairie biomass at Lux Arbor. The magnitudes of the estimated coefficients of early season (April to June) cumulative precipitation and late season (July to September) cumulative precipitation were substantially higher than the estimated coefficient s of soil features on the spatial variation in [Glc], [Xyl] and lignin content of switchgrass and restored prairie biomass at Lux Arbor. At Marshall, late season (July to September) cumulative precipitation was selected 100% of the time over 1000 bootstrapping models for [Glc], [Xyl] and lignin content of switchgrass and restored prairie biomass. Within farm, the magnitude of late season (July to September) cumulative precipitation on [Glc], [Xyl] and lignin content was lower for switchgrass than restored prairie at both farms.

Discussion

A key component of optimizing biomass logistic systems and biorefinery performance lies in understanding and controlling biomass quality from the farm gate. This study sheds light on within-field and year-to-year biomass quality variability. The [Glc] ranged from 95.7 to 161.1 mg g^{-1} and 91.3 to 167.3 mg g^{-1} for switchgrass and restored prairie, respectively. The [Xyl] ranged from 61.7 mg g^{-1} to 93.6 mg g^{-1} and 52.8 mg g^{-1} to 89.3 mg g^{-1} for switchgrass and restored prairie, respectively. The lignin content ranged from 177.4 mg g^{-1} to 199.1 mg g^{-1} and

159.3 mg g^{-1} to 195.9 mg g^{-1} for switchgrass and restored prairie, respectively.

Previous studies reported [Glc] (wt %) of harvested switchgrass as high as 32.2 wt % after diluted sulfuric acid pretreatment for 20 minutes at 160 °C (Shi et al., 2011). Compared to other studies, the lower [Glc] and [Xyl] yields reported here were due to less intensive pretreatment, as described above in the Methods section. Most previous studies reported structural polysaccharide glucan and xylan content rather than glucose and xylose release. Hoover et al. (2022) reported that glucan ranged from 28 to 37 wt % and xylan ranged from 18 to 24 wt % for an upland switchgrass variety. Without 100% conversion, glucose and xylose content is lower than glucan and xylan content. Previous studies have shown that plant biomass is composed of 15-30 wt % lignin (Agblevor et al., 1994, Thammasouk et al., 1997, Waliszewska et al., 2021). This is consistent with the lignin content in this study. In the present study, restored prairie had lower [Xyl] than switchgrass at Marshall over the study period (2018-2020). Generally, no significant [Glc] difference was detected between switchgrass and restored prairie in this study over the study period (2018-2020). Previous studies have shown that higher species richness leads to low biomass cellulose and hemicellulose levels (Adler et al., 2009). The CVs of [Glc], [Xyl] and lignin content were all substantially lower indicating low within-field spatial variability. In addition, the estimated spatial variance of [Glc], [Xyl] and lignin content was considerably lower than the corresponding interannual variance.

To the best of our knowledge, this study is the only one to examine within-field spatial variability of sugar and lignin yields from ligno-cellulosic biomass feedstocks at the field scale. Templeton et al. (2009) demonstrated that harvest year had a significant effect on corn stover biomass composition. The interannual variability of biomass structural sugar content is more likely influenced by precipitation and temperature patterns (Barbosa et al., 2013, Emerson et al.,

2014). The effect of drought on biomass structural sugar content was investigated recently. Hoover et al. (2018) and Ong et al. (2016) reported that drought significantly lowered structural glucan and xylan in miscanthus and switchgrass. In addition, Ong et al. (2016) found that drought increased inhibitory compounds (imidazoles and pyrazine) in ammonia fiber expansion pretreated switchgrass, thus negatively impacting fermentation for biofuel conversion. Emerson et al. (2014) showed that drought decreased cellulose content but increased hemicellulose content in mixed grasses. Previous studies have argued that drought conditions induced plant physiological change to divert carbon from cell wall polysaccharides synthesis to maintain turgor pressure (Iraki et al., 1989, Gall et al., 2015). In this study, the low [Glc] and [Xyl] in 2018 could be attributed to relatively low precipitation during the growing season.

We observed that both early season cumulative precipitation (April-June) and late season cumulative precipitation (July to September) were strongly related to [Glc], [Xyl] and lignin content. The drought effect on biomass lignin content varies in the literature with some studies showing a negative effect (Emerson et al., 2014) and some showing a positive or no effect (Jiang et al., 2012, van der Weijde et al., 2017). The observed drought-induced lignin content increase in crops can be explained by activation of lignifying enzymes (Hu et al., 2009, Yang et al., 2021). Even though the 2018 growing season with relatively low precipitation was not considered severe enough to be designated as a drought, the biomass lignin content was higher in 2018 than 2019 and 2020 for switchgrass and restored prairie at the two study farms. Lignin has been considered as a major contributor to biomass recalcitrance, which makes plant biomass more resistant to microbial or enzymatic deconstruction (Himmel et al., 2007). Santos et al. (2012) identified that lignin content is the most significant factor that reduces enzymatic hydrolysis efficiency in kraft-pretreated woody biomass. The modes of action by which lignin

contributes to biomass recalcitrance can be summarized into two: one is acting as a physical barrier to reduce accessibility of cellulose and hemicellulose, the other one is irreversibly adsorbing enzymes in enzymatic hydrolysis (Himmel et al., 2007). Nonetheless, lignin is a potential energy resource through thermochemical conversion such as pyrolysis and gasification. Extensive research has been conducted demonstrating lignin valorization utilizing an integrated biorefinery framework (Ragauskas et al., 2014, Sethupathy et al., 2022).

High positive correlations between glucan and xylan and glucan and lignin have been observed in corn stover (Templeton et al., 2009, Lorenzana et al., 2010). Da Costa et al. (2019) reported a high positive correlation between glucose and xylose in *Miscanthus* biomass. Similarly, [Glc] and [Xyl] were positively correlated in this study, but with variable direction of the correlation between [Glc] and lignin content, as well as biomass yield and [Xyl]. Correlations between biomass yield and [Glc] were mostly negative with the exception of switchgrass at Marshall in 2019. Sanford et al. (2017) reported a negative and positive correlation between biomass yield and [Glc] at two different sites. Recent studies demonstrated that conventional breeding and selection of high yield switchgrass did not reduce sugar release from biomass hydrolysis (Casler et al., 2022). In this study, none of the negative correlations between biomass yield and [Glc] were statistically significant. In contrast, the only statistically significant positive correlation between biomass yield and [Glc] of switchgrass was observed at Marshall in 2019.

The lack of spatial dependency of [Glc], [Xyl] and lignin content indicates there was no underlying spatially correlated soil feature associated with spatial variability of [Glc], [Xyl] and lignin content. Most of the soil fertility and topographical feature effects on [Glc], [Xyl] and lignin content cannot be reliably estimated. This is expected because of the low spatial variability of biomass [Glc] and [Xyl], especially for switchgrass. Soil fertility features (K, P and Ca) were

frequently selected as factors that might influence restored prairie quality. Soil topographical features such as TWI, slope and elevation were more frequently selected in the models to explain variability of [Glc] and [Xyl] in switchgrass. The negative effects of P and Ca on [Glc], [Xyl] of restored prairie could be due to forb growth favored by relatively higher P and Ca levels in the restored prairie. Garlock et al. (2012) showed that forb dominated feedstocks had lower sugar content and were less digestible than grass dominated feedstocks. Extensive research has shown that nitrogen fertilization increases hemicellulose and has no effect on cellulose in energy grasses (Guo et al., 2017, Emery et al., 2020, Ali et al., 2022). The present study showed that soil nitrogen content was not selected consistently as correlating with monosaccharides and lignin yield from switchgrass and restored prairie. Slope and elevation positively impacted [Glc] and [Xyl] of switchgrass biomass at Marshall. In contrast, TWI negatively impacted [Glc] and [Xyl] of restored prairie at Marshall. This suggests that high soil water holding capacity slightly reduced [Glc] and [Xyl] in switchgrass biomass. To the best of our knowledge, there is no field-scale study examining soil topographical effects on [Glc] and [Xyl] release from switchgrass biomass. Hoover et al. (2018) demonstrated that drought had no impact on [Glc] and [Xyl] release from switchgrass biomass, possibly due to the drought resistance of switchgrass. In addition, we found that the magnitude of slope, elevation and TWI were all under 15 mg g^{-1}. Templeton et al. (2010) showed that uncertainty of cell wall compositional analysis expressed as standard deviation was about 10 mg g^{-1}. More research is needed to elucidate the effects of soil fertility and topographical features on biomass quality.

Within season variability of biomass quality is well documented (Patton & Gieseker, 1942, Adler et al., 2006, Peng et al., 2017). One study at Nashville, Tennessee, USA showed that cellulose and hemicellulose contents of switchgrass reached highest levels in July and stayed

relatively constant until November, while lignin content increased from June to November (Saini et al., 2017). Moreover, studies demonstrated that delayed spring harvest slightly increased cellulose and hemicellulose content of switchgrass while substantially decreasing biomass yield (Aurangzaib et al., 2016, Ibrahim et al., 2017, Massey et al., 2020). While the present study focused on within-field variability of biomass quality, harvesting date should also be an important consideration when designing an efficient biomass production system.

Conclusion

Substantial temporal variability of [Glc], [Xyl] and lignin content was found in both switchgrass and restored prairie. Compared to temporal variability, the within-field spatial variability of [Glc], [Xyl] and lignin content was smaller in both switchgrass and restored prairie. Given the same field conditions and climate, spatial variability of [Glc], [Xyl] and lignin content was greater in restored prairie than switchgrass. Soil P, Ca, sand content, elevation, slope and topographical wetness index were each related to [Glc], [Xyl] and lignin content of switchgrass and restored prairie, however the magnitudes of their effects were low. With the expected climatic variability in the future due to climate change, temporal variability of biomass quality could increase considerably. The implications from this study for downstream biomass logistics planning and biorefinery operation are (1) within-field spatial variability switchgrass quality is not a significant concern; (2) Due to potential changes in grass: forb ratios, it is worthwhile to take account within-field spatial variability of restored prairie when modeling biomass logistics and biorefinery production; and (3) Interannual variability of biomass quality should be taken into consideration when modeling biomass logistics and biorefinery production.

REFERENCES

Adler, P. R., Sanderson, M. A., Boateng, A. A., Weimer, P. J., & Jung, H. J. G. (2006). Biomass yield and biofuel quality of switchgrass harvested in fall or spring. Agronomy Journal, 98(6), 1518–1525. https://doi.org/10.2134/agronj2005.0351

Adler, P. R., Sanderson, M. A., Weimer, P. J., & Vogel, K. P. (2009). Plant species composition and biofuel yields of conservation grasslands. Ecological Applications, 19(8), 2202–2209. https://doi.org/10.1890/07-2094.1

Agblevor, F. A., Evans, R. J., & Johnsonb, K. D. (1994). Lignocellulosic materials I. Herbaceous biomass. Journal of Analytical and Applied Pyrolysis, 30, 125–144.

Ali, I., Adnan, M., Iqbal, A., Ullah, S., Khan, M. R., Yuan, P., Zhang, H., Nasar, J., Gu, M., & Jiang, L. (2022). Effects of Biochar and Nitrogen Application on Rice Biomass Saccharification, Bioethanol Yield and Cell Wall Polymers Features. International Journal of Molecular Sciences, 23(21). https://doi.org/10.3390/ijms232113635

Allison, G. G. (2018). Blended Feedstocks for Thermochemical Conversion : Biomass Characterization and Bio-Oil Production from Switchgrass-Pine Residues Blends. 6(August), 1–16. https://doi.org/10.3389/fenrg.2018.00079

Aurangzaib, M., Moore, K. J., Archontoulis, S. V., Heaton, E. A., Lenssen, A. W., & Fei, S. (2016). Compositional differences among upland and lowland switchgrass ecotypes grown as a bioenergy feedstock crop. Biomass and Bioenergy, 87, 169–177. https://doi.org/10.1016/j.biombioe.2016.02.017

Barbosa, R., Benedito, T., Gonzaga, L., Vieira, E., Regina, M., Boeger, T., Lúcia, C., & Petkowicz, D. O. (2013). Heat stress causes alterations in the cell-wall polymers and anatomy of coffee leaves (*Coffea arabica L.).* Carbohydrate Polymers, 93(1), 135–143. https://doi.org/10.1016/j.carbpol.2012.05.015

Bates, D., Maechler, M., Bolker, B., Walker, S., 2015. Fitting Linear Mixed-Effects Models Using lme4. Journal of Statistical Software, 67(1), 1-48. doi:10.18637/jss.v067.i01.

Bergs, M., Völkering, G., Kraska, T., Pude, R., Do, X. T., Kusch, P., Monakhova, Y., Konow, C., & Schulze, M. (2019). Miscanthus x giganteus stem versus leaf-derived lignins differing in monolignol ratio and linkage. International Journal of Molecular Sciences, 20(5). https://doi.org/10.3390/ijms20051200

Bhandari, H. S., Walker, D. W., Bouton, J. H., & Saha, M. C. (2014). Effects of ecotypes and morphotypes in feedstock composition of switchgrass (Panicum virgatum L.). GCB Bioenergy, 6(1), 26–34. https://doi.org/10.1111/gcbb.12053

Bivand, R., Keitt, T. and Rowlingson, B., 2021. rgdal: Bindings for the 'Geospatial' Data Abstraction Library. R package version 1.5-23. https://CRAN.R-project.org/package=rgdal

Bivand, R. and Lewin-Koh, N., 2021. maptools: Tools for Handling Spatial Objects. R package version 1.1-1. https://CRAN.R-project.org/package=maptools

Brethauer, S., & Studer, M. H. (2015). Biochemical conversion processes of lignocellulosic biomass to fuels and chemicals - A review. Chimia, 69(10), 572–581. https://doi.org/10.2533/chimia.2015.572

Calvin, K., Cowie, A., Berndes, G., Arneth, A., Portugal-, F. C. J., Grassi, G., House, J., & Smith, P. (2021). Bioenergy for climate change mitigation : Scale and sustainability. December 2020, 1346–1371. https://doi.org/10.1111/gcbb.12863

Carpita, N. C., Mccann, M. C., Sciences, B., & Lafayette, W. (2020). Redesigning plant cell walls for the biomass-based bioeconomy. 295(13), 15144–15157. https://doi.org/10.1074/jbc.REV120.014561

Casler, M. D., Lee, D. K., Mitchell, R. B., Moore, K. J., Adler, P. R., Sulc, R. M., Johnson, K. D., Kallenbach, R. L., Boe, A. R., Mathison, R. D., Cassida, K. A., Min, D., Zhang, Y., Ong, R. G., & Sato, T. K. (2022). Biomass Quality Responses to Selection for Increased Biomass Yield in Perennial Energy Grasses. Bioenergy Research, Ivdmd. https://doi.org/10.1007/s12155-022-10513-2

Castillo-Villar, K. K., Eksioglu, S., & Taherkhorsandi, M. (2017). Integrating biomass quality variability in stochastic supply chain modeling and optimization for large-scale biofuel production. Journal of Cleaner Production, 149, 904–918. https://doi.org/10.1016/j.jclepro.2017.02.123

Castillo-villar, K. K., Minor-popocatl, H., & Webb, E. (2016). Quantifying the Impact of Feedstock Quality on the Design of Bioenergy Supply Chain Networks. https://doi.org/10.3390/en9030203

Cheali, P., Posada, J. A., & Gernaey, K. V. (2015). ScienceDirect Upgrading of lignocellulosic biorefinery to value- added chemicals : Sustainability and economics of. 5. https://doi.org/10.1016/j.biombioe.2015.02.030

Cosgrove, D. J. (2005). Growth of the plant cell wall. In Nature Reviews Molecular Cell Biology (Vol. 6, Issue 11, pp. 850–861). https://doi.org/10.1038/nrm1746

Crum, J. R., & Collins, H. P. (1995). KBS Soils. Kellogg Biological Station Long-term Ecological Research Special Publication. Zenodo, http://doi.org/10.5281/zenodo.2581504.

Da Costa, R. M. F., Pattathil, S., Avci, U., Winters, A., Hahn, M. G., & Bosch, M. (2019). Desirable plant cell wall traits for higher-quality miscanthus lignocellulosic biomass. Biotechnology for Biofuels, 12(1), 1–19. https://doi.org/10.1186/s13068-019-1426-7

De Bhowmick, G., Sarmah, A. K., & Sen, R. (2018). Lignocellulosic biorefinery as a model for sustainable development of biofuels and value added products. Bioresource Technology, 247(September 2017), 1144–1154. https://doi.org/10.1016/j.biortech.2017.09.163

Emerson, R., Hoover, A., Ray, A., Lacey, J., Cortez, M., Payne, C., Karlen, D., Birrell, S., Laird, D., Kallenbach, R., Egenolf, J., Sousek, M., & Voigt, T. (2014). Drought effects on composition and yield for corn stover, mixed grasses, and Miscanthus as bioenergy feedstocks. Biofuels, 5(3), 275–291. https://doi.org/10.1080/17597269.2014.913904

Emery, S. M., Stahlheber, K. A., & Gross, K. L. (2020). Drought minimized nitrogen fertilization effects on bioenergy feedstock quality. Biomass and Bioenergy, 133(January), 105452. https://doi.org/10.1016/j.biombioe.2019.105452

Gall, H. Le, Philippe, F., & Domon, J. (2015). Cell Wall Metabolism in Response to Abiotic Stress. i, 112–166. https://doi.org/10.3390/plants4010112

Garlock, R. J., Bals, B., Jasrotia, P., Balan, V., & Dale, B. E. (2012). Influence of variable species composition on the saccharification of AFEXTM pretreated biomass from unmanaged fields in comparison to corn stover. Biomass and Bioenergy, 37, 49–59. https://doi.org/10.1016/j.biombioe.2011.12.036

Ghasemi, E., Ghorbani, G. R., Khorvash, M., Emami, M. R., & Karimi, K. (2013). Chemical composition, cell wall features and degradability of stem, leaf blade and sheath in untreated and alkali-treated rice straw. Animal, 7(7), 1106–1112. https://doi.org/10.1017/S1751731113000256

Gill, J. R., Burks, P. S., Staggenborg, S. A., Moore, K. J., Barrett, M., & Rooney, W. L. (2022). Yield Results and Stability Analysis from the Sorghum Regional Biomass Feedstock Trial. 2014, 1026–1034. https://doi.org/10.1007/s12155-014-9445-5

Gorlitsky, L. E., Sadeghpour, A., Hashemi, M., Etemadi, F., & Herbert, S. J. (2015). Biomass vs. Quality tradeoffs for switchgrass in response to fall harvesting period. Industrial Crops & Products, 63, 311–315. https://doi.org/10.1016/j.indcrop.2014.10.012

Guo, J., Thapa, S., Voigt, T., Owens, V., Boe, A., & Lee, D. K. (2017). Biomass Yield and Feedstock Quality of Prairie Cordgrass in Response to Seeding Rate, Row Spacing, and Nitrogen Fertilization. 2485, 2474–2485. https://doi.org/10.2134/agronj2017.03.0179

Hartig, F., 2021. DHARMa: Residual Diagnostics for Hierarchical (Multi-Level / Mixed) Regression Models. R package version 0.4.3. https://CRAN.R-project.org/package=DHARMa

Heaton, E., Voigt, T., & Long, S. P. (2004). A quantitative review comparing the yields of two candidate C 4 perennial biomass crops in relation to nitrogen, temperature and water. 27, 21–30. https://doi.org/10.1016/j.biombioe.2003.10.005

Hiemstra, P.H., Pebesma, E.J., Twenhofel, C.J.W. and G.B.M. Heuvelink, 2008. Real-time automatic interpolation of ambient gamma dose rates from the Dutch Radioactivity Monitoring Network. Computers & Geosciences, accepted for publication.

Hijmans, R.J., 2021. raster: Geographic Data Analysis and Modeling. R package version 3.4-13. https://CRAN.R-project.org/package=raster

Himmel, M. E., Ding, S., Johnson, D. K., & Adney, W. S. (2007). Biomass Recalcitrance: Engineering Plants and Enzymes for Biofuels Production. Science, 315(February), 804–807. https://doi.org/DOI: 10.1126/science.1137016

Hoover, A., Emerson, R., Ray, A., Stevens, D., Morgan, S., Cortez, M., Kallenbach, R., Sousek, M., Farris, R., & Daubaras, D. (2018a). Impact of drought on chemical composition and sugar yields from dilute-acid pretreatment and enzymatic hydrolysis of Miscanthus, a tall fescue mixture, and switchgrass. Frontiers in Energy Research, 6(JUN), 1–15. https://doi.org/10.3389/fenrg.2018.00054

Hoover, A., Emerson, R., Ray, A., Stevens, D., Morgan, S., Cortez, M., Kallenbach, R., Sousek, M., Farris, R., & Daubaras, D. (2018b). Impact of Drought on Chemical Composition and Sugar Yields from Dilute-Acid Pretreatment and Enzymatic Hydrolysis of Miscanthus, a Tall Fescue Mixture, and Switchgrass. 6(June), 1–15. https://doi.org/10.3389/fenrg.2018.00054

Hoover, A., Emerson, R., Williams, C. L., Ramirez-Corredores, M. M., Ray, A., Schaller, K., Hernandez, S., Li, C., & Walton, M. (2019). Grading Herbaceous Biomass for Biorefineries: a Case Study Based on Chemical Composition and Biochemical Conversion. Bioenergy Research, 12(4), 977–991. https://doi.org/10.1007/s12155-019-10028-3

Hoover, A. N., Emerson, R., Cortez, M., Owens, V., Wolfrum, E., Payne, C., Fike, J., Crawford, J., Crawford, R., Farris, R., Hansen, J., Heaton, E. A., Kumar, S., Mayton, H., & Wilson, D. M. (2022). Key environmental and production factors for understanding variation in switchgrass chemical attributes. GCB Bioenergy, 14(7), 776–792. https://doi.org/10.1111/gcbb.12942

Hu, Y., Li, W. C., Xu, Y. Q., Li, G. J., Liao, Y., & Fu, F. L. (2009). Differential expression of candidate genes for lignin biosynthesis under drought stress in maize leaves. Journal of Applied Genetics, 50(3), 213–223. https://doi.org/10.1007/BF03195675

Ibrahim, M., Hong, C. O., Singh, S., Kumar, S., Osborne, S., & Owens, V. (2017). Switchgrass biomass quality as affected by nitrogen rate, harvest time, and storage. Agronomy Journal, 109(1), 86–96. https://doi.org/10.2134/agronj2016.07.0380

Iraki, N. M., Bressan, R. a, Hasegawa, P. M., & Carpita, N. C. (1989). Alteration of the physical and chemical structure of the primary cell wall of growth-limited plant cells adapted to osmotic stress. Plant Physiol., 91, 39–47. https://doi.org/10.1104/pp.91.1.39

Jiang, Y., Yao, Y., & Wang, Y. (2012). Physiological response, cell wall components, and gene expression of switchgrass under short-term drought stress and recovery. Crop Science, 52(6), 2718–2727. https://doi.org/10.2135/cropsci2012.03.0198

Kenney, K. L., Smith, W. A., Gresham, G. L., & Westover, T. L. (2013). Understanding biomass feedstock variability. Biofuels, 4(1), 111–127. https://doi.org/10.4155/bfs.12.83

Kline, K L, Oladosu, G A, Wolfe, A K, Perlack, R D, & Dale, V H. Biofuel Feedstock

Assessment for Selected Countries. United States. https://doi.org/10.2172/924080

Lan, K., Park, S., Kelley, S. S., English, B. C., Yu, T. H. E., Larson, J., & Yao, Y. (2020). Impacts of uncertain feedstock quality on the economic feasibility of fast pyrolysis biorefineries with blended feedstocks and decentralized preprocessing sites in the Southeastern United States. GCB Bioenergy, 12(11), 1014–1029. https://doi.org/10.1111/gcbb.12752

Lee, D. K., Aberle, E., Anderson, E. K., Anderson, W., Baldwin, B. S., Baltensperger, D., Barrett, M., Blumenthal, J., Bonos, S., Bouton, J., Bransby, D. I., Brummer, C., Burks, P. S., Chen, C., Daly, C., Egenolf, J., Farris, R. L., Fike, J. H., Gaussoin, R., … Owens, V. (2018). Biomass production of herbaceous energy crops in the United States: field trial results and yield potential maps from the multiyear regional feedstock partnership. GCB Bioenergy, 10(10), 698–716. https://doi.org/10.1111/gcbb.12493

Liu, Q., Luo, L., & Zheng, L. (2018). Lignins : Biosynthesis and Biological Functions in Plants. https://doi.org/10.3390/ijms19020335

Lorenzana, R. E., Lewis, M. F., Jung, H. G., Bernardo, R., Lorenzana, R. E., Lewis, M. F., Jung, H. G., & Bernardo, R. (2010). Quantitative Trait Loci and Trait Correlations for Maize Stover Cell Wall Composition and Glucose Release for Cellulosic Ethanol. April, 541–555. https://doi.org/10.2135/cropsci2009.04.0182

Ma, X., Liang, H., Panda, S., Yuen, V. K., Fu, J., Zhou, J., & Zhou, K. (2021). ScienceDirect C2 feedstock-based biomanufacturing of value-added chemicals. September. https://doi.org/10.1016/j.copbio.2021.08.017

Maleki, S. S., Mohammadi, K., & Ji, K. S. (2016). Characterization of Cellulose Synthesis in Plant Cells. In Scientific World Journal (Vol. 2016). Hindawi Publishing Corporation. https://doi.org/10.1155/2016/8641373

Massey, J., Antonangelo, J., & Zhang, H. (2020). Nitrogen fertilization and harvest timing affect switchgrass quality. Resources, 9(6). https://doi.org/10.3390/RESOURCES9060061

Metcalfe, P., Beven, K. and Freer, J., 2018. dynatopmodel: Implementation of the Dynamic TOPMODEL Hydrological Model. R package version 1.2.1. https://CRAN.R-project.org/package=dynatopmodel

Metzner, C., Young, T. M., & Rials, T. (2019). Accurately Estimating and Minimizing Costs for the Cellulosic Biomass Supply Chain with Statistical Process Control and the Taguchi Loss Function. February. https://doi.org/10.15376/biores.14.2.2961-2976

Ong, R. G., Higbee, A., Bottoms, S., Dickinson, Q., Xie, D., Smith, S. A., Serate, J., Pohlmann, E., Jones, A. D., Coon, J. J., Sato, T. K., Sanford, G. R., Eilert, D., Oates, L. G., Piotrowski, J. S., Bates, D. M., Cavalier, D., & Zhang, Y. (2016). Inhibition of microbial biofuel production in drought-stressed switchgrass hydrolysate. Biotechnology for Biofuels, 9(1), 1–14. https://doi.org/10.1186/s13068-016-0657-0

Paradis, E. & Schliep, K. 2019. ape 5.0: an environment for modern phylogenetics and evolutionary analyses in R. Bioinformatics 35: 526-528.

Patton, A. R., & Cieseker, L. (1942). Seasonal Changes in the Lignin and Cellulose Content of Some Montana Grasses, Journal of Animal Science, Volume 1, Issue 1, February 1942, Pages 22–26, https://doi.org/10.2527/jas1942.1122

Pebesma, E.J., 2004. Multivariable geostatistics in S: the gstat package. Computers & Geosciences, 30: 683-691.

Pebesma, E.J., Bivand, R.S., 2005. Classes and methods for spatial data in R. R News 5 (2), https://cran.r-project.org/doc/Rnews/.

Pebesma, E.J., 2018. Simple Features for R: Standardized Support for Spatial Vector Data. The R Journal 10 (1), 439-446, https://doi.org/10.32614/RJ-2018-009

Peng, X., Li, C., Liu, J., Yi, Z., & Han, Y. (2017). Bioresource Technology Changes in composition, cellulose degradability and biochemical methane potential of Miscanthus species during the growing season. Bioresource Technology, 235, 389–395. https://doi.org/10.1016/j.biortech.2017.03.128

Prasad, D., & Ankit, M. (2015). An overview of key pretreatment processes for biological conversion of lignocellulosic biomass to bioethanol. 3 Biotech, 597–609. https://doi.org/10.1007/s13205-015-0279-4

Ragauskas, A. J., Beckham, G. T., Biddy, M. J., Chandra, R., Chen, F., Davis, M. F., Davison, B. H., Dixon, R. A., Gilna, P., Langan, P., Naskar, A. K., Saddler, J. N., Tschaplinski, T. J., Tuskan, A., Wyman, C. E., Ragauskas, A., Gregg, T., Beckham, T., Biddy, M., … Wyman, E. (2014). Lignin Valorization : Improving Lignin Processing in the Biorefinery Lignin Valorization : Improving Lignin Processing Processing in the Biorefinery. 16–17. https://doi.org/10.1126/science.l246843

Rai, A. K., Hamoud, N., Makishah, A., Wen, Z., Gupta, G., Pandit, S., & Prasad, R. (2022). Recent Developments in Lignocellulosic Biofuels, a Renewable Source of Bioenergy. Fermentation, 8(4), 161. MDPI AG. Retrieved from http://dx.doi.org/10.3390/fermentation8040161

R Core Team (2021). R: A language and environment for statistical computing. R Foundation for Statistical Computing, Vienna, Austria. URL https://www.R-project.org/.

Rousset, F. and Ferdy, J., 2014. Testing environmental and genetic effects in the presence of spatial autocorrelation. Ecography 37(8): 781-790 URL: http://dx.doi.org/10.1111/ecog.00566

Saini, P., Koff, J. P. De, Allison, A., & Hamilton, C. (2017). Changes in Lignocellulosic Polymers, Carbon and Energy in Switchgrass for Bioenergy Production. May, 1935–1943. https://doi.org/10.2134/agronj2017.02.0063

Sanford, G. R., Oates, L. G., Roley, S. S., Duncan, D. S., Jackson, R. D., Robertson, G. P., & Thelen, K. D. (2017). Biomass production a stronger driver of cellulosic ethanol yield than biomass quality. Agronomy Journal, 109(5), 1911–1922. https://doi.org/10.2134/agronj2016.08.0454

Santoro, N., Cantu, S. L., Tornqvist, C. E., Falbel, T. G., Bolivar, J. L., Patterson, S. E., Pauly, M., & Walton, J. D. (2010). A high-throughput platform for screening milligram quantities of plant biomass for lignocellulose digestibility. Bioenergy Research, 3(1), 93–102. https://doi.org/10.1007/s12155-009-9074-6

Santos, R. B., Lee, J. M., Jameel, H., Chang, H. M., & Lucia, L. A. (2012). Effects of hardwood structural and chemical characteristics on enzymatic hydrolysis for biofuel production. Bioresource Technology, 110, 232–238. https://doi.org/10.1016/j.biortech.2012.01.085

Saxton, K. E., & Rawls, W. J. (2006). Soil Water Characteristic Estimates by Texture and Organic Matter for Hydrologic Solutions. Soil Science Society of America Journal, 70(5), 1569–1578. https://doi.org/10.2136/sssaj2005.0117

Scheller, H. V., & Ulvskov, P. (2010). Hemicelluloses. Annual Review of Plant Biology, 61, 263–289. https://doi.org/10.1146/annurev-arplant-042809-112315

Sethupathy, S., Murillo Morales, G., Gao, L., Wang, H., Yang, B., Jiang, J., Sun, J., & Zhu, D. (2022). Lignin valorization: Status, challenges and opportunities. In Bioresource Technology (Vol. 347, Issue January, p. 126696). Elsevier Ltd. https://doi.org/10.1016/j.biortech.2022.126696

Sharma, G., Kaur, M., Punj, S., & Singh, K. (2020). Biomass as a sustainable resource for value-added modern materials: a review. In Biofuels, Bioproducts and Biorefining (Vol. 14, Issue 3, pp. 673–695). https://doi.org/10.1002/bbb.2079

Shi, J., Ebrik, M. A., & Wyman, C. E. (2011). Sugar yields from dilute sulfuric acid and sulfur dioxide pretreatments and subsequent enzymatic hydrolysis of switchgrass. Bioresource Technology, 102(19), 8930–8938. https://doi.org/10.1016/j.biortech.2011.07.042

Smith, M. D., Cheng, X., Petridis, L., Cai, C. M., Wyman, C. E., & Smith, J. C. (2016). production : effect of tetrahydrofuran-water on lignin structure and dynamics †. 1268–1277. https://doi.org/10.1039/c5gc01952d

Stoof, C. R., Richards, B. K., Woodbury, P. B., Fabio, E. S., Brumbach, A. R., Cherney, J., Das, S., Geohring, L., Hansen, J., Volk, T. A., & Steenhuis, T. S. (2012). US. Untapped Potential : Opportunities and Challenges for Sustainable Bioenergy Production from Marginal Lands in the Northeast USA. November 2017. https://doi.org/10.1007/s12155-014-9515-8

Soil Survey Staff, Natural Resources Conservation Service, United States Department of Agriculture. Web Soil Survey. Available online at http://websoilsurvey.nrcs.usda.gov/ accessed [05/08/2022]

Takkellapati, S., Li, T., & Gonzalez, M. A. (2018). An overview of biorefinery - derived platform chemicals from a cellulose and hemicellulose biorefinery. Clean Technologies and Environmental Policy, 20(7), 1615–1630. https://doi.org/10.1007/s10098-018-1568-5

Tanger, P., Field, J. L., Jahn, C. E., DeFoort, M. W., & Leach, J. E. (2013). Biomass for thermochemical conversion: Targets and challenges. In Frontiers in Plant Science (Vol. 4, Issue JUL, pp. 1–20). https://doi.org/10.3389/fpls.2013.00218

Templeton, D. W., Scarlata, C. J., Sluiter, J. B., & Wolfrum, E. J. (2010). Compositional analysis of lignocellulosic feedstocks. 2. Method uncertainties. Journal of Agricultural and Food Chemistry, 58(16), 9054–9062. https://doi.org/10.1021/jf100807b

Templeton, D. W., Sluiter, A. D., Hayward, T. K., Hames, B. R., & Thomas, S. R. (2009). Assessing corn stover composition and sources of variability via NIRS. Cellulose, 16(4), 621–639. https://doi.org/10.1007/s10570-009-9325-x

Thammasouk, K., Tandjo, D., & Penner, M. H. (1997). Influence of Extractives on the Analysis of Herbaceous Biomass. Journal of Agricultural and Food Chemistry, 45(2), 437–443. https://doi.org/10.1021/jf960401r

Valentine, J., Clifton-brown, J., Hastings, A., & Robson, P. (2012). Food vs. fuel : the use of land for lignocellulosic 'next generation' energy crops that minimize competition with primary food production. 2008, 1–19. https://doi.org/10.1111/j.1757-1707.2011.01111.x

Van der Weijde, T., Huxley, L. M., Hawkins, S., Sembiring, E. H., Farrar, K., Dolstra, O., Visser, R. G. F., & Trindade, L. M. (2017). Impact of drought stress on growth and quality of miscanthus for biofuel production. GCB Bioenergy, 9(4), 770–782. https://doi.org/10.1111/gcbb.12382

Waliszewska, B., Grzelak, M., Gaweł, E., Spek-Dźwigała, A., Sieradzka, A., & Czekała, W. (2021). Chemical characteristics of selected grass species from polish meadows and their potential utilization for energy generation purposes. Energies, 14(6). https://doi.org/10.3390/en14061669

Wi, S. G., Cho, E. J., Lee, D. S., Lee, S. J., Lee, Y. J., & Bae, H. J. (2015). Lignocellulose conversion for biofuel: A new pretreatment greatly improves downstream biocatalytic hydrolysis of various lignocellulosic materials. Biotechnology for Biofuels, 8(1), 1–11. https://doi.org/10.1186/s13068-015-0419-4

Wickham, H. (2016). ggplot2: Elegant Graphics for Data Analysis. Springer-Verlag New York.

Yang, F., Hanna, M. A., & Sun, R. (2012). Value-added uses for crude glycerol – a byproduct of biodiesel production. Biotechnol Biofuels 5, 13 (2012). https://doi.org/10.1186/1754-6834-5-13

Yang, X., Lu, M., Wang, Y., Wang, Y., Liu, Z., & Chen, S. (2021). Response mechanism of plants to drought stress. In Horticulturae (Vol. 7, Issue 3). https://doi.org/10.3390/horticulturae7030050

Zhang, S., Jiang, S. F., Huang, B. C., Shen, X. C., Chen, W. J., Zhou, T. P., Cheng, H. Y., Cheng, B. H., Wu, C. Z., Li, W. W., Jiang, H., & Yu, H. Q. (2020). Sustainable production of value-added carbon nanomaterials from biomass pyrolysis. Nature Sustainability, 3(9), 753–760. https://doi.org/10.1038/s41893-020-0538-1

APPENDIX

Table A3.1. Plant species and seeding rate at Marshall and Lux Arbor Farms.

Cropping System	Species		Seeding Rate (kg ha^{-1})
Restored prairie	*Aster azureus*	forb	0.07
	Asclepias tuberosa L.		0.04
	Monarda fistulosa L.		0.07
	Asclepias syriaca L.		0.07
	Penstemon digitalis		0.07
	Coreopsis lanceolata		0.14
	Verbena stricta Vent.		0.14
	Rudbeckia triloba L.		0.18
	Rudbeckia hirta L.		0.21
	Ratibida pinnata (Vent.) Barnh.		0.21
	Eryngium yuccifolium Michx.		0.21
	Cassia fasciculata Michx.		0.28
	Echinacea purpurea (L.) Moench		0.28
	Heliopsis helianthoides (L.) Sweet		0.28
	Panicum virgatum var. Southlow	grass	0.56
	Andropogon gerardii		0.56
	Schizacyrium scoparium (Michx.) Nash		1.12
	Sorghastrum nutans (L.) Nash ex Small		1.12
	Elymus canadensis		2.24
Switchgrass	*Panicum virgatum* var. Cave-in-Rock	grass	11.21

Table A3.2. Land use history at Marshall and Lux Arbor Farms.

Farm	Cropping System	Field Size	Pre-conversion (from 1987)	2009 Conversion Year	2010 First Establishment Year	2011 Second Establishment Year
Marshall	Switchgrass	13 ha	CRP Brome grass	No-till soybean	Restored prairie species and oats as nurse crop	Restored prairie species
	Restored prairie	11 ha			Switchgrass and oats as nurse crop	Switchgrass
Lux Arbor	Switchgrass	14 ha	Tilled corn-soybean rotation	No-till soybean	Restored prairie species and oats as nurse crop	Restored prairie species
	Restored prairie	13 ha			Switchgrass and oats as nurse crop	Switchgrass

Table A3.3. Number and distance range (meter) of sampling points for swtichgrass and restored prairie at Marshall and Lux Arbor Farms.

		Marshall			Lux Arbor		
Crop	Year	Minimum	Maximum	Number	Minimum	Maximum	Number
Switchgrass	2018	41.1	331.7	30	33.2	297.7	30
	2019	14.4	408.8	42	22.9	398.0	42
	2020	14.4	408.8	42	22.9	398.0	42
	2021	23.0	400.3	42	22.9	397.7	42
Restored prairie	2018	27.6	350.5	30	23.7	374.5	30
	2019	22.0	458.4	42	19.2	401.2	42
	2020	22.0	458.4	42	19.2	401.2	42
	2021	21.6	441.5	42	16.3	402.0	42

Table A3.4. Descriptive statistics of soil fertility characteristics and topographical features at Lux Arbor Farm in 2018.

	Restored prairie				Switchgrass			
	MIN[1]	MAX[1]	MEAN	SD[1]	MIN	MAX	MEAN	SD
Elevation, m	292.56	298.37	296.64	1.61	285.02	294.71	289.85	2.98
pH	5.7	6.4	6.04	0.19	5.8	6.6	6.22	0.22
Phosphorus, mg kg^{-1}	6	37	17.87	7.84	9	61	23.37	10.49
Soil potassium, mg kg^{-1}	30	135	74.83	28.17	37	125	66.07	22.99
Calcium, mg kg^{-1}	566	1455	975.33	238.58	490	1489	1011.70	261.79
Magnesium, mg kg^{-1}	110	313	185.73	52.20	80	302	178.77	51.60
Total soil carbon (C), wt%	0.64	1.75	1.09	0.26	0.40	1.51	1.00	0.28
Ammonium (NH_4^+), mg kg^{-1}	1.70	5.15	2.97	0.78	1.30	5.20	2.73	0.85
Sand content, wt%	10.60	73.75	44.54	14.23	16.90	81.25	50.94	18.29
Clay content, wt%	7.50	30.70	20.48	5.99	0.00	38.10	19.00	10.27
Slope, °	0.23	6.03	1.98	1.55	0.38	5.95	2.95	1.41
Aspect,	42.59	359.42	223.55	84.11	9.71	356.04	279.84	90.96
Plane curvature, km^{-1}	-0.30	0.30	0.01	0.13	-0.30	0.41	0.03	0.16
Profile curvature, km^{-1}	-0.57	0.34	0.00	0.18	-0.23	0.38	0.00	0.14
Topographical wetness index	4.67	11.36	7.07	1.67	4.83	13.35	7.33	1.96
15 bar lower limit of soil water content (LL15), v%	4.4	18.5	12.36	3.61	1.0	22.7	11.36	6.22
Drained upper limit of soil water content (DUL), v%	13.70	35.60	24.48	5.27	7.50	37.20	22.17	8.72
Saturated water content (SAT), v%	38.10	44.40	39.67	1.52	38.10	45.70	40.07	2.06
Whole profile drainage rate coefficient (SWCON)	17.0	59.1	26.45	9.08	16.6	90.0	38.03	25.87
Saturated hydraulic conductivity (Ksat), mm h^{-1}	2.00	44.09	11.45	9.08	1.58	113.16	25.89	32.59

1. Abbreviation: MIN: minimum, MAX: maximum, SD: standard deviation.

Table A3.5. Descriptive statistics of soil fertility characteristics and topographical features at Lux Arbor Farm in 2020.

	Restored prairie				Switchgrass			
	MIN[1]	MAX[1]	MEAN	SD[1]	MIN	MAX	MEAN	SD
Elevation, m	292.05	298.37	296.51	1.61	284.11	296.43	289.80	3.32
pH	5.5	6.4	5.82	0.22	5.5	6.6	5.97	0.27
Phosphorus, mg kg^{-1}	10	69	21.69	13.95	11	56	24.63	11.60
Soil potassium, mg kg^{-1}	27	169	76.15	29.20	49	141	76.32	21.67
Calcium, mg kg^{-1}	442	1477	971.46	254.85	552	1589	1036.18	280.54
Magnesium, mg kg^{-1}	75	275	181.26	50.39	86	296	179.53	49.76
Total soil carbon(C), wt%	0.69	1.81	1.17	0.31	0.58	1.75	0.97	0.31
Ammonium (NH_4^+), mg kg^{-1}	2.26	32.81	5.07	4.99	3.16	10.26	4.96	1.53
Sand content, wt%	10.60	73.75	47.94	14.10	16.90	81.25	54.58	17.44
Clay content, wt%	7.50	30.70	20.58	5.44	0.00	38.10	18.69	8.95
Slope, °	0.14	6.82	2.06	1.81	0.38	6.55	3.15	1.63
Aspect,	29.75	359.42	203.02	88.73	9.71	356.04	271.54	97.10
Plane curvature, km^{-1}	-0.30	0.30	0.02	0.13	-0.30	0.41	0.02	0.14
Profile curvature, km^{-1}	-0.57	0.34	0.00	0.16	-0.23	0.38	-0.01	0.13
Topographical wetness index	4.70	14.64	7.53	2.49	4.67	13.34	7.34	1.96
15 bar lower limit of soil water content (LL15), v%	4.4	18.5	12.27	3.40	1.0	22.7	11.02	5.65
Drained upper limit of soil water content (DUL), v%	13.70	35.60	23.79	5.24	7.50	37.20	21.21	8.17
Saturated water content (SAT), v%	38.10	44.40	39.53	1.37	38.10	45.70	39.78	1.92
Whole profile drainage rate coefficient (SWCON)	17.0	59.1	27.43	9.63	16.6	90.0	38.42	23.35
Saturated hydraulic conductivity (Ksat), mm h^{-1}	2.00	44.09	12.42	9.63	1.58	113.16	25.68	29.20

1. Abbreviation: MIN: minimum, MAX: maximum, SD: standard deviation.

Table A3.6. Descriptive statistics of soil fertility characteristics and topographical features at Marshall Farm in 2018.

	Restored prairie				Switchgrass			
	MIN[1]	MAX[1]	MEAN	SD[1]	MIN	MAX	MEAN	SD
Elevation, m	284.96	294.32	290.40	2.69	289.94	298.48	295.87	2.21
pH	5.40	6.40	6.05	0.25	5.30	5.80	5.60	0.13
Phosphorus, mg kg^{-1}	15	126	54.17	22.51	16	119	61.07	23.11
Soil potassium, mg kg^{-1}	8	363	61.47	65.27	10	333	126.73	66.39
Calcium, mg kg^{-1}	396	1182	671.73	159.01	488	890	715.03	90.05
Magnesium, mg kg^{-1}	44	137	66.33	19.09	77	191	114.10	24.45
Total soil carbon (C), wt%	0.70	2.05	1.12	0.29	0.94	1.88	1.31	0.22
Ammonium (NH_4^+), mg kg^{-1}	3.02	12.85	5.48	2.11	2.95	18.20	6.56	3.61
Sand content, wt%	20.00	88.30	69.58	16.66	24.60	86.25	57.40	12.98
Clay content, wt%	1.25	20.70	9.47	5.09	1.25	27.40	13.69	7.59
Slope, °	0.65	12.64	4.86	2.97	0.44	7.32	2.41	1.68
Aspect,	18.44	318.08	163.87	94.61	120.29	355.52	208.20	67.28
Plane curvature, km^{-1}	-1.00	0.61	0.07	0.36	-1.54	0.31	-0.03	0.37
Profile curvature, km^{-1}	-0.77	0.75	0.08	0.36	-0.26	0.52	0.05	0.17
Topographical wetness index	4.27	14.38	7.02	2.72	4.96	12.43	7.14	1.99
15 bar lower limit of soil water content (LL15), v%	1.0	12.4	5.43	3.21	1.0	16.6	8.18	4.67
Drained upper limit of soil water content (DUL), v%	4.90	28.20	13.27	5.87	5.80	31.90	18.19	6.45
Saturated water content (SAT), v%	38.10	41.60	39.25	0.99	38.00	42.20	39.05	0.96
Whole profile drainage rate coefficient (SWCON)	20.1	90.0	61.98	23.83	18.1	90.0	45.17	24.31
Saturated hydraulic conductivity (Ksat), mm h^{-1}	5.07	144.82	58.60	41.84	3.11	137.14	35.83	37.64

1. Abbreviation: MIN: minimum, MAX: maximum, SD: standard deviation.

Table A3.7. Descriptive statistics of soil fertility characteristics and topographical features at Marshall Farm in 2020.

	Restored prairie				Switchgrass			
	MIN[1]	MAX[1]	MEAN	SD[1]	MIN	MAX	MEAN	SD
Elevation, m	284.96	294.32	290.34	2.62	289.94	299.01	295.61	2.31
pH	5.70	7.50	6.17	0.38	5.10	7.70	5.59	0.43
Phosphorus, mg kg^{-1}	17	127	50.54	23.75	16	124	58.64	23.87
Soil potassium, mg kg^{-1}	22	245	66.43	48.57	25	266	105.81	49.58
Calcium, mg kg^{-1}	405	2023	818.73	329.05	393	3438	687.94	489.28
Magnesium, mg kg^{-1}	45	126	74.78	22.17	58	177	91.97	25.37
Total soil carbon (C), wt%	0.64	2.28	1.31	0.37	0.87	2.04	1.33	0.31
Ammonium (NH_4^+), mg kg^{-1}	3.15	14.30	6.10	2.48	3.35	31.40	9.47	6.20
Sand content, wt%	20.00	88.30	72.30	14.80	24.60	86.25	60.31	13.58
Clay content, wt%	1.25	20.70	9.89	4.45	1.25	27.40	14.36	7.06
Slope, °	0.65	12.64	4.71	2.93	0.21	7.32	2.33	1.66
Aspect,	10.16	353.16	164.70	104.53	22.84	355.52	205.70	76.38
Plane curvature, km^{-1}	-1.00	0.61	0.01	0.38	-1.54	0.36	-0.04	0.36
Profile curvature, km^{-1}	-0.83	0.86	0.04	0.42	-0.26	0.52	0.03	0.16
Topographical wetness index	4.27	14.38	7.06	2.66	4.96	12.40	7.54	2.16
15 bar lower limit of soil water content (LL15), v%	1.0	12.5	5.60	2.96	1.0	16.6	8.42	4.47
Drained upper limit of soil water content (DUL), v%	4.90	28.20	13.05	5.35	5.80	31.90	18.09	6.26
Saturated water content (SAT), v%	38.10	41.60	39.21	0.91	38.10	42.20	39.03	0.88
Whole profile drainage rate coefficient (SWCON)	20.1	90.0	62.18	21.91	18.1	90.0	44.74	23.12
Saturated hydraulic conductivity (Ksat), mm h^{-1}	5.07	144.82	56.64	38.10	3.11	137.14	34.46	35.04

1. Abbreviation: MIN: minimum, MAX: maximum, SD: standard deviation.

Table A3.8. Moran's I values of observed glucose content (mg g^{-1}) for switchgrass and restored prairie at Marshall and Lux Arbor Farms during the study period (2018-2020).

		Marshall			
Crop	Year	Observed Value	Expected Value	Standard Deviation	P-value
Switchgrass	2018	-0.37	-0.34	0.25	0.932
	2019	-0.42	-0.24	0.20	0.388
	2020	0.04	-0.24	0.21	0.183
Restored prairie	2018	-0.65	-0.34	0.28	0.279
	2019	-0.50	-0.24	0.23	0.264
	2020	-0.15	-0.24	0.23	0.685
		Lux Arbor			
		Observed Value	Expected Value	Standard Deviation	P-value
Switchgrass	2018	-0.28	-0.34	0.26	0.811
	2019	-0.48	-0.24	0.22	0.292
	2020	-0.04	-0.24	0.20	0.310
Restored prairie	2018	-0.62	-0.34	0.25	0.271
	2019	-0.20	-0.24	0.23	0.866
	2020	-0.29	-0.24	0.24	0.841

Table A3.9. Moran's I values of observed xylose content (mg g^{-1}) for switchgrass and restored prairie at Marshall and Lux Arbor Farms during the study period (2018-2020).

		Marshall			
Crop	Year	Observed Value	Expected Value	Standard Deviation	P-value
Switchgrass	2018	-0.23	-0.34	0.25	0.638
	2019	-0.10	-0.24	0.20	0.472
	2020	-0.29	-0.24	0.22	0.824
Restored prairie	2018	-0.60	-0.34	0.28	0.367
	2019	-0.49	-0.24	0.23	0.281
	2020	-0.36	-0.24	0.23	0.603
		Lux Arbor			
		Observed Value	Expected Value	Standard Deviation	P-value
Switchgrass	2018	-0.46	-0.34	0.27	0.680
	2019	-0.56	-0.24	0.21	0.137
	2020	-0.40	-0.24	0.18	0.380
Restored prairie	2018	-0.53	-0.34	0.27	0.487
	2019	0.00	-0.24	0.23	0.300
	2020	-0.46	-0.24	0.24	0.369

Table A3.10. Moran's I values of observed lignin content (mg g^{-1}) for switchgrass and restored prairie at Marshall and Lux Arbor Farms during the study period (2018-2020).

		Marshall			
Crop	Year	Observed Value	Expected Value	Standard Deviation	P-value
Switchgrass	2018	0.34	-0.34	0.25	0.006
	2019	-0.50	-0.24	0.22	0.246
	2020	-0.43	-0.24	0.22	0.391
Restored prairie	2018	-0.71	-0.34	0.28	0.193
	2019	-0.39	-0.24	0.23	0.524
	2020	-0.13	-0.24	0.23	0.605
		Lux Arbor			
		Observed Value	Expected Value	Standard Deviation	P-value
Switchgrass	2018	-0.43	-0.34	0.27	0.756
	2019	-0.23	-0.24	0.22	0.957
	2020	-0.45	-0.24	0.21	0.338
Restored prairie	2018	-0.61	-0.34	0.31	0.400
	2019	-0.38	-0.24	0.24	0.578
	2020	-0.07	-0.24	0.24	0.488

Table A3.11. Results of full model, backward selection model and bootstrap models with backward selection procedure (1000 replications) for glucose content (mg g^{-1}) of switchgrass at Lux Arbor Farm.

	Full Model		Backward Select Model		Bootstrap (1000 replications)			
	Coef[1]	SE[1]	Coef[1]	SE[1]	Inclusion[1]	M[1]	2.5%[1]	97.5%[1]
(Intercept)	132.48	1.40	132.26	0.79	1	132.53	129.90	135.13
Early growing season precipitation (Early), mm	678.93	33.18	669.28	26.88	1	679.50	610.12	753.11
Late growing season precipitation (Late), mm	678.92	33.47	668.82	26.90	1	679.45	607.84	754.06
Potassium, mg kg^{-1}	-4.19	1.48	-3.39	0.98	0.959	-4.08	-7.16	0
Phosphorus, mg kg^{-1}	2.47	1.61			0.671	2.20	0	5.56
Clay content, wt%	-2.13	90.57			0.640	0	-194	192.96
Sand content, wt%	17.20	51.98			0.617	0	-83	128.86
Magnesium, mg kg^{-1}	2.69	2.66	2.33	0.96	0.576	2.23	-3.51	8
Saturated water content (SAT), v%	5.76	16.46	0.00	0.00	0.556	0.00	-25	41.63
Slope, °	1.47	2.27	2.35	0.83	0.547	1.73	0.00	6.10
Drained upper limit of soil water content (DUL), v%	27.66	103.71			0.523	0	-171.81	247.05
Calcium, mg kg^{-1}	1.48	3.03			0.478	0.00	-4.74	7.62
Topographical wetness index (TWI)	-1.42	2.41			0.460	0.00	-6.32	4
Saturated hydraulic conductivity (Ksat), mm h^{-1}	-3.14	11.30			0.447	0	-25.76	19.16
15 bar lower limit of soil water content (LL15), v%	-19.96	37.65			0.439	0	-116.43	58.11
Ammonium (NH_4^+), mg kg^{-1}	-1.53	1.49			0.436	0	-4.35	0.00
Plane curvature, km^{-1}	-3.32	14.48			0.415	0	-30.52	27.61
Total soil carbon, wt%	-0.93	1.39			0.393	0	-3.71	2.27
Aspect	-0.32	1.26			0.386	0	-3.61	2.73
Whole profile drainage rate coefficient (SWCON)	-4.52	9.83			0.367	0	-25.11	15.00
Elevation, m	0.45	1.59			0.362	0	-2.53	3.80
Profile curvature, km^{-1}	-3.42	8.91			0.362	0	-25.24	17.87
pH	-0.19	1.40			0.265	0	-2.84	2.90

1. Abbreviation: Coef: estimation of coefficient, SE: standard error for the estimation of coefficient, Inclusion: inclusion probability, M: median, 2.5%: 2.5 percentile, 97.5%: 97.5 percentile.

Table A3.12. Results of full model, backward selection model and bootstrap models with backward selection procedure (1000 replications) for glucose content (mg g^{-1}) of restored prairie at Lux Arbor Farm.

	Full Model		Backward Select Model		Bootstrap (1000 replications)			
	Coef[1]	SE[1]	Coef[1]	SE[1]	Inclusion[1]	M[1]	2.5%[1]	97.5%[1]
(Intercept)	127.60	7.28	127.60	5.46	1	128.23	113.13	144.31
Early growing season precipitation (Early), mm	1102.73	54.22	1097.91	45.99	1	1106.15	1020.19	1198.57
Late growing season precipitation (Late), mm	1105.87	54.61	1100.89	45.99	1	1109.81	1021.82	1203.39
Clay content, wt%	-624.19	303.42	-637.66	227.22	0.918	-586.59	-1189.34	0
Phosphorus, mg kg^{-1}	-7.86	2.75	-7.05	1.93	0.913	-7.97	-14.16	0
15 bar lower limit of soil water content (LL15), v%	635.39	319.79	624.79	229.39	0.858	634.06	0	1262.20
Saturated water content (SAT), v%	47.20	29.76	52.46	16.75	0.796	39.39	0	101.09
Aspect	3.71	2.06	3.67	1.52	0.751	3.31	0	8.73
Calcium, mg kg^{-1}	-7.80	5.24	-4.86	2.10	0.735	-6.26	-16.08	0
Whole profile drainage rate coefficient (SWCON)	-444.14	796.90	-23.94	10.17	0.650	-19.70	-2076.34	1011.55
Sand content, wt%	42.72	85.45	64.49	20.41	0.641	0	-159.20	209.34
Potassium, mg kg^{-1}	3.79	2.54	2.96	1.81	0.633	3.18	0	8.04
Drained upper limit of soil water content (DUL), v%	-36.26	130.65			0.574	0	-367.87	239.69
Topographical wetness index (TWI)	-2.60	2.77	-3.13	1.91	0.500	0	-8.44	4.18
Saturated hydraulic conductivity (Ksat), mm h^{-1}	421.35	794.11			0.499	0	-1019.99	2057.36
Elevation, m	0.61	3.00			0.442	0	-6.50	8.10
Profile curvature, km^{-1}	5.40	16.44			0.409	0	-36.41	43.84
Magnesium, mg kg^{-1}	2.16	5.53			0.335	0	-7.84	12.32
pH	0.41	2.71			0.333	0	-5.31	6.03
Ammonium (NH_4^+), mg kg^{-1}	-0.01	2.83			0.306	0	-11.21	7.10
Total soil carbon, wt%	0.52	3.75			0.303	0	-7.55	7.18
Plane curvature, km^{-1}	0.42	14.37			0.274	0	-26.29	32.39
Slope, °	-0.23	2.87			0.237	0	-4.93	5.58

1. Abbreviation: Coef: estimation of coefficient, SE: standard error for the estimation of coefficient, Inclusion: inclusion probability, M: median, 2.5%: 2.5 percentile, 97.5%: 97.5 percentile.

Table A3.13. Results of full model, backward selection model and bootstrap models with backward selection procedure (1000 replications) for glucose content (mg g^{-1}) of switchgrass at Marshall Farm.

	Full Model		Backward Select Model		Bootstrap (1000 replications)			
	Coef[1]	SE[1]	Coef[1]	SE[1]	Inclusion[1]	M[1]	2.5%[1]	97.5%[1]
(Intercept)	130.46	1.89	130.30	0.82	1	130.12	125.75	133.22
Early growing season precipitation (Early), mm	16.16	0.96	15.21	0.77	1	15.83	13.87	18.05
Late growing season precipitation (Late), mm	19.75	0.83	20.42	0.74	1	20.03	18.26	21.63
Slope, °	3.41	1.42	2.78	1.07	0.813	3.00	0	6.47
Elevation, m	3.08	1.69	3.94	1.15	0.770	2.81	0	6.77
Saturated hydraulic conductivity (Ksat), mm h^{-1}	-13.52	9.38	-13.68	5.45	0.751	-10.21	-29.80	0
Sand content, wt%	16.63	38.14	8.70	2.87	0.740	4.18	-58.39	80.05
Saturated water content (SAT), v%	7.09	6.51	7.22	3.05	0.681	4.48	-4.69	18.53
Whole profile drainage rate coefficient (SWCON)	-8.91	6.65	-9.37	4.85	0.612	-7.25	-21.93	0
Profile curvature, km^{-1}	-10.69	7.87	-12.03	6.47	0.610	-10.27	-28.95	0
Clay content, wt%	-30.47	58.39	-14.57	6.12	0.583	0	-142.44	72.82
Magnesium, mg kg^{-1}	-2.14	1.47			0.553	-1.22	-5.33	2.33
Drained upper limit of soil water content (DUL), v%	14.96	77.34			0.525	0	-140.96	142.25
Aspect	1.46	1.13			0.499	0	0	3.68
Phosphorus, mg kg^{-1}	-1.23	1.35			0.495	0	-4.78	1.97
Total soil carbon, wt%	1.24	1.35			0.469	0	-1.49	4.61
Ammonium (NH_4^+), mg kg^{-1}	0.88	0.95			0.447	0	0	2.62
Topographical wetness index (TWI)	1.46	1.75			0.445	0	-1.27	5.14
Plane curvature, km^{-1}	3.89	5.07			0.412	0	-3.83	17.69
Potassium, mg kg^{-1}	1.16	1.62			0.390	0	-1.80	5.32
pH	-0.98	2.28	-1.40	0.89	0.382	0	-5.90	3.41
Calcium, mg kg^{-1}	-0.20	2.28			0.346	0	-10.15	5.13
15 bar lower limit of soil water content (LL15), v%	7.65	41.15			0.332	0	-58.61	110.43

1. Abbreviation: Coef: estimation of coefficient, SE: standard error for the estimation of coefficient, Inclusion: inclusion probability, M: median, 2.5%: 2.5 percentile, 97.5%: 97.5 percentile.

Table A3.14. Results of full model, backward selection model and bootstrap models with backward selection procedure (1000 replications) for glucose content (mg g^{-1}) of restored prairie at Marshall Farm.

	Full Model		Backward Select Model		Bootstrap (1000 replications)			
	Coef[1]	SE[1]	Coef[1]	SE[1]	Inclusion[1]	M[1]	2.5%[1]	97.5%[1]
(Intercept)	127.80	5.29	127.13	4.83	1	130.37	116.88	140.20
Late growing season precipitation (Late), mm	21.36	2.42	21.45	2.30	1	21.53	17.-7	25.76
Early growing season precipitation (Early), mm	10.78	2.62	10.59	2.46	0.997	10.75	5.34	17.00
Topographical wetness index (TWI)	-13.04	5.67	-16.93	3.42	0.850	-14.21	-25.09	0.00
Drained upper limit of soil water content (DUL), v%	-280.91	211.59	-325.58	192.62	0.779	-91.38	-681.38	284.33
Total soil carbon, wt%	-8.02	4.92	-8.80	3.57	0.761	-8.64	-18.70	0
Sand content, wt%	-163.43	131.60	-189.43	119.35	0.752	-40.34	-410.56	191.76
Saturated water content (SAT), v%	23.02	14.35	24.24	10.17	0.727	21.11	0.00	54.80
Saturated hydraulic conductivity (Ksat), mm h^{-1}	-36.90	24.91	-39.32	19.00	0.700	-37.26	-97.39	0.22
pH	6.91	4.92	5.99	2.86	0.653	5.67	0	17.46
Magnesium, mg kg^{-1}	6.49	4.81	6.16	3.59	0.598	5.81	0	15.34
Whole profile drainage rate coefficient (SWCON)	-21.71	19.93	-26.96	12.87	0.568	-16.38	-56.17	17.72
Clay content, wt%	94.20	118.71	112.28	83.60	0.537	0	-217.88	320.49
Plane curvature, km^{-1}	8.00	9.40			0.507	0	-9.82	32.81
Slope, °	3.41	3.46			0.482	0	-3.58	10.01
Ammonium (NH_4^+), mg kg^{-1}	3.14	3.40			0.406	0	-3.22	10.42
Phosphorus, mg kg^{-1}	-1.46	4.36			0.387	0	-10.63	8.22
Elevation, m	2.67	4.10			0.365	0	-5.59	12.50
Profile curvature, km^{-1}	-0.76	9.52			0.358	0	-21.73	22.65
15 bar lower limit of soil water content (LL15), v%	4.61	80.54			0.344	0	-142.64	178.24
Calcium, mg kg^{-1}	-2.07	5.85			0.321	0	-14.29	13.02
Potassium, mg kg^{-1}	-1.64	4.67			0.320	0	-12.89	8.18
Aspect	0.57	3.30			0.296	0	-6.25	7.68

1. Abbreviation: Coef: estimation of coefficient, SE: standard error for the estimation of coefficient, Inclusion: inclusion probability, M: median, 2.5%: 2.5 percentile, 97.5%: 97.5 percentile.

Table A3.15. Results of full model, backward selection model and bootstrap models with backward selection procedure (1000 replications) for xylose content (mg g^{-1}) of switchgrass at Lux Arbor Farm.

	Full Model		Backward Select Model		Bootstrap (1000 replications)			
	Coef[1]	SE[1]	Coef[1]	SE[1]	Inclusion[1]	M[1]	2.5%[1]	97.5%[1]
(Intercept)	80.84	0.69	80.57	0.40	1	80.78	79.35	82.29
Early growing season precipitation (Early), mm	299.18	16.22	288.30	13.48	1	298.44	265.46	330.37
Late growing season precipitation (Late), mm	295.57	16.36	284.29	13.49	1	294.75	261.69	327.44
Topographical wetness index (TWI)	-1.75	1.18			0.696	-1.30	-3.66	0.02
Sand content, wt%	11.01	25.41			0.661	0	-38.46	67.48
Clay content, wt%	5.29	44.27			0.652	0	-97.14	91.11
Saturated water content (SAT), v%	0.25	8.04			0.628	0	-14.57	17.82
Total soil carbon, wt%	-0.75	0.68	-0.71	0.40	0.574	-0.79	-2.35	1.34
Drained upper limit of soil water content (DUL), v%	23.87	50.69			0.563	0	-73.28	139.30
15 bar lower limit of soil water content (LL15), v%	-18.83	18.40			0.55	-0.35	-58.56	20.52
pH	0.69	0.69			0.542	0.68	0.00	2.16
Magnesium, mg kg^{-1}	1.34	1.30			0.533	0	-1.95	3.98
Slope, °	-1.14	1.11			0.531	0	-3.05	1.13
Saturated hydraulic conductivity (Ksat), mm h^{-1}	0.57	5.52			0.523	0	-11.94	12.66
Phosphorus, mg kg^{-1}	0.96	0.78			0.516	0.59	0	2.46
Elevation, m	-0.46	0.78			0.483	0	-2.41	1.35
Plane curvature, km^{-1}	-5.13	7.08			0.426	0	-16.67	9.50
Calcium, mg kg^{-1}	-0.50	1.48			0.42	0	-3.74	2.69
Potassium, mg kg^{-1}	-0.64	0.72			0.414	0	-1.94	0.89
Ammonium (NH_4^+), mg kg^{-1}	-0.36	0.73			0.351	0	-1.91	1.19
Aspect	-0.27	0.62			0.345	0	-1.65	0.69
Profile curvature, km^{-1}	-0.24	4.36			0.311	0	-9.16	9.79
Whole profile drainage rate coefficient (SWCON)	-0.11	4.80			0.267	0	-9.43	8.39

1. Abbreviation: Coef: estimation of coefficient, SE: standard error for the estimation of coefficient, Inclusion: inclusion probability, M: median, 2.5%: 2.5 percentile, 97.5%: 97.5 percentile.

Table A3.16. Results of full model, backward selection model and bootstrap models with backward selection procedure (1000 replications) for xylose content (mg g^{-1}) of restored prairie at Lux Arbor Farm.

	Full Model		Backward Select Model		Bootstrap (1000 replications)			
	Coef[1]	SE[1]	Coef[1]	SE[1]	Inclusion[1]	M[1]	2.5%[1]	97.5%[1]
(Intercept)	74.43	4.20	73.80	3.25	1	74.48	66.40	82.44
Early growing season precipitation (Early), mm	325.89	31.30	325.30	26.78	1	326.48	268.09	390.05
Late growing season precipitation (Late), mm	322.65	31.52	322.06	26.79	1	323.23	265.36	387.44
Phosphorus, mg kg^{-1}	-4.26	1.59	-4.33	1.18	0.906	-4.24	-7.30	0
Clay content, wt%	-256.61	175.15	-288.79	128.22	0.811	-255.66	-575.13	36.35
15 bar lower limit of soil water content (LL15), v%	289.10	184.60	315.37	141.72	0.802	298.05	-6.65	625.68
Calcium, mg kg^{-1}	-5.25	3.02	-3.70	1.35	0.785	-4.07	-11.22	0
Drained upper limit of soil water content (DUL), v%	-59.00	75.42	-50.30	18.55	0.698	-54.02	-234.52	99.98
Sand content, wt%	-8.44	49.32	0.00	0.00	0.688	0	-121.22	81.38
Potassium, mg kg^{-1}	2.21	1.47	2.19	1.05	0.682	2.19	0.00	5.09
Whole profile drainage rate coefficient (SWCON)	-321.57	460.01	-9.31	5.04	0.611	-8.64	-1288.16	604.73
Saturated water content (SAT), v%	14.77	17.18	18.20	6.50	0.597	7.93	-22.25	47.00
Aspect	1.52	1.19	1.49	0.88	0.548	1.30	0	4.03
Saturated hydraulic conductivity (Ksat), mm h^{-1}	313.21	458.40			0.504	0	-612.72	1274.46
Total soil carbon, wt%	1.40	2.16	2.16	1.37	0.433	0	-3.27	5.25
Topographical wetness index (TWI)	-1.30	1.60	-1.75	1.18	0.404	0	-4.57	0.04
Magnesium, mg kg^{-1}	1.65	3.19			0.374	0	-5.03	7.66
Ammonium (NH_4^+), mg kg^{-1}	0.76	1.63			0.362	0	-3.14	4.63
Elevation, m	-0.04	1.73			0.356	0	-3.94	3.48
Profile curvature, km^{-1}	3.06	9.49			0.335	0	-17.18	22.50
pH	0.10	1.56			0.320	0	-3.02	3.16
Plane curvature, km^{-1}	1.83	8.29			0.307	0	-14.24	20.24
Slope, °	-0.12	1.66			0.229	0	-2.94	3.07

1. Abbreviation: Coef: estimation of coefficient, SE: standard error for the estimation of coefficient, Inclusion: inclusion probability, M: median, 2.5%: 2.5 percentile, 97.5%: 97.5 percentile.

Table A3.17. Results of full model, backward selection model and bootstrap models with backward selection procedure (1000 replications) for xylose content (mg g^{-1}) of switchgrass at Marshall Farm.

	Full Model		Backward Select Model		Bootstrap (1000 replications)			
	Coef[1]	SE[1]	Coef[1]	SE[1]	Inclusion[1]	M[1]	2.5%[1]	97.5%[1]
(Intercept)	80.63	1.33	80.71	0.84	1	80.37	75.89	83.43
Early growing season precipitation (Early), mm	8.04	0.67	7.91	0.54	1	7.92	6.51	9.31
Late growing season precipitation (Late), mm	9.65	0.58	9.78	0.51	1	9.74	8.58	10.81
Sand content, wt%	64.93	26.73	66.61	21.29	0.98	62.10	4.54	105.33
Saturated hydraulic conductivity (Ksat), mm h^{-1}	-22.40	6.57	-23.89	5.72	0.979	-21.74	-33.42	-2.40
Saturated water content (SAT), v%	13.60	4.56	14.48	3.73	0.94	13.20	0	21.45
Elevation, m	3.73	1.18	4.29	0.92	0.927	3.53	0	5.95
Clay content, wt%	-97.18	40.92	-95.07	30.02	0.919	-97.02	-199.53	0
Whole profile drainage rate coefficient (SWCON)	-11.63	4.66	-11.98	3.51	0.85	-10.90	-21.11	0
Profile curvature, km^{-1}	-12.52	5.51	-13.44	4.59	0.835	-11.84	-25.53	0
Drained upper limit of soil water content (DUL), v%	112.13	54.20	116.01	42.68	0.793	105.57	0	194.62
Slope, °	1.86	1.00	1.47	0.83	0.718	1.72	0	4.30
Phosphorus, mg kg^{-1}	-1.49	0.94	-1.08	0.70	0.673	-1.45	-4.39	1.01
pH	-1.29	1.60	-1.19	0.73	0.55	-0.88	-5.12	1.62
Aspect	0.94	0.79			0.517	0	0	2.35
Plane curvature, km^{-1}	3.60	3.55			0.51	0	-4.16	16.47
Potassium, mg kg^{-1}	1.09	1.13			0.486	0	0	3.76
Magnesium, mg kg^{-1}	-0.77	1.03			0.464	0	-3.46	1.80
Topographical wetness index (TWI)	1.10	1.22			0.443	0	-1.41	4.27
15 bar lower limit of soil water content (LL15), v%	5.74	28.84			0.39	0	-69.98	130.59
Total soil carbon, wt%	-0.03	0.94			0.358	0	-2.20	2.41
Calcium, mg kg^{-1}	0.33	1.60			0.309	0	-1.99	7.09
Ammonium (NH_4^+), mg kg^{-1}	-0.07	0.66			0.247	0	-1.58	1.20

1. Abbreviation: Coef: estimation of coefficient, SE: standard error for the estimation of coefficient, Inclusion: inclusion probability, M: median, 2.5%: 2.5 percentile, 97.5%: 97.5 percentile.

Table A3.18. Results of full model, backward selection model and bootstrap models with backward selection procedure (1000 replications) for xylose content (mg g^{-1}) of restored prairie at Marshall Farm.

	Full Model		Backward Select Model		Bootstrap (1000 replications)			
	Coef[1]	SE[1]	Coef[1]	SE[1]	Inclusion[1]	M[1]	2.5%[1]	97.5%[1]
(Intercept)	68.74	2.87	68.26	1.30	1	68.50	62.54	75.24
Late growing season precipitation (Late), mm	9.76	1.31	9.78	1.25	1	9.77	7.18	12.05
Early growing season precipitation (Early), mm	5.37	1.43	5.49	1.34	0.990	5.56	2.55	8.48
Total soil carbon, wt%	-7.22	2.68	-6.50	1.84	0.921	-7.18	-13.12	0
Saturated hydraulic conductivity (Ksat), mm h^{-1}	-32.86	13.54	-36.22	9.67	0.883	-32.08	-67.12	0
Magnesium, mg kg^{-1}	5.43	2.61	4.02	1.84	0.842	5.20	0	10.91
Saturated water content (SAT), v%	16.29	7.80	17.48	5.03	0.835	15.91	0	33.00
Topographical wetness index (TWI)	-6.29	3.08	-6.96	1.76	0.807	-6.39	-12.38	0
Sand content, wt%	20.95	71.55	10.99	3.74	0.756	5.16	-119.27	178.73
Clay content, wt%	-53.24	64.54	-55.90	26.06	0.713	-21.15	-194.36	70.01
Drained upper limit of soil water content (DUL), v%	19.35	115.04			0.553	0.00	-203.72	269.94
pH	2.58	2.67			0.529	1.79	-1.91	8.40
Plane curvature, km^{-1}	5.36	5.11			0.525	2.08	-0.12	16.68
15 bar lower limit of soil water content (LL15), v%	32.91	43.79	42.38	27.06	0.465	0	-25.96	128.78
Ammonium (NH_4^+), mg kg-1	1.67	1.85			0.458	0	-2.61	5.92
Calcium, mg kg^{-1}	-2.20	3.18			0.430	0	-10.18	5.36
Profile curvature, km^{-1}	-2.08	5.17			0.349	0	-14.40	9.79
Whole profile drainage rate coefficient (SWCON)	1.01	10.84			0.346	0	-18.93	23.19
Phosphorus, mg kg^{-1}	0.42	2.37			0.315	0	-4.44	5.39
Aspect	-0.69	1.79			0.305	0	-4.22	2.79
Slope, °	-0.17	1.88			0.274	0	-4.28	4.06
Elevation, m	0.14	2.23			0.25	0	-4.05	5.04
Potassium, mg kg^{-1}	-0.88	2.54			0.25	0	-6.90	4.36

1. Abbreviation: Coef: estimation of coefficient, SE: standard error for the estimation of coefficient, Inclusion: inclusion probability, M: median, 2.5%: 2.5 percentile, 97.5%: 97.5 percentile.

Table A3.19. Results of full model, backward selection model and bootstrap models with backward selection procedure (1000 replications) for lignin content (mg g^{-1}) of switchgrass at Lux Arbor Farm.

	Full Model		Backward Select Model		Bootstrap (1000 replications)			
	Coef[1]	SE[1]	Coef[1]	SE[1]	Inclusion[1]	M[1]	2.5%[1]	97.5%[1]
(Intercept)	188.04	1.54	188.16	0.92	1	187.98	185.72	190.53
Early growing season precipitation (Early), mm	-188.63	36.44	-179.42	29.69	1	-187.65	-278.01	-102.29
Late growing season precipitation (Late), mm	-181.33	36.76	-171.76	29.69	1	-179.89	-269.62	-95.58
Whole profile drainage rate coefficient (SWCON)	25.12	10.80	21.77	9.02	0.942	22.22	0	43.19
Sand content, wt%	-48.85	57.10	-46.76	27.19	0.788	-11.70	-160.58	53.10
Clay content, wt%	63.43	99.48	66.04	37.51	0.681	15.56	-83.96	237.79
Saturated water content (SAT), v%	-18.70	18.08	-16.98	8.65	0.669	-11.92	-51.13	4.52
Drained upper limit of soil water content (DUL), v%	-81.17	113.91	-79.57	53.91	0.626	0	-307.13	129.01
Phosphorus, mg kg^{-1}	1.54	1.76	188.16	0.92	0.539	1.55	-1.29	5.02
Plane curvature, km^{-1}	9.69	15.90			0.468	0	-18.39	35.94
Aspect	-1.18	1.39			0.429	0	-3.59	1.80
Saturated hydraulic conductivity (Ksat), mm h^{-1}	-0.26	12.41			0.397	0	-19.56	19.27
Topographical wetness index (TWI)	0.92	2.65			0.382	0	-4.11	5.76
Potassium, mg kg^{-1}	0.36	1.62			0.359	0	-3.06	3.83
Magnesium, mg kg^{-1}	0.58	2.93			0.358	0	-5.46	5.38
Slope, °	-0.53	2.49			0.357	0	-4.67	3.46
pH	-0.28	1.54			0.331	0	-4.70	2.35
Calcium, mg kg^{-1}	-0.27	3.33			0.305	0	-5.09	7.51
Elevation, m	0.71	1.75			0.29	0	-2.46	3.37
Ammonium (NH_4^+), mg kg^{-1}	0.77	1.64			0.271	0	-1.97	3.54
15 bar lower limit of soil water content (LL15), v%	6.35	41.35			0.266	0	-69.00	78.10
Total soil carbon, wt%	-0.38	1.53			0.231	0	-3.37	1.54
Profile curvature, km^{-1}	-0.40	9.79			0.225	0	-17.69	15.80

1. Abbreviation: Coef: estimation of coefficient, SE: standard error for the estimation of coefficient, Inclusion: inclusion probability, M: median, 2.5%: 2.5 percentile, 97.5%: 97.5 percentile.

Table A3.20. Results of full model, backward selection model and bootstrap models with backward selection procedure (1000 replications) for lignin content (mg g^{-1}) of restored prairie at Lux Arbor Farm.

	Full Model		Backward Select Model		Bootstrap (1000 replications)			
	Coef[1]	SE[1]	Coef[1]	SE[1]	Inclusion[1]	M[1]	2.5%[1]	97.5%[1]
(Intercept)	182.40	4.01	182.21	0.73	1	182.16	173.83	189.87
Early growing season precipitation (Early), mm	-250.43	29.86	-252.92	26.24	1	-258.07	-313.50	-195.69
Late growing season precipitation (Late), mm	-242.90	30.08	-245.37	26.31	1	-250.85	-306.75	-187.06
Potassium, mg kg^{-1}	2.42	1.40	2.09	0.96	0.699	2.03	0	4.98
Topographical wetness index (TWI)	-1.95	1.52			0.611	-1.86	-5.10	0
Phosphorus, mg kg^{-1}	-2.17	1.52	-2.08	0.82	0.605	-1.66	-5.04	1.72
Clay content, wt%	5.82	167.10			0.564	0.00	-350.16	307.39
Calcium, mg kg^{-1}	-3.02	2.89	-2.50	1.11	0.554	-1.84	-8.92	0.00
Sand content, wt%	-1.97	47.06			0.541	0	-83.89	106.36
15 bar lower limit of soil water content (LL15), v%	-5.00	176.12			0.511	0	-316.56	375.09
Whole profile drainage rate coefficient (SWCON)	266.70	438.89			0.496	0	-621.23	1084.84
Elevation, m	-1.54	1.65			0.489	0	-5.14	2.89
Saturated water content (SAT), v%	-0.30	16.39			0.487	0	-27.58	38.76
Saturated hydraulic conductivity (Ksat), mm h^{-1}	-266.90	437.35			0.455	0	-1084.29	618.17
Total soil carbon, wt%	1.95	2.07			0.452	0	-2.08	5.57
Drained upper limit of soil water content (DUL), v%	-4.81	71.96	-1.68	0.90	0.445	0	-129.79	153.04
pH	1.31	1.49	1.30	0.89	0.432	0	-1.81	4.12
Magnesium, mg kg^{-1}	-0.15	3.04			0.424	0	-5.95	6.04
Plane curvature, km^{-1}	-5.69	7.91			0.371	0	-21.21	9.62
Aspect	0.45	1.13			0.365	0	-2.01	2.74
Profile curvature, km^{-1}	4.73	9.06			0.363	0	-16.20	22.74
Ammonium (NH_4^+), mg kg^{-1}	-0.74	1.56			0.337	0	-5.21	3.81
Slope, °	-0.42	1.58			0.262	0	-2.80	3.22

1. Abbreviation: Coef: estimation of coefficient, SE: standard error for the estimation of coefficient, Inclusion: inclusion probability, M: median, 2.5%: 2.5 percentile, 97.5%: 97.5 percentile.

Table A3.21. Results of full model, backward selection model and bootstrap models with backward selection procedure (1000 replications) for lignin content (mg g^{-1}) of switchgrass at Marshall Farm.

	Full Model		Backward Select Model		Bootstrap (1000 replications)			
	Coef[1]	SE[1]	Coef[1]	SE[1]	Inclusion[1]	M[1]	2.5%[1]	97.5%[1]
(Intercept)	187.19	2.22	188.76	1.35	1	187.40	183.03	191.98
Late growing season precipitation (Late), mm	-7.65	0.97	-7.83	0.84	1	-7.65	-9.69	-5.75
Early growing season precipitation (Early), mm	3.62	1.13	3.80	0.88	0.988	3.51	1.54	5.74
Clay content, wt%	114.95	68.39	55.22	32.40	0.886	80.78	0.00	236.94
Drained upper limit of soil water content (DUL), v%	-98.54	90.59	-7.38	4.25	0.689	-54.59	-235.90	0
Slope, °	-2.17	1.67	-1.71	1.21	0.658	-2.32	-5.80	0
Sand content, wt%	-45.32	44.67			0.591	-20.63	-111.66	7.60
Phosphorus, mg kg^{-1}	-2.12	1.58	-1.52	0.95	0.564	-1.65	-5.04	0.00
15 bar lower limit of soil water content (LL15), v%	-48.83	48.20	-51.09	35.83	0.543	0	-167.55	53.45
Saturated water content (SAT), v%	-5.89	7.63			0.535	0	-18.59	6.69
Elevation, m	1.52	1.98	2.52	1.20	0.508	0	-2.26	5.74
Plane curvature, km^{-1}	-2.95	5.94			0.491	0	-17.85	14.52
Profile curvature, km^{-1}	-7.94	9.22	-8.50	5.98	0.473	0	-31.23	0.00
Saturated hydraulic conductivity (Ksat), mm h^{-1}	6.89	10.98			0.452	0	-14.15	28.05
pH	1.24	2.67			0.451	0	-5.31	7.94
Magnesium, mg kg^{-1}	-0.10	1.72			0.431	0	-3.87	4.94
Topographical wetness index (TWI)	-0.87	2.04			0.412	0	-6.07	3.38
Aspect	-1.03	1.32			0.407	0	-3.54	1.66
Calcium, mg kg^{-1}	-0.06	2.67			0.396	0	-6.98	9.07
Total soil carbon, wt%	-0.54	1.58			0.386	0	-4.26	2.64
Potassium, mg kg^{-1}	1.05	1.89			0.323	0	-2.82	4.42
Whole profile drainage rate coefficient (SWCON)	2.23	7.79			0.312	0	-14.50	15.92
Ammonium (NH_4^+), mg kg^{-1}	0.01	1.11			0.166	0	-1.82	2.02

1. Abbreviation: Coef: estimation of coefficient, SE: standard error for the estimation of coefficient, Inclusion: inclusion probability, M: median, 2.5%: 2.5 percentile, 97.5%: 97.5 percentile.

Table A3.22. Results of full model, backward selection model and bootstrap models with backward selection procedure (1000 replications) for lignin content (mg g^{-1}) of restored prairie at Marshall Farm.

	Full Model		Backward Select Model		Bootstrap (1000 replications)			
	Coef[1]	SE[1]	Coef[1]	SE[1]	Inclusion[1]	M[1]	2.5%[1]	97.5%[1]
(Intercept)	166.28	2.34	169.03	1.05	1	167.02	161.63	171.64
Early growing season precipitation (Early), mm	5.29	1.16	5.61	1.09	1	5.52	3.15	7.93
Late growing season precipitation (Late), mm	-10.63	1.07	-10.75	1.03	1	-10.78	-12.82	-8.73
Magnesium, mg kg^{-1}	5.72	2.12	4.22	1.65	0.926	5.19	0	9.75
Topographical wetness index (TWI)	-5.22	2.50	-5.04	1.52	0.784	-4.75	-10.26	0
Calcium, mg kg^{-1}	-5.00	2.58	-5.18	2.06	0.716	-4.32	-11.52	0
Drained upper limit of soil water content (DUL), v%	-99.71	93.49	-20.48	8.61	0.7	-52.53	-294.15	24.42
Slope, °	-2.79	1.53	-1.72	1.26	0.677	-2.31	-5.89	0
Sand content, wt%	-59.74	58.15	-9.40	4.80	0.667	-30.05	-183.03	10.67
pH	2.87	2.17	3.50	1.86	0.599	2.74	0	7.61
Saturated water content (SAT), v%	6.27	6.34	10.00	4.82	0.572	2.13	-9.72	21.08
15 bar lower limit of soil water content (LL15), v%	32.11	35.59			0.556	7.64	-36.67	113.63
Saturated hydraulic conductivity (Ksat), mm h^{-1}	-9.81	11.00	-18.94	8.85	0.548	0	-38.06	17.63
Potassium, mg kg^{-1}	-2.35	2.06	-2.46	1.69	0.54	-2.22	-7.90	0
Whole profile drainage rate coefficient (SWCON)	6.56	8.81			0.524	0	-9.22	24.36
Plane curvature, km^{-1}	3.69	4.15			0.522	0	-4.70	14.28
Total soil carbon, wt%	-2.20	2.18			0.514	0	-7.37	2.88
Elevation, m	-2.26	1.81			0.509	0	-5.18	2.69
Clay content, wt%	15.92	52.46			0.498	0	-95.37	136.09
Profile curvature, km^{-1}	3.82	4.21			0.485	0	-8.38	13.13
Ammonium (NH_4^+), mg kg^{-1}	0.87	1.50			0.383	0	-3.05	4.32
Phosphorus, mg kg^{-1}	1.21	1.93			0.357	0	-2.75	5.45
Aspect	-0.06	1.46			0.333	0	-3.40	3.22

1. Abbreviation: Coef: estimation of coefficient, SE: standard error for the estimation of coefficient, Inclusion: inclusion probability, M: median, 2.5%: 2.5 percentile, 97.5%: 97.5 percentile.

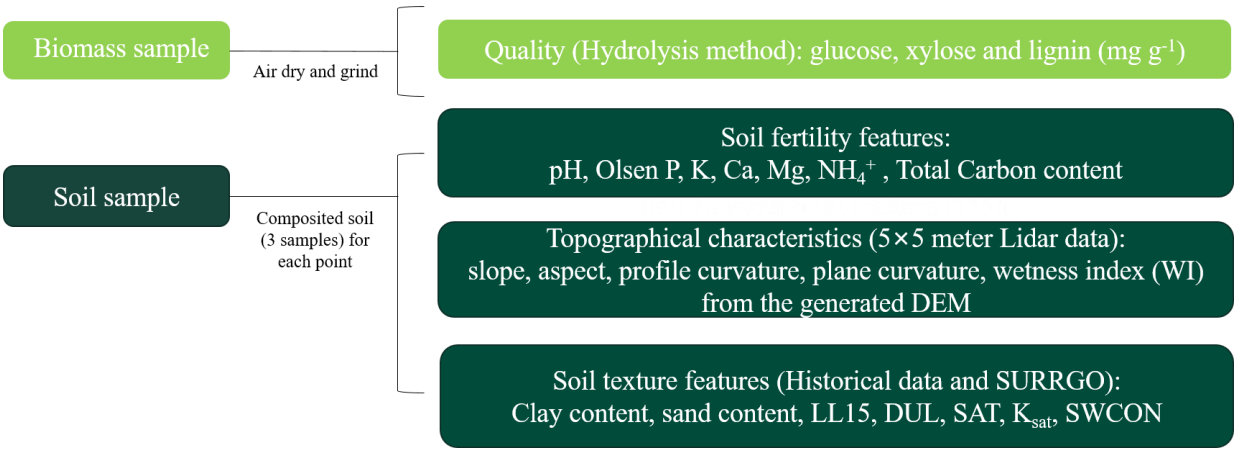

Figure A3.1. Flow chart of biomass samples and soil samples parameters.

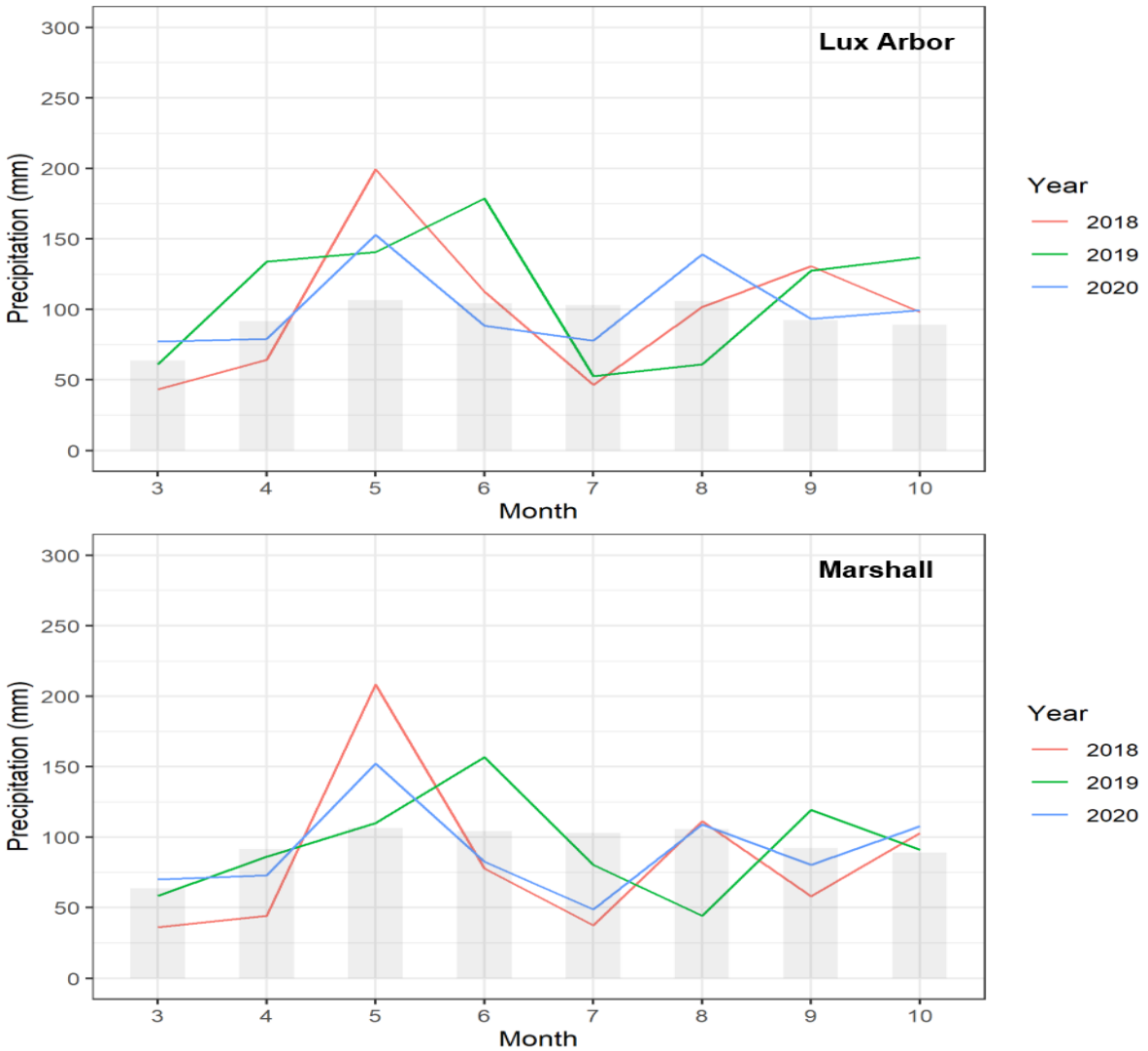

Figure A3.2. Monthly precipitation (mm) during growing season (March-October) at Lux Arbor Farm and Marshall Farm over the study period (2018-2020) and 30 years average.

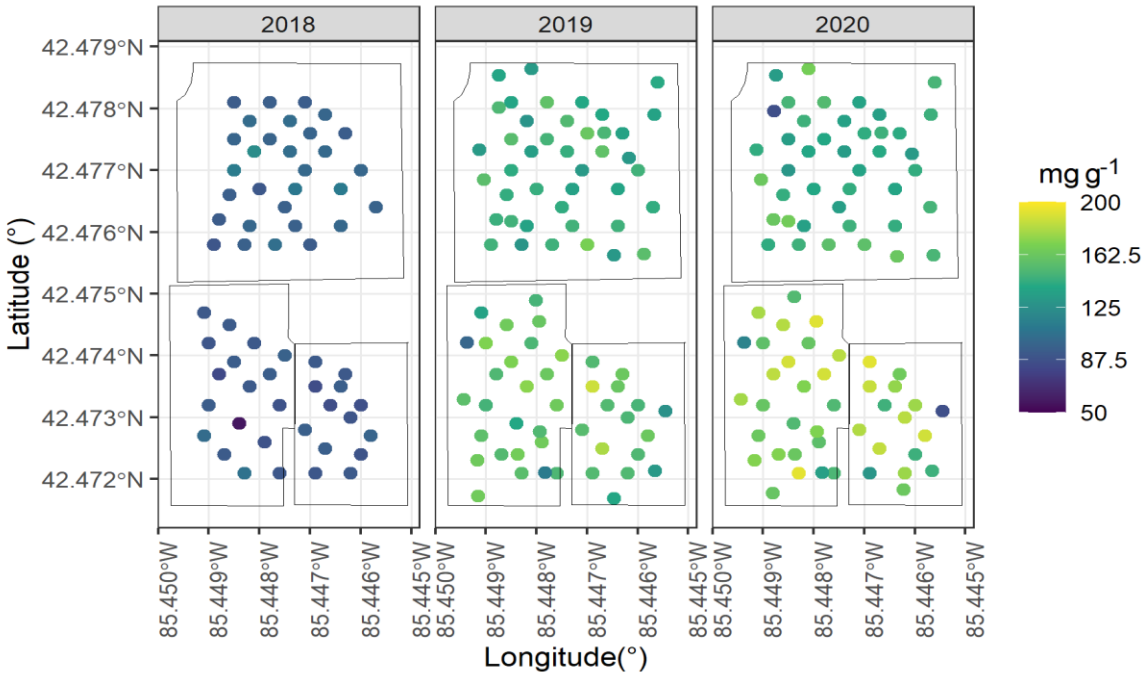

Figure A3.3. Glucose content (mg g^{-1}) of switchgrass (upper panel) and restored prairie (lower panel) during the study period (2018-2020) at Lux Arbor Farm.

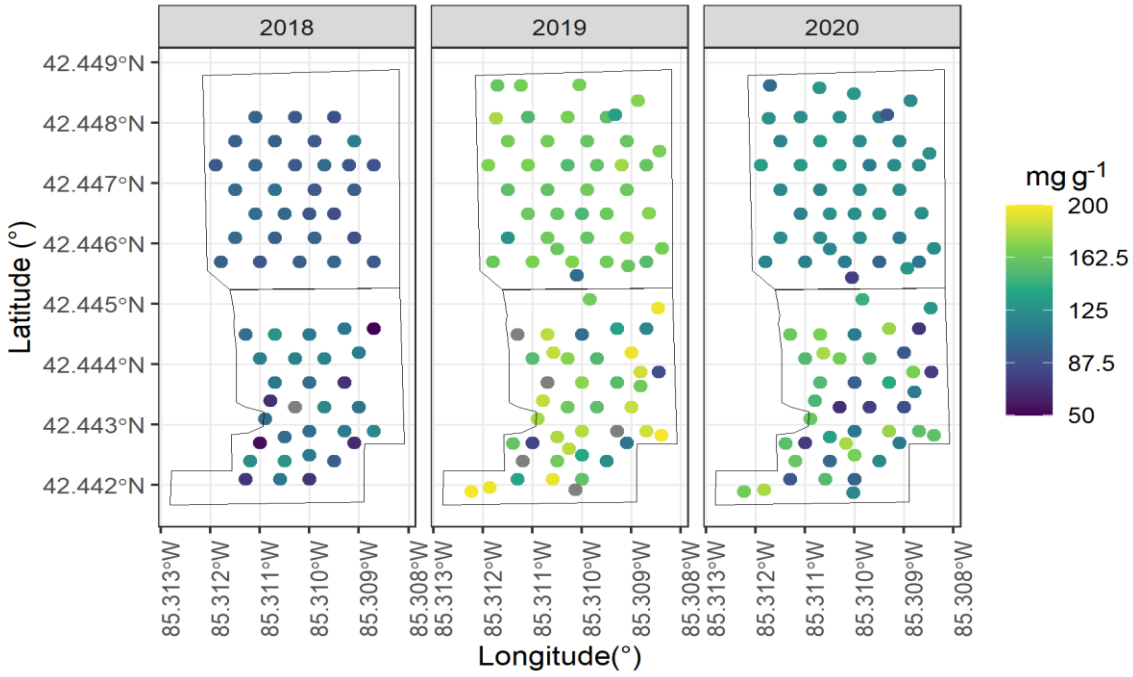

Figure A3.4. Glucose content (mg g^{-1}) of switchgrass (upper panel) and restored prairie (lower panel) during the study period (2018-2020) at Marshall Farm.

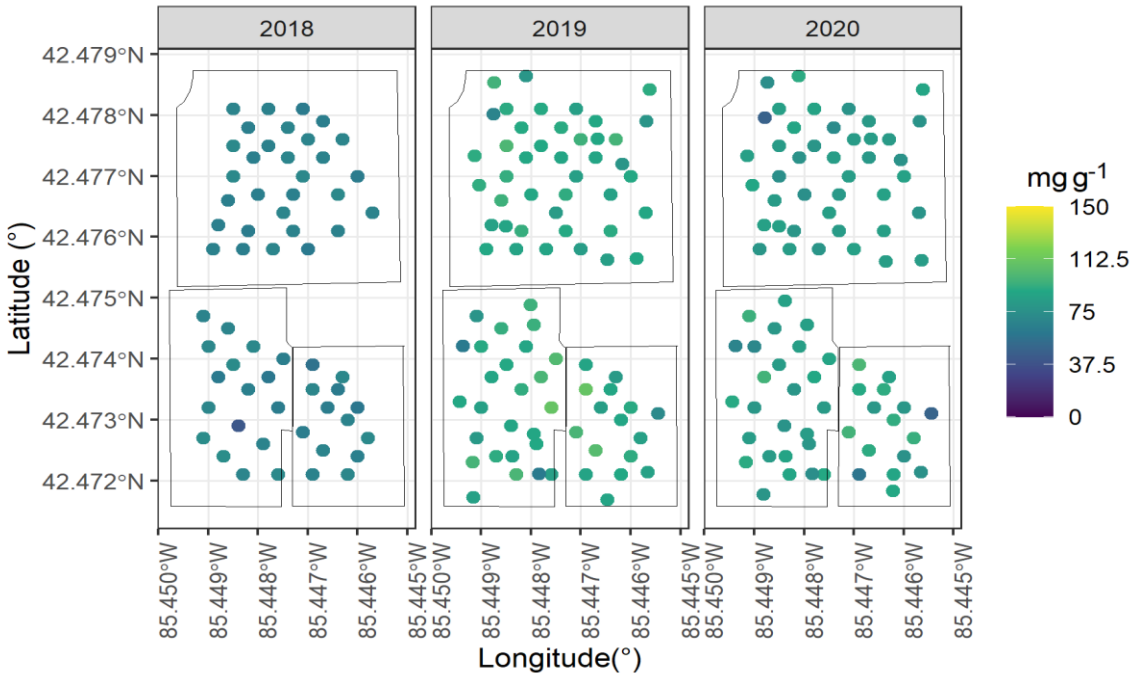

Figure A3.5. Xylose content (mg g^{-1}) of switchgrass (upper panel) and restored prairie (lower panel) during the study period (2018-2020) at Lux Arbor Farm.

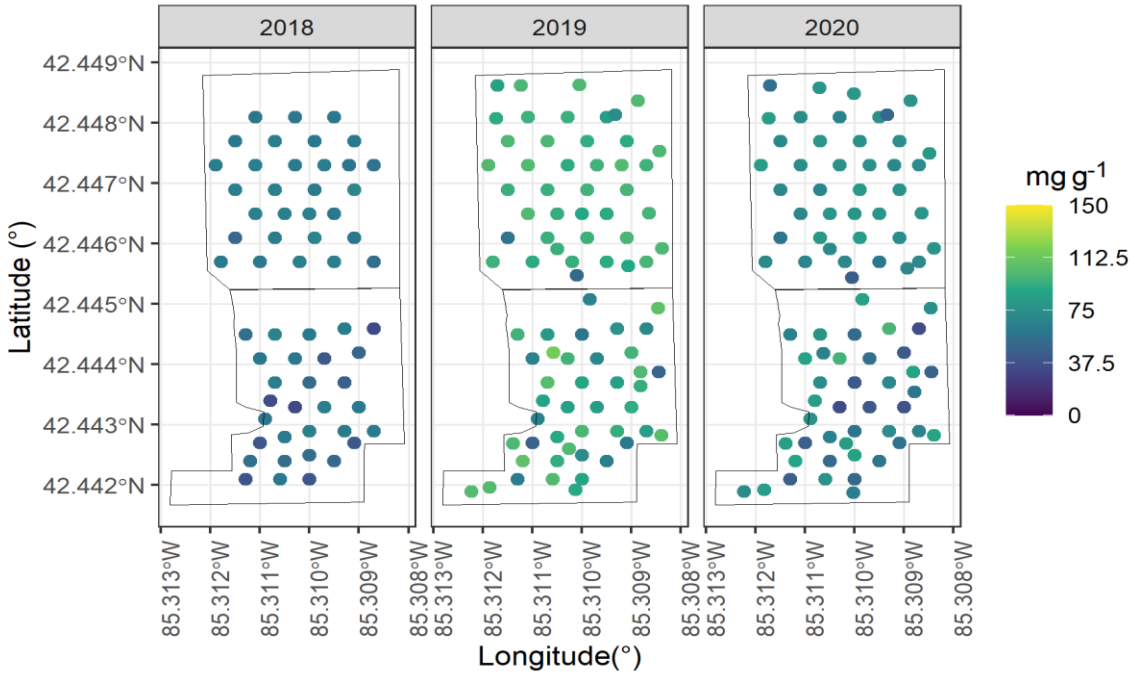

Figure A3.6. Xylose content (mg g^{-1}) of switchgrass (upper panel) and restored prairie (lower panel) during the study period (2018-2020) at Marshall Farm.

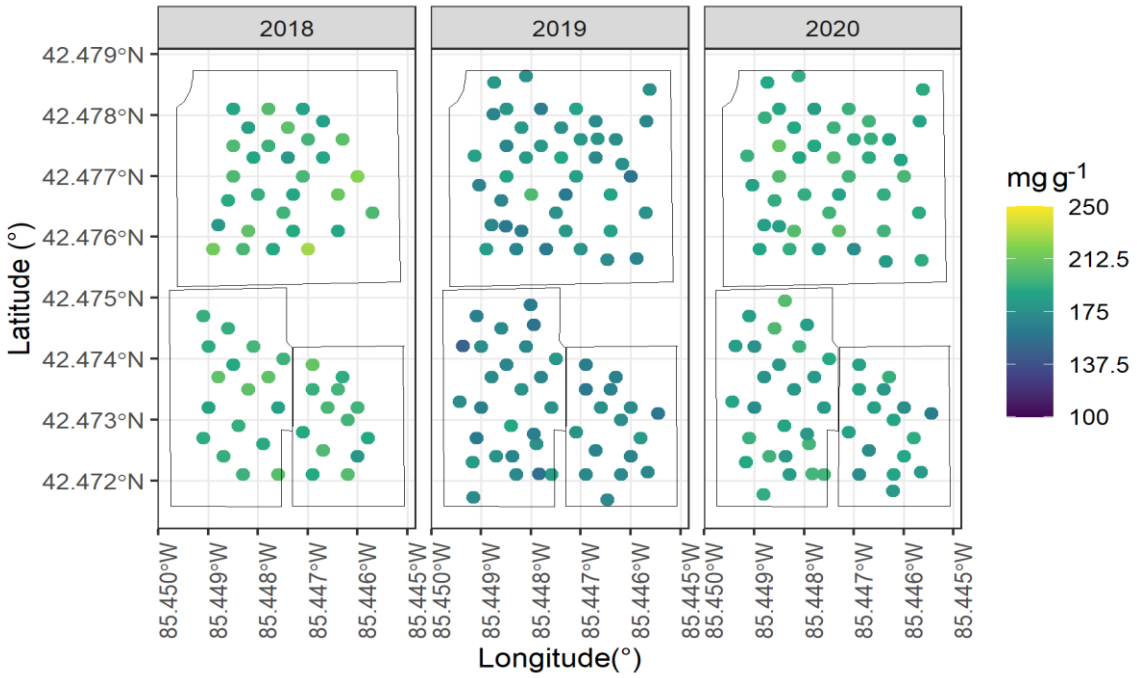

Figure A3.7. Lignin content (mg g^{-1}) of switchgrass (upper panel) and restored prairie (lower panel) during the study period (2018-2020) at Lux Arbor Farm.

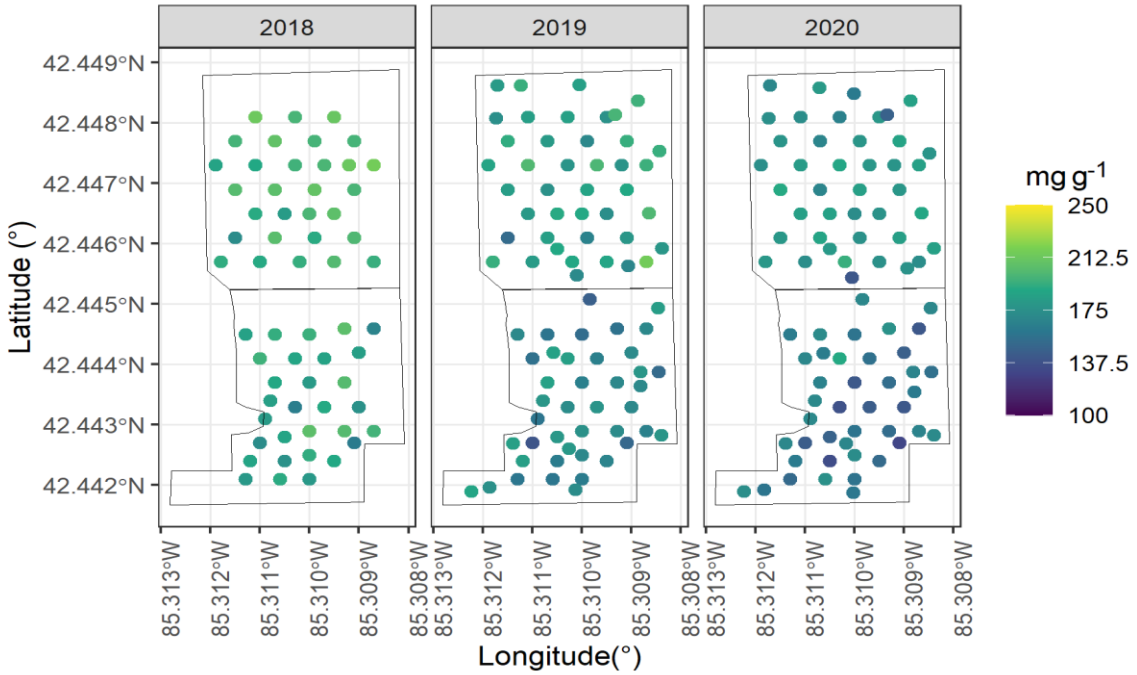

Figure A3.8. Lignin content (mg g^{-1}) of switchgrass (upper panel) and restored prairie (lower panel) during the study period (2018-2020) at Marshall Farm.

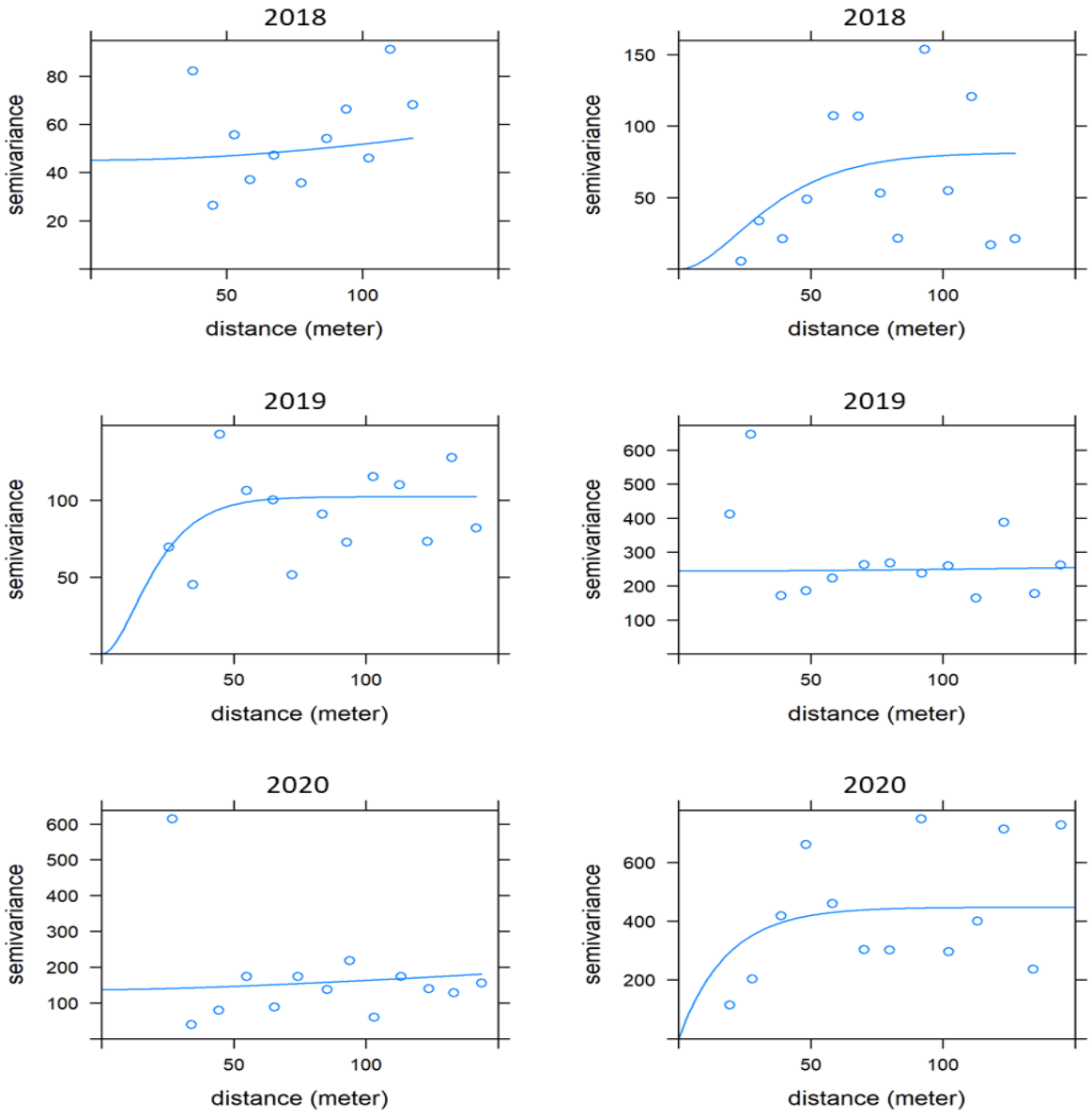

Figure A3.9. Empirical semi-variograms with best fitted Matern correlation models of glucose content (mg g^{-1}) of switchgrass (left panel) and restored prairie (right panel) at Lux Arbor Farm over the study period (2018-2020.

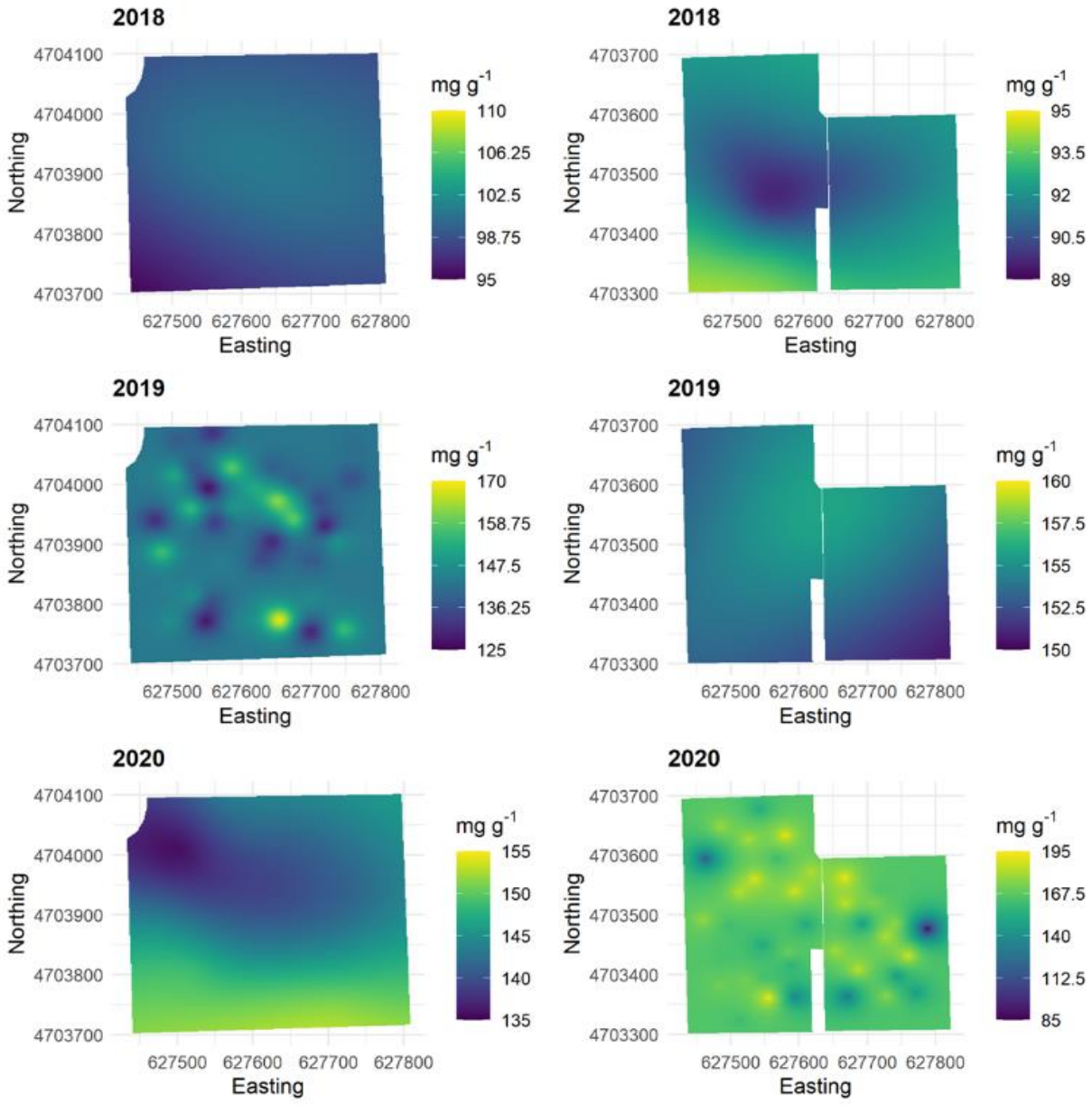

Figure A3.10. Ordinary kriging maps of glucose content (mg g^{-1}) of switchgrass (left panel) and restored prairie (right panel) at Lux Arbor Farm over the study period (2018-2020).

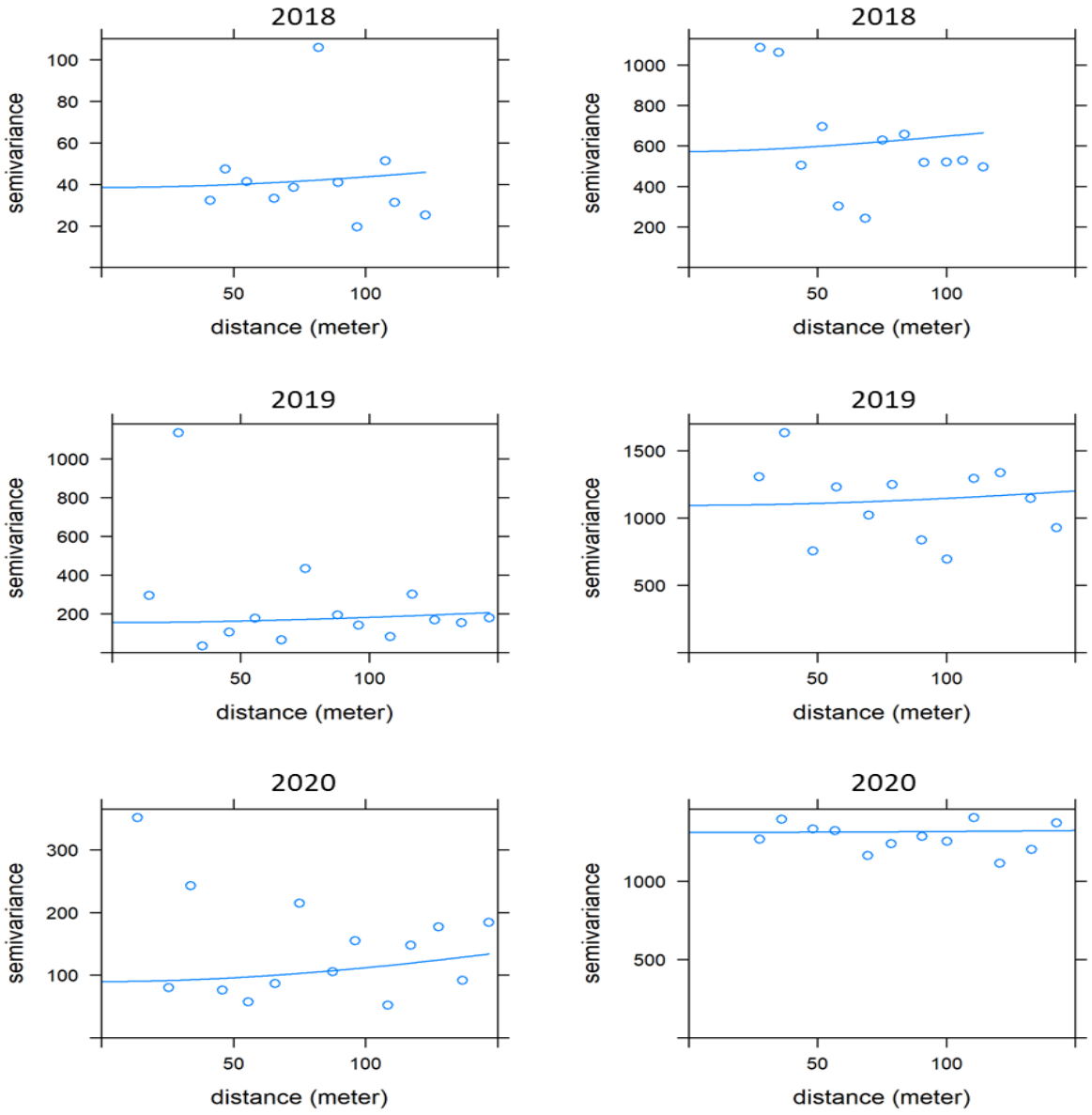

Figure A3.11. Empirical semi-variograms with best fitted Matern correlation models of glucose content (mg g^{-1}) of switchgrass (left panel) and restored prairie (right panel) at Marshall Farm over the study period (2018-2020).

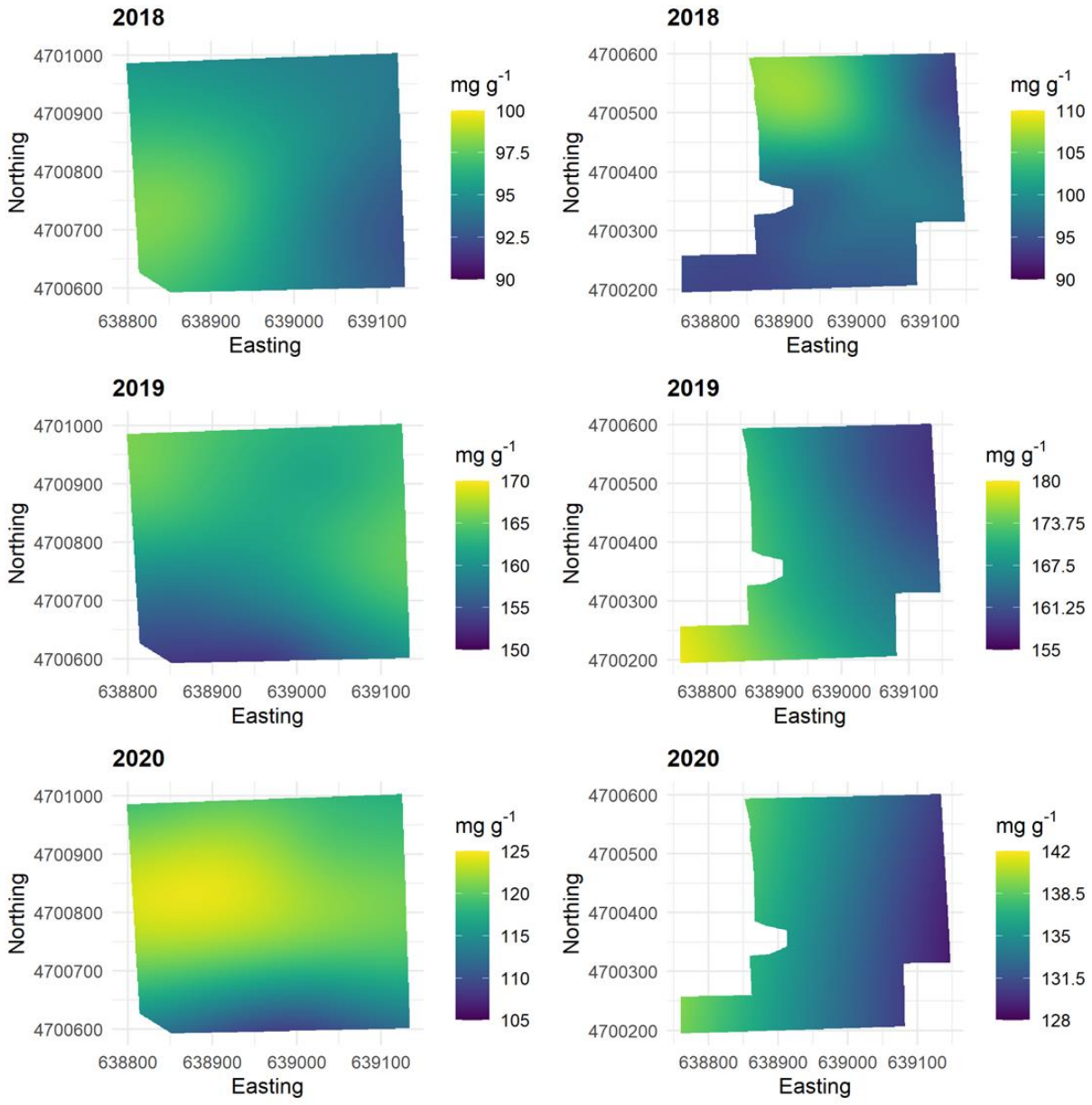

Figure A3.12. Ordinary kriging maps of glucose content (mg g^{-1}) of switchgrass (left panel) and restored prairie (right panel) at Marshall Farm over the study period (2018-2020).

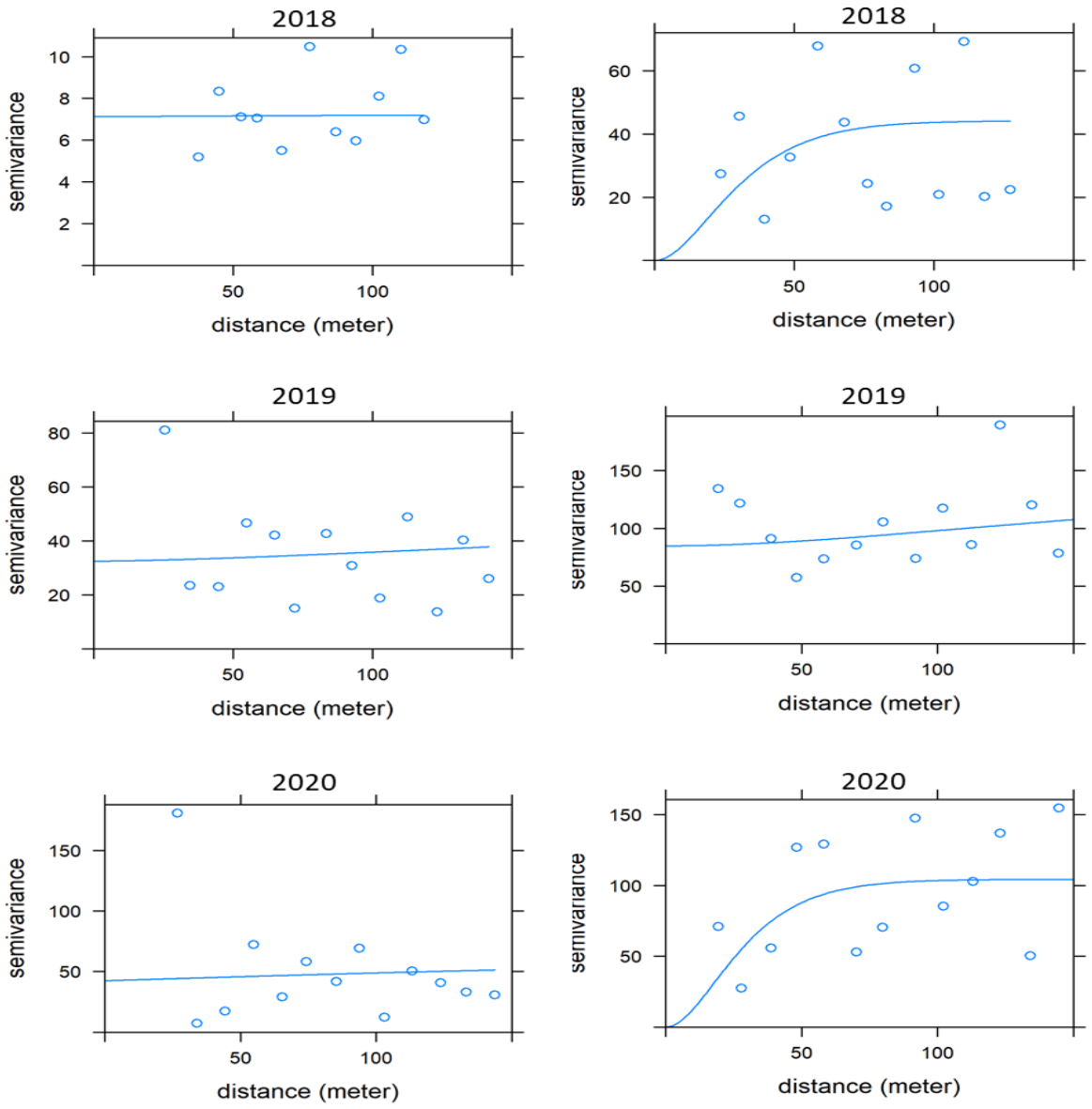

Figure A3.13. Empirical semi-variograms with best fitted Matern correlation models of xylose content (mg g^{-1}) of switchgrass (left panel) and restored prairie (right panel) at Lux Arbor Farm over the study period (2018-2020).

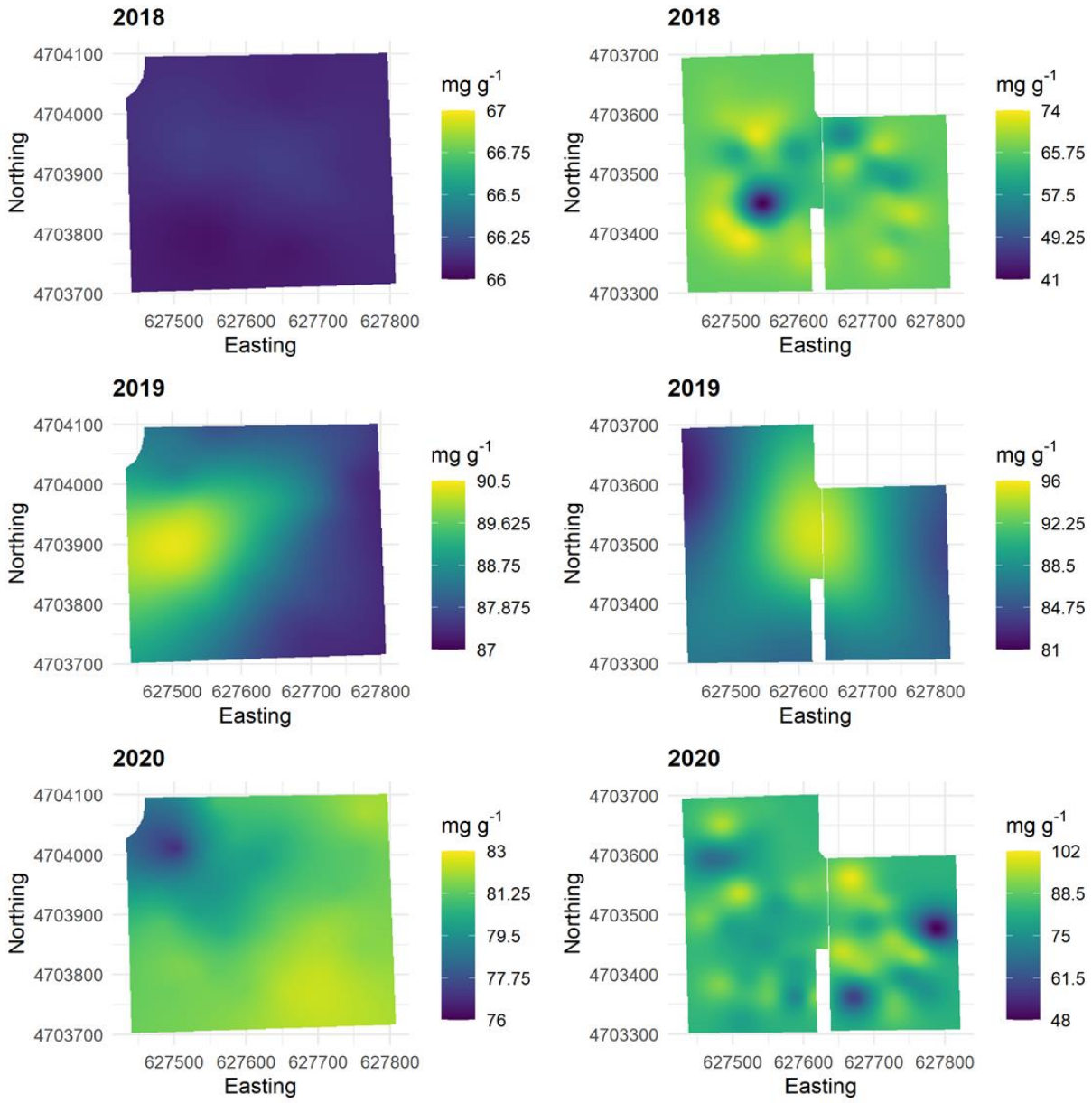

Figure A3.14. Ordinary kriging maps of xylose content (mg g-1) of switchgrass (left panel) and restored prairie (right panel) at Lux Arbor Farm over the study period (2018-2020).

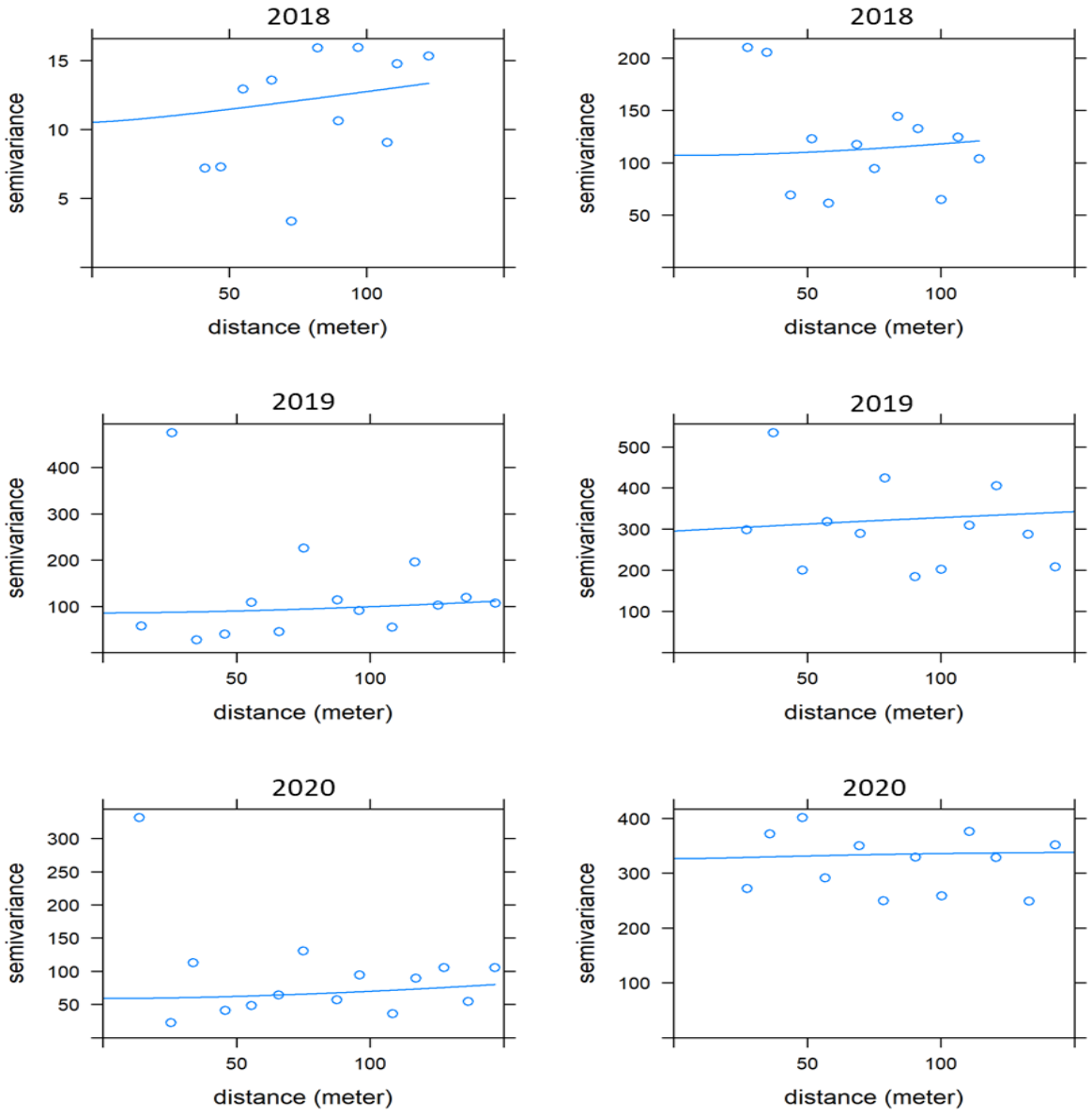

Figure A3.15. Empirical semi-variograms with best fitted Matern correlation models of xylose content (mg g^{-1}) of switchgrass (left panel) and restored prairie (right panel) at Marshall Farm over the study period (2018-2020).

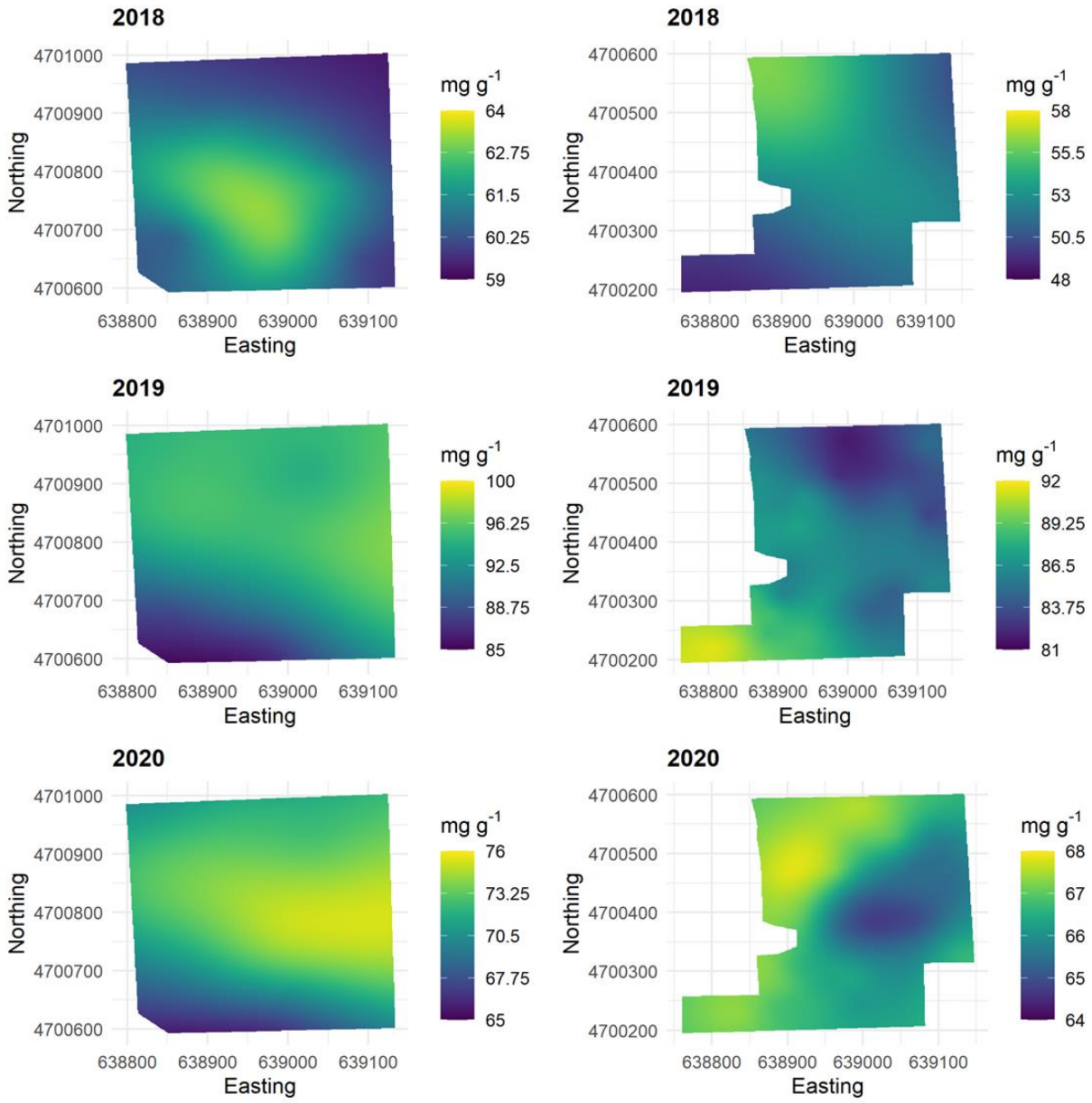

Figure A3.16. Ordinary kriging maps of xylose content (mg g^{-1}) of switchgrass (left panel) and restored prairie (right panel) at Marshall Farm over the study period (2018-2020).

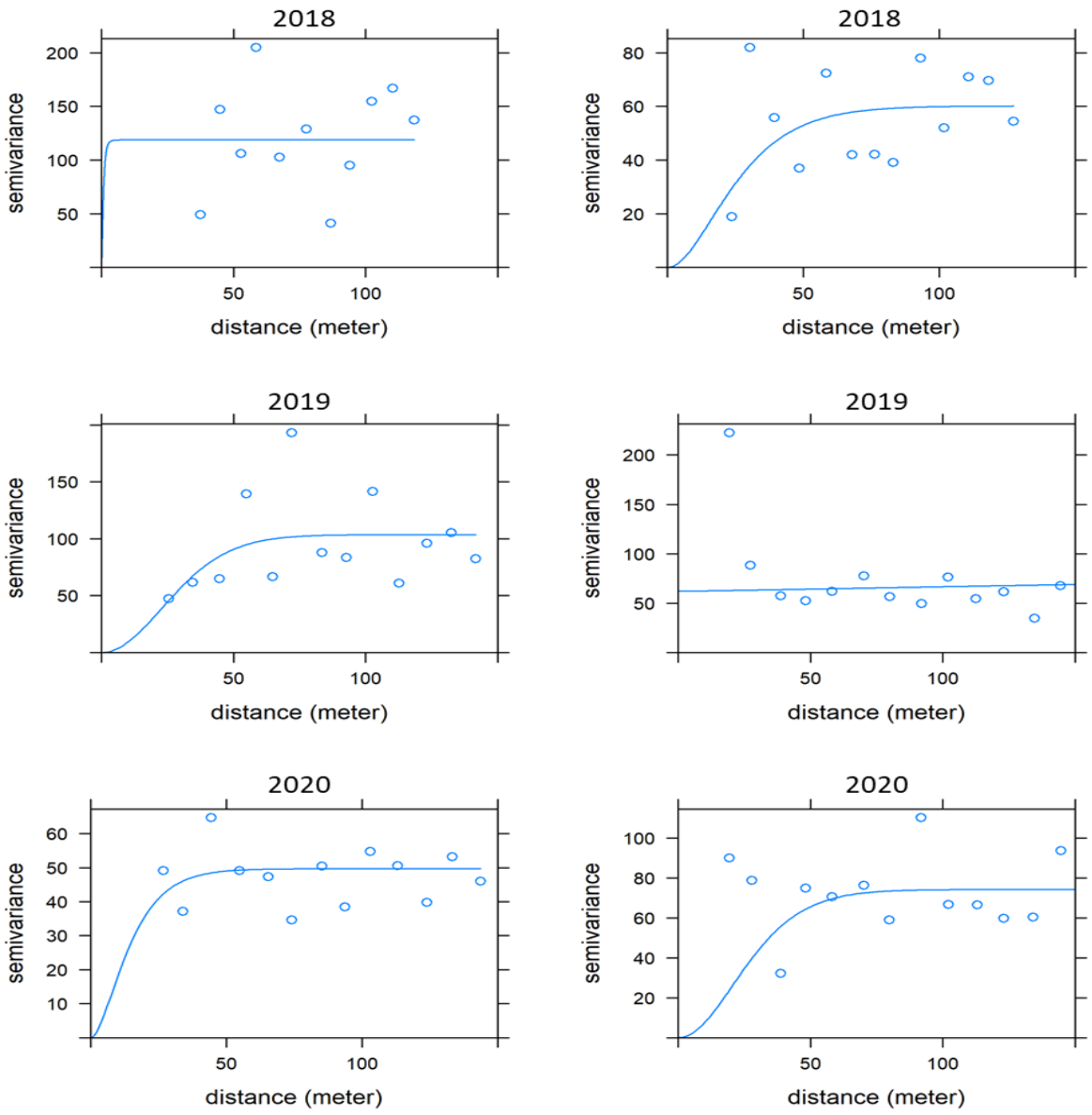

Figure A3.17. Empirical semi-variograms with best fitted Matern correlation models of lignin content (mg g^{-1}) of switchgrass (left panel) and restored prairie (right panel) at Lux Arbor Farm over the study period (2018-2020).

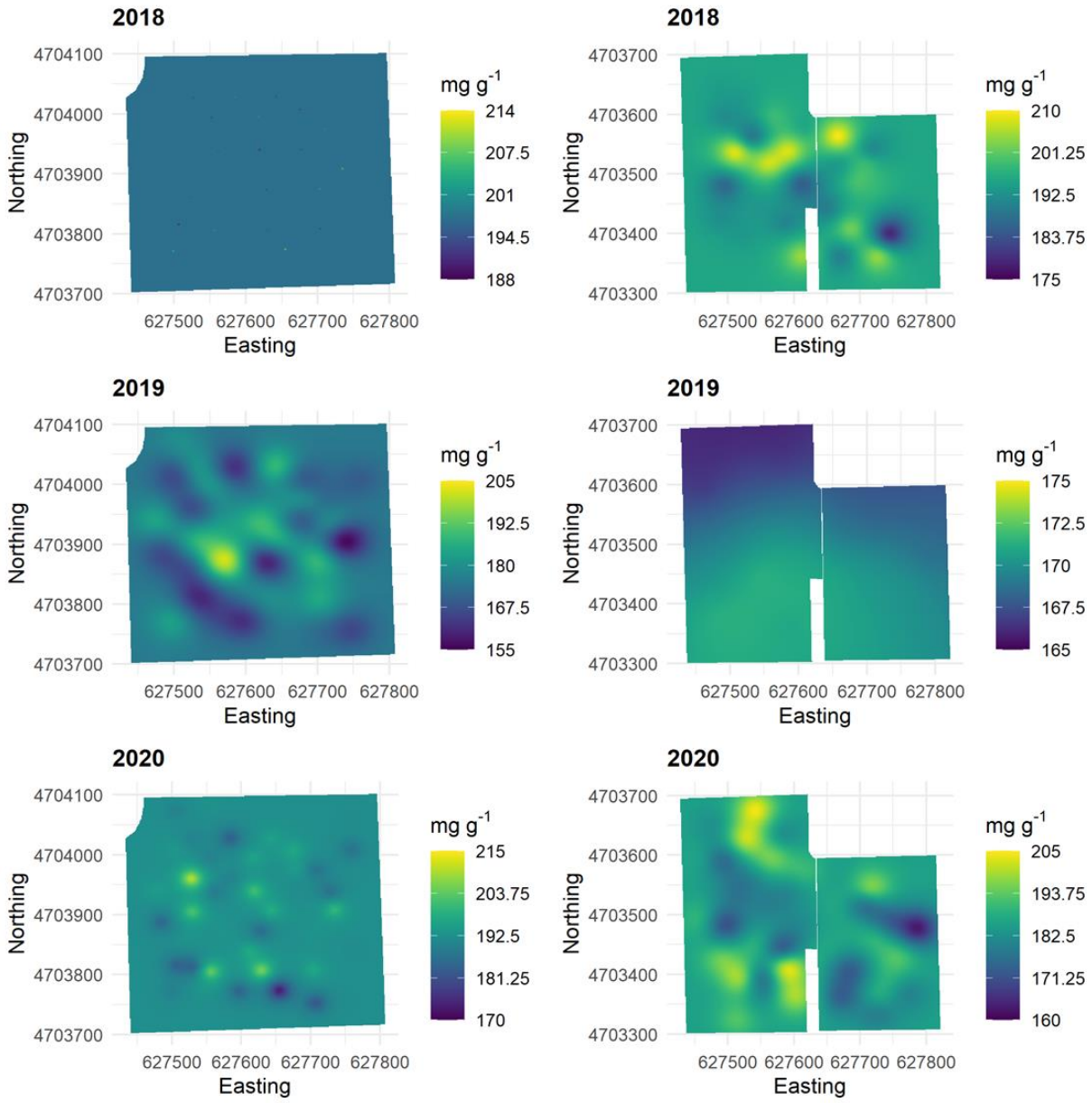

Figure A3.18. Ordinary kriging maps of lignin content (mg g^{-1}) of switchgrass (left panel) and restored prairie (right panel) at Lux Arbor Farm over the study period (2018-2020).

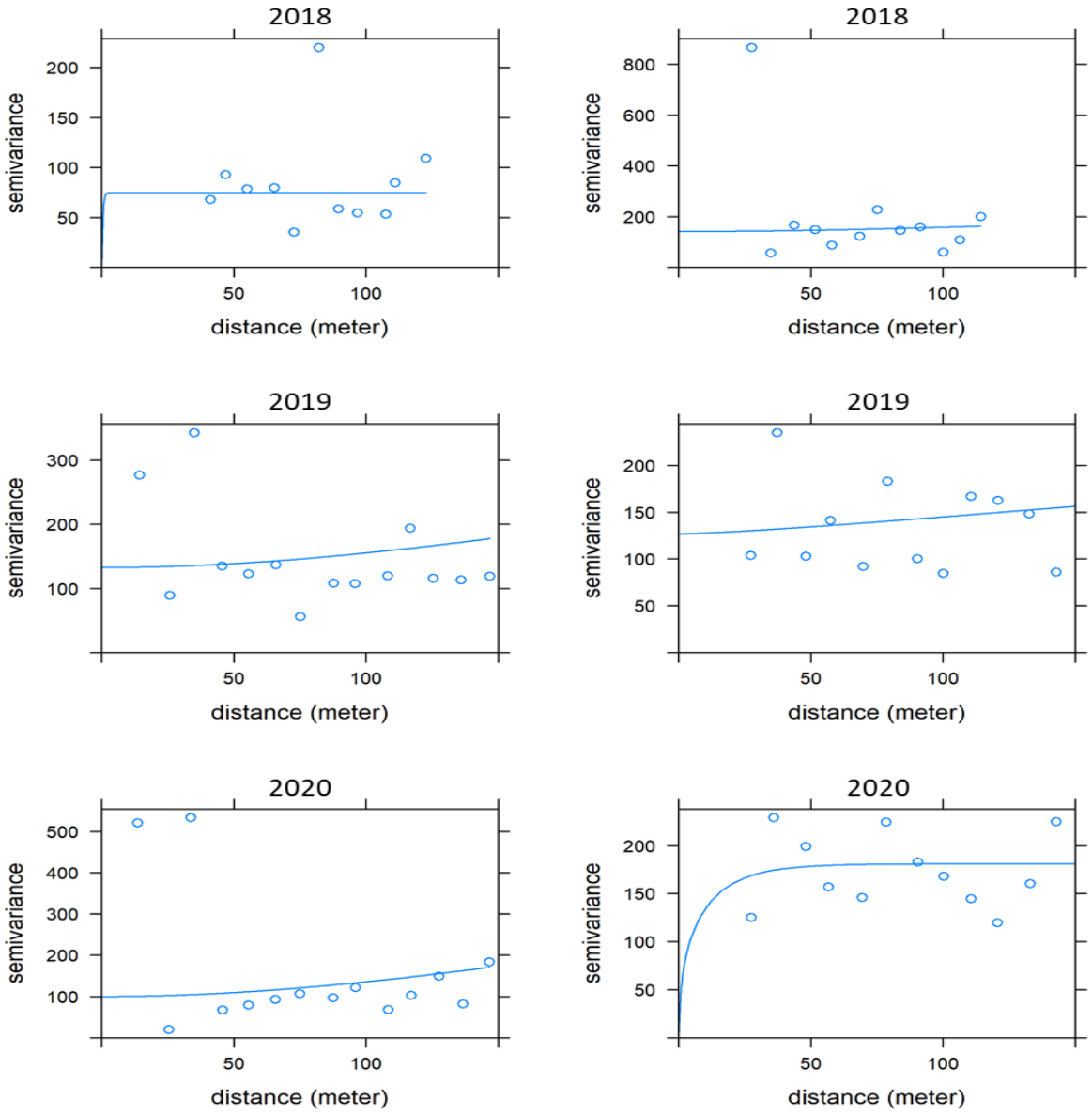

Figure A3.19. Empirical semi-variograms with best fitted Matern correlation models of lignin content (mg g^{-1}) of switchgrass (left panel) and restored prairie (right panel) at Marshall Farm over the study period (2018-2020).

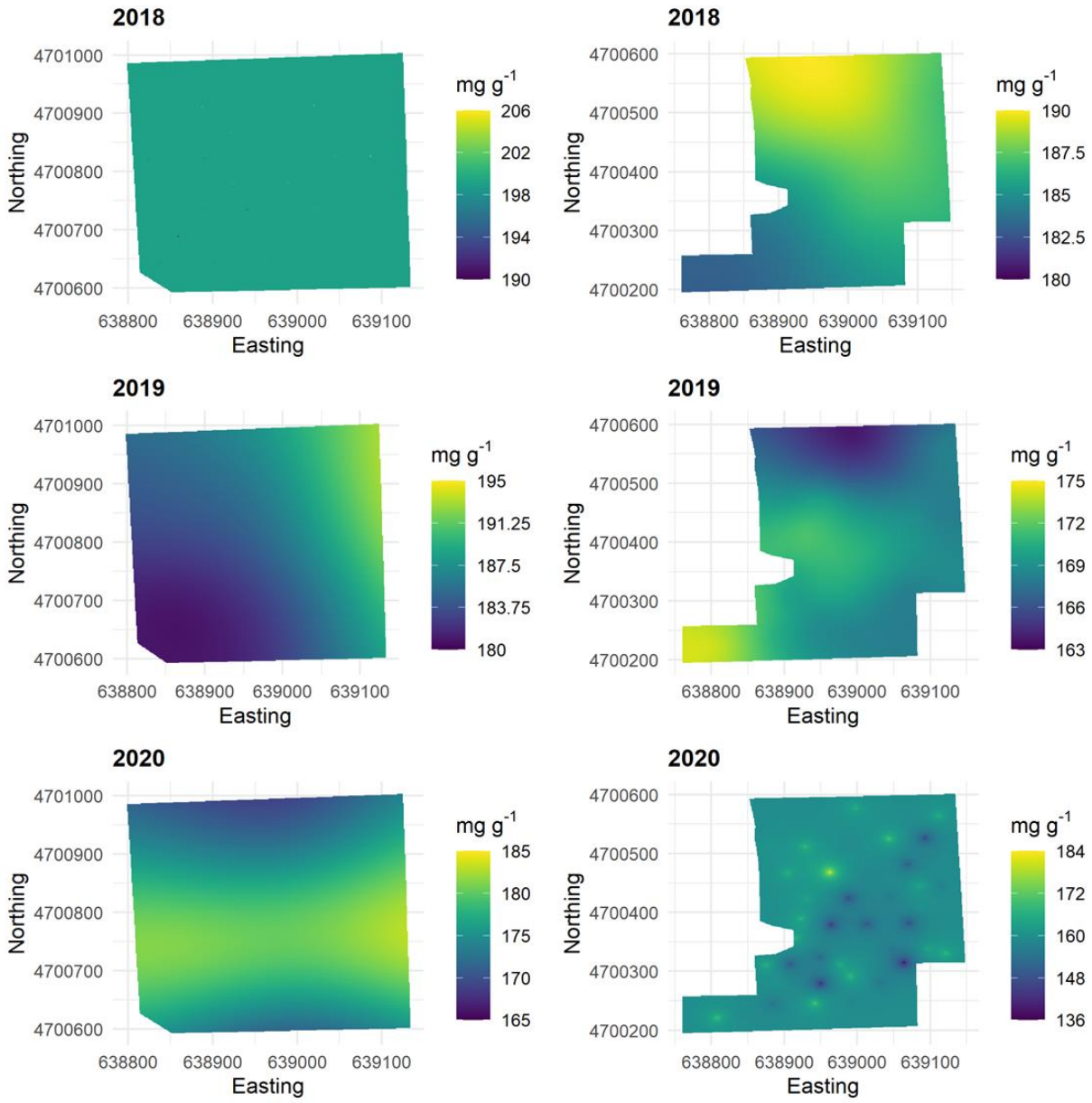

Figure A3.20. Ordinary kriging maps of lignin content (mg g^{-1}) of switchgrass (left panel) and restored prairie (right panel) at Marshall Farm over the study period (2018-2020).

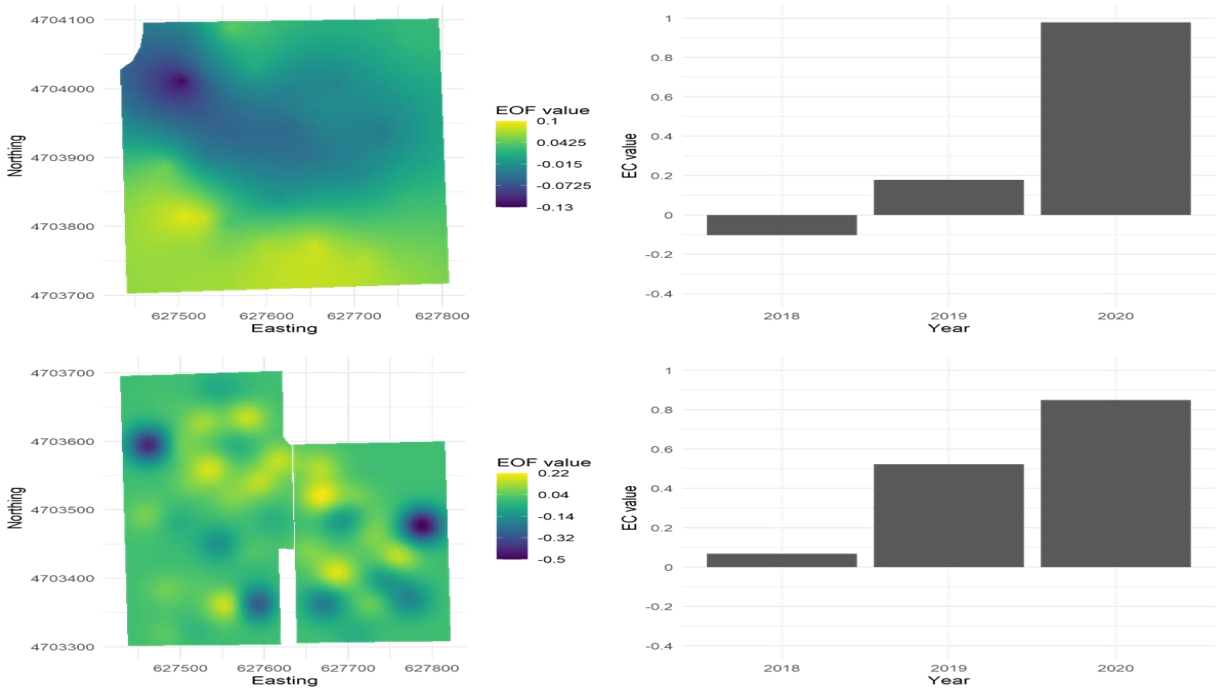

Figure A3.21. The leading spatial empirical orthogonal function (EOF) and time series of expansion efficient (EC) for switchgrass glucose content (upper panel) and restored prairie glucose content (lower panel) at Lux Arbor Farm.

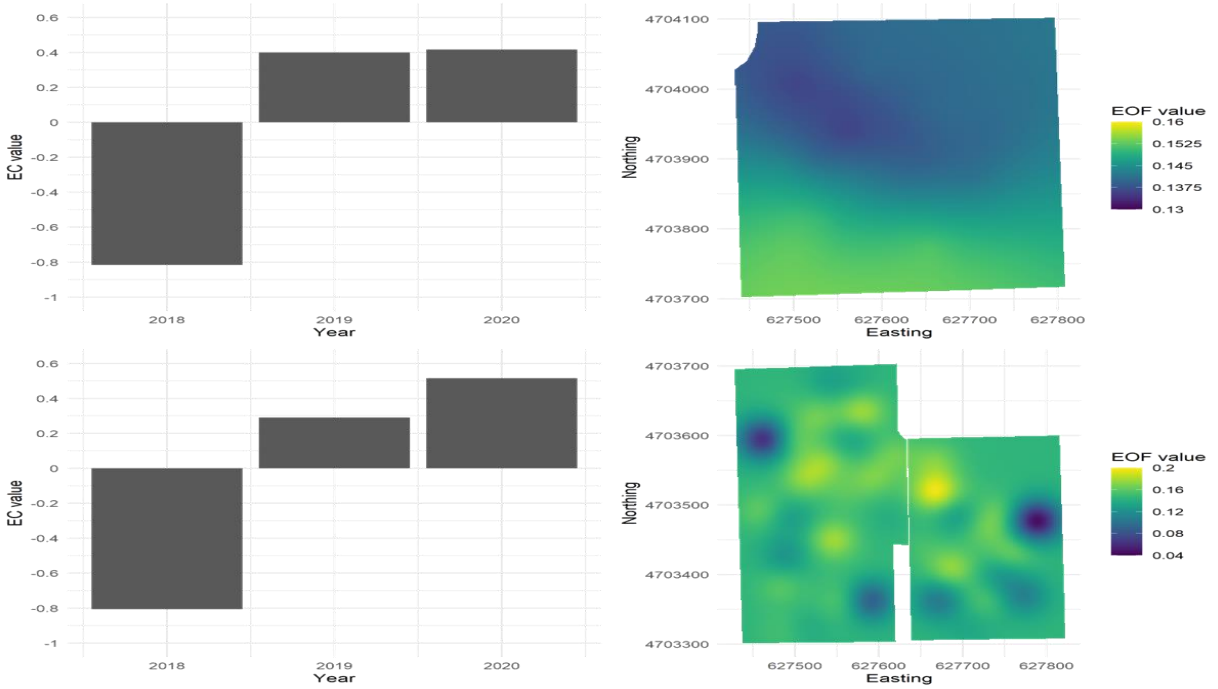

Figure A3.22. The leading temporal empirical orthogonal function (EOF) and time series of expansion efficient (EC) for switchgrass glucose content (upper panel) and restored prairie glucose content (lower panel) at Lux Arbor Farm.

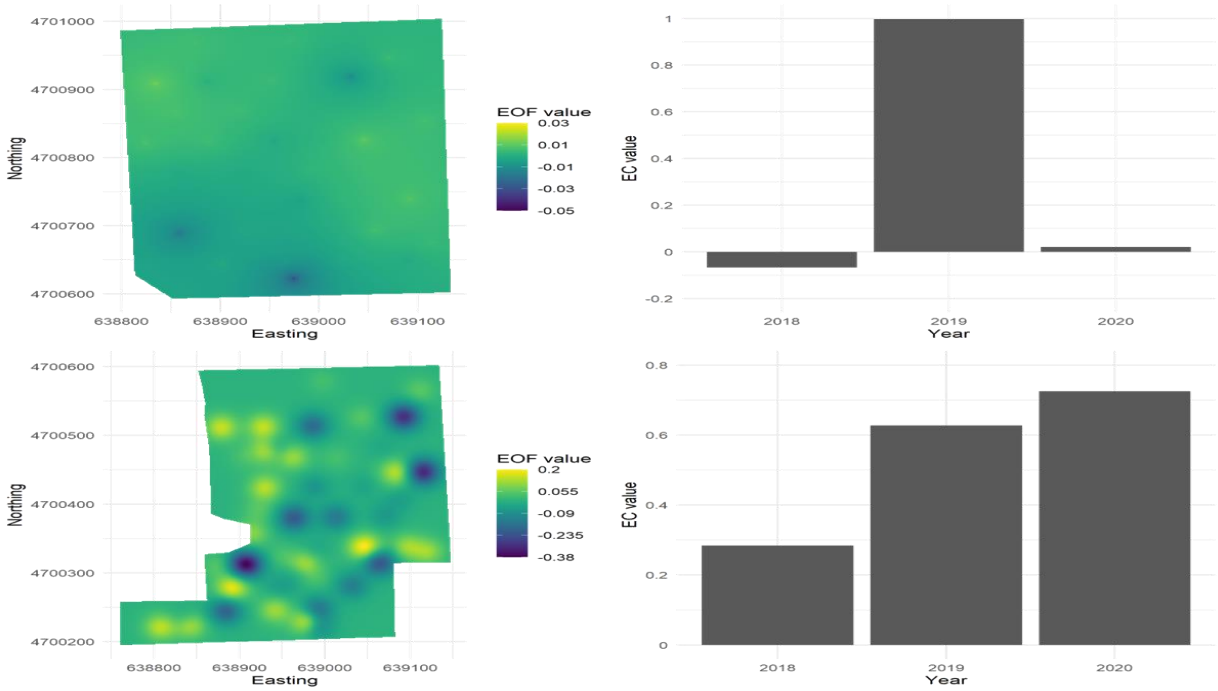

Figure A3.16. The leading spatial empirical orthogonal function (EOF) and time series of expansion efficient (EC) for switchgrass glucose content (upper panel) and restored prairie glucose content (lower panel) at Marshall Farm.

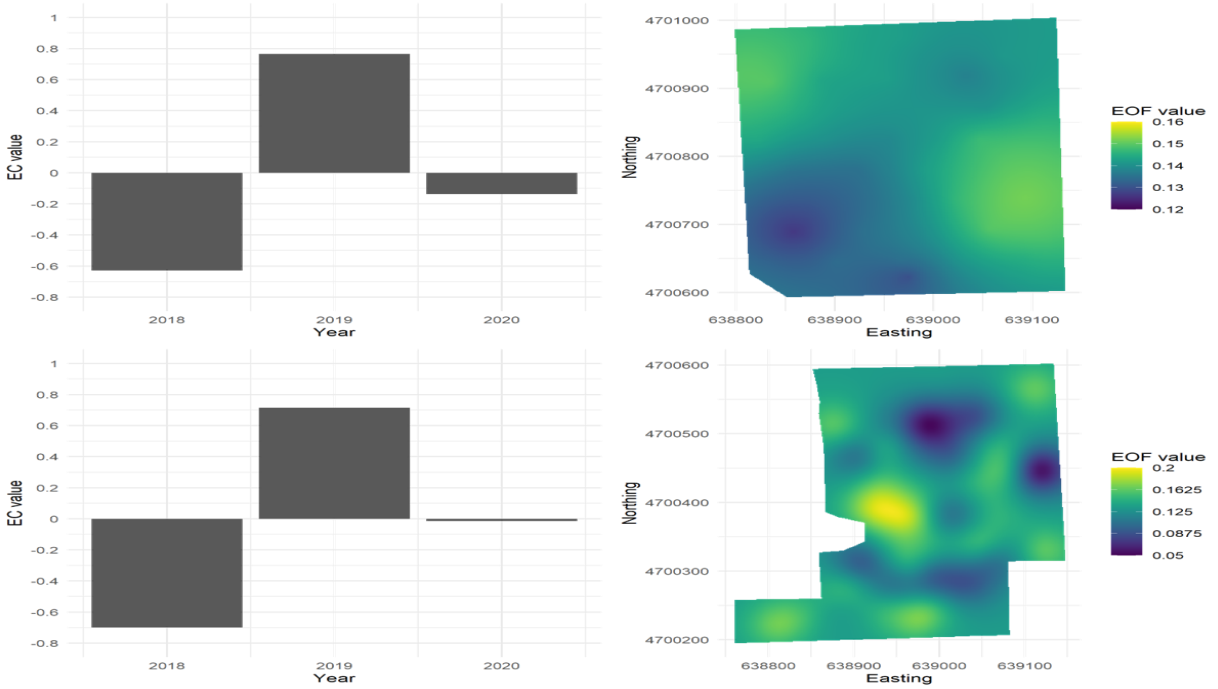

Figure A3.24. The leading temporal empirical orthogonal function (EOF) and time series of expansion efficient (EC) for switchgrass glucose content (upper panel) and restored prairie glucose content (lower panel) at Marshall Farm.

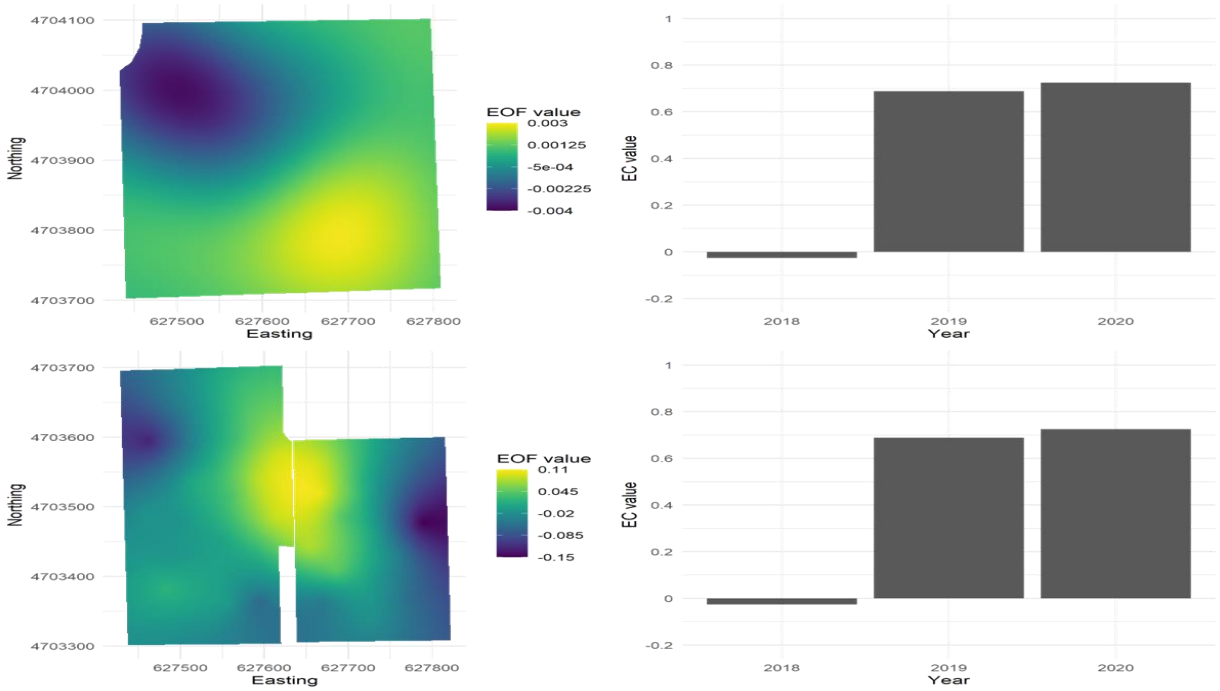

Figure A3.25. The leading spatial empirical orthogonal function (EOF) and time series of expansion efficient (EC) for switchgrass xylose content (upper panel) and restored prairie xylose content (lower panel) at Lux Arbor Farm.

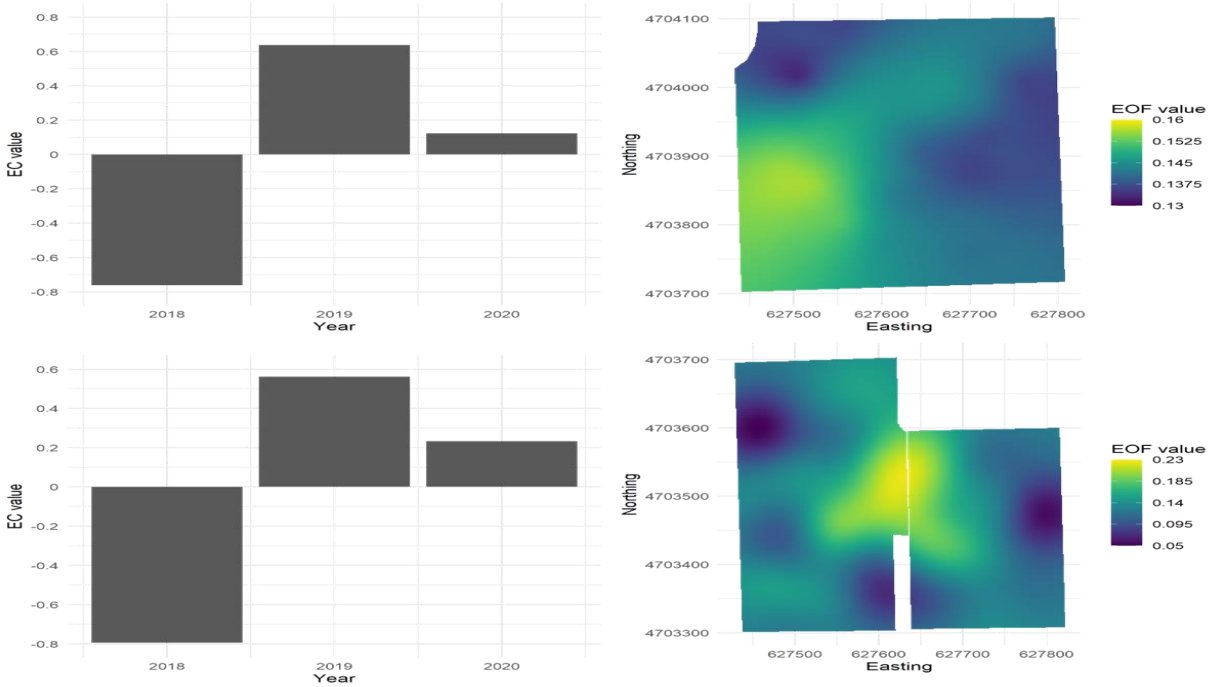

Figure A3.26. The leading temporal empirical orthogonal function (EOF) and time series of expansion efficient (EC) for switchgrass xylose content (upper panel) and restored prairie xylose content (lower panel) at Lux Arbor Farm.

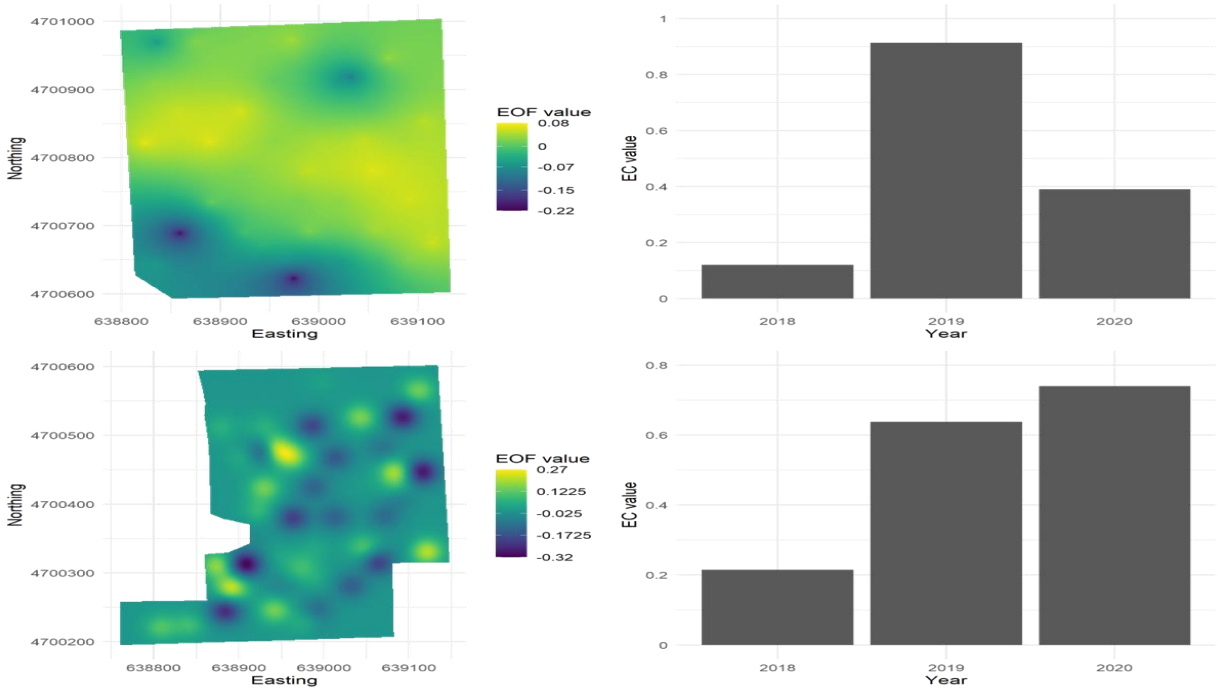

Figure A3.27. The leading spatial empirical orthogonal function (EOF) and time series of expansion efficient (EC) for switchgrass xylose content (upper panel) and restored prairie xylose content (lower panel) at Marshall Farm.

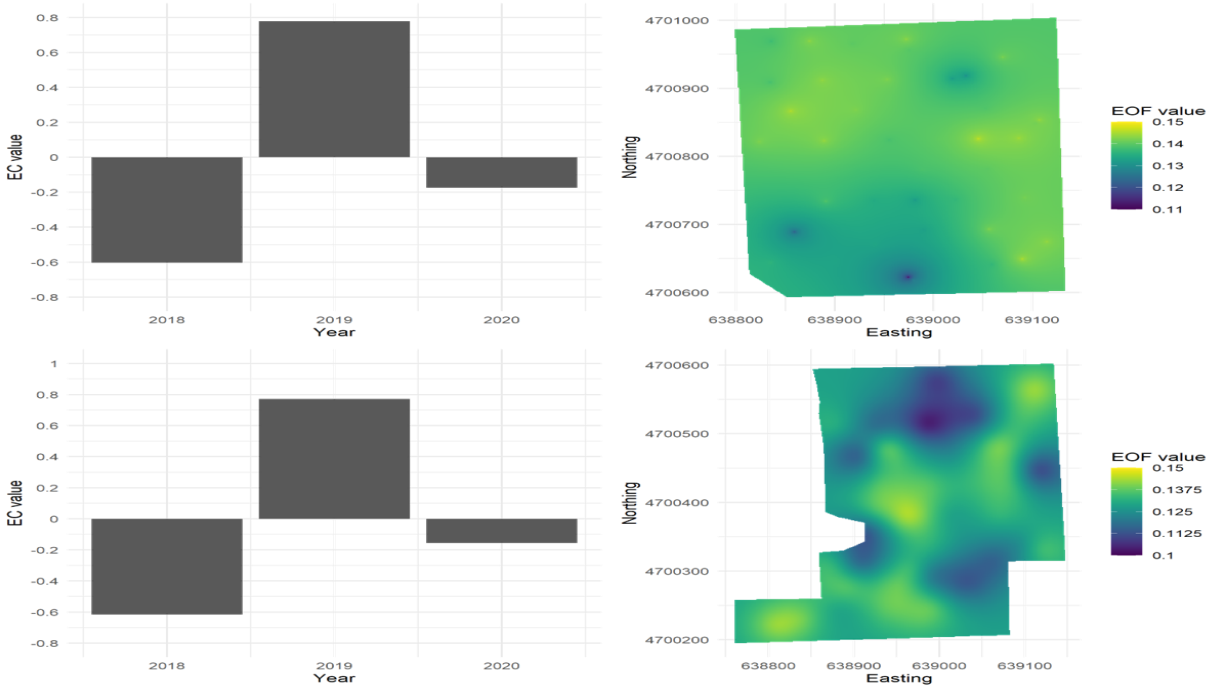

Figure A3.28. The leading temporal empirical orthogonal function (EOF) and time series of expansion efficient (EC) for switchgrass xylose content (upper panel) and restored prairie xylose content (lower panel) at Marshall Farm.

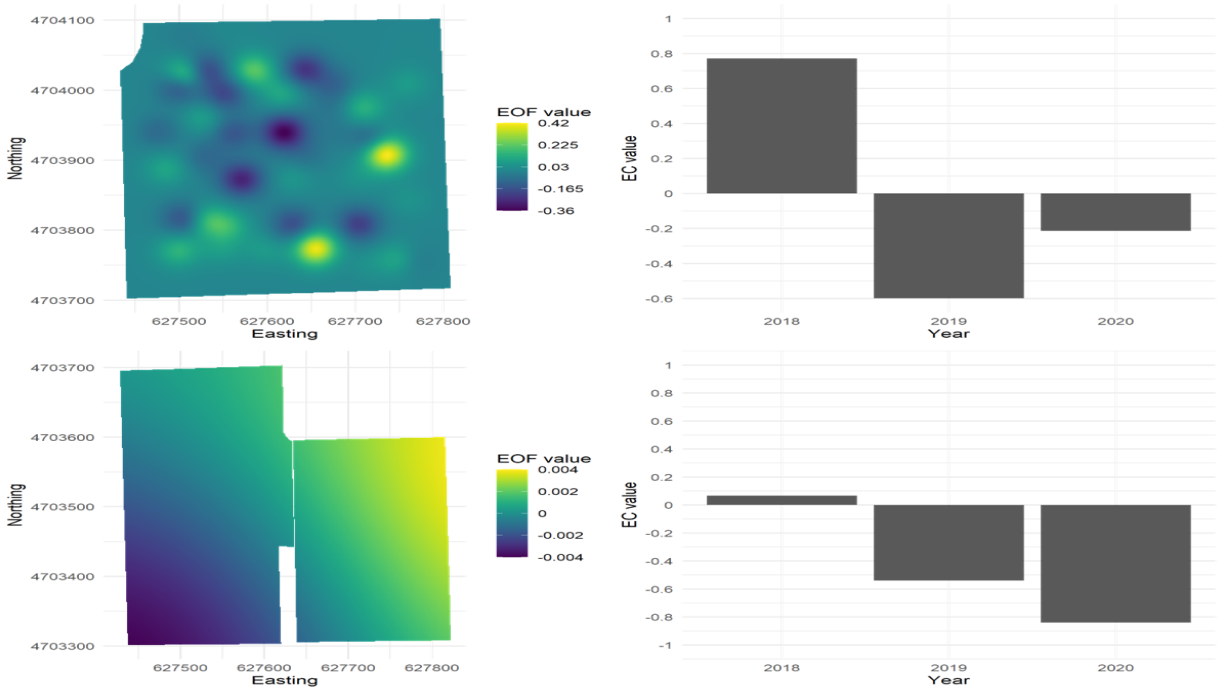

Figure A3.29. The leading spatial empirical orthogonal function (EOF) and time series of expansion efficient (EC) for switchgrass lignin content (upper panel) and restored prairie lignin content (lower panel) at Lux Arbor Farm.

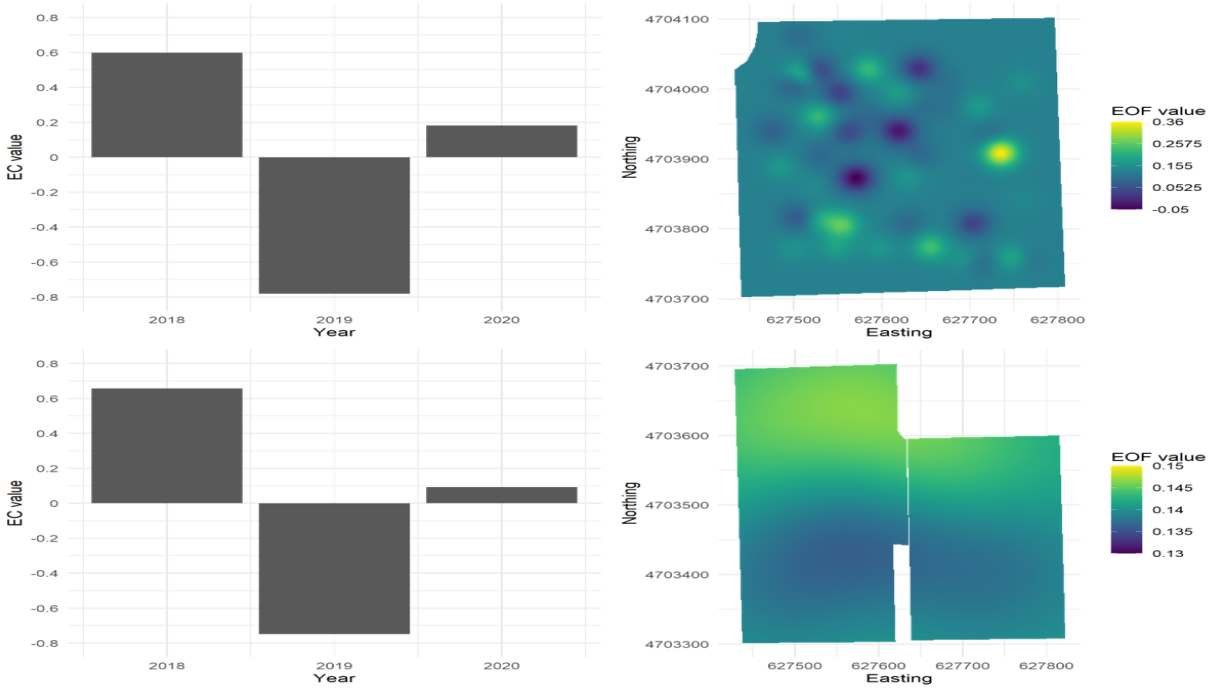

Figure A3.30. The leading temporal empirical orthogonal function (EOF) and time series of expansion efficient (EC) for switchgrass lignin content (upper panel) and restored prairie lignin content (lower panel) at Lux Arbor Farm.

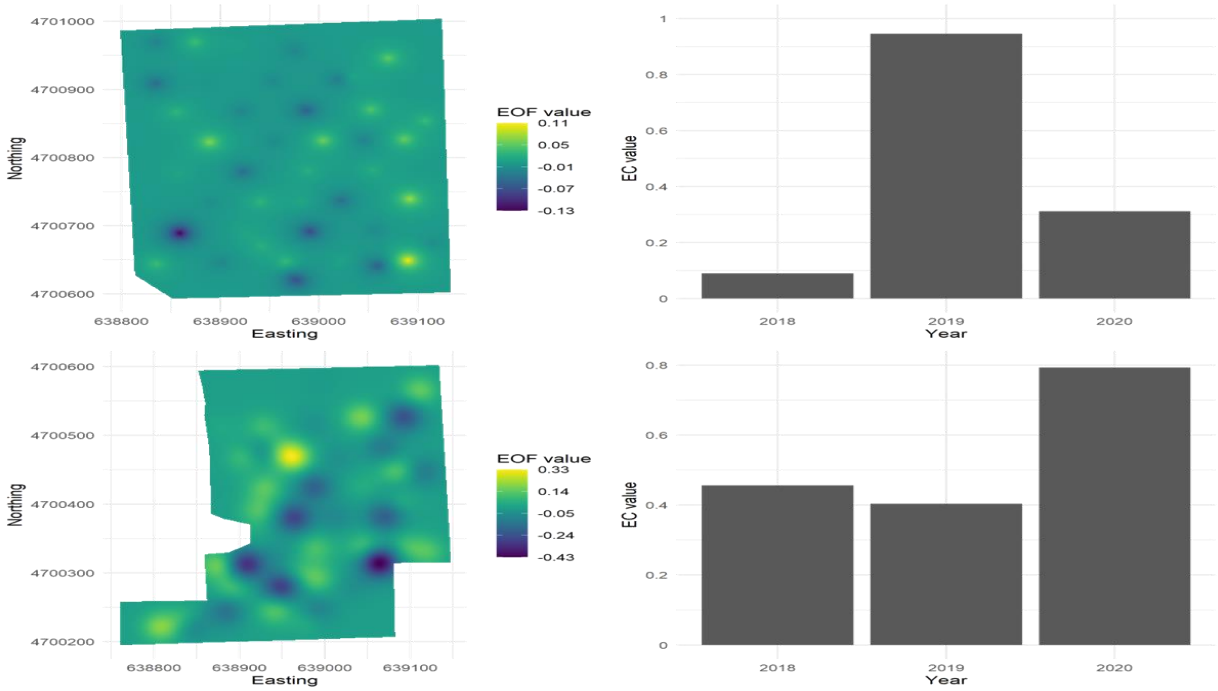

Figure A3.31. The leading spatial empirical orthogonal function (EOF) and time series of expansion efficient (EC) for switchgrass lignin content (upper panel) and restored prairie lignin content (lower panel) at Marshall Farm.

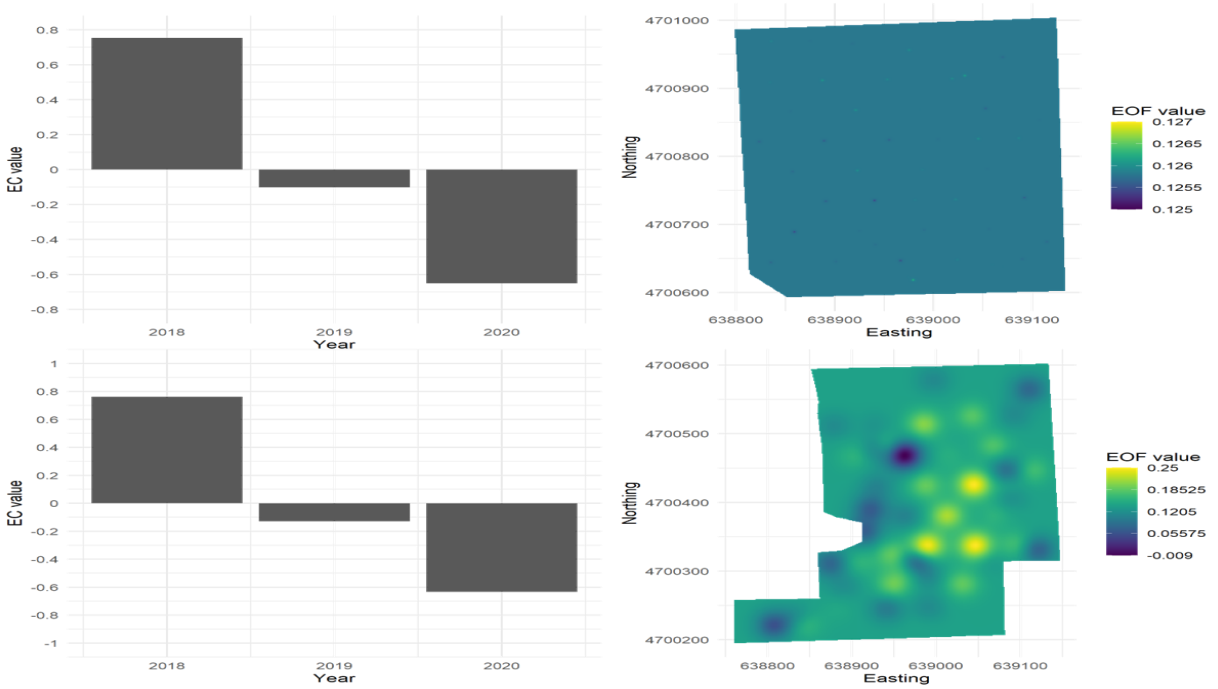

Figure A3.32. The leading temporal empirical orthogonal function (EOF) and time series of expansion efficient (EC) for switchgrass lignin content (upper panel) and restored prairie lignin content (lower panel) at Marshall Farm.

CHAPTER 4 NEAR-INFRARED SPECTROSCOPY AS AN ANALYTICAL PLATFORM FOR EVALUATING PLANT CELL WALL COMPOSITION

Abstract

Identifying analytical instrumentation and methods to quickly and accurately assess variability in biomass quality is valuable to facilitate development of best management practices on farms as well as process optimization techniques at the biorefinery level. Near-infrared spectroscopy is a promising technique to estimate structural glucose, structural xylose and lignin content of biomass feedstocks. In this study, structural glucose, structural xylose and lignin content of 168 switchgrass (*Panicum virgatum*) samples and 168 restored prairie samples were determined both by standard chemical analysis and near-infrared spectroscopy with partial least square algorithm. Compared to chemical analyses, near-infrared spectroscopy measurements had a bias of -72.5 mg g^{-1} (95% CI: -74.7 to -70.4 mg g^{-1}) and -78.5 mg g^{-1} (95% CI: -82.3 to -74.7 mg g^{-1}) for structural glucose content, and a bias of -99.6 mg g^{-1} (95% CI: -102.3 to -96.9 mg g^{-1}) and -91.4 mg g^{-1} (95% CI: -93.7 to -89.0 mg g^{-1}) for structural xylose content of switchgrass and restored prairie, respectively. After bias correction, the highest Lin's concordance correlation coefficient was 0.94 (95%: 0.913, 0.958) for structural xylose content of restored prairie. Near-infrared spectroscopy measurements had the lowest absolute bias of 32.6 mg g^{-1} (95% CI: 30.8 to 34.4 mg g^{-1}) and 47.8 mg g^{-1} (95% CI: 44.7 to 51.0 mg g^{-1}). However, the Lin's concordance correlation coefficient was lowest between standard chemical measurements and bias corrected near-infrared measurements of lignin content for switchgrass (0.465, 95% CI: 0.336 to 0.576) and restored prairie (0.108, 95%: -0.075, 0.284). With appropriate bias correction, near-infrared spectroscopy is a viable rapid analytical method to estimate biomass structural glucose, structural xylose and lignin content.

Introduction

To meet the increasing demand for renewable energy and reduction of greenhouse gas emissions from the energy sector, lignocellulosic bioenergy feedstocks for conversion to liquid fuels have been garnering considerable attention (Liu et al., 2021; Rai et al., 2022). In addition to liquid fuel, lignocellulosic bioenergy feedstocks can also provide other value-added biochemical products (Den et al., 2018). Lignocellulosic bioenergy feedstocks include two major resources: forest-derived resources and agriculture-derived resources. Fuelwood, forest residues, municipal solid wastes (MSW), etc. are considered as forest-derived resources. Corn stover, crop residues, dedicated energy crops, etc. are considered as agriculture-derived resources. The U.S Billion Ton Update (2011) projected there will be 1094 million dry tons of biomass available in the contiguous U.S in 2030, under a baseline scenario. Among all the biomass feedstocks assessed in the report, dedicated energy crops contribute the highest potential quantity (U.S. Department of Energy, 2011).

Cellulose, hemicellulose and lignin are the key cell wall compositional components for producing fuel and biochemicals from lignocellulosic feedstocks. Efforts have been made to optimize biomass cell wall compositions through genetic engineering and breeding (Bhatia et al., 2017; Da Costa et al., 2019; van der Cruijsen et al., 2021). Therefore, rapid analytical methods for biomass cell wall composition determination are needed to accurately analyze large quantities of samples in order to develop uniform and sustainable lignocellulosic feedstocks (Harman-Ware et al., 2022). In addition, rapid analytical data of feedstock cell wall composition from intermediate samples acquired during the conversion process help monitor and improve conversion efficiency (Hames et al., 2003).

Analytical methods for biomass composition determination date back to early 20th century

(Sluiter et al., 2010). The famous Klason method for lignin quantification in wood was proposed by Klason in 1906 (McCarthy & Islam, 1999). In the following three decades, multiple methods for wood lignin determination were suggested by researchers by modifying the concentration of sulfuric acid pretreatment and hydrolysis temperature (Mahood & Cable, 1922; Ritter et al., 1932). Methods for sugar quantification in wood were explored by Ritter et al. (1933) and later modified by Saeman et al. (1945). The modified paper chromatography methods were widely used for sugar quantification in wood industry for a few decades. From 1980 to 1990, researchers tested different methods for fiber analysis of food and feed such as utilizing gas liquid chromatography to measure hydrolyzed sugar content (Petterson, 1984). Van Soest et al. (1991) suggested a widely used method for forage fiber analysis of animal feed, which is still in use today. In the 1990s, scientists at the National Renewable Energy Laboratory published books summarizing biomass analysis methods for biofuel application and provided a suite of laboratory analytical procedures (LAP) for woody and herbaceous biomass compositional analysis (Milne et al., 1990; Sluiter et al., 2008).

Analytical methods for biomass cell wall composition determination can be generally grouped into two types: 1) destructive and 2) non-destructive. Among destructive methods, two subtypes exist. They are gravimetric and chromographic/spectrometric. Gravimetric methods are widely used for forage fiber analysis and are based on a sequence of extraction and fractionation of biomass to determine the weight of different cell wall compositions. After hot neutral solution extraction, a neutral detergent fiber (NDF) value is obtained to represent total cell wall composition. Acid detergent fiber (ADF) values represent least digestible cell wall composition cellulose and lignin derived from acid treated biomass. The difference between NDF and ADF is the hemicellulose content. Cellulose is removed from ADF residue through use of a sulfuric acid

solution to derive the acid detergent lignin (ADL) value. It was recognized that the ADL value underestimated the true lignin content due to partial solubilization of lignin. A more reliable method of lignin content determination is the Klason method. The ADL method used diluted sulfuric acid at high temperature precede concentrated acid and heat. In contrast, the Klason method used higher concentrations of sulfuric acid at low temperature and heat. The major limitation of gravimetric methods is the lack of capability to distinguish structural carbohydrates such as glucan and xylan content in biomass. Similar to gravimetric methods, spectrophotometric methods start with pretreatment step to solubilize lignin in a solvent such as acetylbromide (Barnes & Anderson, 2017), HCl triethylene glycol (Yin et al., 2021), or thioglycolate (Wang et al., 2022). In the following step, spectrometric measurements are taken at 280 nm using extinction coefficients to quantify lignin content. For structural carbohydrates, gas-liquid chromatography, high performance liquid chromatography, or anion exchange chromatography with pulsed amperometric detection are used to measure hydrolysate sugar content (Alberheim et al., 1967; Bhattacharyya, 2012). The destructive methods are time and labor consuming, and therefore they are not suitable for analyzing large volumes of biomass samples that are typical for genetic screening of biomass feedstocks.

The widely used noninvasive methods are nuclear magnetic resonance (NMR) spectroscopy and near infrared spectroscopy (NIR). Partial least square regression or other multivariate algorithms are used to develop predictive models with spectral data and true compositional data from standard methods (Roggo et al., 2007). The advantage of noninvasive methods is no pretreatment and minimum preparation of biomass samples. On the other hand, the disadvantage of noninvasive methods is the requirement of standard methods to calibrate and update predictive models.

Research has been ongoing to develop high-throughput analytical methods, which generally involve modification of pretreatments and utilization of autosampler and plate reading techniques (Decker et al., 2018). DeMartini et al. (2011) developed a scaled-down version of a two-stage acid hydrolysis high-throughput method for cell wall composition analysis with the help of robots to automate sample dispensing and heating. Selig et al. (2011) developed a high-throughput method based on two-stage acid hydrolysis using a 96-well reactor plate equipped with a spectrophotometer to quantify sugar content. However, the scaled-down, high-throughput wet chemistry methods require costly customized equipment and multiple steps to process the samples. By comparison, the non-destructive methods such as near infrared spectroscopy are promising rapid analytical methods for high-throughput analysis of cell wall composition. Studies have been shown that near infrared spectroscopy is a reliable method for biomass cell wall composition analysis (Li et al., 2021; Adnan et al., 2022). As the computational speed keeps increasing, biomass composition analysis via near infrared spectroscopy can harness the power of more advanced machine learning methods (Bai et al., 2022; Zhang et al., 2022).

This study was conducted with the objectives of 1) Examining the agreement of near-infrared spectroscopy and hydrolysis analysis for structural glucose, structural xylose and lignin content in switchgrass and restored prairie; and 2) Investigating the bias and precision of the near-infrared spectroscopy compared to hydrolysis analysis for structural glucose, structural xylose and lignin content in switchgrass and restored prairie.

Materials and methods

Biomass materials

Switchgrass (cultivar Cave-in-rock) and restored prairie (5 grass and 14 forb species) were hand harvested at ground level by using 1×1 m^2 quadrat and clipper at two farms after the first killing

frost for 42 randomly selected sampling points each at Marshall Farm (42.44° N, -85.32° W) and Lux Arbor Farm (42.48° N, -85.44° W) in 2019 and 2020, respectively. A total of 168 biomass samples for switchgrass and restored prairie were analyzed for biomass composition. Before composition analysis, all samples were ground to pass a 2-mm mesh and dried at 65 °C to a constant weight.

Chemical compositional analysis (Reference method)

All biomass samples were processed and analyzed at the MSU Biomass Analysis Facility for structural glucose, xylose and lignin content (mg g^{-1}). Roughly 60-70 mg of dry biomass subsamples were transferred into plastic tubes and loaded on a robotic arm system to further mill them with 5.56 mm stainless steel balls (Salem Specialty Ball Co, Canton, CT). For monosaccharide composition determination, 2 mg subsamples were mixed with 100 μg of an inositol solution (5mg/ml) as an internal standard, then pretreated with 250 μl of 2M trifluoroacetic acid and incubated for 90 min at 121°C. After cooling on ice, samples were centrifuged at 10,000 rpm for 10 min. 100 μl of the acidic supernatant was transferred to a glass screw cap vials for the alditol acetate derivatization procedure. Then, 200 μl of a sodium borohydride solution was added to the dried sample and left at room temperature for 1.5 hours, after which 150 μl of glacial acetic acid was added to neutralize the solution. 50 μl of acetic anhydride and 50 μl of pyridine were then added to acetylate alditols, then incubated for 20 min at 121°C. After samples reached room temperature, 500 μl of ethyl acetate and 2 ml water were added and the material was centrifuged at 2,000 RPM for 5 min to obtain an ethyl acetate layer. A 50 μl aliquot of the ethyl acetate layer was pipetted into GC/MS vials with inserts for quantified structural xylose content. For crystalline cellulose content, the trifluoroacetic acid pretreated pellet was added to a screw-capped glass tube with 1 ml of Updegraff reagent (Acetic

acid: nitric acid: water, 8:1:2 v/v). Then, the glass tube was heated at 100°C for 30 min. Cooled samples were centrifuged at 10,000 rpm for 15 min. Supernatant was discarded and a pellet with only crystalline cellulose was obtained. Saeman hydrolysis was used to hydrolyze the pellet into glucose with 175 µl of 72% sulfuric acid. After 45 min incubation at room temperature, samples were further centrifuged with 825 µl water added at 10,000 rpm for 5 min to obtain supernatant with glucose. The colorimetric anthrone assay was used to assay glucose content of the supernatant in a 96 well polystyrene microtiter plate. For lignin content determination, 1-1.5 mg subsample of each dry biomass sample was mixed with 100 µl of freshly made acetyl bromide solution (25% v/v acetyl bromide in glacial acetic acid) and heated in a capped flask at 50°C for 2 hours initially. Then, the samples were heated for an additional hour with vertexing every 15 minutes. After cooling on ice to room temperature, 400 µl of 2 M sodium hydroxide and 70 µl of freshly prepared 0.5 M hydroxylamine hydrochloride were added to the samples in flasks. Then, flasks were filled with glacial acetic acid to the 2.0 ml mark. Absorbance (abs) was read in an ELISA reader at 280 nm using a UV specific 96 well plate with 200 µl of the solution. A detailed protocol is available in Foster et al. (2010).

Near-Infrared Spectrometers compositional analysis

About 20 mg dry biomass samples were first passed through a 2 mm screen via hammer mill (Schutte Hammermill, Buffalo NY, USA) and then a 0.5 mm screen via cyclone mill (UDY Corporation, Fort Collins Co, USA) before analysis by near-infrared spectroscopy for glucan, xylan and lignin content (mg g^{-1}). A Foss XDS near-infrared (NIR) spectrometer (Foss North America, Eden Prairie MN, USA) was used to collect NIR spectra. The spectrometer lamp was warmed up for thirty minutes before scanning. The ground biomass samples were transferred into Foss “quarter cup” vials and spectra of samples were scanned in reflectance mode from 400-

2500 nm with a resolution of 0.5 nm averaged over 32 scans, resulting in 1 minute total scan time. The NIR biomass compositional analysis followed the general calibrate-collect-predict cycle. Predictive models were developed by using representative biomass samples with known glucan, xylan and lignin content (mg g^{-1}). Normalizing, detrending and smoothing were applied to the spectral data of representative biomass samples. Partial least squares models were adopted for developing predictive models of final glucan, xylan and lignin concentrations (mg g^{-1}). The "leave one out" cross-validation technique was used to validate the predictive models. The predictive models were compared by root mean square error and coefficient of determination (R^2). Best predictive models were used to predict glucan, xylan and lignin concentrations (mg g^{-1}). Detailed methods are given in Wolfrum et al., (2020).

Statistical Analysis

Pearson's correlation coefficients are often used as a measure of linear relationships between two variables. However, examining the possibility of one measurement being substituted by another measurement requires assessing agreement between the two measurements, which also be referred to as reproducibility assessment. Lin's concordance correlation coefficient is a metric that assesses not only association but also agreement. It is more sensitive to detect the deviation from a 1:1 relationship of two measurements (Lin, 1989). Therefore, Lin's concordance correlation coefficients were calculated between structural glucose and near-infrared glucan, structural xylose and near-infrared xylan, and acetyl bromide soluble lignin and near-infrared lignin for switchgrass and restored prairie, respectively. 1:1 identity plots between two measurements were used to visually examine the agreements between two measurements for cell wall composition of switchgrass and restored prairie. As a comparison, Pearson's correlation coefficients were calculated as well.

Lin's concordance correlation coefficient:

$$\hat{\rho}_c = \frac{2s_{xy}\sqrt{s_x s_y}}{s_x^2 + s_y^2 + (\bar{x} - \bar{y})^2}$$

Where s_{xy} is sample covariance between x and y, s_x^2 is sample variance of x, s_y^2 is sample variance of y, $\bar{x}$ is sample mean of x, $\bar{y}$ is sample mean of y.

Lin's concordance correlation coefficient is relative metric to measure agreement. More direct assessment of agreement can utilize a Bland-Altman plot, which is often used in the medical field to check the agreement between the same measurement by two different techniques or instruments (Bland & Altman, 1986). Bland-Altman plots were made for structural glucose and near-infrared glucan, structural xylose and near-infrared xylan, acetyl bromide soluble lignin and near-infrared lignin for both switchgrass and restored prairie.

In addition, Passing-Bablok regressions were fitted for structural glucose and near-infrared glucan, structural xylose and near-infrared xylan, acetyl bromide soluble lignin and near-infrared lignin for switchgrass and restored prairie, respectively. Passing-Bablok regression was proposed by Passing & Bablok (1983) as a non-parametric regression analysis for methods comparison. In comparison of least square regression, Passing-Bablok regression is more robust to outliers.

All statistical analysis were done in R statistical computation environment (R Core Team, 2022) with package SimplyAgree (Caldwell, 2022). All figures were made in R statistical computational environment with package ggplot2 (Wickham, 2016).

Bias = $\frac{1}{n}\sum_i^n (Method1i - Method2i)$

Where n is number of paired measurements from both methods. Method1i is the measurement from method1, and Method2i is the measurement from method2 (Reference measurement).

95% Limit of agreement (LoA):

Upper LoA = Bias + 1.96 × S_d

Lower LoA = Bias + 1.96 × S_d

Where S_d is the standard deviation of differences between results from the two methods.

Standard error of the estimated limits of agreement:

$$SE_{LoA} = \sqrt{\left(\frac{1}{n} + \frac{1.96^2}{2(n-1)}\right) S_d}$$

Where n is number of paired measurements from both method. S_d is the standard deviation of difference between two methods` measurements.

Results

Descriptive statistics

In Table 4.1, the structural glucose measurement by chemical analysis of switchgrass samples ranged from 345.9 to 443.6 mg g^{-1}, whereas the near-infrared glucan measurement of switchgrass samples ranged from 279.2 to 362.1 mg g^{-1}. The structural glucose measurement by chemical analysis of restored prairie samples ranged from 270.1 to 458.5 mg g^{-1}, whereas the near-infrared glucan measurement of restored prairie samples ranged from 277.8 to 363.6 mg g^{-1}. The mean and median of structural glucose measurements by chemical analysis were higher than near-infrared glucan measurements for both types of biomass samples. As shown in Figures 4.1 and 4.2, the distributional shapes of measurements for compositional glucose content from two methods were similar for both types of biomass samples. However, the distributions of structural glucose measurements by chemical analysis shifted to higher values than near-infrared glucan measurements.

The structural xylose measurement by chemical analysis of switchgrass samples ranged from 191.8 to 343.4 mg g^{-1}, whereas the near-infrared xylan measurement of switchgrass samples ranged from 102.2 to 230 mg g^{-1}. The structural xylose measurement by chemical analysis of

restored prairie samples ranged from 172.9 to 335.5 mg g^{-1}, whereas the near-infrared xylan measurement of restored prairie samples ranged from 93.6 to 222.7 mg g^{-1}. Similar to structural glucose measurements, the mean and median of structural xylose measurements by chemical analysis were higher than near-infrared xylan measurements for both types of biomass samples. The structural xylose measurements by chemical analysis tended to be higher than near-infrared xylan measurements.

The ABSL measurement of switchgrass ranged from 152.7 to 216 mg g^{-1}, whereas near-infrared lignin measurement of switchgrass ranged from 183.6 to 238.3 mg g^{-1}. The ABSL measurement of restored prairie ranged from 131.2 to 198 mg g^{-1}, whereas the near-infrared lignin measurements of restored prairie ranged from 176.7 to 254.2 mg g^{-1}. In contrast to structural glucose and xylose measurements, the mean and median of ABSL measurements were lower than near-infrared lignin measurement for both types of biomass samples. The ABSL measurements tended to be lower than near-infrared lignin measurements.

Table 4.1. Descriptive statistics of structural glucose and near-infrared glucan, structural xylose and near-infrared xylan, acetyl bromide soluble lignin and near-infrared lignin content for swtichgrass and restored prairie. Unit: mg g^{-1}.

	Structural glucose (mg g^{-1})				Near-infrared glucan (mg g^{-1})			
Crop	Mean(SD[1])	Median	Min	Max	Mean(SD[1])	Median	Min	Max
Switchgrass	394.3(18.6)	390.6	345.9	443.6	321.8(19.0)	319.4	279.2	362.1
Restored prairie	401.8(32.7)	408.8	270.1	458.5	323.3(18.8)	326	277.8	363.6
	Structural xylose (mg g^{-1})				Near-infrared xylan (mg g^{-1})			
	Mean(SD[1])	Median	Min	Max	Mean(SD[1])	Median	Min	Max
Switchgrass	301.9(19.8)	302.7	191.8	343.4	202.3(17.2)	203.8	102.2	230
Restored prairie	269.7(37.2)	279	172.9	335.5	178.3(34.1)	187	93.6	222.7
	ABSL[1] (mg g^{-1})				Near-infrared lignin (mg g^{-1})			
	Mean(SD[1])	Median	Min	Max	Mean(SD[1])	Median	Min	Max
Switchgrass	183.4(11.0)	184.2	152.7	216	215.0(10.7)	217.4	183.6	238.3
Restored prairie	169.1(12.8)	170.1	131.2	198	217.6(12.4)	217.2	176.7	254.2

1. Abbreviation: SD: standard deviation, ABSL: acetyl bromide soluble lignin.

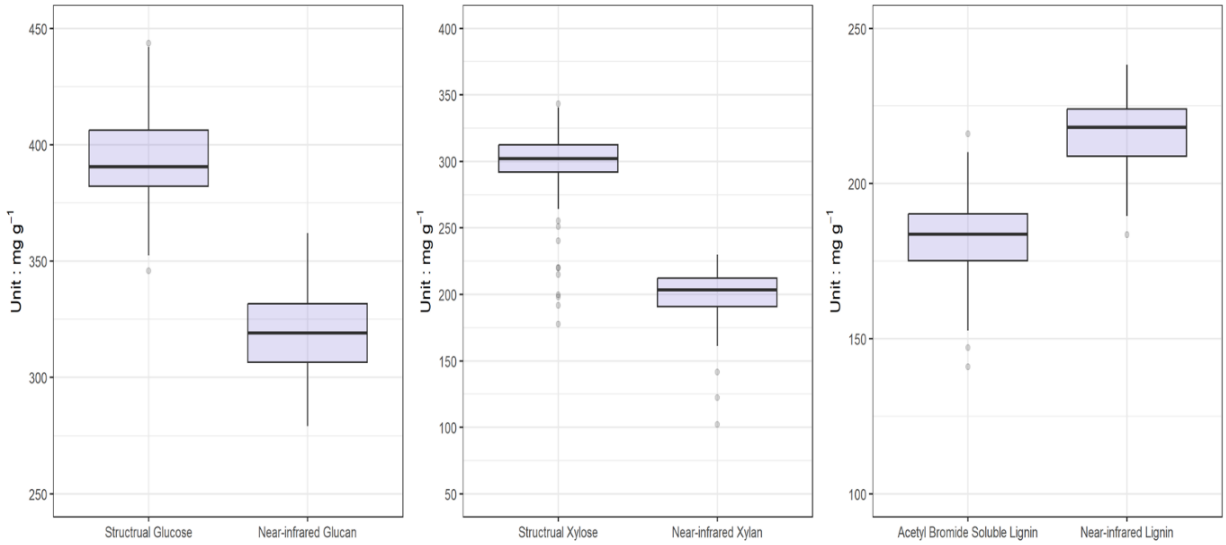

Figure 4.1. Boxplots of switchgrass quality data. Left panel shows structural glucose content (mg g^{-1}) and near infrared glucan content (mg g^{-1}). Middle panel shows structural xylose (mg g^{-1}) and near infrared xylan content (mg g^{-1}). Right panel shows acetyl bromide soluble lignin content (mg g^{-1}) and near infrared lignin content (mg g^{-1}).

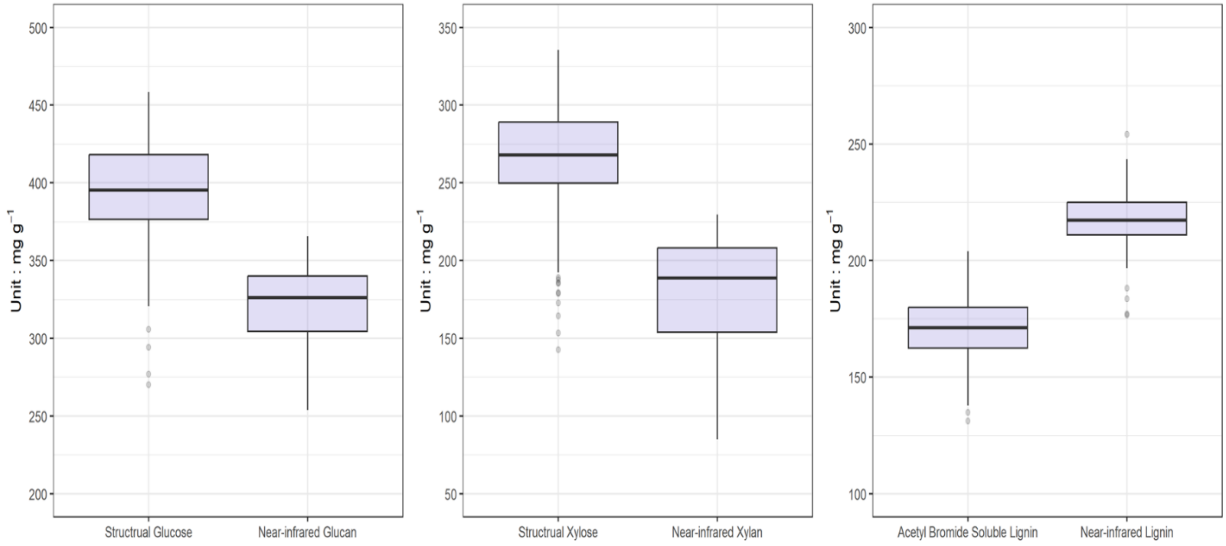

Figure 4.2. Boxplots of restored prairie quality data. Left panel shows structural glucose (mg g^{-1}) and near-infrared glucan content (mg g^{-1}). Middle panel shows structural xylose (mg g^{-1}) and near-infrared xylan content (mg g^{-1}). Right panel shows acetyl bromide soluble lignin content (mg g^{-1}) and near-infrared lignin content (mg g^{-1}).

Pearson's correlation coefficients and Lin's concordance correlation coefficients

As shown in Table 4.2, structural glucose by chemical analysis and near-infrared glucan had the highest Pearson's correlation coefficient of 0.731 (95% CI: 0.650, 0.792) among all three

compositional components measurements of switchgrass. ABSL and near-infrared lignin had the lowest Pearson's correlation coefficient of 0.468 (95% CI: 0.311, 0.555) among all three compositional components measurements of switchgrass. In contrast, ABSL and near-infrared lignin had the highest Lin's concordance correlation coefficient of 0.088 (95% CI: 0.057, 0.119) among all three compositional components measurements of switchgrass.

Structural xylose by chemical analysis and near-infrared xylan had the highest Pearson's correlation coefficient of 0.943 (95%: 0.911, 0.962) among all three compositional components measurements of restored prairie (Table 4.2). In consistent, structural xylose and near-infrared xylan had the highest Lin's concordance correlation coefficient of 0.218 (95% CI: 0.169, 0.267) among all three compositional components measurements of restored prairie. Similar to switchgrass, both Pearson's correlation coefficient and Lin's concordance correlation coefficient exhibited lowest value for ABSL and near-infrared lignin of restored prairie.

Table 4.2. Pearson correlation coefficients with 95% bootstrap confidence intervals and Lin's concordance correlation coefficients with 95% confidence intervals of biomass cell wall composition of switchgrass and restored prairie between chemical compositional analysis and near-infrared spectrometer compositional analysis.

Crop	Methods	Pearson's Correlation Coefficient	Lin's concordance correlation coefficient
Switchgrass	Structural glucose and NIR[1] glucan	0.731[0.650, 0.792][a]	0.086[0.065, 0.107][b]
	Structural xylose and NIR[1] xylan	0.560[0.336, 0.743]	0.036[0.025, 0.047]
	ABSL[1] and NIR[1] lignin	0.468 [0.269, 0.593]	0.088[0.057, 0.119]
Restored prairie	Structural glucose and NIR[1] glucan	0.637[0.270, 0.760]	0.103[0.069, 0.136]
	Structural xylose and NIR[1] xylan	0.943[0.911, 0.962]	0.218[0.169, 0.267]
	ABSL[1] and NIR[1] lignin	0.108[-0.101, 0.326]	0.013[-0.001, 0.036]

1: Abbreviations: ABSL: Acetyl bromide soluble lignin, NIR: near-infrared.
a: 95% bootstrap confidence interval of pearson correlation coefficient.
b: 95% confidence interval of Lin's concordance correlation coefficient.

Bland-Altman plots

The biases of near-infrared glucan measurement compared to structural glucose measurement by chemical analysis of switchgrass and restored prairie were -72.5 mg g^{-1} (95% CI:-74.7 to -70.4

mg g^{-1}) and -78.5 mg g^{-1} (95% CI: -82.3 to -74.7 mg g^{-1}), respectively (Table. 4.3). As shown in Figure 4.3, most of the measurements differences of structural glucose content for switchgrass and restored prairie from two methods fell within the range of 95% limits of agreement (LoA). There was no relation of structural glucose measurement differences of switchgrass with the absolute concentrations. In contrast, a downward trend showing higher negative bias associated with higher measurement value was observed for restored prairie structural glucose content.

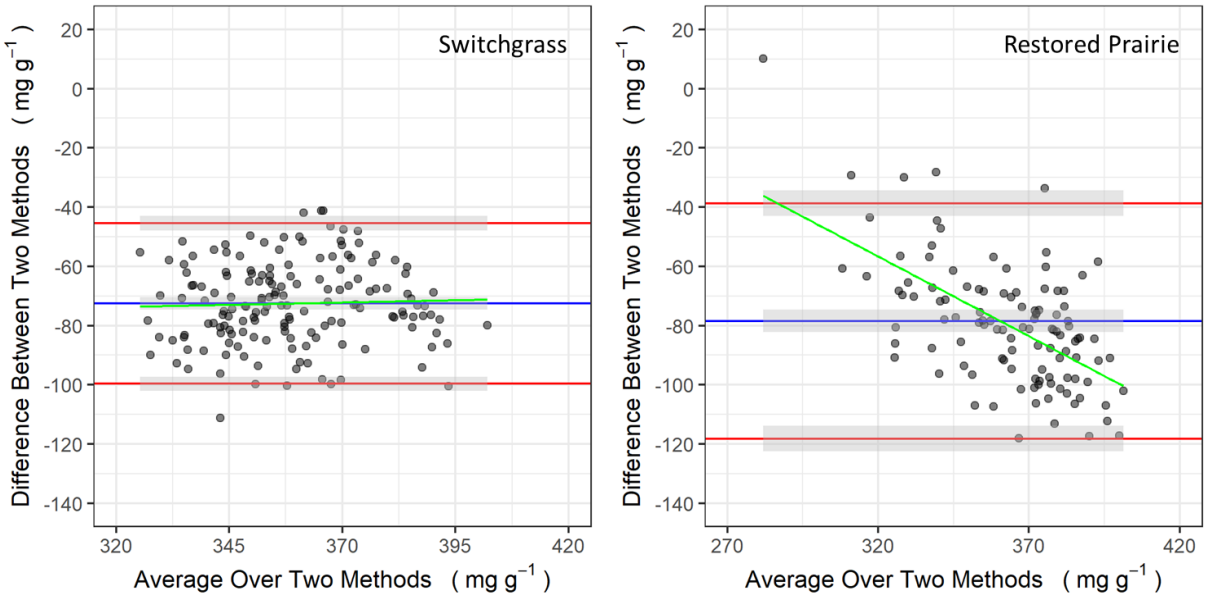

Figure 4.3. Bland-Altman plots for structural glucose measurements (mg g^{-1}) and near-infrared glucan measurements (mg g^{-1}) of switchgrass (left panel) and restored prairie (right panel). Horizontal blue line is bias (near-infrared glucan measurement – structural glucose measurement) between two measurement methods and gray shaded area is 95% confidence interval. Top horizontal red line is upper bound of 95% limit of agreement (LoA) of two measurement methods and gray shaded area is 90% confidence interval. Bottom horizontal red line is lower bound of 95% limit of agreement (LoA) of two measurement methods and gray shaded area is 90% confidence interval.

Similarly, biases were observed between near-infrared xylan measurement and structural xylose measurements by chemical analysis of switchgrass (-99.6 mg g^{-1}, 95% CI: -102.3 to -96.9 mg g^{-1}) and restored prairie (-91.4 mg g^{-1}, 95% CI: -93.7, -89.0 mg g^{-1}) (Table. 4.3). Most of the measurement differences in structural xylose content for switchgrass and restored prairie from two methods fell within the range of 95% limits of agreement. A slight downward trend showing

higher negative bias associated with higher measurement value was observed for structural xylose content in both switchgrass and restored prairie (Figure 4.4).

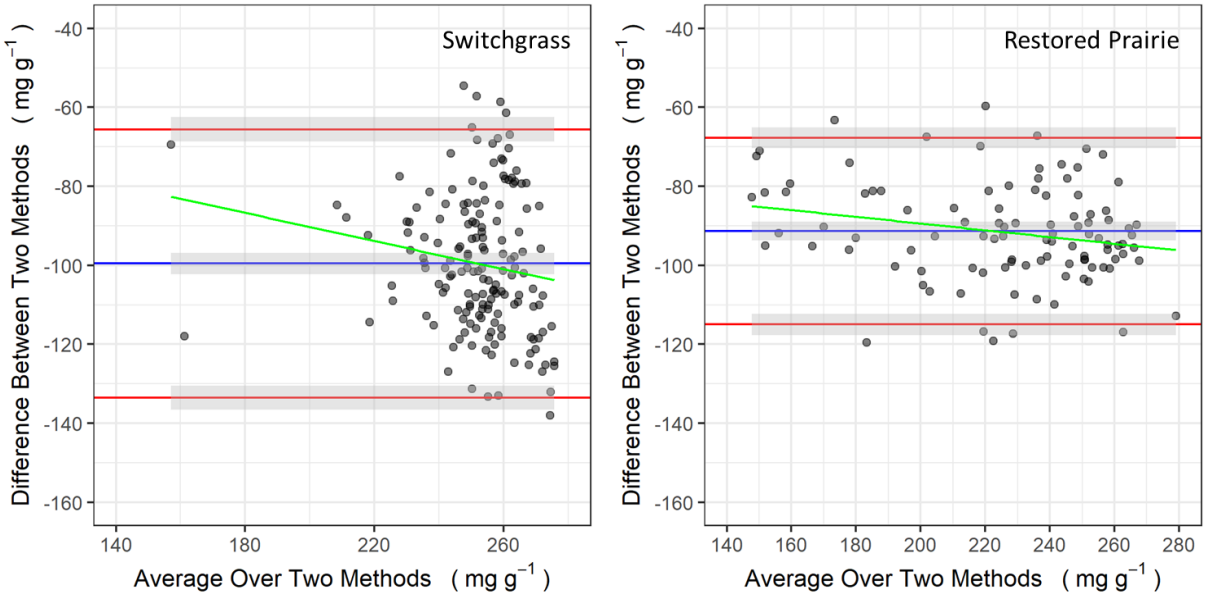

Figure 4.4. Bland-Altman plots for structural xylose measurements (mg g^{-1}) and near-infrared xylan measurements (mg g^{-1}) of switchgrass (left panel) and restored prairie (right panel). Horizontal blue line is bias (near-infrared xylan measurement – structural xylose measurement) between two measurement methods and gray shaded area is 95% confidence interval. Top horizontal red line is upper bound of 95% limit of agreement (LoA) of two measurement methods and gray shaded area is 90% confidence interval. Bottom horizontal red line is lower bound of 95% limit of agreement (LoA) of two measurement methods and gray shaded area is 90% confidence interval.

In contrast, Table 4.3 shows that the bias between near-infrared lignin and ABSL was positive for switchgrass (32.6 mg g^{-1}, 95% CI: 30.8 to 34.4 mg g^{-1}) and restored prairie (47.8, 95% CI: 44.7 to 51.0 mg g^{-1}). Most of the measurement differences for lignin content of switchgrass and restored prairie from two methods were tightly scattered around the corresponding bias and showed no systematic relation with the absolute concentrations (Figure 4.5).

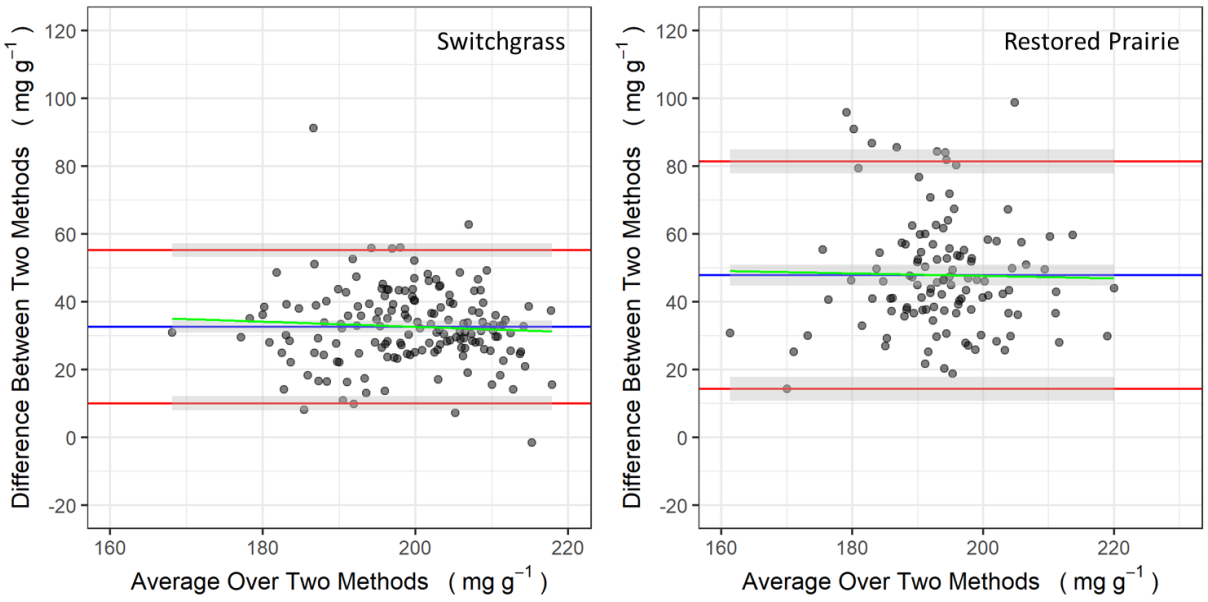

Figure 4.5. Bland-Altman plots for acetyl bromide soluble lignin measurements (mg g^{-1}) and near-infrared lignin measurements (mg g^{-1}) of switchgrass (left panel) and restored prairie (right panel). Horizontal blue line is bias (near-infrared lignin measurement –acetyl bromide soluble lignin measurement) between two measurement methods and gray shaded area is 95% confidence interval. Top horizontal red line is upper bound of 95% limit of agreement (LoA) of two measurement methods and gray shaded area is 90% confidence interval. Bottom horizontal red line is lower bound of 95% limit of agreement (LoA) of two measurement methods and gray shaded area is 90% confidence interval.

As shown in Table 4.3, the absolute value of the bias of compositional glucose measurements and lignin measurements from the two methods was higher for restored prairie compared to switchgrass. In contrast, the absolute value of compositional xylose measurements from the two methods was lower for restored prairie compared to switchgrass. In comparing compositional glucose and xylose measurements, the absolute value of the bias between acetyl bromide soluble lignin measurements and near-infrared lignin measurements was the lowest for both types of biomass materials. The absolute value of the bias of compositional xylose measurements from two methods was slightly higher than the bias of compositional glucose measurements from two methods.

Table 4.3. Bias, 95% limits of agreement for near-infrared glucan and structrual glucose, near-infrared xylan and structrual xylose, near-infrared lignin and acetyl bromide soluble lignin (ABSL) content of switchgrass and restored prairie samples. Unit: mg g^{-1}.

	Near-infrared glucan and Structural glucose (mg g^{-1})	
	Switchgrass	Restored prairie
Bias[1]	-72.5[-74.7, -70.4][a]	-78.5[-82.3, -74.7]
Lower LoA[4]	-99.7[-102.1, -97.2][b]	-118.2[-122.5, -113.9]
Upper LoA	-45.4[-47.9, -43.0][b]	-38.7[-43.0, -34.4]
	Near-infrared xylan and Structural xylose (mg g^{-1})	
	Switchgrass	Restored prairie
Bias[2]	-99.6[-102.3, -96.9]	-91.4[-93.7, -89.0]
Lower LoA	-133.6[-136.6, -130.5]	-114.99[-117.7, -112.3]
Upper LoA	-65.6[-68.6, -62.5]	-67.72[-70.4, -65.1]
	Near-infrared lignin and ABSL[4] (mg g^{-1})	
	Switchgrass	Restored prairie
Bias[3]	32.6[30.8, 34.4]	47.8[44.7, 51.0]
Lower LoA	10.0[8.0, 12.1]	14.3[10.7, 17.8]
Upper LoA	55.2[53.2, 57.2]	81.4[77.8, 85.0]

1. Bias = near-infrared glucan measurement – structural glucose measurement.
2. Bias = near-infrared xylan measurement – structural xylose measurement.
3. Bias = near-infrared lignin measurement – structural acetyl bromide lignin measurement.
4. Abbreviation: LoA: Limit of Agreement, ABSL: Acetyl Bromide Soluble Lignin.
a. Values within square brackets for biases are 95% confidence intervals.
b. Values within square brackets for 95% limits of agreement are 90% confidence intervals.

Passing-Bablok regression

As shown in Figure 4.6, structural glucose measurements and near-infrared glucan measurements did not lie on the 1:1 line for either switchgrass or restored prairie. Structural glucose measurements were consistently higher than near-infrared glucan measurements for switchgrass. There were only two near-infrared glucan measurements that were higher than structural glucose measurements for restored prairie. The bias-corrected near-infrared glucan measurements and structural glucose measurements were closer to the 1:1 relationship (Figure 4.6). The least squared regression fitted line exhibited a proportional bias (slope: 0.72, 95% CI of slope: 0.61, 0.82) of compositional glucose content between measurements from two methods for switchgrass. The Passing-Bablok regression fitted line was parallel with bias-corrected identity line with the median slope of 0.96 (95% CI: 0.84 to 1.09) for switchgrass. In contrast, the least

square regression fitted line (Slope: 1.11, 95% CI of slope: 0.86 to 1.36) for restored prairie was parallel with bias-corrected identity line. However, the Passing-Bablok regression fitted line exhibited a considerable proportional bias (Slope: 1.65, 95% CI of slope: 1.39 to 1.97) for restored prairie, implying that bias increases as measurement value increases.

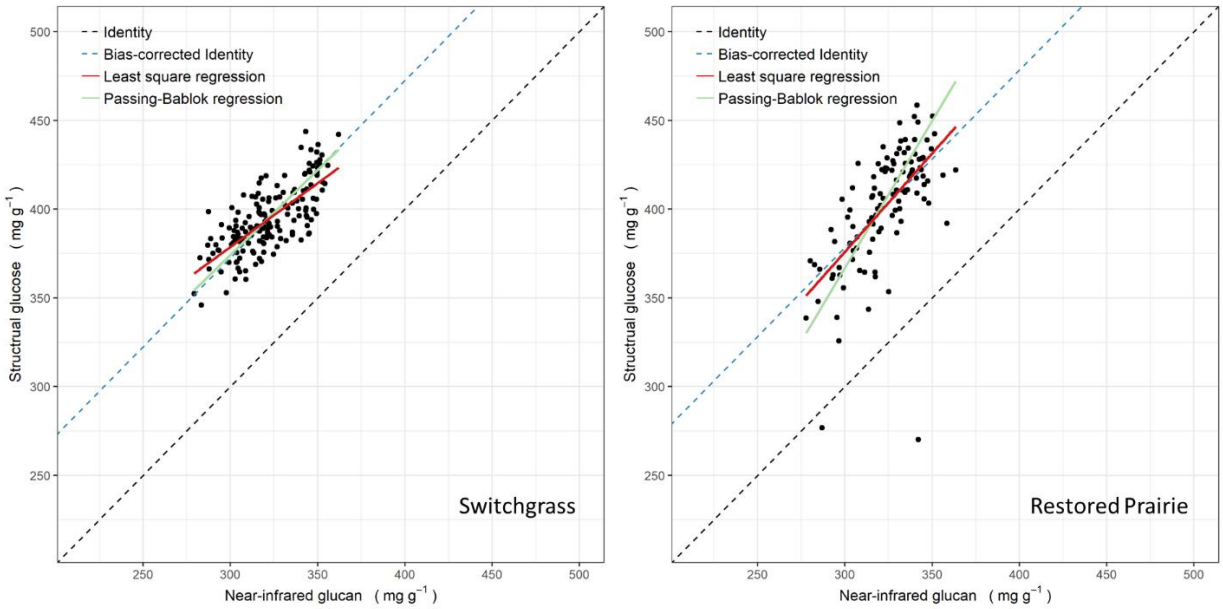

Figure 4.6. Regression plots for structural glucose measurements (mg g^{-1}) and near-infrared glucan measurements (mg g^{-1}) of switchgrass (left panel) and restored prairie (right panel). Black dotted line is 45 degree one on one identity line. Light blue dotted line is the 45 degree one on one bias-corrected (near-infrared glucan - bias) identity line. Red solid line is fitted line from least square regression. Green solid line is fitted line from Passing-Bablok regression.

Structural xylose measurements and near-infrared xylan measurements did not lie on the 1:1 line for either switchgrass or restored prairie (Figure 4.7). Structural xylose measurements were consistently higher than near-infrared xylan measurements for switchgrass and restored prairie. For switchgrass, the least squared regression line exhibited a downward proportional bias (slope: 0.64, 95% CI of slope: 0.49 to 0.79) of compositional xylose content between measurements. In contrast, the Passing-Bablok regression line showed upward proportional bias (Slope: 1.31, 95% CI of slope: 1.04 to 1.60) for switchgrass, which was driven by the two low values of compositional xylose content. For restored prairie, both the least squared regression line (Slope:

1.03, 95% CI of slope: 0.96 to 1.10) and the Passing-Bablok regression line (Slope: 1.08, 95% CI of slope: 1 to 1.16) were nearly parallel with the bias-corrected identity line.

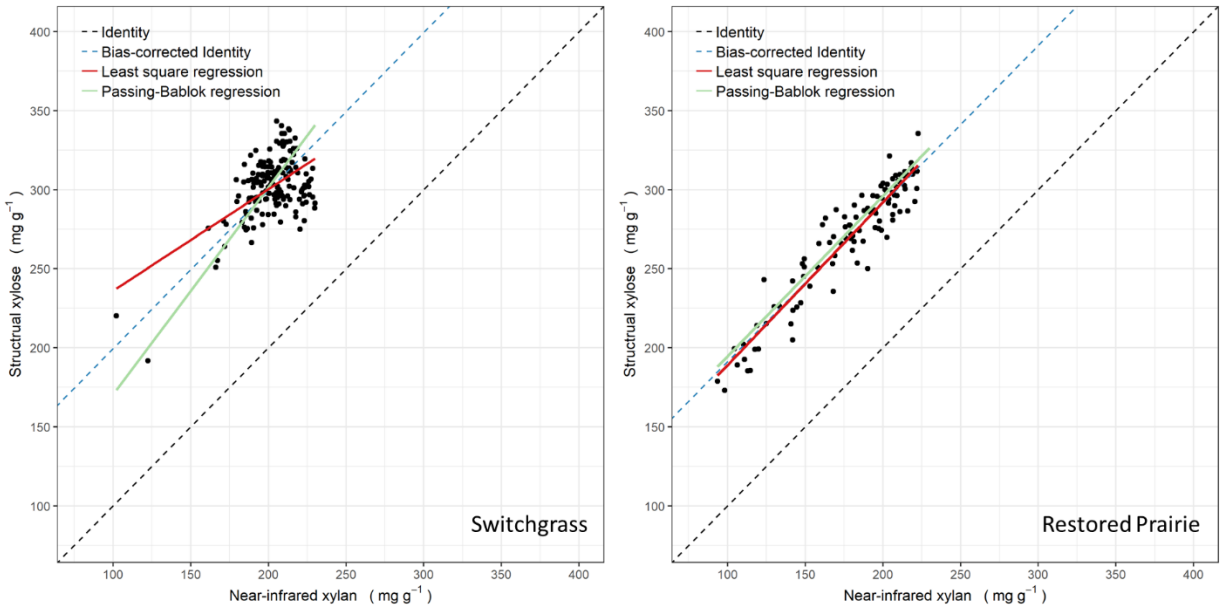

Figure 4.7. Regression plots for structural xylose measurements (mg g^{-1}) and near-infrared xylan measurements (mg g^{-1}) of switchgrass (left panel) and restored prairie (right panel). Black dotted line is 45 degree one on one identity line. Light blue dotted line is the 45 degree one on one bias-corrected (near-infrared xylan - bias) identity line. Red solid line is fitted line from least square regression. Green solid line is fitted line from Passing-Bablok regression.

Acetyl bromide soluble measurements and near-infrared lignin measurements did not lie on the 1:1 line for either switchgrass or restored prairie (Figure 4.8). In contrast to compositional glucose and xylose content, acetyl bromide soluble measurements were consistently lower than near-infrared lignin measurements for switchgrass and restored prairie with the exception of only one datum for switchgrass. The least squared regression line exhibited a substantial downward proportional bias of lignin content between measurements for switchgrass (slope: 0.53, 95% CI of slope: 0.39 to 0.69) and restored prairie (slope: 0.08, 95% CI of slope: 0.39 to 0.69). In contrast, the Passing-Bablok regression line showed an upward proportional bias for switchgrass (Slope: 1.27, 95% CI of slope: 1.08 to 1.53) and restored prairie (Slope: 1.06, 95% CI of slope: -1.54 to 1.48).

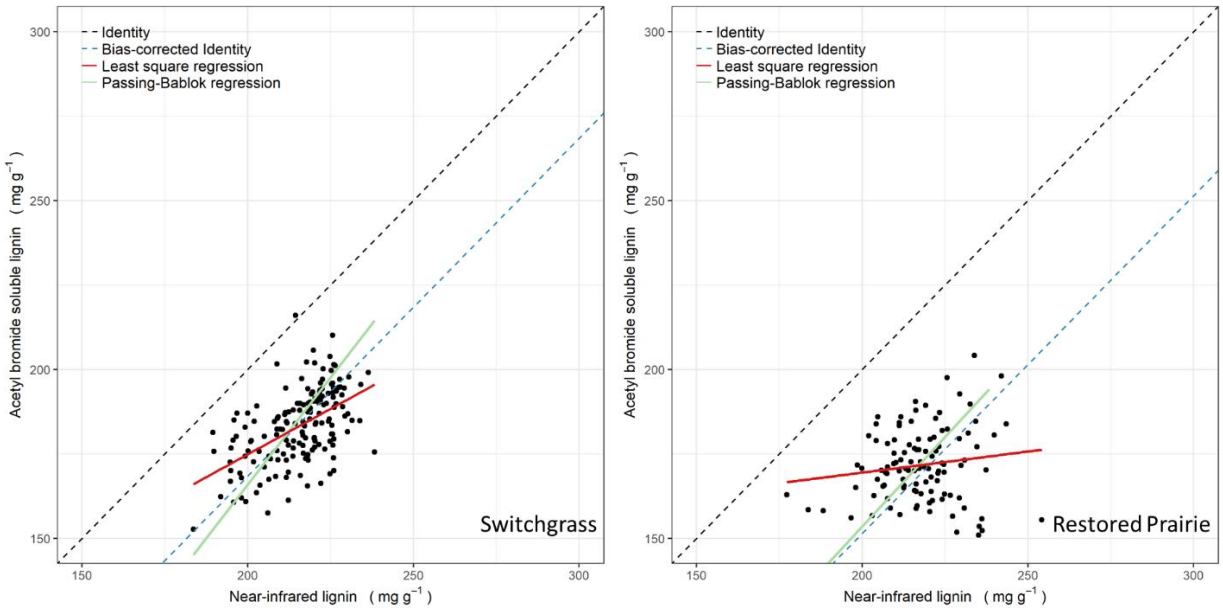

Figure 4.8. Regression plots for acetyl bromide soluble lignin measurements (mg g^{-1}) and near-infrared lignin measurements (mg g^{-1}) of switchgrass (left panel) and restored prairie (right panel). Black dotted line is 45 degree one on one identity line. Light blue dotted line is the 45 degree one on one bias-corrected (near-infrared lignin - bias) identity line. Red solid line is fitted line from least square regression. Green solid line is fitted line from Passing-Bablok regression.

Table 4.4 shows that bias correction improved the relationship between two measurement methods for structural glucose, structural xylose and lignin content. Lin's concordance correlation coefficient increased from 0.086 to 0.731 and 0.103 to 0.551 for structural glucose contents of switchgrass and restored prairie, respectively. Lin's concordance correlation coefficient increased from 0.036 to 0.554 and 0.218 to 0.94 for structural xylose content of switchgrass and restored prairie, respectively. For lignin content measurement, Lin's concordance correlation coefficient increased from 0.088 to 0.465 and 0.013 to 0.108 for switchgrass and restored prairie, respectively.

Table 4.4. Lin's concordance correlation coefficients with 95% confidence intervals of biomass cell wall composition of switchgrass and restored prairie between chemical compositional analysis and near-infrared analysis Spectrometers compositional analysis after bias correction.

Crop	Methods	Lin's concordance correlation coefficient
Switchgrass	Structural glucose and NIR[1] glucan	0.731[0.651, 0.795][a]
	Structural xylose and NIR[1] xylan	0.554[0.439, 0.651]
	ABSL[1] and NIR[1] lignin	0.465[0.336, 0.576]
Restored prairie	Structural glucose and NIR[1] glucan	0.551[0.438, 0.646]
	Structural xylose and NIR[1] xylan	0.940[0.913, 0.958]
	ABSL[1] and NIR[1] lignin	0.108[-0.075, 0.284]

1: Abbreviations: ABSL: Acetyl bromide soluble lignin, NIR: near-infrared.
a: 95% confidence interval of Lin's concordance correlation coefficient.

Discussion

In this study, the structural glucose content from chemical analysis for switchgrass ranged from 345.9 to 443.6 mg g^{-1}, which is comparable with other studies. Previous studies showed that the structural glucose of switchgrass ranged from 38 to 43 wt% as determined by similar chemical analysis (Hu et al., 2010; Shi et al., 2011). The structural xylose content of switchgrass from chemical analysis had relatively high values (191.8 to 343.4 mg g^{-1}). Frederick et al. (2016) reported structural xylose content of switchgrass of 24.35 wt% (standard deviation: 2.51 wt%). Previous studies reported that the lignin content of switchgrass determined by Klason method ranged from 17.5% (Kgblevo et al., 1994) to 21.4% (Thammasouk et al., 1997). This is consistent with the range (184.2 to 216 mg g^{-1}) of lignin content of switchgrass observed in this study.

A study investigating mixed grass biomass from several CRP grasslands in Oregon, USA reported that structural glucose content ranged from 28.76 to 36.01 wt%, structural xylose content ranged from 14.21 to 21.98 wt%, and lignin content ranged from 13.4 to 17.45 wt% (Juneja et al., 2011). Another study examined chemical composition of big bluestem (*Andropogon gerardii*) and showed that structural glucose content ranged from 31.8 to 36.5 wt%,

structural xylose content ranged from 24.96 to 39.74 wt%, and lignin content ranged from 14.4 to 18.0 wt% (Zhang et al., 2012). Compared to these two studies (Juneja et al., 2011; Zhang et al., 2012), structural glucose content (270.1 to 458.5 mg g^{-1}), structural xylose content (172.9 to 335.5 mg g^{-1}) of restored prairie were relatively higher in this study. The structural glucose content and structural xylose content of restored prairie were more variable than switchgrass in this study. This is expected because of the multi-species nature of restored prairie.

To the best of our knowledge, the literature has focused on reporting coefficients of determination and prediction errors to evaluate performance of near-infrared spectroscopy for determining cell wall composition. Understanding bias is also critical for applying near-infrared spectroscopy in the research and industry setting.

Because the chemical analysis conducted in this study was in a different lab as the reference chemical analysis used in developing predictive model with near-infrared spectra data, biases were expected between chemical analysis in this study and near-infrared spectroscopy measurements for the three cell wall compositional components. Interlaboratory variability of measurements on the same substance is a common phenomenon but the causes are multifactorial (La Bastide & Van Goor, 1978). Templeton et al. (2016) observed the high variability of glucan content measurements from 14 different labs on the same biomass samples. The multi-factors associated with interlaboratory variability include instrument differences, modified protocols, analysts' differences, etc. It is noteworthy that measurements from near-infrared measurements varied less than standard chemical analysis. This could be explained by the random errors introduced by multiple steps involved in traditional chemical analysis.

Near-infrared spectroscopy utilizes the spectrum absorption of molecular bonds (such as C-H, O-H, etc.) in the sample to qualitatively and quantitatively determine the chemical composition

(Manley, 2014).There are four common measurement modes of near-infrared spectroscopy: transmittance, transflectance, diffuse reflectance and transmittance through scattering medium (Skvaril et al., 2017). For solid material in this study, transflectance mode was used to collect near-infrared spectra. The thickness of the samples, the heterogeneity of the sample and moisture in the sample may contribute to the variability of the measurements for solid material (Hong & Chia, 2021). Consequently, less useful information can be derived through predictive models. Measures need to be taken to account for these factors when building the predictive model.

The predictive model in this study for near-infrared spectra data used leave-one-out cross validation to validate model performance. Leave-one-out cross validation is one of the preferred methods to estimate out of sample prediction error (Magnusson et al., 2020). However, there is an ongoing debate in the literature on whether leave-one-out cross validation could bias the prediction error (Varma & Simon, 2006; Tibshirani & Tibshirani, 2009). In this study, all the Pearson's coefficient of correlation between the two methods for cell wall composition is below 0.90 (coefficient of determination is 0.81) with exception of structural xylose content of restored prairie (Pearson's coefficient of correlation: 0.94, coefficient of determination: 0.89). This low coefficient of determination could be attributed to optimistically underestimated prediction error of the predictive model selected based on lowest prediction error in this study. More advanced calibration techniques have been explored to realistically estimate the prediction error (Tian et al., 2007; Baumann & Baumann, 2014; Efron, 2021).

A few studies demonstrated that coupling partial least square regression (PLS) with various variable selection techniques could increase predictive accuracy for determination of cell wall components. These includes genetic algorithms (Lestander et al., 2003; Yang et al., 2017), competitive adaptive reweighted sampling (Ai et al., 2022) and variable combination population

analysis (Bonah et al., 2020; Mishra & Woltering, 2021). Elle et al., 2019 showed that partial least square regression with competitive adaptive reweighted sampling (CARS) effectively increased the accuracy for lignin content determination compared to PLS with full spectrum. Likewise, Liang et al. (2020) showed that partial least square regression with genetic algorithms increased the accuracy for lignin content determination compared to PLS with full spectrum for lignin content of pulp wood.

A typical pipeline of developing a predictive model with near-infrared spectral data begins with preprocessing the spectral data. The main goal of this critical step is to reduce the noise in spectral data, and therefore improve the quality of the data for the model training step (Rinnan et al., 2009). The present study used standard normal variate (SNV) normalization, detrending and Savitzky-Golay smoothing as preprocessing treatment. Xu et al. (2008) proposed an ensemble preprocessing method to improve the spectral data quality from NIR. Furthermore, the systematic and proportional biases found in the present study emphasize the importance of continuing maintenance of predictive model. The predictive model performance utilizing near-infrared spectroscopy and multivariate analysis depends heavily on the coverage of training data (Balabin & Smirnov, 2012). The predictive model should be regularly recalibrated for a wide range of biomass material to improve the predictive performance. Researchers have identified the need of calibration maintenance for the predictive model to ensure wide application of NIR spectroscopy technique (Workman, 2018; Qiao et al. 2021). The commonly used calibration maintenance methods are piecewise standardization, bias/slope correction and model updating (Bouveresse & Massart, 1996).

Despite there being room for improvement in the NIR spectroscopy analytical method, it is appealing for process monitoring in a biorefinery setting due to its non-destructive nature and

minimal sample preparation requirements. For biochemical conversion from biomass to biofuel, timely monitoring the quality of biomass assists adjustment of yeast mass loading, thereby increasing conversion efficiency (Gomes et al., 2018). NIR spectroscopy has been demonstrated to be useful as an inline monitoring tool for biodiesel production by inserting a probe directly in the reactor (López-Fernández et al., 2022).

The speed of the NIR spectroscopy analytical method is much faster relative to traditional chemical analysis. In this study, the NIR spectroscopic method takes 32 reads within 1 minute on average per instrument (Wolfrum et al., 2020). In contrast, only 20-30 samples on average can be processed per day per analyst using current wet-chemistry analytical techniques (Foster et al., 2010b). In addition, the near-infrared spectroscopy analytical method does not consume any laboratory reagents. Therefore, it is more environmentally friendly.

Recently, a new research direction on miniaturization and portability of NIR spectrometers has been explored (Beć et al., 2020; Beć et al., 2021). The satisfactory performance of portable NIR spectrometers has been shown in the food and wood industries (Teixeira Dos Santos et al., 2013; Pan et al., 2015; Diniz et al., 2019). The increasing portability of NIR spectrometers combined with reduced cost of instruments opens more opportunities for NIR spectrometer application along the life cycle of bioenergy products. Zhu et al., (2022) summarized and compared the main types of commercial portable NIR spectrometers. The weight of the currently available commercial portable NIR spectrometer ranges from 15 to 1180 g. With more and more advancement in NIR spectroscopy techniques, the method has the potential to be an increasingly valuable analytical tool in bioenergy research and in commercial biorefinery applications.

Conclusion

Near-infrared spectroscopy underestimated both structural glucose and structural xylose content

of switchgrass and restored prairie. In contrast, NIR spectroscopy overestimated lignin content of switchgrass and restored prairie. On a positive note, the biases for structural glucose, structural xylose and lignin content of switchgrass and restored prairie from chemical analysis and near-infrared spectroscopy measurements were maintained within the limits of agreement. A higher absolute value of bias was associated with higher values of restored prairie structural glucose measurements and switchgrass structural xylose measurements. The absolute value of bias was lowest for lignin measurements of switchgrass and restored prairie. After bias correction, Lin's concordance correlation coefficient for all three cell wall compositional components of switchgrass and restored prairie improved substantially.

In summary, near-infrared spectroscopy shows promise as a high throughput analytical instrument for measurement of structural glucose and xylose content of biomass with correction for potential biases. Furthermore, accuracy would be expected to increase over time using conventional predictive equation recalibration methods from new sample comparisons. The current NIR spectroscopy method for lignin content measurements needs further improvement to reduce measurement noise before widespread adoption can be recommended. Analytical instrumentation and methods to accurately assess variability in biomass quality are valuable to facilitate field and biorefinery management practices.

REFERENCES

Adnan, M., Shen, Y., Ma, F., Wang, M., Jiang, F., Hu, Q., Mao, L., Lu, P., Chen, X., He, G., Khan, M. T., Deng, Z., Chen, B., Zhang, M., & Huang, J. (2022). A quick and precise online near-infrared spectroscopy assay for high-throughput screening biomass digestibility in large scale sugarcane germplasm. Industrial Crops and Products, 189(October). https://doi.org/10.1016/j.indcrop.2022.115814

Ai, N., Jiang, Y., Omar, S., Wang, J., Xia, L., & Ren, J. (2022). Rapid Measurement of Cellulose, Hemicellulose, and Lignin Content in Sargassum horneri by Near-Infrared Spectroscopy and Characteristic Variables Selection Methods. Molecules, 27(335). https://doi.org/https:// doi.org/10.3390/molecules27020335

Alberheim, P., Nevins, D.J., English, P.D., Karr, A. (1967). Analyzing the Acid Hydrolyzates of Polysaccharides. A Method for the Analysis of Sugars in Plant Cell-Wall Polysaccharides by Gas-Liquid Chromatography, Carbohydrate Research, 5, 340–345. https://doi.org/10.1016/S0008-6215(00)80510-8

Bai, X., Zhang, L., Kang, C., Quan, B., Zheng, Y., Zhang, X., Song, J., Xia, T., & Wang, M. (2022). Near-infrared spectroscopy and machine learning-based technique to predict quality-related parameters in instant tea. Scientific Reports, 12(1), 1–8. https://doi.org/10.1038/s41598-022-07652-z

Balabin, R. M., & Smirnov, S. V. (2012). Interpolation and extrapolation problems of multivariate regression in analytical chemistry: Benchmarking the robustness on near-infrared (NIR) spectroscopy data. Analyst, 137(7), 1604–1610. https://doi.org/10.1039/c2an15972d

Barnes, W., & Anderson, C. (2017). Acetyl Bromide Soluble Lignin (ABSL) Assay for Total Lignin Quantification from Plant Biomass. Bio-Protocol, 7(5), 1–11. https://doi.org/10.21769/bioprotoc.2149

Baumann, D., & Baumann, K. (2014). Reliable estimation of prediction errors for QSAR models under model uncertainty using double cross-validation. Journal of Cheminformatics, 6(1), 1–19. https://doi.org/10.1186/s13321-014-0047-1

Beć, K. B., Grabska, J., & Huck, C. W. (2021). Principles and Applications of Miniaturized Near-Infrared (NIR) Spectrometers. Chemistry - A European Journal, 27(5), 1514–1532. https://doi.org/10.1002/chem.202002838

Beć, K. B., Grabska, J., Siesler, H. W., & Huck, C. W. (2020). Handheld near-infrared spectrometers: Where are we heading? NIR News, 31(3–4), 28–35. https://doi.org/10.1177/0960336020916815

Bhatia, R., Gallagher, J. A., Gomez, L. D., & Bosch, M. (2017). Genetic engineering of grass cell wall polysaccharides for biorefining. Plant Biotechnology Journal, 15(9), 1071–1092. https://doi.org/10.1111/pbi.12764

Bhattacharyya, L. (2012). Glycan Analysis by High Performance Anion Exchange Chromatography with Pulsed Amperometric Detection. In Applications of Ion Chromatography for Pharmaceutical and Biological Products (eds L. Bhattacharyya and J.S. Rohrer). https://doi.org/10.1002/9781118147009.ch17

Bonah, E., Huang, X., Aheto, J. H., Yi, R., Yu, S., & Tu, H. (2020). Comparison of variable selection algorithms on vis-NIR hyperspectral imaging spectra for quantitative monitoring and visualization of bacterial foodborne pathogens in fresh pork muscles. Infrared Physics and Technology, 107(January). https://doi.org/10.1016/j.infrared.2020.103327

Bouveresse, E., & Massart, D. L. (1996). Improvement of the piecewise direct standardisation procedure for the transfer of NIR spectra for multivariate calibration. Chemometrics and Intelligent Laboratory Systems, 32(2), 201–213. https://doi.org/10.1016/0169-7439 (95)00074-7

Caldwell, A. R. (2022). SimplyAgree: An R package and jamovi Module for Simplifying Agreement and Reliability Analyses. Journal of Open Source Software, 7(71), 4148. https://doi.org/10.21105/joss.04148

Da Costa, R. M. F., Pattathil, S., Avci, U., Winters, A., Hahn, M. G., & Bosch, M. (2019). Desirable plant cell wall traits for higher-quality miscanthus lignocellulosic biomass. Biotechnology for Biofuels, 12(1), 1–18. https://doi.org/10.1186/s13068-019-1426-7

Decker, S. R., Harman-Ware, A. E., Happs, R. M., Wolfrum, E. J., Tuskan, G. A., Kainer, D., Oguntimein, G. B., Rodriguez, M., Weighill, D., Jones, P., & Jacobson, D. (2018). High Throughput Screening Technologies in Biomass Characterization. Frontiers in Energy Research, 6(November), 1–18. https://doi.org/10.3389/fenrg.2018.00120

DeMartini, J. D., Studer, M. H., & Wyman, C. E. (2011). Small-scale and automatable high-throughput compositional analysis of biomass. Biotechnology and Bioengineering, 108(2), 306–312. https://doi.org/10.1002/bit.22937

Den, W., Sharma, V. K., Lee, M., Nadadur, G., & Varma, R. S. (2018). Lignocellulosic biomass transformations via greener oxidative pretreatment processes: Access to energy and value added chemicals. Frontiers in Chemistry, 6(APR), 1–23. https://doi.org/10.3389/fchem.2018.00141

Diniz, C., Grattapaglia, D., & de Alencar Figueiredo, L. (2019). Comparative performance of bench and portable near infrared spectrometers for measuring wood samples of two Eucalyptus species (E. pellita and E. benthamii). Proceedings of the 18th International Conference on Near Infrared Spectroscopy, 31–38. https://doi.org/10.1255/nir2017.031

Efron, B. (2021). Resampling Plans and the Estimation of Prediction Error. Stats, 4(4), 1091–1115. https://doi.org/10.3390/stats4040063

Elle, O., Richter, R., Vohland, M., & Weigelt, A. (2019). Fine root lignin content is well predictable with near-infrared spectroscopy. Scientific Reports, 9(1), 1–11.

https://doi.org/10.1038/s41598-019-42837-z

Foster, C. E., Martin, T. M., & Pauly, M. (2010a). Comprehensive compositional analysis of plant cell walls (Lignocellulosic biomass) part I: Lignin. Journal of Visualized Experiments, 37. https://doi.org/10.3791/1745

Foster, C. E., Martin, T. M., & Pauly, M. (2010b). Comprehensive compositional analysis of plant cell walls (Lignocellulosic biomass) part II: Carbohydrates. Journal of Visualized Experiments, 37, 10–13. https://doi.org/10.3791/1837

Frederick, N., Li, M., Julie Carrier, D., D. Buser, M., & R. Wilkins, M. (2016). Switchgrass storage effects on the recovery of carbohydrates after liquid hot water pretreatment and enzymatic hydrolysis. AIMS Bioengineering, 3(3), 389–399. https://doi.org/10.3934/bioeng.2016.3.389

Gomes, J., Batra, J., Chopda, V. R., Kathiresan, P., & Rathore, A. S. (2018). Monitoring and control of bioethanol production from lignocellulosic biomass. Waste Biorefinery: Potential and Perspectives, 727–749. https://doi.org/10.1016/B978-0-444-63992-9.00025-2

Hames, B. R., Thomas, S. R., Sluiter, A. D., Roth, C. J., & Templeton, D. W. (2003). Rapid biomass analysis: new tools for compositional analysis of corn stover feedstocks and process intermediates from ethanol production. Appl Biochem Biotechnol. 2003 Spring;105 -108:5-16. doi: 10.1385/abab:105:1-3:5. PMID: 12721471.

Harman-Ware, A. E., Happs, R. M., Macaya-Sanz, D., Doeppke, C., Muchero, W., & DiFazio, S. P. (2022). Abundance of Major Cell Wall Components in Natural Variants and Pedigrees of Populus trichocarpa. Frontiers in Plant Science, 13(February), 1–10. https://doi.org/10.3389/fpls.2022.757810

Hong, F. W., & Chia, K. S. (2021). A review on recent near infrared spectroscopic measurement setups and their challenges. Measurement: Journal of the International Measurement Confederation, 171(November 2020). https://doi.org/10.1016/j.measurement.2020.108732

Hu, Z., Sykes, R., Davis, M. F., Charles Brummer, E., & Ragauskas, A. J. (2010). Chemical profiles of switchgrass. Bioresource Technology, 101(9), 3253–3257. https://doi.org/10.1016/j.biortech.2009.12.033

Juneja, A., Kumar, D., Williams, J. D., Wysocki, D. J., & Murthy, G. S. (2011). Potential for ethanol production from conservation reserve program lands in Oregon. Journal of Renewable and Sustainable Energy, 3(6). https://doi.org/10.1063/1.3658399

Kgblevo, F. A., Evans, R. J., & Johnsonb, K. D. (1994). Molecular-beam mass-spectrometric lignocellulosic materials I. Herbaceous biomass. Journal of Analytical and Applied Pyrolysis, 30, 125–144.

La Bastide, J.G.A. & Van Goor, C.P. (1978). Interlaboratory variability in the chemical analysis

of leaf samples. Plant and Soil, 49(1), 1–7. http://www.jstor.org/stable/42933562

Lestander, T. A., Leardi, R., & Geladi, P. (2003). Selection of near infrared wavelengths using genetic algorithms for the determination of seed moisture content. Journal of Near Infrared Spectroscopy, 11(6), 433–446. https://doi.org/10.1255/jnirs.394

Liang, L., Wei, L., Fang, G., Xu, F., Deng, Y., Shen, K., Tian, Q., Wu, T., & Zhu, B. (2020). Prediction of holocellulose and lignin content of pulp wood feedstock using near infrared spectroscopy and variable selection. Spectrochimica Acta - Part A: Molecular and Biomolecular Spectroscopy, 225. https://doi.org/10.1016/j.saa.2019.117515

Lin, L. I. (1989). A Concordance Correlation Coefficient to Evaluate Reproducibility Author (s): Lawrence I-Kuei Lin Published by : International Biometric Society Stable URL : http://www.jstor.org/stable/2532051 REFERENCES Linked references are available on JSTOR for thi. Biomatrics, 45(1), 255–268.

Liu, Y., Tang, Y., Gao, H., Zhang, W., Jiang, Y., Xin, F., & Jiang, M. (2021). Biotechnologies for Lignocellulosic Biorefinery. Molecules, 26, 5411.

López-Fernández, J., Moya, D., Dolors Benaiges, M., Valero, F., & Alcalà, M. (2022). Near Infrared Spectroscopy: A useful technique for inline monitoring of the enzyme catalyzed biosynthesis of third-generation biodiesel from waste cooking oil. Fuel, 319(March). https://doi.org/10.1016/j.fuel.2022.123794

Magnusson, M., Andersen, M. R., Jonasson, J., & Vehtari, A. (2020). Leave-One-Out Cross-Validation for Bayesian Model Comparison in Large Data. http://arxiv.org/abs/2001.00980

Mahood, S. A., & Cable, D. E. (1922). The Chemistry of Wood IV—The Analysis of the Wood of Eucalyptus globulus and Pinus montícola. 12(1920), 933–934.

Manley, M. (2014). Near-infrared spectroscopy and hyperspectral imaging: Non-destructive analysis of biological materials. Chemical Society Reviews, 43(24), 8200–8214. https://doi.org/10.1039/c4cs00062e

Martin Bland, J., & Altman, D. G. (1986). Statistical Methods for Assessing Agreement Between Two Methods of Clinical Measurement. The Lancet, 327(8476), 307–310. https://doi.org/10.1016/S0140-6736 (86)90837-8

McCarthy, J. L., & Islam, A. (1999). Lignin chemistry, technology, and utilization: A brief history. ACS Symposium Series, 742, 2–66. https://doi.org/10.1021/bk-2000-0742.ch001

Milne, T. A., Brennan, A. H., & Glenn, B. H. (1990). Sourcebook of methods of analysis for biomass and biomass conversion processes. https://doi.org/10.5860/choice.28-6021

Mishra, P., & Woltering, E. J. (2021). Identifying key wavenumbers that improve prediction of amylose in rice samples utilizing advanced wavenumber selection techniques. Talanta, 224. https://doi.org/10.1016/j.talanta.2020.121908

Perlack, R.D., & Stokes, B.J. (Leads), U.S. Department of Energy. 2011. U.S. Billion-Ton Update: Biomass Supply for a Bioenergy and Bioproducts Industry. ORNL/TM-2011/224. Oak Ridge National Laboratory, Oak Ridge, TN. 227p

Pan, L., Zhu, Q., Lu, R., & McGrath, J. M. (2015). Determination of sucrose content in sugar beet by portable visible and near-infrared spectroscopy. Food Chemistry, 167, 264–271. https://doi.org/10.1016/j.foodchem.2014.06.117

Passing, H., & Bablok, W. (1983). A New Biometrical Procedure for Testing the Equality of Measurements from Two Different Analytical Methods. Application of linear regression procedures for method comparison studies in Clinical Chemistry, Part I. Cclm, 21(11), 709–720. https://doi.org/10.1515/cclm.1983.21.11.709

Qiao, L., Mu, Y., Lu, B., & Tang, X. (2021). Calibration Maintenance Application of Near-infrared Spectrometric Model in Food Analysis, Food Reviews International, DOI: 10.1080/87559129.2021.1935999

Rai, A. K., Al Makishah, N. H., Wen, Z., Gupta, G., Pandit, S., & Prasad, R. (2022). Recent Developments in Lignocellulosic Biofuels, a Renewable Source of Bioenergy. Fermentation, 8(4). https://doi.org/10.3390/fermentation8040161

R Core Team (2021). R: A language and environment for statistical computing. R Foundation for Statistical Computing, Vienna, Austria. URL https://www.R-project.org/.

Rinnan, Å., Berg, F. van den, & Engelsen, S. B. (2009). Review of the most common pre-processing techniques for near-infrared spectra. TrAC - Trends in Analytical Chemistry, 28(10), 1201–1222. https://doi.org/10.1016/j.trac.2009.07.007

Ritter, G. J., Mitchell, R. L., & Seboro, R. M. (1933). Some Factors that Influence the Conversion of Cellulosic Materials to Sugar. Journal of the American Chemical Society, 55(7), 2989–2991. https://doi.org/10.1021/ja01334a063

Ritter, G. J., Seborg, R. M., & Mitchell, R. L. (1932). Factors Affecting Quantitative Determination of Lignin by 72 Per Cent Sulfuric Acid Method. Industrial and Engineering Chemistry - Analytical Edition, 4(2), 202–204. https://doi.org/10.1021/ac50078a017

Roggo, Y., Chalus, P., Maurer, L., Lema-Martinez, C., Edmond, A., & Jent, N. (2007). A review of near infrared spectroscopy and chemometrics in pharmaceutical technologies. Journal of Pharmaceutical and Biomedical Analysis, 44(3 SPEC. ISS.), 683–700. https://doi.org/10.1016/j.jpba.2007.03.023

Saeman, J. F., Bubl, J. L., & Harris, E. E. (1945). Quantitative saccharification of wood and cellulose. Industrial and Engineering Chemistry, 17, 35–37. https://doi.org/10.1021/i560137a008

Selig, M. J., Tucker, M. P., Law, C., Doeppke, C., Himmel, M. E., & Decker, S. R. (2011). High throughput determination of glucan and xylan fractions in lignocelluloses. Biotechnology

Letters, 33(5), 961–967. https://doi.org/10.1007/s10529-011-0526-7

Shi, J., Ebrik, M. A., & Wyman, C. E. (2011). Sugar yields from dilute sulfuric acid and sulfur dioxide pretreatments and subsequent enzymatic hydrolysis of switchgrass. Bioresource Technology, 102(19), 8930–8938. https://doi.org/10.1016/j.biortech.2011.07.042

Skvaril, J., Kyprianidis, K. G., & Dahlquist, E. (2017). Applications of near-infrared spectroscopy (NIRS) in biomass energy conversion processes: A review. Applied Spectroscopy Reviews, 52(8), 675–728. https://doi.org/10.1080/05704928.2017.1289471

Sluiter, A., Hames, B., Ruiz, R., Scarlata, C., Sluiter, J., Templeton, D., & Crocker, D. (2008). Determination of Structural Carbohydrates and Lignin in Biomass: Laboratory Analytical Procedure (LAP). In Technical Report NREL/ TP -510 -42618. http://www.nrel.gov/biomass/pdfs/42618.pdf

Sluiter, J. B., Ruiz, R. O., Scarlata, C. J., Sluiter, A. D., & Templeton, D. W. (2010). Compositional analysis of lignocellulosic feedstocks. 1. Review and description of methods. Journal of Agricultural and Food Chemistry, 58(16), 9043–9053. https://doi.org/10.1021/jf1008023

Teixeira Dos Santos, C. A., Lopo, M., Páscoa, R. N. M. J., & Lopes, J. A. (2013). A review on the applications of portable near-infrared spectrometers in the agro-food industry. Applied Spectroscopy, 67(11), 1215–1233. https://doi.org/10.1366/13-07228

Templeton, D. W., Wolfrum, E. J., Yen, J. H., & Sharpless, K. E. (2016). Compositional Analysis of Biomass Reference Materials: Results from an Interlaboratory Study. Bioenergy Research, 9(1), 303–314. https://doi.org/10.1007/s12155-015-9675-1

Thammasouk, K., Tandjo, D., & Penner, M. H. (1997). Influence of Extractives on the Analysis of Herbaceous Biomass. Journal of Agricultural and Food Chemistry, 45(2), 437–443. https://doi.org/10.1021/jf960401r

Tian, L. U., Cai, T., Goetghebeur, E., & Wei, L. J. (2007). Model evaluation based on the sampling distribution of estimated absolute prediction error. Biometrika, 94(2), 297–311. https://doi.org/10.1093/biomet/asm036

Tibshirani, R. J., & Tibshirani, R. (2009). A bias correction for the minimum error rate in cross-validation. Annals of Applied Statistics, 3(2), 822–829. https://doi.org/10.1214/08-AOAS224

Van der Cruijsen, K., Al Hassan, M., Van Erven, G., Dolstra, O., & Trindade, L. M. (2021). Breeding targets to improve biomass quality in miscanthus. Molecules, 26(2), 1–28. https://doi.org/10.3390/molecules26020254

Van Soest, P. J., Robertson, J. B., & Lewis, B. A. (1991). Methods for Dietary Fiber, Neutral Detergent Fiber, and Nonstarch Polysaccharides in Relation to Animal Nutrition. Journal of Dairy Science, 74(10), 3583–3597. https://doi.org/10.3168/jds.S0022-0302(91)78551-2

Varma, S., & Simon, R. (2006). Bias in error estimation when using cross-validation for model selection. BMC Bioinformatics, 7, 1–8. https://doi.org/10.1186/1471-2105-7-91

Wang, Z., Huang, Y., Zhang, F., Xie, H., Jiang, G., Lv, D., Zhang, H., Lam, S. S., & Song, A. (2022). Improving enzymatic saccharification of corn stover via thioglycolic acid-mediated Fenton pretreatment. Journal of Cleaner Production, 365(May). https://doi.org/10.1016/j.jclepro.2022.132804

Wickham, H. (2016). ggplot2: Elegant Graphics for Data Analysis. Springer-Verlag New York.

Wolfrum, E. J., Payne, C., Schwartz, A., Jacobs, J., & Kressin, R. W. (2020). A Performance Comparison of Low-Cost Near-Infrared (NIR) Spectrometers to a Conventional Laboratory Spectrometer for Rapid Biomass Compositional Analysis. Bioenergy Research, 13(4), 1121–1129. https://doi.org/10.1007/s12155-020-10135-6

Workman, J. J. (2018). A Review of Calibration Transfer Practices and Instrument Differences in Spectroscopy. Applied Spectroscopy, 72(3), 340–365. https://doi.org/10.1177/0003702817736064

Xinru Li, Ma, F., Liang, C., Wang, M., Zhang, Y., & Shen, Yufei, Chengping Liang1, Maoyao Wang1, Yan Zhang1, Yufei Shen1, Muhammad Adnan1, Pan Lu1, Muhammad Tahir Khan2, J. H. and M. Z. (2021). Precise high-throughput online near-infrared spectroscopy assay to determine key cell wall features associated with sugarcane bagasse digestibility. In Clinical PET/MRI (pp. 289–312). https://doi.org/10.1016/B978-0-323-88537-9.00012-X

Xu, L., Zhou, Y. P., Tang, L. J., Wu, H. L., Jiang, J. H., Shen, G. L., & Yu, R. Q. (2008). Ensemble preprocessing of near-infrared (NIR) spectra for multivariate calibration. Analytica Chimica Acta, 616(2), 138–143. https://doi.org/10.1016/j.aca.2008.04.031

Yang, M., Chen, Q., Kutsanedzie, F. Y. H., Yang, X., Guo, Z., & Ouyang, Q. (2017). Portable spectroscopy system determination of acid value in peanut oil based on variables selection algorithms. Measurement: Journal of the International Measurement Confederation, 103, 179–185. https://doi.org/10.1016/j.measurement.2017.02.037

Yin, X., Wei, L., Pan, X., Liu, C., Jiang, J., & Wang, K. (2021). The Pretreatment of Lignocelluloses With Green Solvent as Biorefinery Preprocess: A Minor Review. Frontiers in Plant Science, 12(June). https://doi.org/10.3389/fpls.2021.670061

Zhang, K., Johnson, L., Nelson, R., Yuan, W., Pei, Z., & Wang, D. (2012). Chemical and elemental composition of big bluestem as affected by ecotype and planting location along the precipitation gradient of the Great Plains. Industrial Crops and Products, 40(1), 210–218. https://doi.org/10.1016/j.indcrop.2012.03.016

Zhang, W., Kasun, L. C., Wang, Q. J., Zheng, Y., & Lin, Z. (2022). A Review of Machine Learning for Near-Infrared Spectroscopy. Sensors, 22(24), 1–32. https://doi.org/10.3390/s22249764

Zhu, C., Fu, X., Zhang, J., Qin, K., & Wu, C. (2022). Review of portable near infrared spectrometers: Current status and new techniques. Journal of Near Infrared Spectroscopy, 30(2), 51–66. https://doi.org/10.1177/09670335211030617

CHAPTER 5 GENERAL CONCLUSION

This study was undertaken to fill the gap in understanding interannual temporal and within-field spatial variability of biomass yield and quality of two bioenergy crops - switchgrass and restored prairie. The main objectives of the study were to (1) evaluate interannual temporal and within-field spatial variability of biomass yield and quality of switchgrass and restored prairie; (2) examine the relationships of soil fertility characteristics and topographical features with biomass yield and quality of switchgrass and restored prairie; and (3) assess the viability of using near-infrared spectroscopy to determine cell wall composition of bioenergy feedstock biomass.

In chapter 2, we found that both switchgrass and restored prairie showed within-field variability of biomass yield. The monoculture cropping system of switchgrass had more within-field spatial variability of biomass yield than the polyculture cropping system of restored prairie under the same field and climate conditions. Moreover, the interannual temporal variability of biomass yield in the monoculture cropping system of switchgrass was also higher than in the polyculture cropping system of restored prairie. Among all the soil fertility characteristics and topographical features examined, there were considerable uncertainties in their relationships with biomass yield. Nonetheless, soil $NH4^{+}$, Mg, and topographical wetness index were significantly related to switchgrass biomass yield; and, soil Ca, P and SAT were significantly related to biomass yield of restored prairie.

In chapter 3, we provided the first comprehensive assessment of within-field variability of biomass quality of switchgrass and restored prairie as bioenergy feedstocks at the field scale. The three major components of cell wall composition—glucose, xylose and lignin—were selected to represent biomass quality. The within-field spatial variability of glucose, xylose and lignin contents was considerably lower than the corresponding annual temporal variability for

switchgrass and restored prairie. Restored prairie had a higher interannual temporal variability of glucose and xylose content than switchgrass. There were no clear relationships of the examined soil fertility characteristics and topographical features with our measures of biomass quality.

In chapter 4, we assessed the viability of substituting traditional wet chemistry analysis of biomass with near-infrared spectroscopy to determine structural glucose, xylose and lignin content of biomass materials. Biases were found between chemical analysis and near-infrared spectroscopy methods for determining glucose, xylose and lignin content. After bias correction, near-infrared spectroscopy had better agreement with the chemical analysis according to Lin's concordance correlation coefficient. We concluded that near-infrared spectroscopy with bias correction is a promising analytical method for rapid cell wall composition determination.

The Insights gained from this study will benefit agronomic management of bioenergy crops, as well as bioenergy feedstock supply chain design and biorefinery operation planning. Scientists have reached a general consensus that the frequency and intensity of extreme weather is expected to increase in the future. And, like all agriculture in general, bioenergy crop production will be impacted by the expected extreme weather events. Therefore, it is important to understand the variability of bioenergy feedstock biomass yield and quality in order to adapt to future climatic uncertainty. The biomass yield of switchgrass and restored prairie in this study showed good temporal stability during the study period (2018-2021). However, the within-field spatial variability of switchgrass biomass yield implies the potential to improve field scale biomass yield with site-specific agronomic management practices. More research is needed to elucidate the causes of within-field spatial variability of switchgrass biomass yield.

The relatively lower within-field spatial variability of restored prairie biomass yield makes it a good candidate for growing in marginal lands with low-input field management strategies. Since

biomass quality of switchgrass and restored prairie is more subject to interannual variability than within-field spatial variability, biomass quality of restored prairie may be more consistent from year to year at the field scale. Currently, most supply chain biomass quality research focuses on moisture content. Incoporating more biomass quality component parameters, such as cell wall composition, into biomass supply chain design will more accurately evaluate the efficiency of the supply chain. At the biorefinery level, efforts should be made to reduce year to year variability in biomass quality in order to improve conversion efficiency. In addition, near-infrared spectroscopy with chemometrics will be a powerful analytical tool to assess and monitor biomass quality variability throughout the field to fuel production pipeline.